

**Understanding, Engineering and Chemical
Modification of Pyrichalasin H Biosynthesis
from *Magnaporthe grisea* NI980**

Von der Naturwissenschaftlichen Fakultät der Gottfried Wilhelm
Leibniz Universität Hannover

zur Erlangung des Grades

Doktor der Naturwissenschaften (Dr. rer. nat.)

genehmigte Dissertation

von

Chongqing Wang, Master (China)

2020

Referent: Prof. Dr. Russell Cox

Korreferent: Prof. Dr Mark Brönstrup

Tag der Promotion: 29.06.2020

Abstract

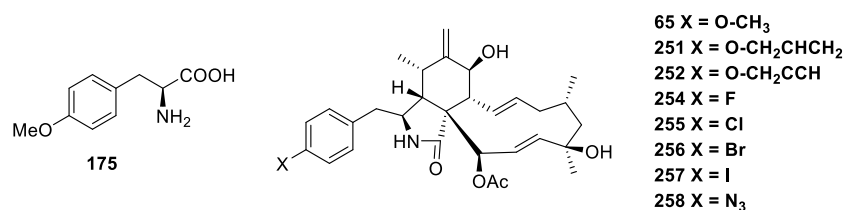
Keywords: natural products, biosynthesis, pyrichalasin

Pyrichalasin H **65** belongs to the cytochalasan family of fungal natural products, and is the major phytotoxic metabolite produced by the fungal plant pathogen *Magnaporthe grisea* NI980. In a combined chemical and genetic approach, the biosynthesis and chemical modification of **65** were investigated in this work.

Using a bipartite gene knockout strategy targeting the *pyi* biosynthetic gene cluster, two fundamental genes *pyiS* and *pyiC* were disrupted, resulting in the complete abolition of **65**. Five tailoring genes (two P450 encoding genes, one *O*-AcT, one *O*-MeT and one OXR encoding gene) were also inactivated individually; thirteen novel cytochalasans were isolated and identified by HRMS and NMR. For the first time, we discovered that *O*-methyltyrosine **175** was the initial precursor of **65** from the results of *pyiA* KO.

Six cryptic P450 genes were investigated in two pyrichalasin H P450 disruption strains by heterologous expression. HffD and CYP1 were confirmed to catalyse a C-18 hydroxylation reaction, HffG catalyses a C-7 hydroxylation reaction and CYP3 catalyses an epoxidation reaction between C-6 and C-7. Three novel epoxide cytochalasans were obtained.

Four 4'-halogenated phenylalanines, together with 4'-allyl, 4'-propargyl and 4'-azido phenylalanine were fed to a Δ *pyiA* KO strain. This resulted in production of seven new 4'-functionalised pyrichalasins with titres around 30 - 60 mg/L.



Based on seven 4'-substituted pyrichalasins generated by mutasynthesis, many functionalised pyrichalasins were created by various chemical modifications. Triazole pyrichalasins were generated by click chemistry, using azide- **258** and alkyne pyrichalasin **252** as starting materials. Bromo- pyrichalasin **256** is the substrate for the synthesis of dimeric pyrichalasin **318** via Suzuki cross coupling, while Iodo-pyrichalasin **257** is a substrate for Sonogashira coupling reactions. Moreover, dye linked

pyrichalasin **308 - 316** were generated for actin visualization in cell biology. In total, eighteen novel functional pyrichalasin were synthesized.

Zusammenfassung

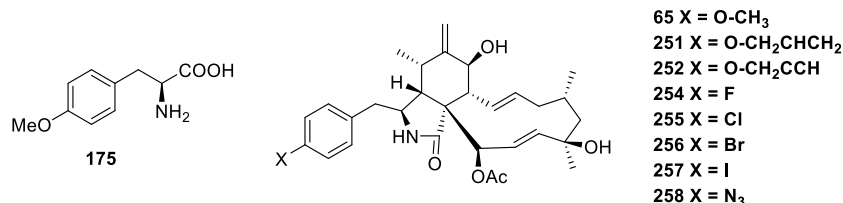
Schlagwörter: naturstoffe, biosynthese, pyrichalasin

Pyrichalasin H **65** gehört der Familie der Cytochalasine an und ist das Haupttoxin welches von dem Pflanzenpathogen *Magnaporthe grisea* NI980 produziert wird. Mittels Kombination von chemischen und genetischen Methoden wurden in dieser Arbeit die Biosynthese und chemischen Modifikationen von **65** erforscht.

Unter Zuhilfenahme einer zweiteiligen Genknockout-Strategy wurden die beiden essentiellen Gene *pyiS* und *pyiC* des *pyi* Genclusters inaktiviert, wodurch die Produktion von **65** komplett unterbunden wurde. Fünf weitere Gene (zwei P450 codierende Gene, ein *O*-AcT, ein *O*-MeT and ein OXR codierendes Gen) wurden ebenfalls individuell inaktiviert, was zur Bildung dreizehn neuer Cytochalasane führte. Diese wurden isoliert und mittels HRMS und NMR charakterisiert. Durch Knockout von *pyiA* haben wir erstmalig nachgewiesen, dass *O*-Methyltyrosin **175** der initiale Vorläufer von **65** ist.

Die Funktion sechs kryptischer P450-Gene wurde durch heterologe Expression in dem Pyrichalasin H P450-Deletionsstamm untersucht. HffD und CYP1 katalysieren eine Hydroxylierung an C-18, HffG katalysiert eine Hydroxylierung an C-7 und CYP3 katalysiert eine Epoxidierung zwischen C-6 und C-7. Drei neue epoxidierte Cytochalasane wurden erhalten.

Vier 4'-halogenierte Phenylalaninvarianten wurden zusammen mit 4'-allyl-, 4'-propargyl- und 4'-azido-Phenylalanin an den Δ *pyiA* Knockoutstamm verfüttert. Dies resultierte in der Bildung von sieben neuartigen 4'-funktionalisierten Pyrichalasanen mit Ausbeuten von 30 - 60 mg/L.



Ausgehend von den 4'-substituierten Pyrichalasanen wurden viele weitere funktionalisierte Pyrichalasane durch nachfolgende chemische Modifikationen erhalten. Triazol-Pyrichalasane wurden aus Azid **258** und dem Alkin-Pyrichalasin **252** als Startmaterial durch Click-Chemie hergestellt. Bromo-Pyrichalasin **256** ist das Substrat für die Herstellung des dimeren Pyrichalasins **318** *via* Suzuki Kreuz-Kopplung, während Iodo-Pyrichalasin **257** das Substrat für Sonogashira-Reaktionen darstellt. Des Weiteren wurden fünf Farbstoff-gekoppelte Pyrichalasane **308** - **316** für die Visualisierung von Aktin in der Zellbiologie hergestellt. In der Summe wurden achtzehn neue Pyrichalasane synthetisiert.

Acknowledgement

First of all, I would like to thank Prof. Russell Cox for giving me the opportunity to do this PhD. I am greatly thankful to his support and professional supervision throughout the last three years.

Especially, I want to give my sincere gratitude to Dr. Elizabeth Skellam. She is always very patient with all my questions, always gives me detailed explanations of all the theories and experiments. Moreover, she also helped me a lot of my personal troubles when I first came in Germany.

I also want to thank our cooperation partners, thank Prof. Marc-Henri Lebrun and Dr. Didier Tharreau providing us *Magnaporthe grisea* NI980 strain. Thank Prof. Jörn Kalinowski and Dr. Daniel Wibberg for their efforts with sequencing and bioinformatics matters. Thank Prof. Marc Stadler and Christopher Lambert for their hard work for bioassays on cell and microorganism. Thanks for Dr. Eric Kuhnert for the offer the fungal strain *Xylaria hypoxylon*, *Hypoxylon fragiforme* and *Daldinia concentrica*. Thank Prof. Theresia Stradal and Klemens Rottner for their precious suggestion on cell imaging assay. Thanks for the dye molecules provided by Prof. Mark Brönstrup. I am also grateful to Dr. Carsten Zeilinger for his contribution on living cell assay.

Thanks for the strong support from BMWZ media kitchen team and all the analytical departments at the OCI, this work would not have been possible without the generous help from all of you. Particularly, I thank Dr. Jörg Fohrer and Dr. Gerald Dräger for their help with NMR and mass related questions. And thank Katja, Doreen, Monika for making almost everything possible.

I would like to thank all past and current Cox group members, in particular Hao, Sen, Dongsong, Jin, Lei, Tian, Lukas, Carsten, Raissa, Verena, Karen, Francesco, Steffen, Eman, Mary, Oliver, Vjaceslavs, Haili and all my students (Haoxuen, Yan, Maurice, Adrian, Teresa and Michelle).

Special thanks to Dr Kun Fang, Hongyu Wang, Prof. Jingsong Han, Guidong Wang, Hao Zhou, Dechao Zhao, Dr Yu Fang for constant support throughout my studies.

Finally, I would like to thank my parents, family and friends for their unparalleled love and care. I won't make it without their strong and unselfish support.

Abbreviations and Units

A	adenylation domain	Kb	kilobase
aa	amino acid	KR	β -ketoreductase
ACE1	avirulence conferring enzyme 1	KS	β -ketosynthase
ACP	acyl carrier protein	KO	knockout
AMT	agrobacterium mediated transformation	L	liter
ATP	adenosine triphosphate	LB	lysogeny broth
AT	acyl transferase	LCMS	liquid chromatography- mass spectrometry
aq.	aqueous	LDKS	lovastatin diketide synthase
bar	basta resistance gene	LNKS	lovastatin nonketide synthase
BGC	biosynthesis gene cluster	M	mol/l
BLAST	basic local alignment search tool	mg	milligram
bp	base pair	mRNA	messenger RNA
$^{\circ}$ C	Celsius	<i>m/z</i>	mass tocharge ratio
CDNA	complementary DNA	mFAS	mamalian
C-MeT	<i>c</i> -methyl transferase	min	minute
CoA	co-enzyme A	mL	millilitre
COSY	correlation spectroscopy	MS	mass spectrometry
CuI	copper iodide	MT	methyltransferase
CuSO ₄	copper(II) sulfate	NADPH	nicotinamide adenine dinucleotide (phosphate)
DA	Diels Alder(ase)	NHEJ	non-homologous end-joining
DAD	diode array detector	NMR	nuclear magnetic resonance
ddH ₂ O	double distilled H ₂ O	ORF	open reading frame
DMAP	dimethylaminopyridine	PAM	protospacer adjacent motif
DMF	dimethylformamide	PEG	polyethylene glycol
DMSO	dimethylsulfoxide	PKS	polyketide synthase
DNA	deoxynucleic acid	PT	product template
DH	dehydratase	PMT	protoplast mediated transformation
DIPEA	<i>N,N</i> -diisopropylethylamine	PCR	polymerase chain reaction
DKC	Dieckmann cyclisation	PCP	peptide carrier protein
dNTP	deoxynucleotide triphosphate	Q-TOF	quadrupole time- of-flight
EDTA	ethylenediaminetetraacetic acid	R	reductive release domain
EtOH	ethanol	RT	room temperature
EDC	<i>N</i> -(3-dimethylaminopropyl)- <i>N'</i> -ethylcarbodiimide	RT-PCR	reverse transcriptase
EtOAc	ethyl acetate	RNA	ribonucleic acid
ER	enoyl reductase	rpm	revolutions per minute
eGFP	enhanced green fluorescent protein	SAM	<i>S</i> -adenosyl methionine
eq	equivalent	SAT	starter unit acyl carrier protein
ESI	electron-spray ionisation	SDR	short chain dehydrogenase/reductase
ELSD	evaporative light scattering detector	SDS-PAGE	sodium dodecyl sulfate polyacrylamide gel electrophoresis
FAD	flavin adenine dinucleotide	<i>S.</i>	<i>Saccharomyces cerevisiae</i>
FAS	fatty acid synthase	<i>sp.</i>	species
g	gram	T	thiolation
gDNA	genomic DNA	TAE	tris-acetate-EDTA
GOI	gene of interest	TCEP	tris(2-carboxyethyl)phosphine
HMBC	heteronuclear multiple bond correction	THF	tetrahydrofuran
HPLC	high performance liquid chromatography	TE	thiolesterase
hyg	hygromycin B resistance cassette	TFA	trifluoroacetic acid
HR	homologous recombination	U	uracil
HRMS	high resolution mass spectrometry	UV	ultra violet
HSQC	heteronuclear single quantum correlation	<i>v/v</i>	volume per volume
Hz	hertz	<i>w/v</i>	weight per volume
IR	infrared	WT	wild type

Contents

Abstract	1
Zusammenfassung.....	3
Acknowledgement	5
Abbreviations and Units	6
1. Introduction.....	11
1.1 Natural Products in Fungi.....	11
1.1.1 Alkaloids.....	12
1.1.2 Terpenes.....	12
1.1.3 Polyketides.....	13
1.1.4 Peptides.....	20
1.1.5 Polyketide Synthase – Nonribosomal Peptide Synthetase (PKS - NRPS) Hybrids	24
1.2 Cytochalasans	27
1.2.1 Isotopic Labelling Experiment of Cytochalasin E.....	28
1.2.2 Biosynthesis of Cytochalasin E and Cytochalasin K.....	29
1.3 Tailoring Modifications in Natural Product Biosynthesis.....	31
1.3.1 Cytochrome P450 Monooxygenase.....	31
1.3.2 Alpha Keto Glutarate Dependent Dioxygenase	34
1.3.3 Methyltransferase	36
1.3.4 Acetyltransferase.....	37
1.3.5 Short-Chain Dehydrogenase/Reductase.....	38
1.4 Pyrichalasin H	39
1.4.1 Introduction.....	39
1.4.2 Bioinformatic Analysis of the <i>Pyrichalasin H</i> Gene Cluster	40
1.4.3 Bioinformatic Analysis of the ACE1 Gene Cluster	42
1.5 Diversifying Natural Products through Mutasynthesis and Semisynthesis	46

1.5.1 Application of Mutasynthesis in Natural Products	46
1.5.2 Application of Semisynthesis in Natural Products	47
1.6 Project Aims	48
2 Investigation the Biosynthesis of Pyrichalasin H by Gene Disruption	51
2.1 Introduction	51
2.1.1 Bipartite Gene Targeting Strategy	52
2.1.2 Protoplast-Mediated Transformation.....	53
2.2 Aims	54
2.3 Results	55
2.3.1 Chemical Investigation of <i>Magnaporthe grisea</i> WT.....	55
2.3.2 <i>pyiS</i> Gene Knockout.....	63
2.3.3 Targeted Inactivation of Tailoring Genes in Pyrichalasin BGC	67
2.4 Discussion & Conclusion	86
3 Combinatorial Biosynthesis of Late Stage Cytochalasan Tailoring Cytochrome P450 Monooxygenases	92
3.1 Introduction	92
3.1.1 Heterologous Expression.....	92
3.1.2 Benzenediol Lactone Engineering.....	94
3.2 Aims	96
3.3 Results	97
3.3.1 Combinatorial Biosynthesis with <i>ccsB</i> into <i>Magnaporthe grisea</i> NI980 <i>pyiH</i> Disruption Strain.....	97
3.3.2 Heterologous Expression of Cryptic Cytochalasan P450s into <i>Magnaporthe grisea</i> NI980 P450 Disruption Strain	102
3.4 Discussion & Outlook	119
4. Generating New Pyrichalasin by Mutasynthesis	125

4.1 Introduction to Mutasynthesis and Other Methods of Pathway Engineering	125
4.2 Aims	128
4.3 Results	129
4.3.1 Synthesis of Substrates	129
4.4 Discussion & Conclusion	132
5. Chemical Modification of Mutasynthetic Pyrichalasan	134
5.1 Introduction	134
5.1.1 Total synthesis of Cytochalasin B	135
5.1.2 Chemical Modification of Cytochalasin D	136
5.2 Aims	137
5.3 Results	137
5.3.1 Generating New Hybrid Molecular Pyrichalasan by Copper-Catalyzed Azide-Alkyne Huisgen Cycloaddition (CuAAC)	137
5.3.2 Application of Huisgen Cycloaddition	138
5.3.3 Result	139
5.3.4 Synthesis, Bioevaluation and Application of Fluorescent Dye Linked Pyrichalasan in Cell Visualization	142
5.3.5 Results	144
5.3.6 Generating Dimeric Pyrichalasan with Different Chain Length Linkers	146
5.3.7 Results	147
5.3.8 Generating New Pyrichalasan by Sonogashira Reaction	149
5.3.9 Result	150
5.4 Discussion & Outlook	150
6 Overall Conclusion and Outlook	154
7. Experimental	157

7.1 Biology Parts	157
7.1.1 General	157
7.1.2 Enzymes	157
7.1.3 Antibiotics	158
7.1.4 plasmids and Vectors	158
7.1.5 Primers and Their Sequences	159
7.1.6 Media, Buffers and Solutions	163
7.1.7 Growth and Storage Conditions for Microorganisms	166
7.1.8 Feeding Studies	167
7.1.9 DNA and RNA Visualization, Isolation and Purification	168
7.1.10 DNA Amplification from DNA and RNA Templates	170
7.1.11 Fungal Transformations	171
7.2 Chemistry parts	173
7.2.1 General	173
7.2.2 Analytical LCMS	173
7.2.3 Preparative LCMS	174
7.2.4 High Resolution Mass Spectrometry (HRMS) Analysis	174
7.2.5 Infrared Spectrum (IR) Analysis	175
7.2.6 Nuclear Magnetic Resonance (NMR) Analysis	175
7.2.6 Software	175
7.2.7 Synthetic Procedures	176
References	198
8. Appendix	209
8.1 NMR Data for Chapter 2	209
8.2 NMR Data for Chapter 4	213
8.3 NMR Data for Chapter 5	217
Curriculum Vitae	236
List of Publications	236

1. Introduction

1.1 Natural Products in Fungi

Fungi are important eukaryotic microorganisms.¹ Many fungi can produce a wide range of organic compounds, including primary metabolites and secondary metabolites.^{2,3} Primary metabolism can be divided into sugars, organic acids, amino acids, proteins and lipids.⁴ They are essential for growth, development and reproduction of cells. The primary metabolites participate in the primary response by the regulation of carbohydrates, protein and lipids.⁵

Fungi are important producers of secondary metabolites. Many fungal secondary metabolites exhibit potent biological activities. For example: penicillin V **1** is a useful antibacterial agent; aflatoxins **2** are potent toxic and carcinogenic compounds which threaten human, animal, and plant health; cephalosporin C **3** can cure Gram-positive and some Gram-negative bacterial infections; compactin **4** reduces the risk of cardiovascular disease by preventing conversion of mevalonate into cholesterol; and kojic acid **5** is currently used to lighten skin color and treat abnormal hyperpigmentation.⁶ In China, Japan and Korea, mizoribine **6** is used for renal transplants (Figure 1.1).⁷

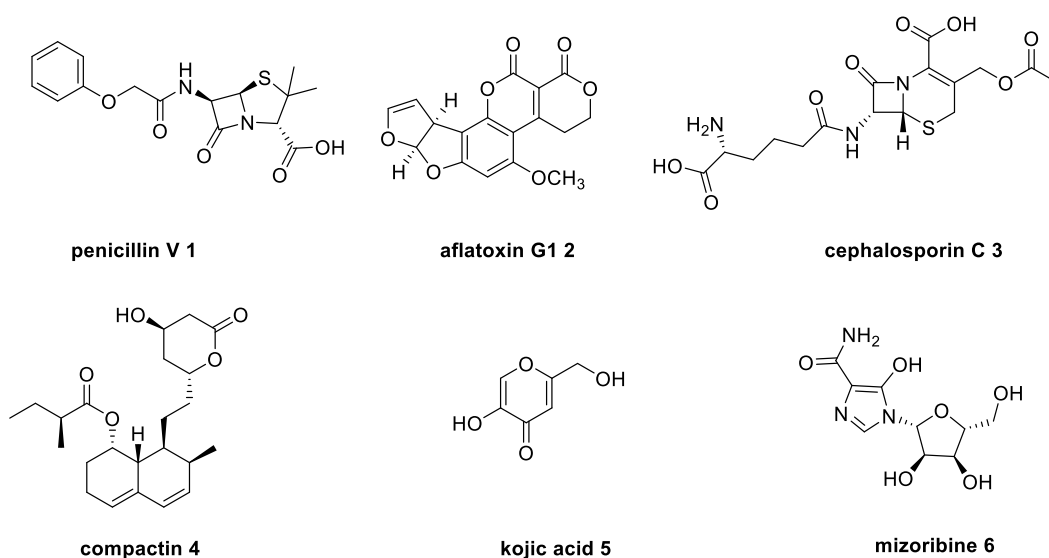


Figure 1.1 Examples of natural products produced by fungi.^{6,7}

In general, natural products can be divided into four major classes. They are alkaloids, terpenes, polyketides and peptides.⁵⁻⁷

1.1.1 Alkaloids

Alkaloids are a group of basic nitrogen-containing, low molecular-weight compounds, mostly derived from amino acids. Different from other kinds of secondary metabolites, most of alkaloids have unique biosynthetic origins. Clavicipitaceae and Trichocomaceae are the main fungal producers of ergot alkaloids **7 - 9** which have both harmful and beneficial effects to humans and have possibly been known for thousands of years.⁸ Due to their potent biological activity, many of them have been exploited as pharmaceuticals, narcotics and poisons, such as compounds **10 - 12** (Figure 1.2).^{6,8}

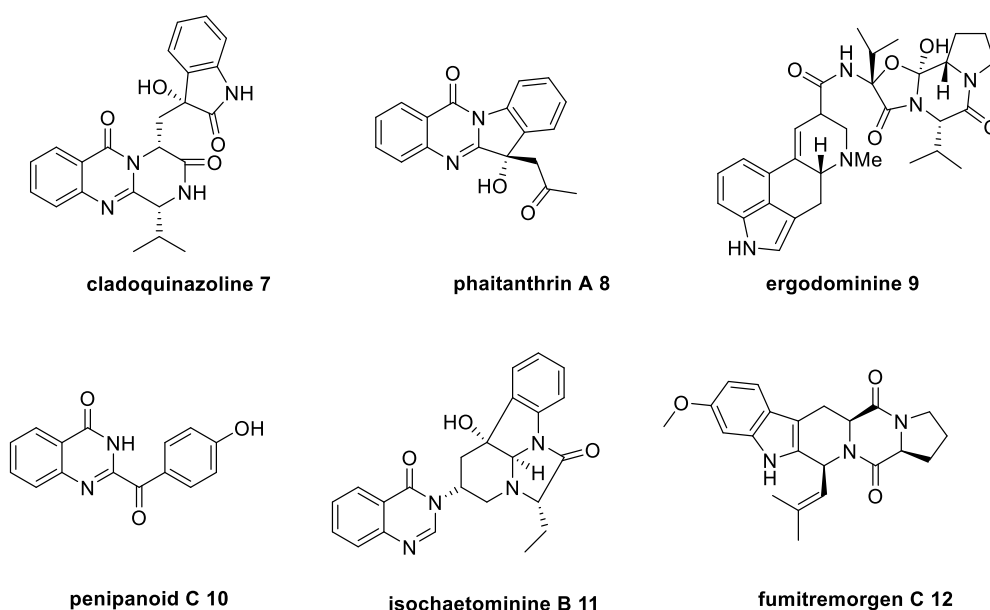


Figure 1.2 Examples of fungal alkaloids.^{6,8}

1.1.2 Terpenes

Terpenes are mainly produced by odoriferous plants, for example, camphor and turpentine. However, fungi also biosynthesize many important terpenes, including aristolochenes **13**, gibberellins **14**, oleanone **15**,⁹ myrcene **16** and carotenoids **17**. All terpenes are built from isoprene units and can be linear or cyclic, unsaturated or

saturated. Furthermore, they can be modified in many ways. Common terpenes can be divided into four classes: monoterpenes (C_{10}), which are generated from geranyl pyrophosphate; sesquiterpenes (C_{15}) come from farnesyl pyrophosphate; diterpenes (C_{20}) and carotenoids originate from geranylgeranyl pyrophosphate. Triterpenes (C_{30}) are classified among an extensive and structurally diverse group of natural substances, referred to as triterpenoids.¹⁰ Their structure includes 30 carbon atoms. Derivatives of squalene, are usually tetracyclic and pentacyclic, containing respectively four and five rings (Figure 1.3).^{9,10}

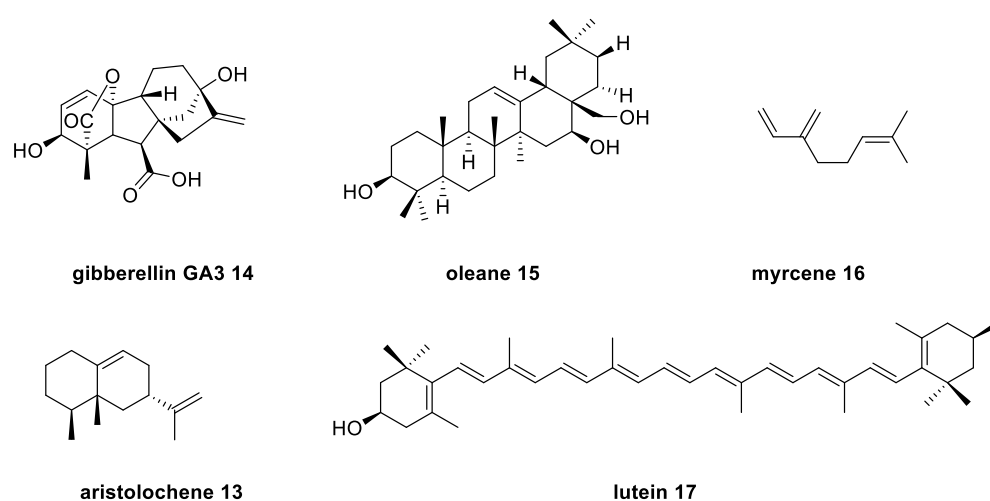


Figure 1.3 Examples of fungal terpenes.^{9,10}

1.1.3 Polyketides

Polyketides have been regarded as one of the most important classes of secondary metabolites.¹¹ They are produced by plants, bacteria and marine organisms as well as fungi.¹² The best-characterized fungal polyketides include: the yellow spore-pigment intermediate naphthopyrone (WA) **18**,¹¹ produced by *Aspergillus nidulans*; the carcinogen aflatoxin B1 **19**; the commercially useful cholesterol-lowering compound lovastatin **20**; and the mycotoxin acyl-pyrrolidone family compound fusarin C **21** (Figure 1.4).^{6,12}

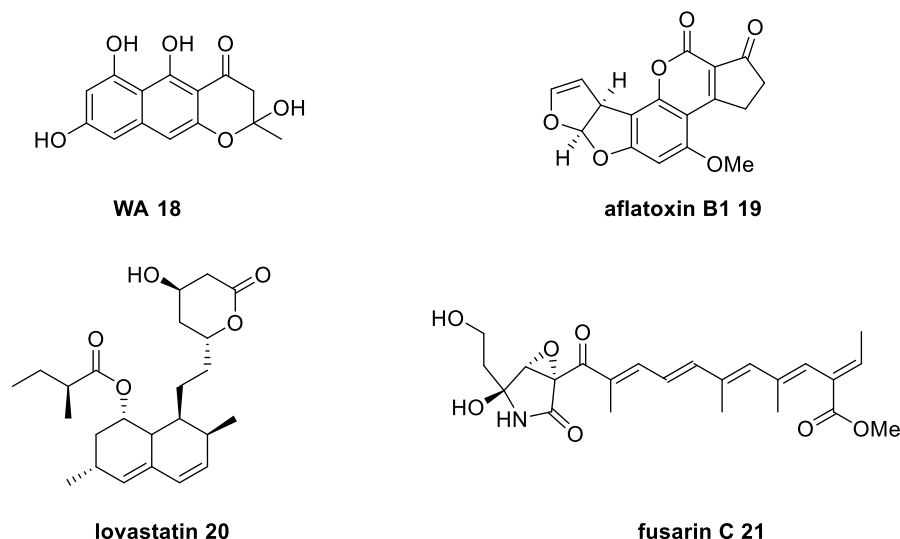


Figure 1.4 Examples of fungal polyketides.^{6,12}

Polyketides are biosynthesized by large multifunctional enzymes called polyketide synthases (PKS).⁶ PKS proteins are characterised into three types: Types I, II and III. Type I PKS are found in bacteria and fungi. Type II PKS consist of individual monofunctional proteins and are restricted to bacteria. Type III PKS (chalcone and stilbene synthases) are very simple systems found in plants, bacteria and fungi (Figure 1.5).¹⁰

Fatty acids serve as central components of membrane lipids and act as energy storage compounds in the form of triacylglycerols. They play important role in life. In the 1970s, it was reported that eukaryotic fatty acid biosynthesis is executed by large, multifunctional proteins known as type I fatty acid synthases (FAS). Type I FAS can be divided into yeast FAS (yFAS) and metazoan FAS (mFAS) based on the complete different domain organisation.¹³

Both type I FAS and PKS catalyse multiple rounds of precursor elongation by the same set of enzymatic domains in one multienzyme. Polyketides are synthesised from small coenzyme-A (CoA) esters, such as, acetyl-CoA **22**, malonyl-CoA **23**, propionyl-CoA **24** and butyryl-CoA **25** by continuous decarboxylation condensation catalysed by polyketide synthase enzymes. The vast diversity of polyketides originates from the use of small units like acetyl CoA, after elongation and modification. Fungal polyketide biosynthesis is closely related to fatty acid biosynthesis, which is often used as a guide for polyketide research (Figure 1.5).^{14,15}

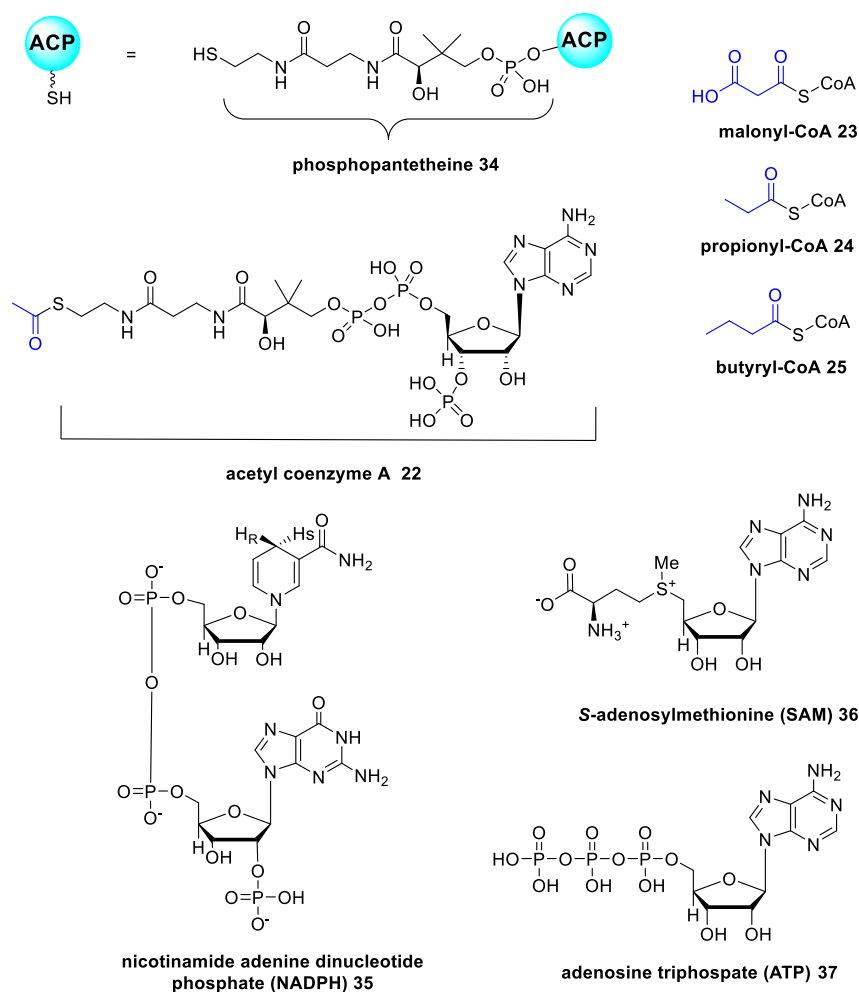
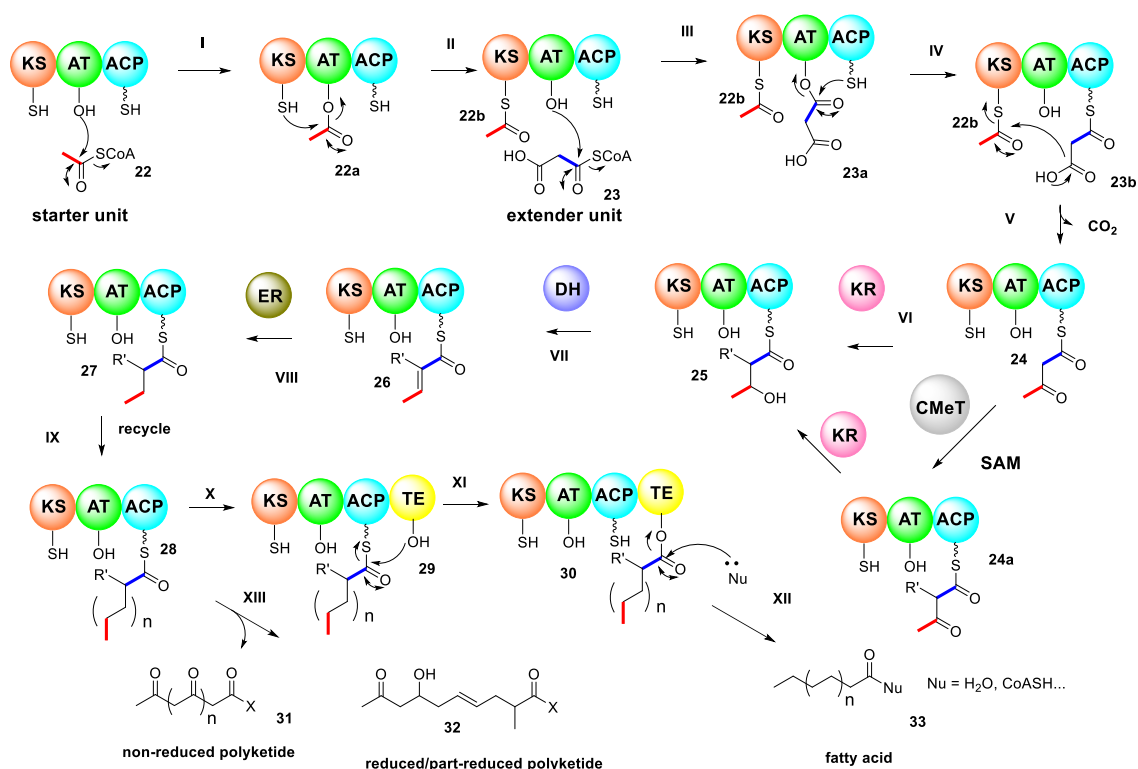


Figure 1.5 Chemical structures of Acetyl-CoA, NADPH, ATP and SAM.^{14,15}

Both fatty acid and polyketide biosynthesis begin by using an acyltransferase (AT) to load an acetyl-CoA starter unit **22** onto the ketosynthase (KS) domain. A malonyl-CoA extender unit **23** is then loaded onto an acyl carrier protein (ACP), which has a phosphopantetheine (PP) moiety **34** from CoA (Scheme 1.1, steps I-III).¹⁶ Then, triggered by decarboxylation, the KS domain catalyses a Claisen condensation between the starter unit **22** and extender unit **23**, resulting in carbon chain extension intermediate compound **24** attached to the PP arm of the ACP domain (Scheme 1.1, steps IV-V). Both polyketide and fatty acid biosynthesis requires the KS domain, while the ACP domain used by all FAS is not needed in Type III polyketide biosynthesis.¹⁷ Similarly, all FAS enzymes need an AT domain, however type III PKS enzymes do not require an AT domain.¹⁸

After the condensation, fatty acid biosynthesis continues with processing of the β -keto group, attached to the phosphopantetheine (PP) arm of the ACP domain. The β -keto group is first reduced to an alcohol **25** by the ketoreductase (KR) domain. The alcohol is dehydrated by the dehydratase (DH) domain to form olefin **26**, which is then reduced again by the enoyl reductase (ER) domain to yield a fully reduced thiolester **27** (Scheme 1.1, steps VI-VIII). The KR and ER domains use the cofactor NADPH **35** (Figure 1.5) to reduce the β -keto group in **25** and **27** respectively (Scheme 1.1). The AT domain then transfers this newly formed saturated thiolester from the PP arm of the ACP domain back to the KS domain. The cycle repeats with the condensation of malonyl units until the chain reaches a critical length **28** (usually 16-18 carbons, step IX). Finally, the thiolesterase (TE) releases the fatty acid **33** (Scheme 1.1, steps X-XII).¹⁹



Scheme 1.1 Biosynthesis of polyketides and fatty acids.¹⁹

Polyketide biosynthesis proceeds through all the same catalytic steps, however the growing chain does not always need to be fully reduced and transferred back to the KS domain from the PP arm of the ACP domain at either the KR **25**, DH **26**, or ER **27** stages. In addition, the growing chain can be methylated by a C-methyltransferase (C-

MeT) domain, the methyl group come from *S*-adenosyl methionine (SAM) **36** (Figure 1.5).¹⁸ This occurs at the β -keto **24** stage, then either KR, DH, or ER are involved and yield the non-reduced **31** or reduced/partly-reduced polyketide **32** (Scheme 1.1, step XIII). Fungal PKS are also known to use alternative starter units including benzoate, *e.g.* strobilurin.^{20,21} Finally, once the polyketides have been assembled, a series of ‘tailoring’ enzymes can further modify the core structure by post-assembly modifications (reduction, oxidation, cyclisation, *etc.*).^{22,23,24}

The major catalytic domains of fungal PKS are closely related to those of mFAS. They include KS, DH, ER, KR and *C*-MeT domains. There is very little structural data for fungal PKS, but there are good crystal structures of mFAS.¹³ mFAS consists of a dimeric polypeptide with domains in the order (N to C) KS, AT, DH, ψ *C*-MeT, ψ KR, ER, KR, ACP and TE. The ψ *C*-MeT domain is a non-functional methyl transferase. The ψ KR domain is a structural (non-catalytic) domain of the KR. The mFAS protein forms an X-shaped dimer (Figure 1.6). The dimeric structure is divided into two subunits and connected by a narrow polypeptide linker in the center. The *N*-terminal KS domain is linked to the AT domain through an α/β fold linker domain. The KS, and AT domains were defined as the “condensing region”. The second subregion consists of KR, DH and ER domains, which are required for β -carbon modification and referred to as the “modifying region” (Figure 1.6). The modifying and condensing regions are connected by a covalent peptide linker. The crystal structure of dimeric mFAS suggests that the linker area around the central connection is quite flexible, like a hinge.

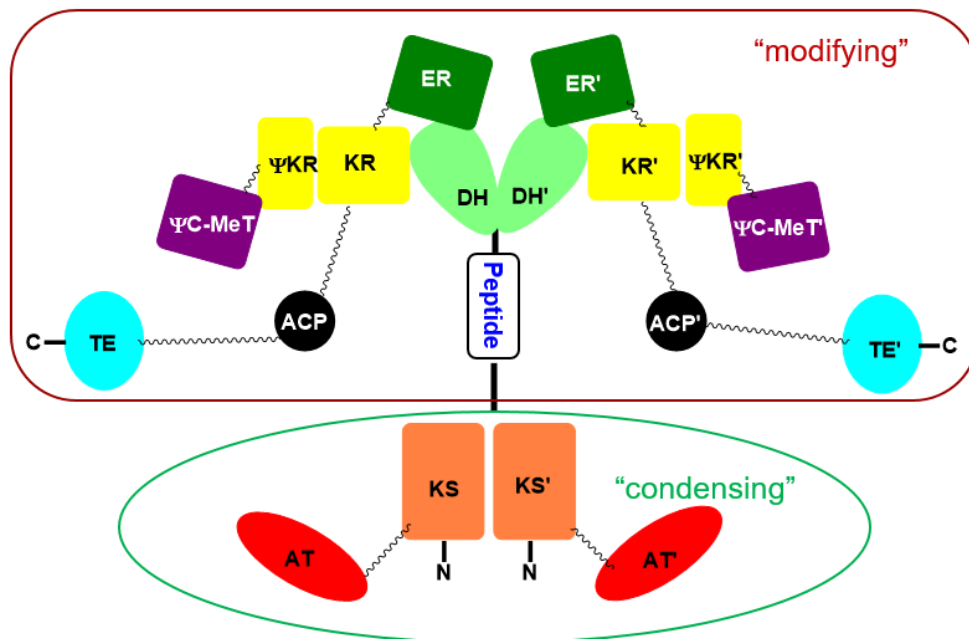


Figure 1.6 Schematic architecture of mFAS domain connectivity.¹³ Abbreviations: KS, ketosynthase; AT, acetyl transferase; DH, dehydratase; C-MeT, C-methyltransferase; ER, enoylreductase; KR, ketoreductase; ACP, acyl-carrier protein; TE, thiolesterase.

Type I PKS consist of very large multifunctional proteins with individual functional domains, they can be either modular or iterative. All fungal PKS belong to the iterative type I class (iPKS). Modular type I PKS systems are found in bacteria.^{10,25} In iterative type I PKS systems, the chain is reloaded to the single KS after each extension and β -modification cycle. Each β -processing cycle can be different. The variation in β -processing is referred to as programming.

Based on the degree of programming and extent of β - processing, fungal iterative PKS can be further grouped into three major subtypes: non-reducing (NR-PKS); partially reducing (PR-PKS); and highly reducing (HR-PKS).^{26,27,28}

To date, all HR-PKS consist of an N-terminal KS domain, followed by AT and DH domains. The DH is often followed by a functional C-methyltransferase (C-MeT) domain in many cases.^{10,29,30} Some HR-PKS have a functional ER, but in many HR-PKS, there is a broken ER domain, and these systems often have a *trans*-acting ER encoded by a separate gene. After the ER domain is the KR domain and the PKS is terminated by an ACP domain. Fungal HR-PKS thus have the same catalytic domains

arranged in the same order as mFAS, but with the difference that C-MeT is usually functional. T-toxin **38** and squalstatin **39** are examples of polyketides produced by HR-PKS (Figure 1.7 A).¹⁰

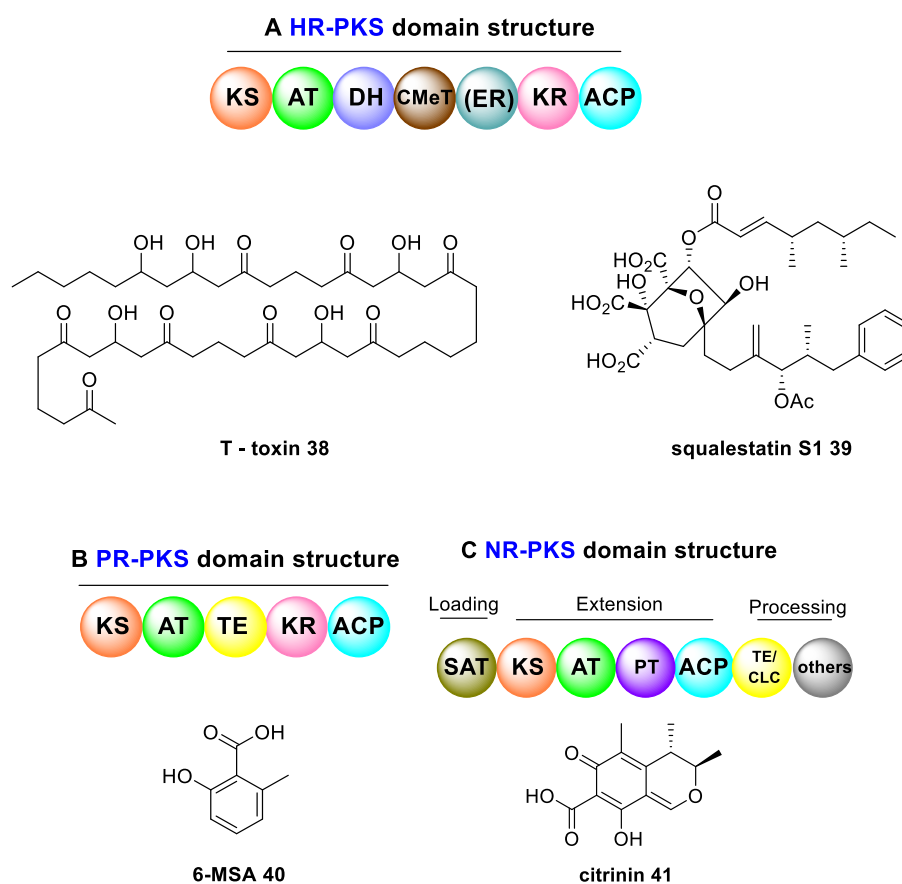


Figure 1.7 A, Domain structure of HR-PKS and related metabolites; **B**, Domain structure of PR-PKS and related metabolites; **C**, Domain structure of NR-PKS and related metabolites.¹⁰

The enzymology of PR-PKS is much less understood. The domain structure is similar to mFAS. They consist of an N-terminal KS domain, followed by AT, TE, KR and ACP domain. In some cases, there is a DH domain, but an ER domain has never been found. 6-MSA **40** is an example of a polyketide produced by a PR-PKS (Figure 1.7 B).¹⁰

The final class of fungal PKS are the NR-PKS. They usually begin with a starter unit ACP transacylase (SAT) domain, which is responsible for starter unit loading. KS and AT domains follow, and as usual are involved in the chain extension.¹⁰ A product template (PT) domain is unique in NR-PKS, and has a cyclisation function. The PT

domain is followed by a C-terminal ACP domain.^{31,32} Many additional domains have been reported at the C-terminus, such as the Claisen-cyclase-thiolesterase (CLC-TE), and C-methyltransferase (C-MeT) domains. A reductive release (R) domain can be found in some NR-PKS domains, playing a role to release the polyketide as an aldehyde or primary alcohol.^{10,31} An example of a polyketide produced by NR-PKS is citrinin **41** (Figure 1.7 C).¹⁰

1.1.4 Peptides

Peptides are another extremely diverse group of natural products produced by fungi.⁴ Both proteinogenic and non-proteinogenic amino acids can be the building blocks of peptides.³³ Their structural diversity is vast, with variations in the length of peptide, cyclisation pattern, and very many possible tailoring modifications. Peptides have already shown great potential.^{33,34} For example, the bioactive cyclosporin A **42**, the antifungal compounds threoninepeptide **43** and valinepeptide **44**, and the glucan synthase inhibitor phalloidin **45** (Figure 1.8).^{7,18,32,35,36}

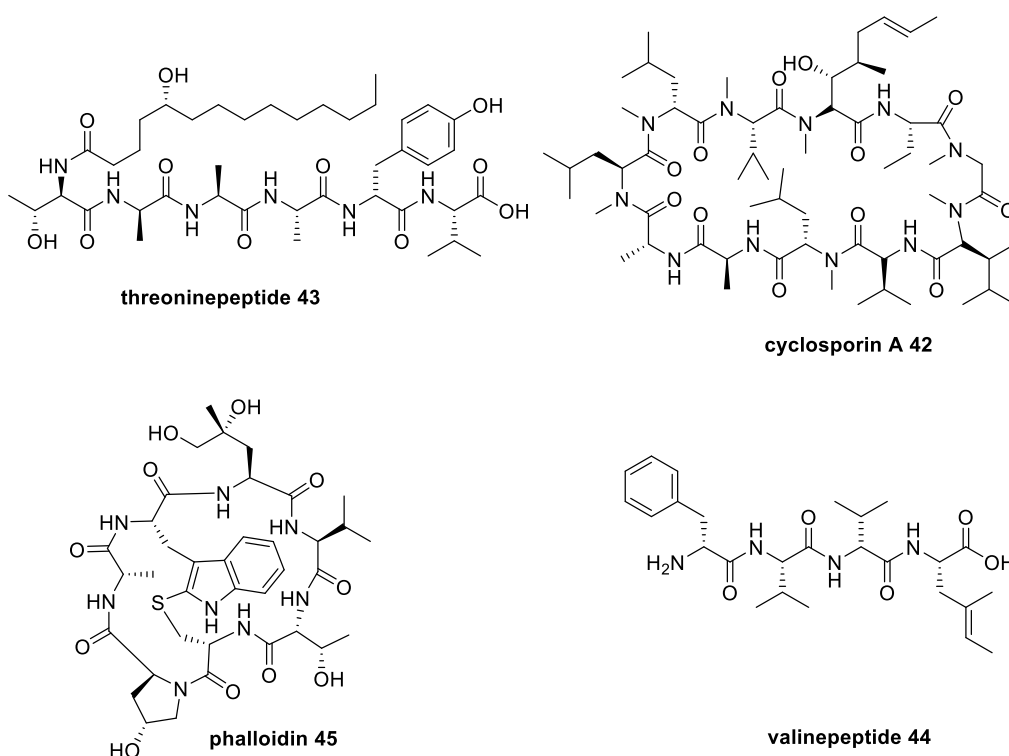
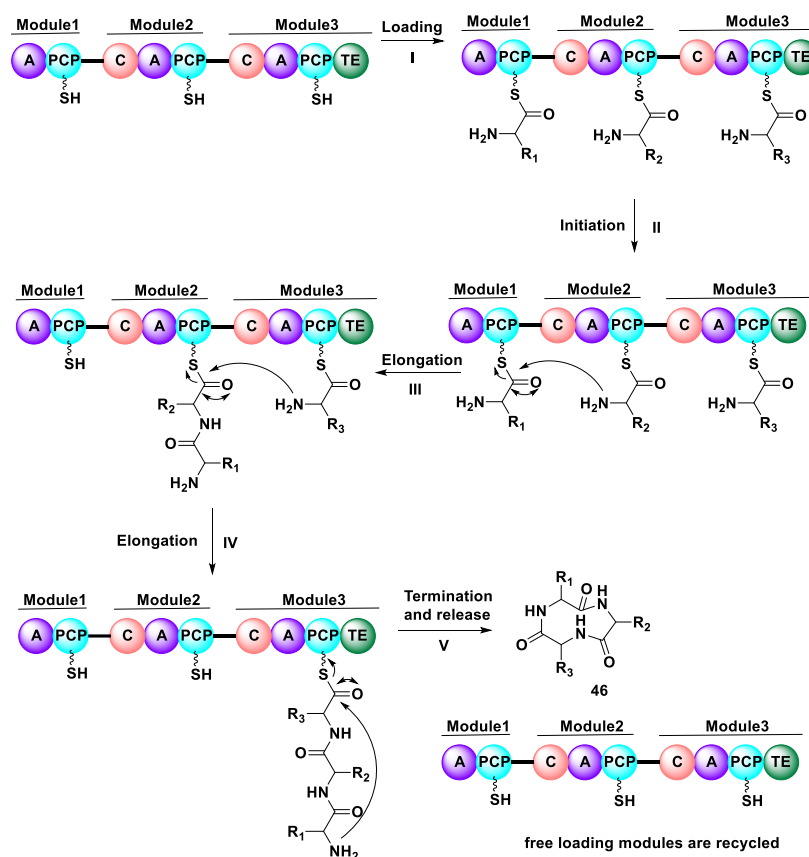


Figure 1.8 Examples of fungal ribosomal peptide natural products.

Peptides are made by two different systems. These are ribosomal and the non-ribosomal peptides. Nonribosomal peptides synthetases (NRPS) are responsible for the biosynthesis of nonribosomal peptides. NRPS consist of a large multidomain modular enzymes. These contain three core domains: adenylation (A); condensation (C); and peptidyl carrier protein (PCP) domains. These three domains, working together, constitute the repeating module responsible for activation and incorporation of amino acid into the growing peptide chain.³⁷

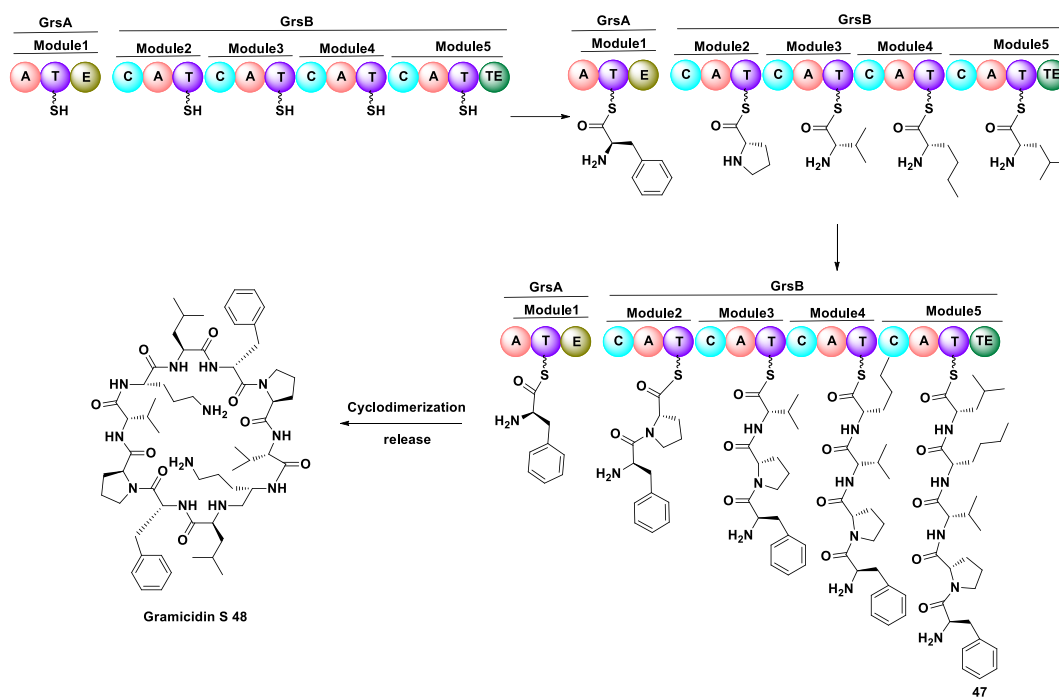
The modules of NRPS are made up of catalytic domains that catalyse single steps (Scheme 1.2). Each amino acid is precisely selected, activated and loaded by the adenylation (A) domain with the participation of ATP, then transferred to the terminal thiol of a phosphopanteteine prosthetic group of a peptidyl carrier protein (PCP), which is the transport unit through the loading step (Scheme 1.2, step I).

PCP are functionally and structurally closely related to ACP in FAS and PKS systems. In the initiation and elongation steps, the condensation (C) domain catalyses the formation of an amide bond between amino acids held by adjacent PCP domains (Scheme 1.2, step II-IV). Once the completed peptide is formed, it can be released either by a thiolesterase (TE) domain or by a modified C domain in the termination step to produce the compound **46** (Scheme 1.2, step V). The free loading module can be recycled.^{38,39}



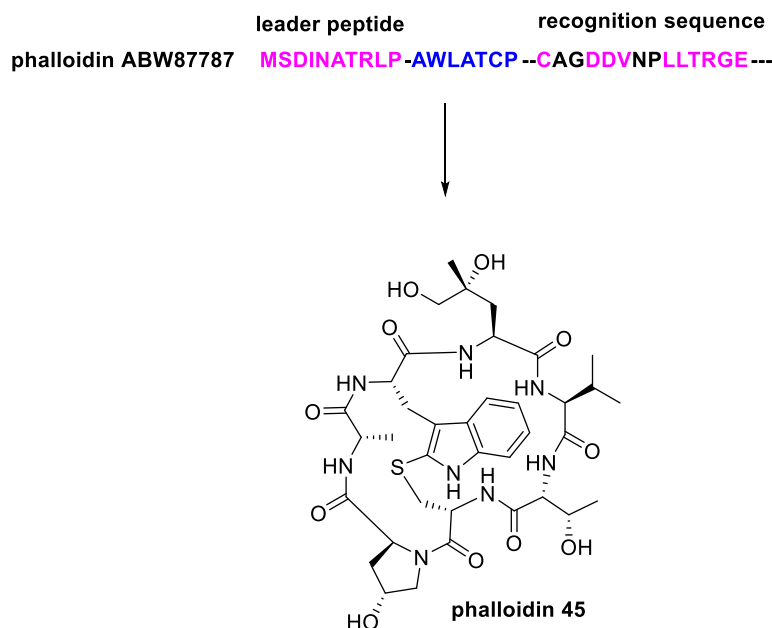
Scheme 1.2 A schematic overview of a general NRPS biosynthetic pathway.^{37,40}

Gramicidin S **48** is one of the most effective antibacterial peptides with regard to its ability to inhibit the growth and kill bacterial cells.⁴¹ **48** is biosynthesized by two NRPS proteins, GrsA and GrsB, that catalyse thiotemplated peptide bond formation and release by cyclodimerization to form the cyclic decapeptide (Scheme 1.3).⁴² Phenylalanine, proline, valine, leucine and asparagine are precisely selected by the A-domain of each module and then transferred to the cognate PCP domains. The condensation domain then catalyses the formation of a linear peptide **47** before final release of **48** by cyclisation.



Scheme 1.3 Gramicidin S **48** biosynthesis.⁴¹

The genome sequencing efforts lead to the finding of ribosomal peptides, they are ribosomally-synthesized and post-translationally-modified peptides (RiPPs).⁷ Phallotoxins are produced by several species of mushrooms in the genera *Amanita*, *Galerina* and *Conocybe*.⁴³ Phallotoxins such as phalloidin can bind to actin and have been used as an imaging tool to stain the cell skeleton. The precursor peptides contain a 10-residue leader peptide, a 7-residue core peptide and a C-terminal recognition sequence (Scheme 1.4). The leader and recognition sequences are highly conserved, but the core peptide is more variable.



Scheme 1.4 The chemical structure of Phalloidin **45**.⁴³

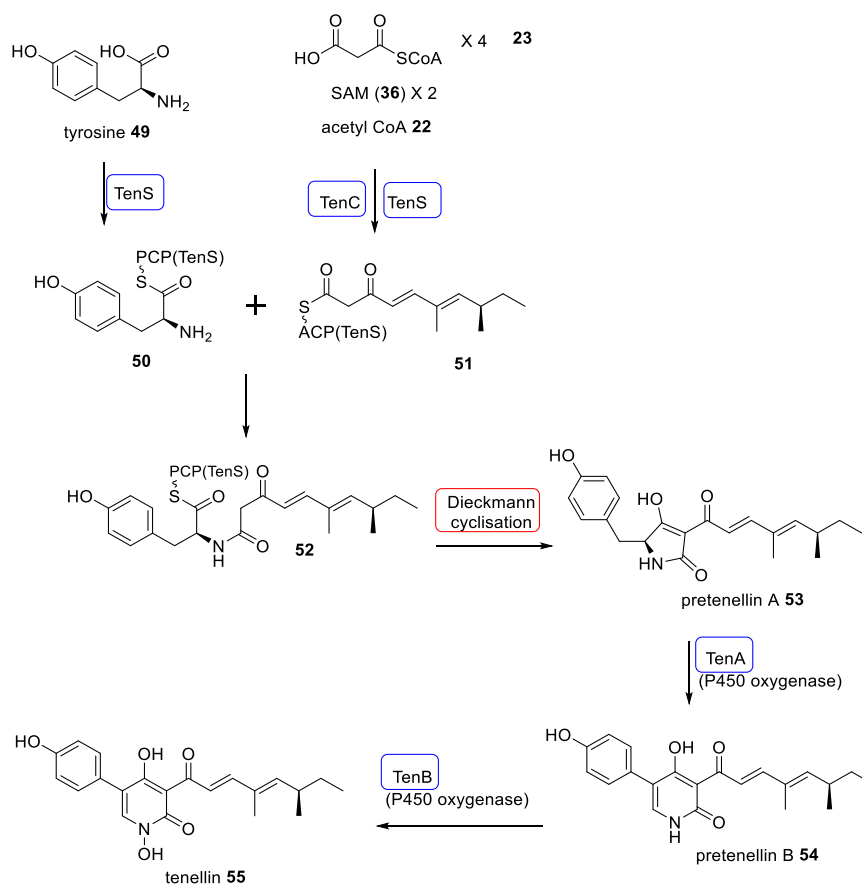
1.1.5 Polyketide Synthase – Nonribosomal Peptide Synthetase (PKS - NRPS) Hybrids

PKS–NRPS hybrids have been known in fungi for more than ten years.^{44,45} These hybrid enzymes are made up of a fungal iterative type I PKS fused to a single NRPS module that is sometimes truncated. Fungal type I PKS–NRPS use a set of catalytically active domains to build up a polyketide-amino acid (PK–AA) hybrid molecule, in an iterative way.⁴⁶ The biosynthetic pathway for PKS-NRPS hybrids cytochalasin E and K can be proposed, based on the deduced gene functions of the *ccs* gene cluster. The domain organization of the PKS-NRPS encoded by *ccsA*, which is similar to other reported PKS-NRPS genes, for example, including CheA in *Penicillium expansum* (35% identity to *ccsA*), TenS in *Beauveria bassiana* (33% identity to *ccsA*) and FusA in *Fusarium venenatum* (36% identity to *ccsA*).^{47,48}

Two different release mechanisms have been demonstrated from PKS-NRPS hybrids. These are, Dieckmann condensation and reductive release. Tenellin **55** is produced by the insect pathogen fungus *Beauveria bassiana* CBS 110,¹⁶ which belongs to fungal 2-pyridones, are also interesting from biosynthesis perspective. The tenellin biosynthetic gene cluster was found by the Cox group by systematic screening of a genome library with degenerate primers based on conserved regions in the C-MeT domain of highly

reducing PKS and fungal PKS-NRPS hybrids.⁴⁹ The positive clone revealed a gene cluster comprised of 4 putative genes: two cytochrome P450 oxygenases (TenA and TenB); a *trans* acting ER (TenC); and the iterative PKS-NRPS hybrid (TenS).

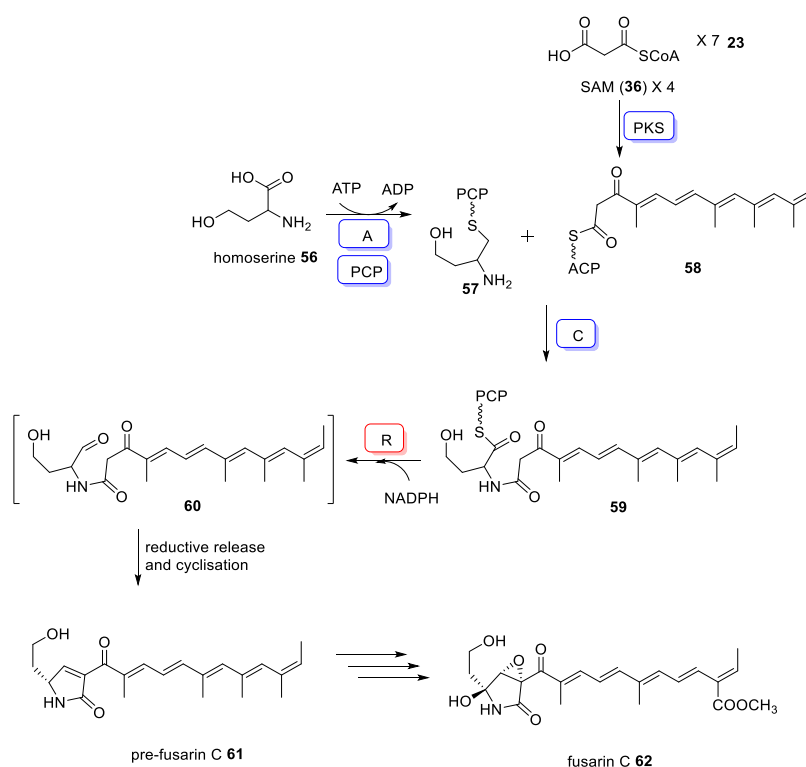
Heterologous expression of TenS in *A. oryzae* M-2-3 showed the PKS-NRPS to produce pretenellin A **53** when expressed together with TenC. However, prototenellin A-C, tetramic acids with incorrect polyketide side chain were produced when express TenS alone.⁵⁰ Formation of tetramic acids without involvement of any oxygenase suggests that the release domain functions as a Dieckmann cyclase in this case rather than as reductase. The biosynthetic pathway then requires ring expansion from tetramic acid precursor **52** to the 2-pyridone pretenellin B **54** is catalysed by TenA. The other cytochrome P450 oxygenase, TenB, then catalyses the *N*-hydroxylation as shown in a combination of heterologous expression, RNA silencing and cell free extract experiments, lead to the production of tenellin **55** (Scheme 1.5).⁵¹



Scheme 1.5 DKC release mechanisms of tenellin **55** biosynthesis.⁵²

Fusarins have been isolated from various species of *Fusaria*.⁵³ These compounds are a group of mycotoxin acyl-pyrrolidones.⁵⁴ The gene cluster involved in the biosynthesis of fusarin C **62** in *Fusarium venenatum* was confirmed by Simpson and co-workers. The *fusA* gene is responsible for the early stages biosynthesis of compound **62**.

Fusarin synthetase (FUSS), encoded by *fusA*, consists of a type I iterative PKS fused to an NRPS. A tetramethylated polyunsaturated heptaketide **58** is generated by the FUSS PKS and held by the ACP domain.⁴⁵ Homoserine **56** is adenylated and transferred to the PCP domain. The condensation domain then catalyses nucleophilic attack by the homoserine nitrogen atom on the ACP-bound polyketide, forming an intermediate amide **59** held by the NRPS of FUSS. The final biosynthetic step is the reduction of the PCP-bound thiolester catalysed by the reductive domain of NRPS. In the biosynthesis of fusarin, the product of the reduction is thought to be a free aldehyde **60**, which then undergoes a cyclisation reaction to form the pre-fusarin **61** in which the polyketide has been fully elaborated and fused to homoserine aldehyde to give the unmodified 1,5-dihydropyrrol-2-one ring **61**. Pre-fusarin then undergoes with several steps of modification reactions to produce the final product fusarin C **62** (Scheme 1.6).



Scheme 1.6 Reductive release mechanisms of fusarin C **62** biosynthesis.⁵⁵

1.2 Cytochalasans

Over 300 cytochalasans have been described in the literature.⁵⁶ Cytochalasans are a large class of structurally diverse fungal hybrid polyketide-non ribosomal peptide secondary metabolites, which possess a wide range of biological activities.

The major biological activity of cytochalasan is targeting the actin cytoskeleton. This affects cellular processes such as cell adhesion, motility, signalling and cytokinesis.⁵⁷ New bioactivities of cytochalasans have been reported, including nematicidal,⁵⁸ antifouling,⁵⁹ and anti-inflammatory properties.⁶⁰ Also including induction of apoptosis in leukemia cells,⁶¹ inhibition of angiogenesis,⁶² and activity against multi-drug resistant bacteria.⁴⁸

Typical cytochalasans contain a tricyclic core, formed from a macrocycle fused to an octahydro isoindole moiety, derived from a highly reduced polyketide backbone and an amino acid. Common cytochalasans are biosynthesized from the amino acids tryptophan⁶³ (*e.g.* chaetoglobosin A **63**) or phenylalanine (*e.g.* cytochalasin E **64**).⁶⁴ Moreover, cytochalasans can also incorporate other amino acids such as tyrosine (*e.g.* pyrivalasin H **65**, phenochalasin **68**),⁶⁵ leucine (*e.g.* periconiasin A **66**),⁶⁶ valine (*e.g.* trichalasin A **67**, Figure 1.9).^{64,67}

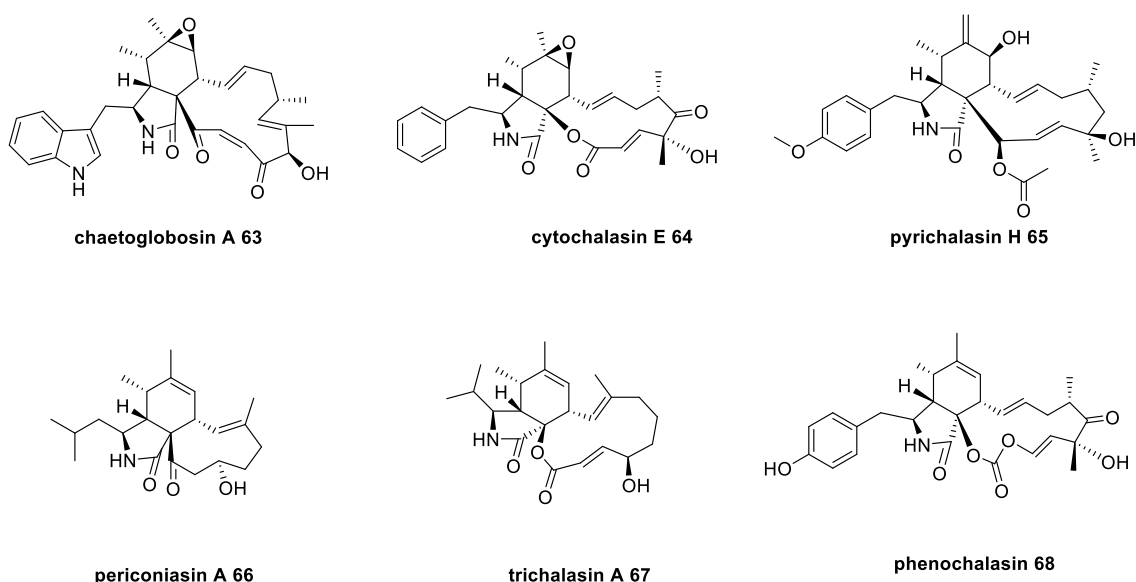
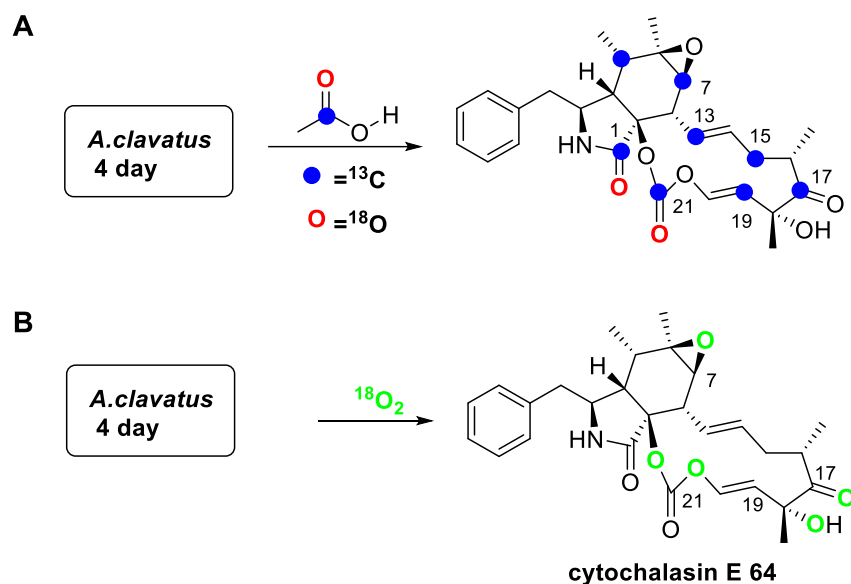


Figure 1.9 Structures of cytochalasans.⁶⁸

1.2.1 Isotopic Labelling Experiment of Cytochalasin E

Tang and co-workers revealed the origin of carbon atoms in cytochalasin E **64** by using isotopic labelling experiments.⁶⁹ Doubly labelled [¹³C and ¹⁸O₂] acetate was fed to *Aspergillus clavatus* grown in potato-extruse (PD) liquid stationary culture at 30 °C for 4 days. Labelled compound was isolated, purified by column chromatography and characterized by ¹H and ¹³C NMR. The result showed that the origin of carbon atoms of both C-1 and C-21 derived from acetate. Also, C-7, C-13, C-15, C-17 and C-19 were shown to originate from acetate through NMR spectra. Both C-1 and C-21 of **64** recovered from culture supplemented with double labelled acetate, indicating that these carbonyl oxygen atoms are derived from acetate during polyketide assembly (Scheme 1.7 A). To confirm the origin of oxygen at C-17, cytochalasin E **64** was isolated from *A. clavatus* grown in a closed system in which the oxygen consumed was replaced by ¹⁸O₂ for 4 days. Labelled **64** was isolated and characterized by ¹H and ¹³C NMR. The result confirmed that the carbonate oxygen atoms are derived from molecular oxygen (Scheme 1.7 B).⁶⁹



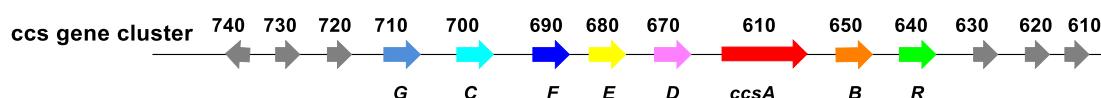
Scheme 1.7 Labelling study showed the origin of O and C in cytochalasin E **64**.^{21,69}

1.2.2 Biosynthesis of Cytochalasin E and Cytochalasin K

The biosynthetic pathway for cytochalasins E **64** and K **82** can be proposed, based on the deduced gene functions of the *ccs* gene cluster (Table 1.1).⁷⁰

Table 1.1 Genes within and flanking the *ccs* gene cluster.⁷⁰

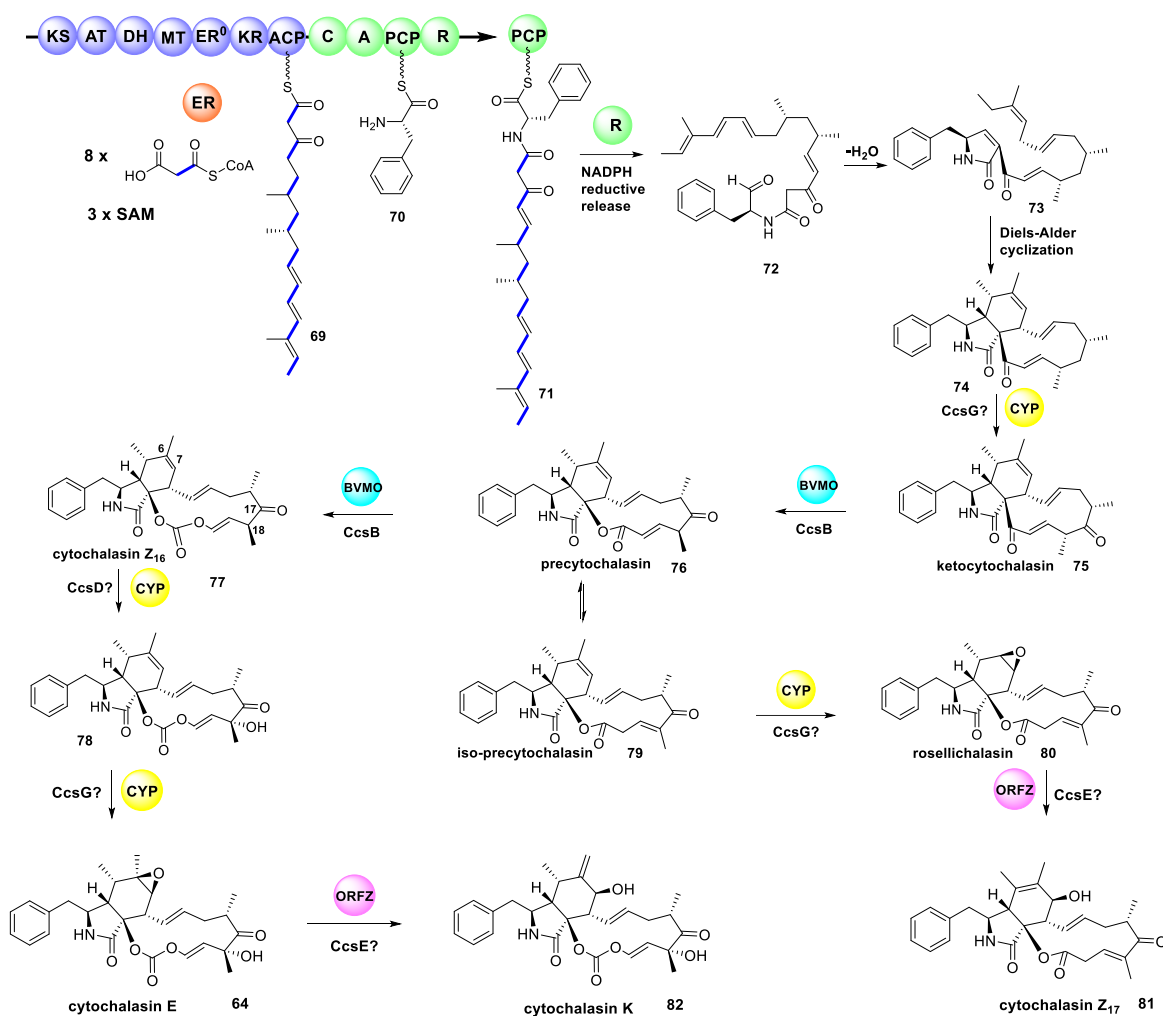
Gene Name	Gene Locus	Conserved Domain	Putative Function
<i>ccsR</i>	78640	Zn(II) cluster DNA-binding domain	Transcription factor
<i>ccsB</i>	78650	Flavin-containing monooxygenase	Monooxygenase
<i>ccsA</i>	78660	KS-AT-DH-MT-ER ⁰ -KR-ACP-C-A-T-R	PKS–NRPS hybrid
<i>ccsD</i>	78670	Cytochrome P450	P450 monooxygenase
<i>ccsE</i>	78680	$\alpha\beta$ -hydrolase	Esterase
<i>ccsF</i>	78690	n/a	Unknown
<i>ccsC</i>	78700	Enoyl reductase of the MDR family	Enoyl_reductase
<i>ccsG</i>	78710	Cytochrome P450	P450 monooxygenase



The ER domain of the PKS – NRPS hybrid encoded by *ccsA* is probably inactive, because it lacks the key NADPH **35** binding motif (LXHXG(A)XGGVG, Scheme 1.5). An octaketide backbone **69** is synthesized by the HR-PKS module of *ccsA*. Then, phenylalanine **70** is selectively activated by the A domain of the NRPS module and transferred to the phosphopantetheinyl arm of the PCP domain. This is followed by a condensation catalysed by the C domain, between the nucleophilic amino group of phenylalanine and the electrophilic carbonyl of the ACP-bound polyketide. This gives

the PCP tethered amide intermediate **71**. The R domain from the NRPS module is then proposed to catalyse reductive release to give an aminoaldehyde intermediate **72**, which then undergoes an intramolecular Knoevenagel condensation to give the 3,5-disubstituted 3-pyrrolin-2-one **73**.^{68,71} Subsequently, this is cyclized by intramolecular [4+2] Diels-Alder reaction between the terminal polyketide diene and the 3-pyrrolin-2-one dienophile to give the 11-membered carbocycle-fused perhydroisoindolone backbone **74** (Scheme 1.8). The Knoevenagel and Diels-Alder reactions have been long-proposed, but currently there is little evidence to show which proteins catalyse these steps.

After the formation of the 11-membered carbocycle-fused perhydroisoindolone intermediate **74**, several steps of oxidation occur to afford the final cytochalasins E **64** and K **82**.^{68,71} Two Baeyer–Villiger oxidations are catalysed by *ccsB* to afford intermediates **76** and **77**. Afterwards, two hydroxylations at C-17 and C-18, catalysed by CcsD and CcsG, produce compounds **78** and **64**. Cytochalasin E then catalyzed by CcsE to give cytochalasin K **82**. Epoxidation at C-6/C-7 to yield **80**, is also catalysed by CcsG. Finally, CcsE catalyse the formation of cytochalasin Z₁₇ **81** (Scheme 1.8).^{72,73}



Scheme 1.8 Proposed biosynthetic pathway of cytochalasin E **64** and K **82**.^{70,74}

1.3 Tailoring Modifications in Natural Product Biosynthesis

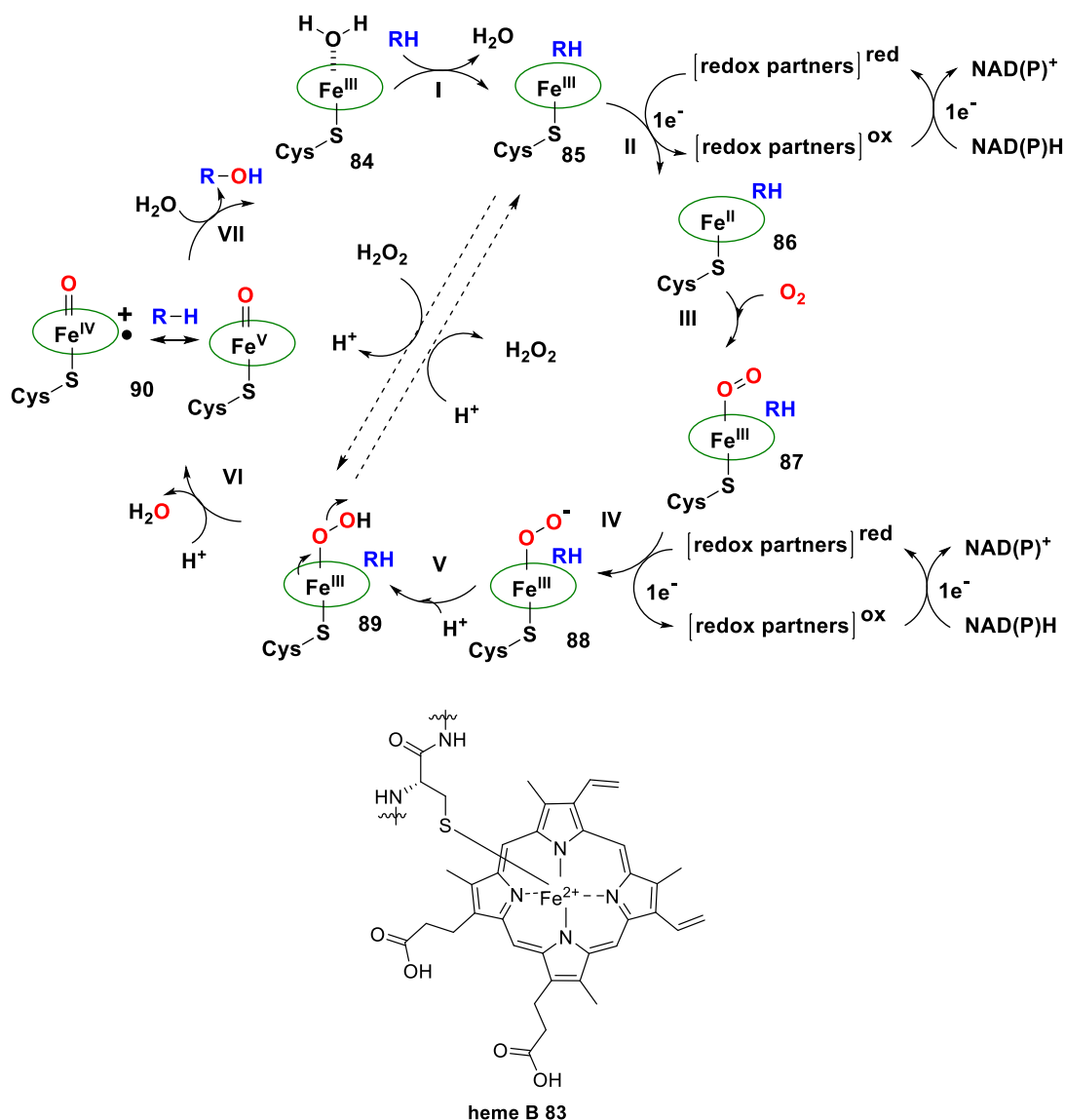
1.3.1 Cytochrome P450 Monooxygenase

Biological oxygenation is often provided by iron-based monooxygenases, in both heme and non-heme varieties. The mechanisms by which electrons are passed from iron to liganded O₂ and for the reaction with bound substrates, by both subclasses have been studied deeply.⁷⁵

Cytochrome P450 monooxygenase enzymes are the most common enzymes to oxygenate natural products. They are heme-proteins in which iron is bound to four nitrogen atoms of a porphyrin *e.g.* heme B **83** (Scheme 1.9) and to a protein cysteine

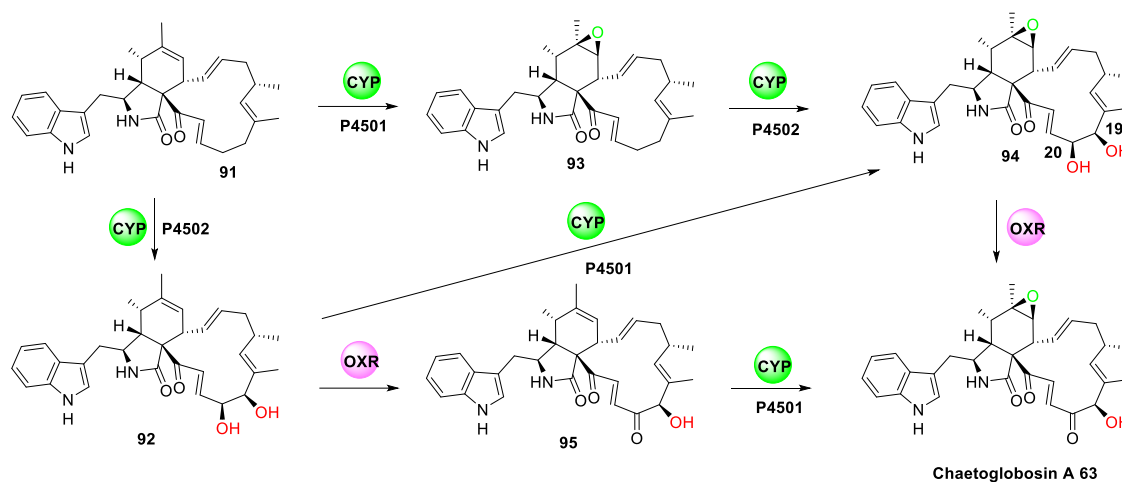
residue. The cytochrome P450 enzymes form a family of heme proteins that participate in the biosynthesis of secondary metabolites. These monooxygenases catalyse many reactions such as hydroxylations, epoxidations and Baeyer-Villiger oxidations. P450 enzymes use NADPH as a source of electrons *via* a redox partner that is required to transfer these electrons between NADPH and the iron centre.

The catalytic cycle is initiated by the substrate (RH) binding to the ferric P450 to yield **85**. The first electron is then transferred from NADPH to P450 to give compound **86** (Scheme 1.9, step I-II). The reduced iron then rapidly binds with oxygen to produce an Fe(II)-O₂ complex **87** (Scheme 1.9, step III). A second electron transfer results in the formation of an iron-peroxide species **88** which is protonated, followed by loss of water to form a high valent oxo-iron cation radical intermediate **90** (Scheme 1.9, step IV-VI). This intermediate is proposed to abstract a hydrogen atom from the substrate to form an Fe^{III}-hydroxide complex. Radical recombination then occurs to produce the oxygenated product (Scheme 1.9, step VII). This step is usually referred to as the rebound step. In the whole process, P450 take two electrons from NADPH and deliver one oxygen atom from O₂ to the organic substrate, and the other oxygen atom is released as water.⁷⁶



Scheme 1.9 Schematic representation of the consensus P450 catalytic cycle and peroxide shunt pathway.⁷⁶

An example is the late stage chaetoglobosin A **63** biosynthesis, after the Diels-Alder cyclization to form the intermediate **91**. This is oxidised by two P450 enzymes and one oxidoreductase in two separate steps to generate the final compound **63**. Deletion of P450-2 led to the production of **93**, revealing that this P450 catalyses iterative hydroxylations at C-19 and C-20 (Scheme 1.10).^{77,78}



Scheme 1.10 The late stage biosynthesis of Chaetoglobosin A **63**.^{77,78}

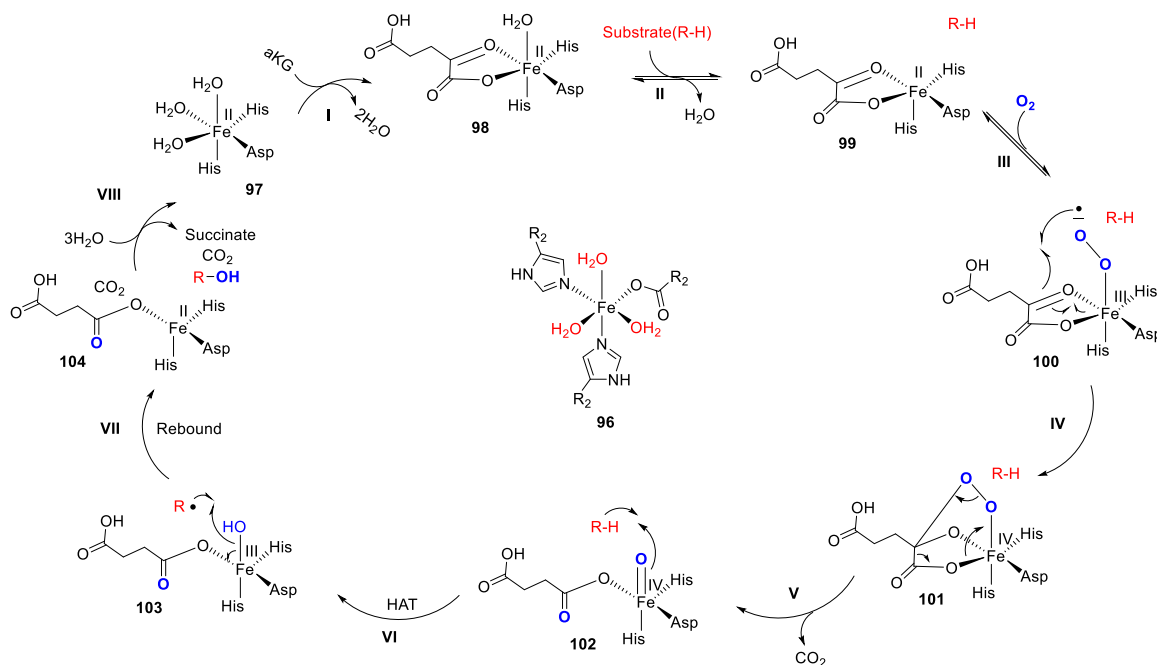
1.3.2 Alpha Keto Glutarate Dependent Dioxygenase

Fe(II)/ α -ketoglutarate (α -KG) dependent oxygenases are a large class of enzymes that catalyse a wide array of oxygenation reactions. α -KG Oxygenases are typically involved in processes, including protein side chain modification, repair of alkylated DNA and RNA, biosynthesis of antibiotics, biosynthesis of plant metabolites and other assorted functions.⁷⁹

Crystal structure and magnetic circular dichroism (MCD) data reveal that the resting form of the enzyme consists of a six coordinate octahedral Fe²⁺ center coordinated to three protein facial triad residues and three water molecules **96**.^{80,81} The first step is binding of α -KG, forming the (Fe + α -KG) **98** form of enzyme (Scheme 1.11, step I). Next, primary substrate binds, inducing water release to give **99** and the opening of a coordination site for O₂ binding (Scheme 1.11, step II). The next steps in the consensus mechanism are not fully understood, but are proposed to involve the same hydrogen atom abstraction (HAT) / rebound paradigm of the P450 oxygenases.

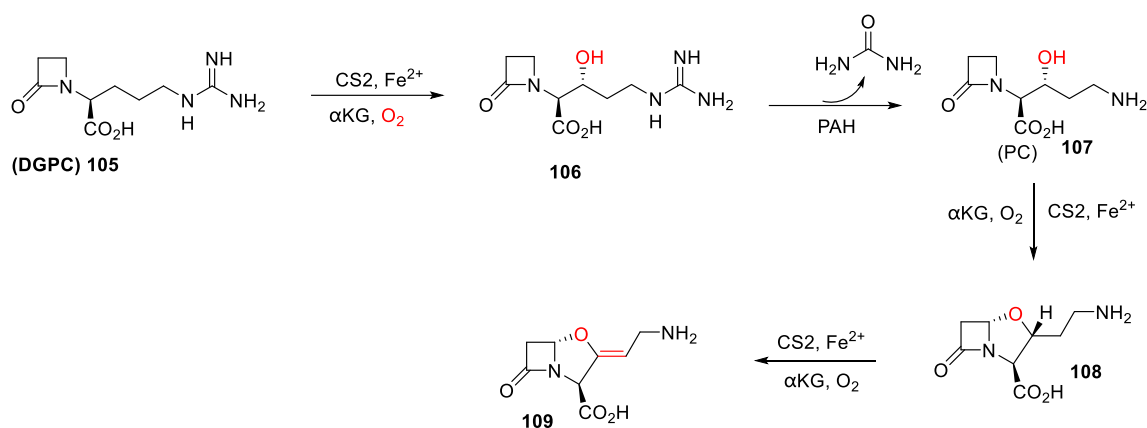
Due to the loss of the water ligand, a binding site for O₂ is created, and the substrate binding reactivity towards O₂ is significantly increased.⁸² It is thought that O₂ binds to form a Fe(III)-peroxyl adduct **100** (Scheme 1.11, step III), which attacks the keto group of α -KG to form an intermediate which can be formulated as a bicyclic peroxybridge Fe⁴⁺ species **101**. Decarboxylation and heterolytic cleavage of the O-O bond leads to the production of an Fe(IV)-oxo intermediate **102** (Scheme 1.11, step IV-V) which was identified as the species responsible for the HAT from the primary substrate.^{83,84}

Hydroxyl rebound to the substrate radical yields the hydroxylated product (Scheme 1.11, step VI-VII).



Scheme 1.11 Chemical mechanism for α -KG oxygenases.^{83,84}

Clavamate synthase-2 (CS2) is an interesting member of the α -KG dependent oxygenase class. It plays an important role in the construction of the strained bicyclic clavam ring structure during the biosynthesis of clavaminic acid **109**, an advanced precursor of the potent β -lactamase inhibitor clavulanic acid.⁸⁵ During the biosynthesis of clavulanic acid **109**, CS2 catalyzes the hydroxylation of deoxyguanidinoproclavaminic acid (DGPC) **105** to guanidinoproclavaminic acid, coupled to the oxidative decarboxylation of the cosubstrate α -KG to succinate and CO_2 . In the first step, one atom of O_2 is incorporated into the hydroxylated product **106** and the other one appears in succinate.^{86,87} Next, proclavamate amidino hydrolase (PAH) removes the guanyl group to yield proclavaminic acid (PC **107**).^{88,89} Then CS2 catalyses the oxidative ring closure of PC **107** to dihydroclavaminic acid **108**, which is subsequently desaturated to clavaminic acid **109**. Both steps are coupled to the oxidative decarboxylation of α -KG. In the ring-closure and desaturation reactions, the second atom of oxygen was not incorporated into the product, but reduced to water.⁹⁰

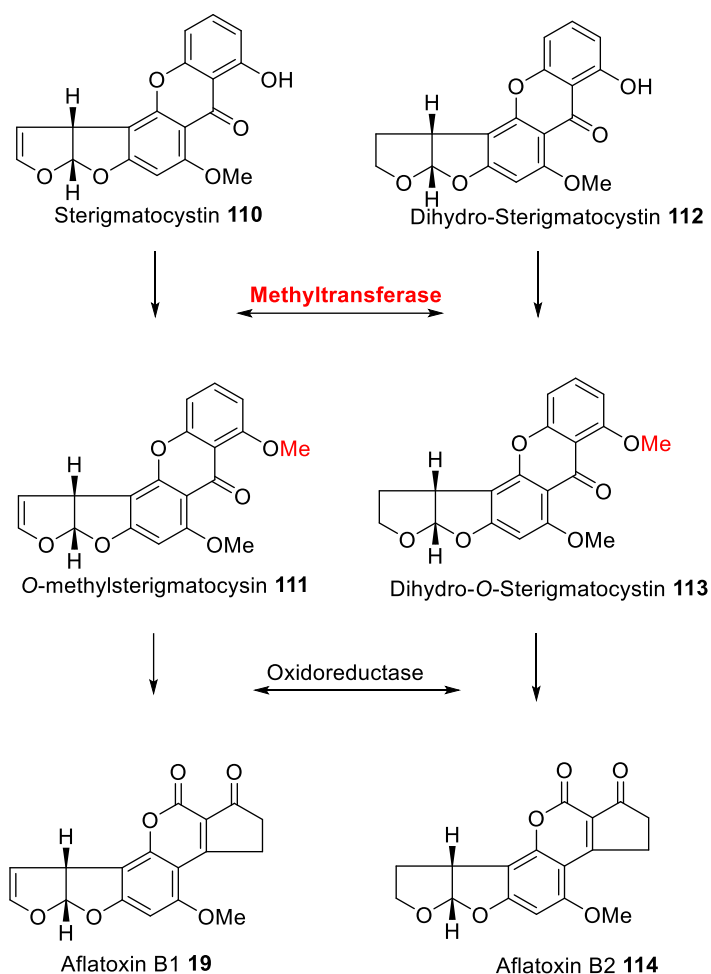


Scheme 1.12 Biosynthetic pathway of clavulanic acid **109**.⁸⁵

1.3.3 Methyltransferase

Methylation can be divided into *S*-, *O*-, *N*-, and *C*-types and are found in various organic compounds from small molecular phenols to macromolecular proteins. *O*-methyltransferases (*O*-MeT), a subgroup of methyltransferases, found in diverse organisms, including plants,⁹¹ animals⁹² and microbes^{93,94} can transfer the methyl group to a hydroxyl or carbonyl group from *S*-adenosyl methionine (SAM, **36**).⁹⁵ Many *O*-MeT in fungi, such as those involved in aflatoxin biosynthesis have been well characterised.

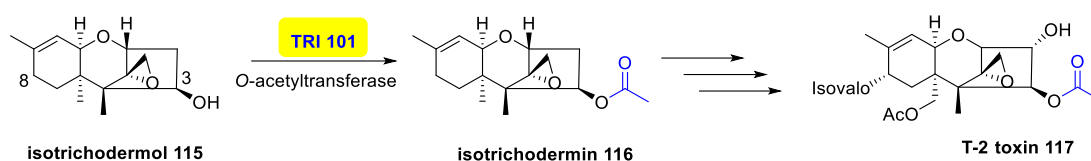
Aflatoxin B1 **19** and B2 **114** are secondary metabolites produced by the filamentous fungi *Aspergillus flavus* and *Aspergillus parasiticus*. These compounds are known to present a potential threat to human health. Many researchers have conducted extensive biomedical and genetic studies to better understand the biosynthesis and molecular regulation of aflatoxin biosynthesis.^{96,97,98} In the later biosynthetic steps of aflatoxin B1 and B2, the conversion of sterigmatocystin **110** to *O*-methyl sterigmatocystin **111** and the conversion of dihydro-sterigmatocystin **112** to dihydro-*O*-sterigmatocystin **113** were found to be catalysed by an *O*-methyltransferase (Scheme 1.13).⁹⁸



Scheme 1.13 Late stages of the aflatoxin B1 and B2 biosynthesis pathway.⁹⁹

1.3.4 Acetyltransferase

O-acetyltransferases play a significant role in the synthesis of many natural products (Scheme 1.14).¹⁰⁰ T-2 toxin **117** is a trichothecene with an ester-linked isovaleryl group at C-8, produced by *Fusarium sporotrichioides*. The core trichothecene ring structure is formed from trichodiene synthase and subsequent multiple oxygenations, yielding the toxic intermediate isotrichodermol **115**. TRI 101 is part of trichothecene gene cluster in *Fusarium sporotrichioides* encodes 3-*O*-acetyltransferase, which converts isotrichodemol **115** to isotrichodemol **116** through acetylation at C-3 hydroxyl position in *F. sporotrichioides*.¹⁰⁰



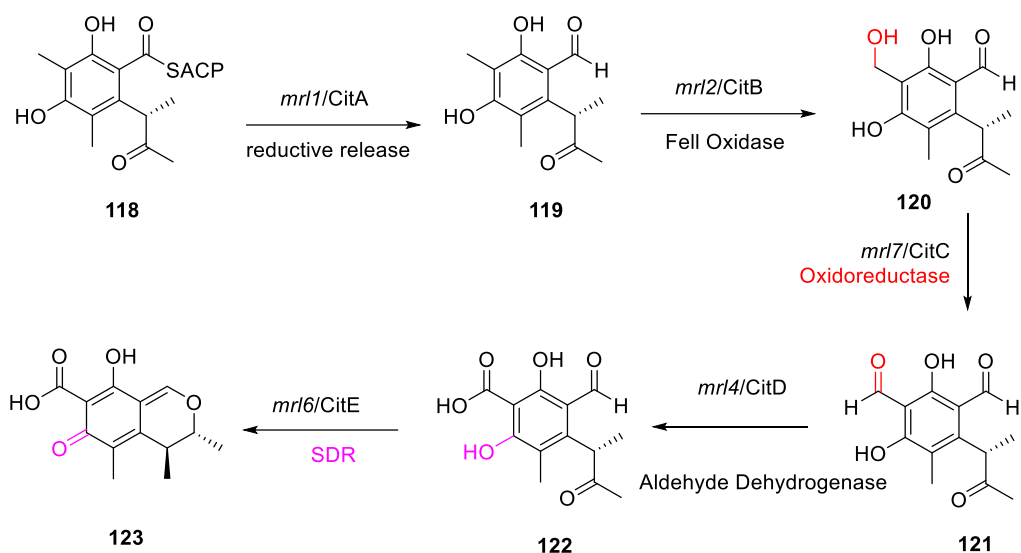
Scheme 1.14 Biosynthesis of isotrichodermin **117** catalyzed by TRI 101 enzyme.¹⁰⁰

1.3.5 Short-Chain Dehydrogenase/Reductase

Short-chain dehydrogenases/reductases (SDR) are defined by few but distinct sequence motifs and form a well-established enzyme family of oxidoreductases. Currently, around 3000 structures of the SDR family are annotated in sequence databases, and the corresponding genomes represent all forms of life.¹⁰¹

Citrinin **123** was discovered by Harold Raistrick and coworkers in 1930s and it was first isolated from *Penicillium citrinum*.¹⁰² The citrinin biosynthesis gene cluster *Penicillium* was systematically analysed. Several genes involved in the biosynthesis include: *citS*, encoding an nr-PKS; *mrl1*, encoding a serine hydrolase of no known function; *mrl2*, encoding a non-heme Fe(II) dependent oxygenase; *mrl4*, encoding an NAD(P)⁺ dependent aldehyde dehydrogenase; *mrl6*, encoding a short-chain dehydrogenase; and there is another NAD(P)⁺ oxidoreductase encoded by *mrl7*.

The ACP-bound thiolester **118** was catalysed by CitA to form **119**, then **119** undergoes an oxidation reaction to give **120**, compound **120** was catalysed by the oxidoreductase CitC to form **121**, the CitD catalyse the aldehyde **121** into acid product **122**, citrinin **123** will be released after catalysed by the short-chain dehydrogenase CitE (Scheme 1.15).¹⁰²



Scheme 1.15 Deduced biosynthetic pathway to citrinin **123**.¹⁰²

1.4 Pyrichalasin H

1.4.1 Introduction

Pyrichalasin H **65** is a member of the cytochalasan family. It is the first cytochalasan known to contain the methoxyphenyl group (Figure 1.10, Section 1.4.2). It is made up of three major parts: a methylated tyrosine, an isoindolone core and a macrocycle. **65** is first isolated as a phytotoxic metabolite from *Pyricularia grisea* (IFO 7287) in 1987, also called *Magnaporthe grisea*, which is a pathogenic fungus which causes blast disease in crabgrass (*Digitaria sanguinalis*).^{103,104} Isolations (thirty one from crabgrass, one from pangolagrass and six from *D. horizontalis*) show that pyrichalasin H is pathogenic to all *Digitaria* species (crabgrass, pangolagrass, *Digitaria horizontalis*, *Digitaria ciliaris* and *Digitaria ischemum*).¹⁰⁵ **65** shows various biological properties,¹⁰⁶ and has some biological activity against rice seedlings,¹⁰⁷ strong effect on cell morphology and actin distribution in C3H-2K cells, and lymphocyte capping.

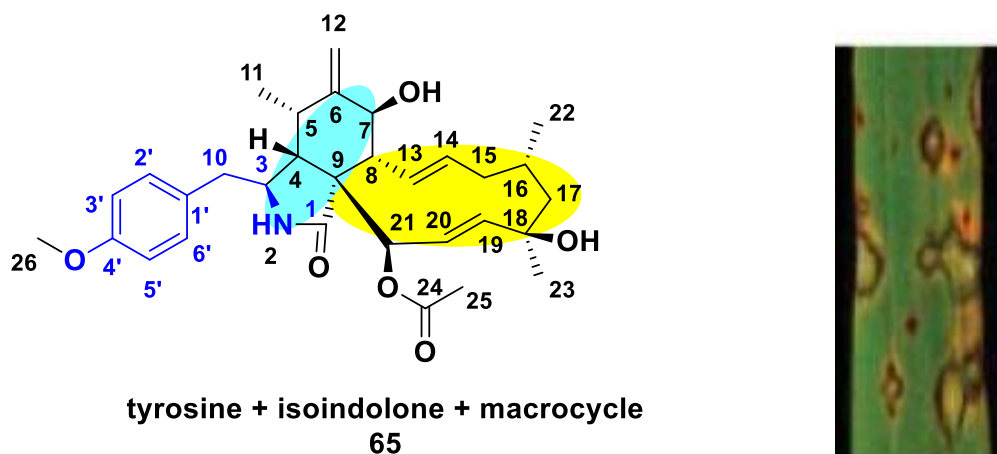


Figure 1.10 Structure of Pyrichalasin H **65** and rice blast disease.¹⁰⁷

1.4.2 Bioinformatic Analysis of the *Pyrichalasin H* Gene Cluster

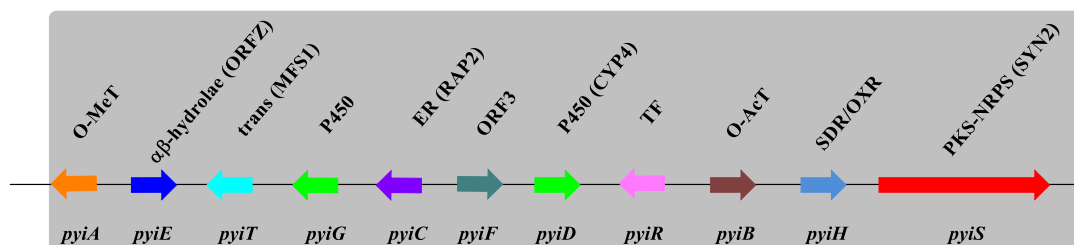
Pyrichalasin H **65** producing strain *M. grisea* NI980 was provided by the Lebrun group. Genomic DNA from *M. grisea* was prepared by Dr Elizabeth J. Skellam and the whole genome was sequenced in collaboration with CeBiTec in Bielefeld and the raw data was assembled to give a high quality draft genome.¹⁰⁸ The whole genome sequence was then submitted to the fungiSMASH database for preliminary identification of secondary metabolite biosynthetic gene clusters (BGC).

Genome annotation of *M. grisea* NI980 was done by Dr Elizabeth Skellam. The sequencing of *M. grisea* NI980 identified 66 BGC including 8 PKS-NRPS clusters. Three cytochalasan-like gene clusters were identified: a putative Avirulence Conferring Enzyme1 (ACE1) gene cluster; and a putative *SYN2* gene cluster (Figure 1.11 A). A putative pyrichalasin H gene cluster located on *M. grisea* Scaffold Mg-Sc00012 was also identified. The putative pyrichalasin H gene cluster was further analysed using Softberry, FGENESH and NCBI Protein Blast (Table 1.2, GenBank accession number MK801691).¹⁰⁹ Dr Elizabeth Skellam designated this putative BGC as the *pyi* gene cluster and assigned trivial names to the genes in analogy to the names of genes from the cytochalasin E **64** cluster.⁷⁰

The *pyi* BGC encodes a PKS-NRPS (*pyiS*), a *trans*-ER (*pyiC*), a putative Diels-Alderase (*pyiF*), and an $\alpha\beta$ -hydrolase (*pyiE*). These are the four core genes which are present in all known cytochalasan BGC. Moreover, a transcriptional regulator (*pyiR*), an oxidoreductase (*pyiH*), and a transporter (*pyiT*) were also found in the BGC. The

presence of an *O*-methyltransferase (*pyiA*) and an *O*-acetyltransferase (*pyiB*) is also good evidence that the identified cluster is involved in the biosynthesis of pyrlichalasin H **65**, corresponding with the *O*-methyl and *O*-acetyl functional groups of **65**.

A *M. grisea* NI980



B *P. oryzae* Guy 11

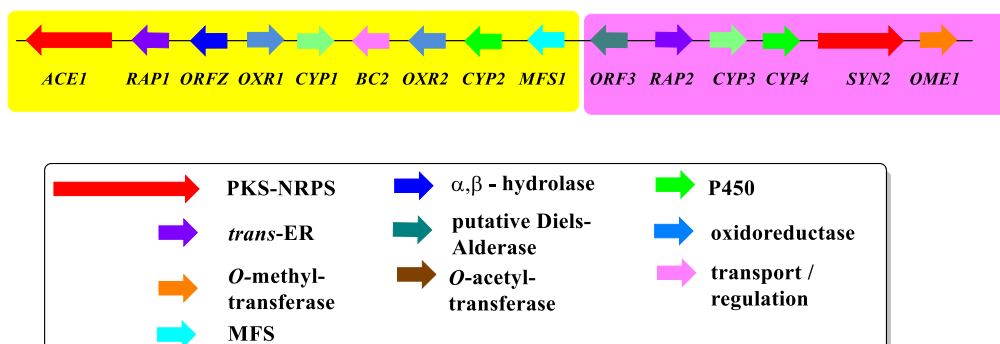


Figure 1.11 Cytochalasan BGC identified in *Magnaporthe* sp. **A**, *M. grisea* NI980; **B**, *P. oryzae* Guy 11. The ACE1 gene cluster from *P. oryzae* are highlighted in yellow, and the SYN2 cluster are highlighted in pink.¹⁰⁹

Table 1.2 Gene annotation of *pyi* cluster located on Scaffold00012.¹⁰⁹

Gene	Trivial name	Putative function	Homolog	Identity (%)	Query coverage
<i>M.grisea_g1694.t1</i>	<i>PyiA</i>	SAM-dependent O-methyl transferase	MGG_0837 7	76%	99%
<i>M.grisea_g1695.t1</i>	<i>PyiE</i>	$\alpha\beta$ -hydrolase	ACLA_078 680	67%	98%
<i>M.grisea_g1696.t1</i>	<i>PyiT</i>	Major Facilitator Superfamily Transporter	ANO14919 _111240	67%	90%
<i>M.grisea_g1697.t1-1</i>	<i>PyiG</i>	Cytochrome P450	MGG_0837 9	48%	88%
			ACLA_078 710	48%	94%
<i>M.grisea_g1697.t1-2</i>	<i>PyiC</i>	Enoyl reductase	H634G_092 56	76%	95%
			MGG_0838 0	64%	95%
<i>M.grisea_g1698.t1</i>	<i>PyiF</i>	pDA	MAJ_10105	75%	100%
			ACLA_078 690	70%	86%
<i>M.grisea_g1699.t1</i>	<i>PyiD</i>	Cytochrome P450	MGU_0882 3	69%	98%
			ACLA_078 670	55%	91%
<i>M.grisea_g1700.t1</i>	<i>PyiR</i>	Zn(2)C6 transcriptional regulator	SAMD0002 3353_55007 20	29%	50%
<i>M.grisea_g1701.t1</i>	<i>PyiB</i>	O-acetyltransferase	SPI_05896	49%	98%
<i>M.grisea_g1702.t1</i>	<i>PyiH</i>	Oxidoreductase	MBR_0816 3	68%	92%
			MGU_0882 4	69%	99%
<i>M.grisea_g1703.t1</i>	<i>PyiS</i>	PKS-NRPS	ACLA_078 660	56%	99%

1.4.3 Bioinformatic Analysis of the ACE1 Gene Cluster

Pyricularia oryzae isolates that carry the gene encoding Avirulence Conferring Enzyme1 (ACE1) are specifically recognized by rice (*Oryza sativa*) cultivars carrying

the resistance gene Pi33.¹¹⁰ The avirulence gene *ACE1* was identified by map-based cloning at one end of *P. oryzae* cosmid clone D31C12.¹¹¹ The genomic sequence of the *ACE1* locus was obtained from *pyricularia oryzae* Guy 11.

Lebrun and co-workers analysed and characterized the *ACE1* BGC from *P. oryzae* Guy 11. The *ACE1* BGC contains 15 genes and consist of two parts (Figure 1.11 B, Table 1.3); the *ACE1* gene cluster (Figure 1.11 B, highlighted in yellow); and the *SYN2* gene cluster (Figure 1.11 B, highlighted in pink). *OME1* encodes a putative SAM-dependent *O*-methyltransferase, *SYN2* encodes a hybrid PKS-NRPS highly similar to *ACE1*. *RAP1* and *RAP2* were identified to encode trans-acting enoyl reductases, *ORF3* (*pDA*) and *ORFZ* ($\alpha\beta$ -hydrolase) were identified between them. *OXR1* (short-chain alcohol dehydrogenase) and *OXR2* (FAD-dependent oxidase), were also identified between *ACE1* and *SYN2*. The gene *MFS1* identified between *CYP2* and *RAP2* encodes a putative transporter. Finally, the gene *BC2* located between *CYP1* and *OXR2* encodes a putative transcriptional regulator.¹¹¹

Table 1.3 predicted function of the ACE1 gene clusters in *P. oryzae*.¹¹²

Gene	Name	Conserved domain	Putative function
MGG_12447.5	ACE1	KS/AT/MT/KR/ACP/C/A/PP	PKS-NRPS
MGG_08391.5	RAP1	Zinc-containing dehydrogenase	Enoyl reductase
MGG_08390.5	ORFZ	Hydrolase	Hydrolase
MGG_08389.5	OXR1	Short-chain dehydrogenase/reductase	Dehydrogenase
MGG_08387.5	CYP1	Cytochrome P450	Cytochrome P450 monooxygenase
MGG_08386.5	BC2	Zn ₂ Cys ₆ DNA-binding domain	Zn(II) ₂ Cys ₆
MGG_08385.5(split)	OXR2	FAD linked oxidase, N-terminal	Transcription factor FAD oxidase
MGG_08385.5(split)	CYP2	Cytochrome P450	Cytochrome P450 monooxygenase
MGG_08384.5	MFS1	Major facilitator superfamily	MFS transporter
MGG_08381.5	ORF3	No hits	Unknown
MGG_08380.5	RAP2	Zinc-containing dehydrogenase	Enoyl reductase
MGG_08379.5	CYP3	Cytochrome P450	Cytochrome P450 monooxygenase
MGG_08378.5	CYP4	Cytochrome P450	Cytochrome P450 monooxygenase
MGG_12451.5	SYN2	KS/AT/MT/KR/PP/ACP	PKS
MGG_08377.5	OME1	<i>S</i> -adenosyl-L-methionine-dependent <i>O</i> -methyltransferase	SAM-dependent <i>O</i> -methyltransferase

Artemis comparison between the *P. oryzae* Guy 11 *ACE1* cluster and the *M. grisea* NI980 *pyi* cluster revealed that 7 genes from the pyrichalasin H **65** cluster are homologs of the genes from the *ACE1* cluster: *OME1*, *SYN2*, *CYP4*, *RAP2*, *ORF3*, *MFS1*, *ORFZ* and *ACE1* (Figure 1.12). The core cluster of *ACE1* (homologs of *ACE1*, *RAP1* and *ORF3*) is present in the putative pyrichalasin H **65** gene cluster. The $\alpha\beta$ -hydrolase *ORFZ*, is similar for pyrichalasin H and the *ACE1* metabolites. The function of *ORF3* and *ORFZ* are particularly interesting as they could play a key role in the cyclization

reactions of cytochalasans. However, previous KO experiments of the *ACE1* gene cluster failed, probably due to the chromatin structure.¹¹¹ Heterologous expression of *ACE1* and *RAP1* in *A. oryzae* lead to the isolation of the shunt product **124** (Scheme 1.16). This is derived from tyrosine and a C₁₈ polyketide. It is thought that the *A. oryzae* host reduces the tyrosine-derived aldehyde to a primary alcohol. However **124** is clearly closely related to proposed cytochalasin intermediates (*e.g.* see cheme 1.8). In particular **124** resembles **125** which is a key proposed intermediate during pyrichalasin H **65** biosynthesis (Scheme 1.16). The structure of the *ACE1* metabolites itself is unknown because the BGC is expressed only for a brief time in single cells (appressoria) during penetration of the rice leaf epidermis.

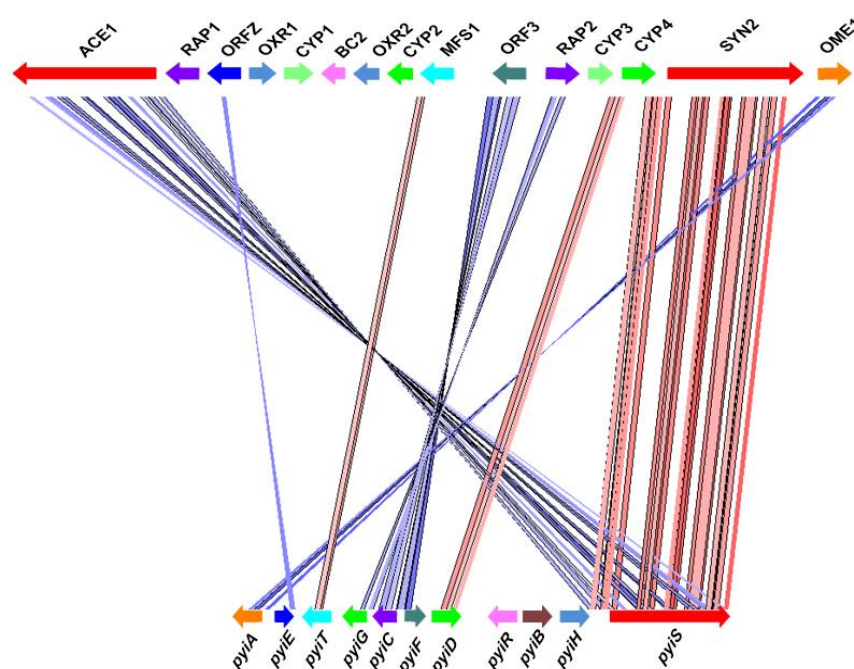
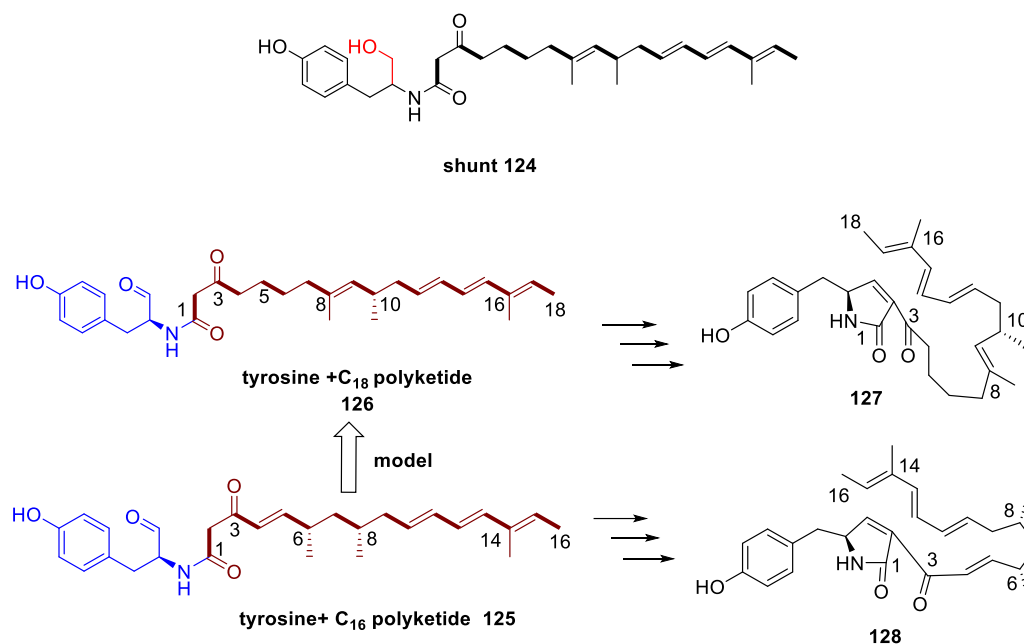


Figure 1.12 Artemis comparison of cytochalasan BGC identified in *Magnaporthe* sp. *M. grisea* NI980 (BGC bottom) and *M. oryzae* Guy 11 (top).



Scheme 1.16 Proposed key precursors from **65** and ACE1 biosynthesis.¹¹³

This project focuses on investigating the tailoring enzymes involved in the late stage biosynthesis of pyrichalasin H **65**. For example, the oxidoreductase encoding gene *pyiH*, the *pyiA* gene encoding an *O*-methyltransferase, the *pyiB* gene encoding an *O*-acetyltransferase and two P450 genes, *pyiD* and *pyiG*. There are also four cytochrome P450 monooxygenase encoding genes, *CYP1*, *CYP2*, *CYP3* and *CYP4* contained in the *ACE1* gene cluster, all predicted to encode monooxygenases with unknown selectivity. Heterologous expression of these cryptic P450 monooxygenase gene will be carried out to elucidate their functions.

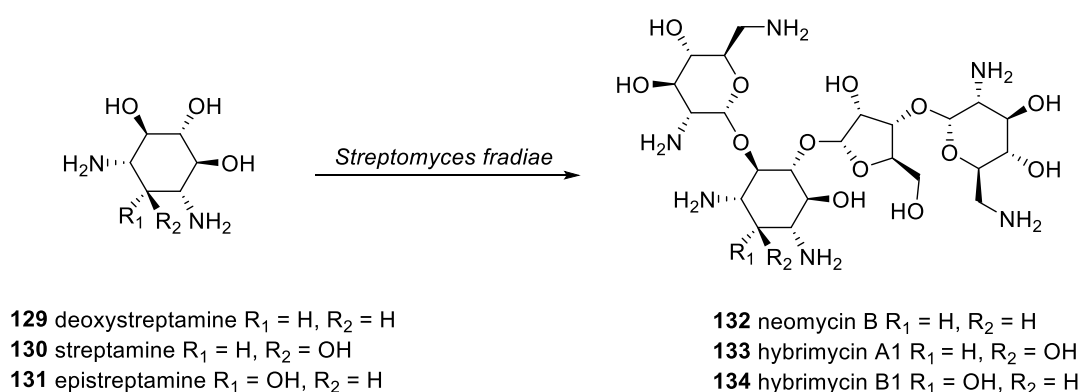
1.5 Diversifying Natural Products through Mutasynthesis and Semisynthesis

1.5.1 Application of Mutasynthesis in Natural Products

Natural products are an important source of lead compounds for drug development. To diversify natural products a number of approaches have been used. Mutasynthesis is built upon precursor-directed biosynthesis but utilises mutant micro-organisms deficient in a key aspect of the biosynthetic pathway.¹¹⁴ A typical strategy used for this approach

would be to supplement a KO strain with a particular precursor, leading to the production of a new natural product.¹¹⁴

One typical example of mutasynthesis was in the production of new analogues of the aminoglycoside-aminocyclitol antibiotic neomycin **132**. A mutant of the producing strain, *Streptomyces fradiae*, was selected. When the mutant strain was supplemented with the aminocyclitol precursor deoxystreptamine **129**, neomycin **132** was produced. When this mutant strain was supplemented with the aminocyclitols streptamine **130** and epistreptamine **131** these unnatural precursors were also utilised by the biosynthetic machinery to produce the novel neomycin analogues, hybrimycin A1 **133** and hybrimycin B2 **134** respectively.¹¹⁵ The successful production of active neomycin analogues by mutasynthesis, lead to the application of this method to generate a whole range of aminoglycoside-aminocyclitol antibiotics (Scheme 1.17).¹¹⁴

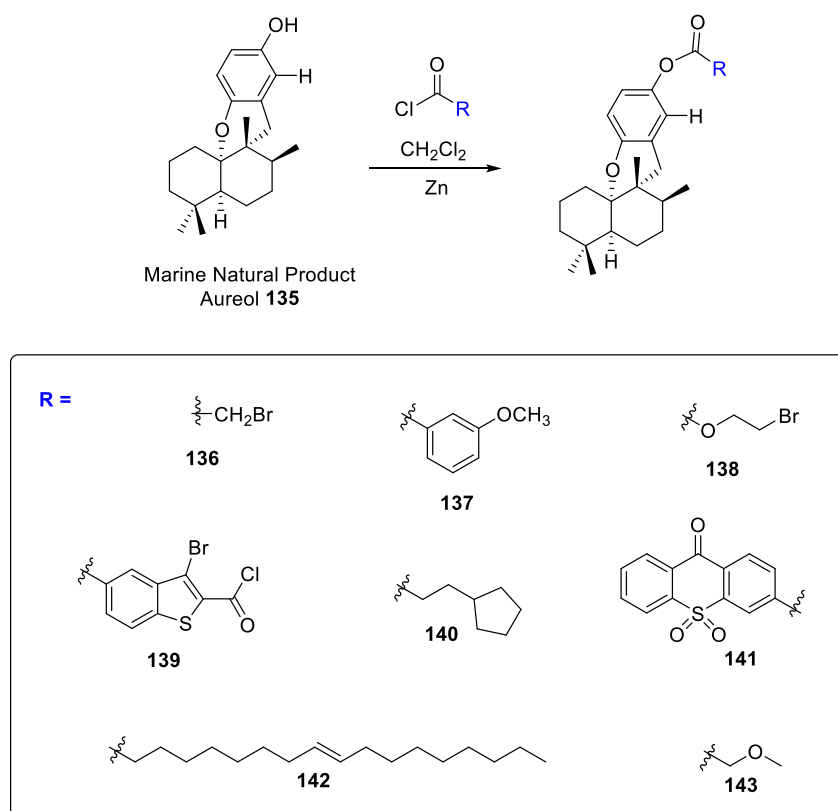


Scheme 1.17 Mutasynthesis of neomycin analogues.¹¹⁴

1.5.2 Application of Semisynthesis in Natural Products

Secondary metabolites generated by microbes have proven to be a valuable source of providing lead compounds for drug and agrochemical discovery. Over the past few decades, the investigation has revealed a portion of biologically active natural products that microorganism can provide. The unique small molecule structures offer an unprecedented potential for the creative application of semisynthetic transformations to the generation of countless analogues for the evaluation in lead discovery and development.¹¹⁶

One famous example of generating a semisynthetic library starting with a marine natural product utilizes the readily available natural product aureole **135** to create a library of semisynthetic products for biological evaluation. The target of this study was the rational and high-throughput modification of a marine natural product into a library of derivatives by utilizing hydroxyl functionality to generate more desirable molecules. Aureol **135** was used to generate a series of new semisynthetics beginning with commercially available acid chlorides with derivatives **136** - **143**. All the derivatives were prepared with a mixture of 1 M eq. of activated zinc dust and an excess of acid-chloride, stirred for 15 min followed by addition of aureol (Scheme 1.18).¹¹⁷



Scheme 1.18 Representative acid chlorides utilized to generate new semisynthetic products.¹¹⁷

1.6 Project Aims

Genome sequencing of *M. grise* NI980 showed there are 8 PKS-NRPS cluster. However, only the *pyi* BGC contains gene encoding all four core enzymes necessary for cytochalasan biosynthesis a PKS-NRPS; a *trans*-ER; a putative Diels-Alderase (pDA);

and an $\alpha\beta$ -hydrolase (section 1.4.2). Therefore, the *pyi* BGC was assumed to be responsible for **65** biosynthesis. Some tailoring genes encoding *O*-MeT, *O*-AcT and P450s are also presented in this BGC (Figure 1.12).

First of all, the gene encoding PKS-NRPS from *pyi* BGC will be disrupted. The abolition of **65** will confirm that the *pyi* BGC is the correct cluster involved in **65** biosynthesis. The mutant strain will be tested on crabgrass for pathogenicity by collaborators. If crabgrass no longer be infected, **65** will have the potential to be a genus-specific natural herbicide.

Our major aims are to elucidate the late stage biosynthetic pathway of pyrichalasin H **65** by knocking out the tailoring genes involved in its biosynthesis individually. Bipartite gene fragments combined with protoplast mediated transformation methods will be used to generate the KO mutants.¹²⁶ The obtained intermediates and shunt metabolites isolated from KO strains will be fully analysed by LCMS and NMR. The structure of the shunts and intermediates will help us understand the function of each tailoring gene and how each catalyst participates in the biosynthesis. Finally, a detailed late stage **65** biosynthetic pathway will be elucidated either in a linear, parallel or spontaneous way.

Then, with some KO strains in hand, we will attempt to develop our mutant strains into a synthetic bioengineering platform by heterologous expression of unknown function genes from other biosynthetic pathways. These are two cryptic P450 genes from *Hypoxylon fragiforme* cytochalasin BGC (Figure 3.7) and four unknown CYP genes from the *ACE1* gene cluster (Figure 1.12). The *hffD* and *hffG* genes will be investigated in P450 disruption strains. CYP gene will be expressed in the same host. We are aiming to achieve three goals: first, clarification of the promiscuity of cryptic P450 enzymes; second, the generation of novel cytochalasins by using combinatorial biosynthesis of different P450 genes; and finally, engineering the confirmed biosynthetic pathway to develop new branches for the main route.

The adenylation domain of NRPS often shows tolerance towards different amino acid substrates. So the A-domain will be investigated in mutasynthesis experiments by feeding various 4'-substituted phenylalanines to *pyiA* KO strain. A small library of 4'-functionalised pyrichalasins will be built during this study.

Based on the library generated by mutasynthesis, a range of different chemical reactions can be executed to introduce interesting pharmacophores to pyrichalasin. For example:

the 4'-iodo-pyrichalasin could be used as substrates for Sonogashira reactions to add alkyne groups, the 4'-bromo-pyrichalasin could be the substrate for Suzuki cross coupling to generate un-natural dimeric pyrichalasin; and 4'-azido- and 4'-alkyne-pyrichalasin could be starting materials for copper catalyzed Huisgen azide alkyne cycloaddition click reactions. Many bioconjugations can be generated by these chemical modifications.

Pyrichalasin H **65** can bind with actin and has strong inhibition on actin polymerization. We can link dye molecules to it by click chemistry. These hybrid molecules could be developed into cell imaging tools to visualize the actin in cells. Finally, all the new cytochalasins generated by pathway elucidation, pathway engineering, mutasynthesis and semisynthesis will be tested systematically on antitumor activity, cytotoxicity and anti-microbial activity by our collaborators. Hopefully, we can find some promising candidates for future investigation.

2 Investigation the Biosynthesis of Pyrivalasin H by Gene Disruption

Partial results of the presented work have been published in *Org. Lett.*, 2019, 21, 4163 – 4167.¹⁰⁹

2.1 Introduction

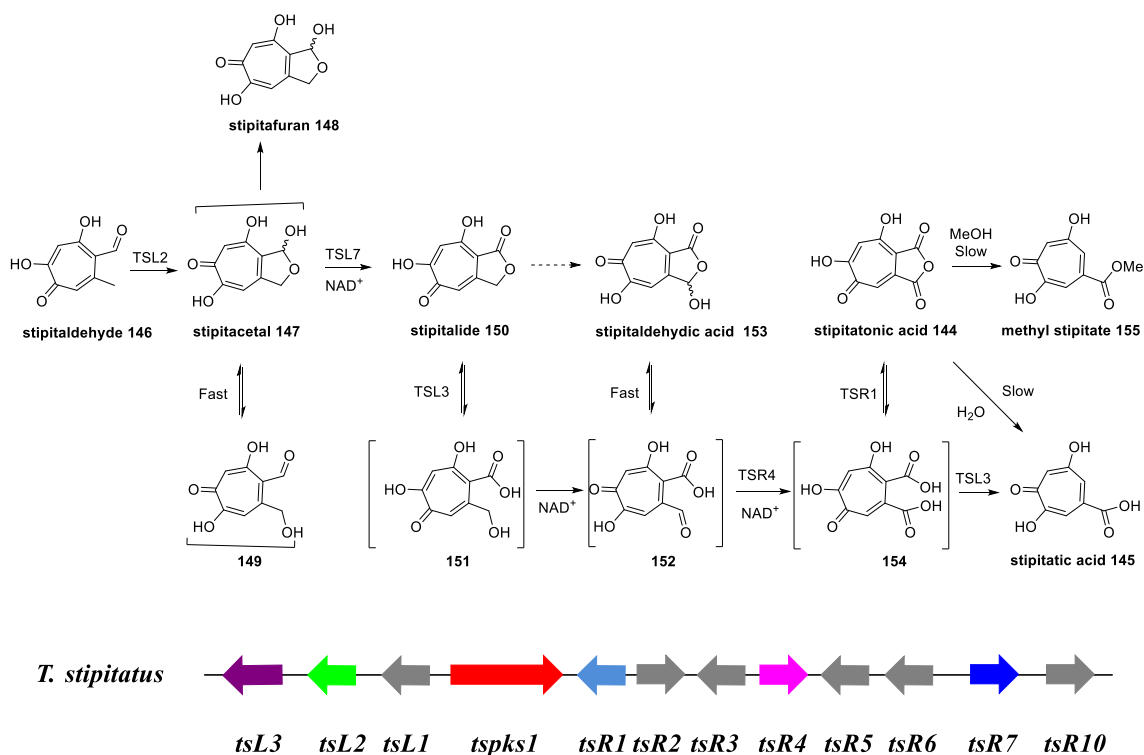
Fungal natural products are very important but they are not always produced in high yields, or they may need to be modified for pharmaceutical / agrochemical use. Before natural products can be engineered, their biosynthesis needs to be understood. One way to do this is through gene knockout (KO) studies – genes individually inactivated to reveal their function.¹¹⁸

A good example of the use of this strategy comes from the investigation of the biosynthesis of the tropolone stipitonic acid. Stipitonic acid **144** is the true precursor of stipitatic acid **145**. Stipitonic acid is produced by the enzymes encoded by the *Talaromyces stipitatus trop* gene cluster, which contains 12 putative open reading frames clustered around the gene *tspks1* (Scheme 2.1).^{119,120}

Cox and co-workers investigated the biosynthesis of stipitatic acid **145** using the bipartite KO strategy in *T. stipitatus*.¹²¹ The *tsL2* gene, which encodes a putative cytochrome P450 monooxygenase, was targeted for KO.^{120,121} The mutant strain was no longer able to synthesize **144**, **145**, **150**, **153** or **155**, but tropolone **146** was formed. Next, the *tsR7* gene, which encodes a putative NAD-dependent dehydrogenase was targeted for KO. Compounds **144**, **145**, **150**, **153** and **155** were abolished from the metabolic profile, the major new compound obtained was stipitafuran **148**. TsL2 is the C-9 hydrolase due to all isolated compounds are oxidized at C-9. The direct-9 oxidation products stipitacetal **147** / **149** was not observed.

Another putative NAD-dependent dehydrogenase encoding gene, *tsR4*, was targeted for KO, and stipitaldehydic acid **153** was produced. The gene *tsR1* encoding a putative hydrolase was targeted.¹²² The LCMS analysis of *tsR1* KO showed that **154** was produced. *In vitro* experiments assay of TsR1 confirmed that it can rapidly hydrolyse

the bright yellow stipitatic acid **144** to give colorless diacid **145**. Compound **145** is the final product of the normal pathway. *In vitro* experiments confirmed that TsL3 can convert **154** to **145**, the conversion speed was much increased by adding TsR1 into the reaction, these results confirmed that the decarboxylase TsL3 most likely reacts with the decarboxylate **154**.¹²¹

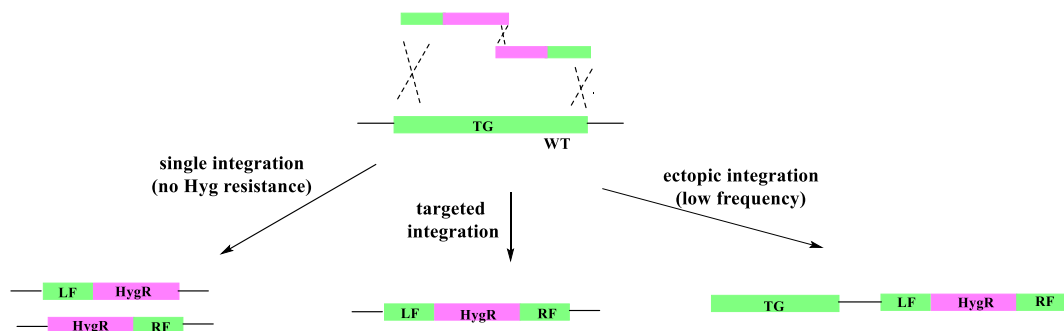


Scheme 2.1 Proposed biosynthetic pathway of stipitatic acid **144**.¹²¹

2.1.1 Bipartite Gene Targeting Strategy

Although gene knock outs are an essential strategy for investigating gene function, it is difficult to achieve the desired genetic modification in fungi. Frequent ectopic integration of the introduced DNA fragments is caused by non-homologous end joining (NHEJ) mechanisms.¹²³ DNA repair mechanisms make it difficult to generate efficient gene targeting frequencies. There have been reports that KO of genes involved in NHEJ in fungi can result in strains which have higher frequencies of desired recombination into target genes. However, the creation of NHEJ deficient strains requires KO experiments which are themselves low efficiency.¹²⁴

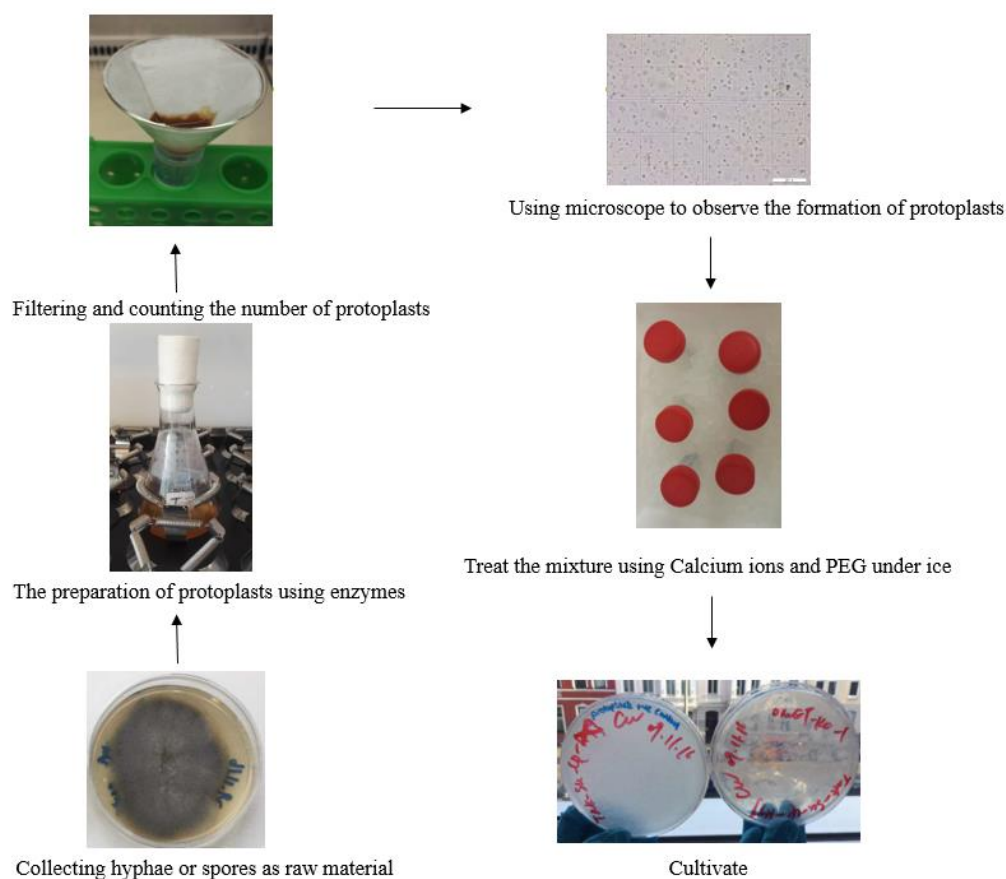
Several strategies have been reported to achieve increased desired homologous recombination (HR) frequencies rather than the application of a NHEJ pathway deficient strain.¹²⁵ One of the most useful methods is the use of a bipartite gene targeting strategy. This strategy involves the creation of two fragments of a KO construct, neither of which can on its own confer antibiotic resistance. When these fragments are introduced into fungi, the two fragments are recombined by HR and only then will the fungal selection marker become functional, leading to the targeted introduction of the full fragment into the genome by the activated HR mechanism (Scheme 2.2). The HR efficiency is much higher, then compared to using a single gene targeting fragment because the frequency of ectopic integration is greatly reduced.¹²⁶



Scheme 2.2 PMT with bipartite gene targeting substrates. TG, target gene; HR, homologous recombination; HygR, hygromycin resistant cassette; LF, left fragment; RF, right fragment; WT, wild type.¹²⁶

2.1.2 Protoplast-Mediated Transformation

Protoplast mediated transformation (PMT) is the most widely used fungal transformation method, which relies on the creation of a large number of competent fungal protoplasts. The principle is to use some commercially available enzymes (such as *Trichoderma harzianum* lysing enzyme and Driselase enzyme) to digest fungal cell wall components, thereby generating protoplasts. Next, some chemical reagents (such as PEG) are used to promote the fusion of exogenous DNA fragments and protoplasts (Scheme 2.3).¹²⁷



Scheme 2.3 Basic steps of the protoplast-mediated transformation.

2.2 Aims

The pyrichalasin H **65** producing strain *M. grisea* NI980 was provided by our collaborator Prof. Marc-Henri Lebrum. Genome sequence results showed that there are only three putative cytochalasin BGC (Chapter 1.4.2). Our first goal is to elucidate the chemical structures of all interesting metabolites produced by the WT strain. Then the *pyiS* gene will be the target for KO to confirm if the *pyi* BGC is responsible for **65** biosynthesis.

Once the *pyi* BGC has been confirmed, all the tailoring genes will be targeted for KO to confirm their possible functions. By systematic KO of these genes, we might also be able to isolate some novel cytochalasins or shunt products from the KO strain. In the end, a possible late-stage biosynthetic pathway will be determined based on the KO metabolites.

2.3 Results

2.3.1 Chemical Investigation of *Magnaporthe grisea* WT

2.3.1.1 Major Compound

Magnaporthe. grisea NI980 was used as the wild type (WT) strain in this study. For pyrichalasin H **65** the WT production strain was cultivated in DPY liquid medium for 7 days at 25 °C, 110 rpm. The liquid culture was extracted. The organic extract was dried and evaporated and the residue was dissolved into 1 mL HPLC MeOH and analysed by LCMS (Figure 2.1).

In the DAD chromatogram several peaks were detected. Six interesting peaks were targeted for purification by Preparative LCMS (Figure 2.1).¹⁰⁹ Approximately 61.6 mg **65** ($t_R = 6.3$ min) was obtained as white powder from 1 L DPY culture extracts. The UV spectra (MeCN / H₂O) showed the maximum absorption at 276 nm (Figure 2.2), which indicated the presence of several isolated double bonds and a substituted aromatic ring. HRMS of **65** confirmed a molecular formula of C₃₁H₄₁NO₆ ([M+Na]⁺ calculated 546.2832, found 546.2834).

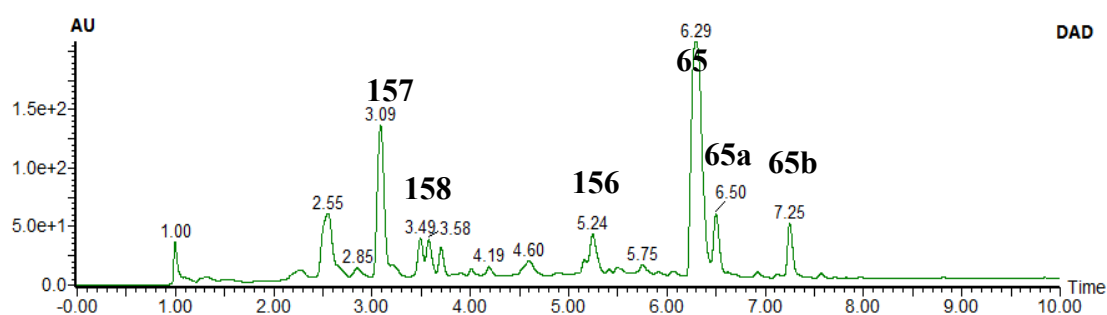


Figure 2.1 LCMS chromatogram (DAD) of liquid extracts from *M. grisea* NI980 WT strain.

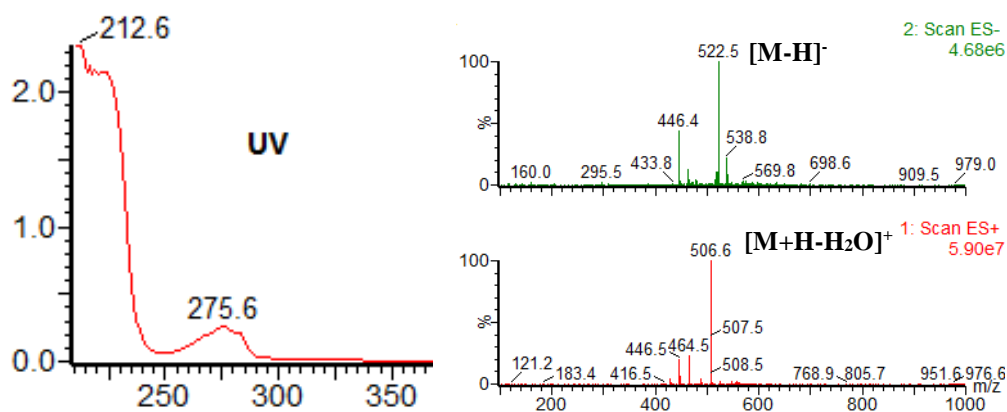
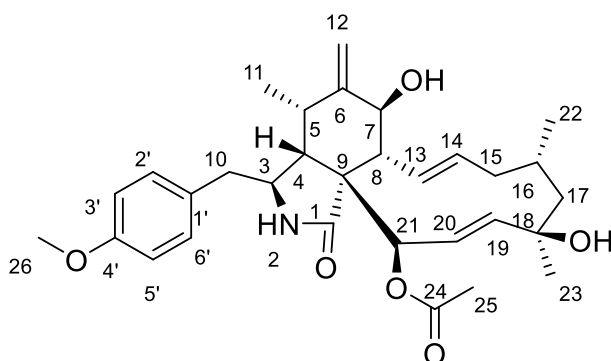


Figure 2.2 UV and mass spectra of compound **65**.

Full NMR was acquired, and analysis of ^1H and ^{13}C NMR data of **65** identified 31 carbons and 41 protons (Table 2.1). The assignment of the ^1H NMR spectrum is based on the results of 2D homonuclear correlation spectroscopy (COSY). Cross peaks were observed between the following pairs of signals: (δ_{H} - δ_{H}) 7.08-6.87, 5.85-5.57, 5.75-5.41, 5.36-5.12, 5.36-3.86, 5.75-2.93, 5.43-2.05, 3.83-2.98, 3.21-2.80, 2.80-2.65, 2.78-0.99, 2.05-1.81, 1.81-1.06. This indicated the presence of a tertiary methyl group, two secondary methyl groups, a *para*-substituted benzene ring, two disubstituted double bonds and a methoxyl group.

Table 2.1 NMR data of **65** recorded at 400 MHz in CDCl₃. Values are in agreement with published data.¹⁰⁹



Position	δ_H	M	J_{H-H}/Hz	δ_C	HSQC	HMBC H to C	H-H COSY
1	-	-	-	174.4	-	-	-
2	5.57	s	-	-	-	-	-
3	3.23	ddd	4.6, 9.5, 4.5	54.0	CH	1', 1, 4, 9	4, 10
4	2.12	dd	4.5, 4.9	50.4	CH	5, 6, 10, 11, 21	3, 5
5	2.79	m	-	33.0	CH	1', 7, 11	4, 12
6	-	-	-	148.1	-	-	-
7	3.84	dd	10.8, 1.3	69.9	CH	5, 6, 8, 9, 13	8, 12
8	2.95	dd	10.8, 9.8	47.3	CH	1, 3, 6, 7, 13, 14	7, 13
9	-	-	-	51.9	-	-	-
10a	2.61	dd	13.6, 9.5	44.8	CH ₂	1', 3, 4	3, 11
10b	2.80	dd	13.6, 4.6	-	-	-	-
11	0.99	d	6.7	14.2	CH ₃	4, 5, 6	10
12a	5.12	brs	-	114.2	CH ₂	5, 6, 7	5, 7, 15
12b	5.36	brs	-	-	-	-	-
13	5.75	ddd	9.8, 15.5, 1.3	127.3	CH	7, 8, 15, 16	8, 14
14	5.41	ddd	15.5, 5.2, 10.4	138.8	CH	8, 15, 16	13, 15
15a	1.83	m	-	42.9	CH ₂	13, 14, 16, 17, 22	12, 14, 22
15b	2.05	m	-	-	-	-	-
16	1.83	m	-	28.4	CH	17	17
17a	1.56	dd	14.3, 2.7	53.8	CH ₂	16	16
17b	1.88	m	-	-	-	-	-
18	-	-	-	74.5	-	-	-
19	5.55	dd	17.1, 2.3	138.2	CH	8, 9, 20, 21, 23	20
20	5.89	dd	17.1, 2.1	126.1	CH	8, 18, 19, 21	19, 21
21	5.56	dd	2.1, 2.3	77.6	CH	8, 19, 20, 23, 24	20
22	1.06	d	6.3	26.6	CH ₃	15, 16, 17	15
23	1.37	s	-	31.3	CH ₃	16, 17, 18, 19	-
1'	-	-	-	129.5	-	-	-
2' 6'	7.07	d	8.6	130.2	2 x CH	3', 4', 5', 10	3', 5'
3' 5'	6.86	d	8.6	114.4	2 x CH	2', 6', 4'	2', 6'
4'	-	-	-	158.8	-	-	-
24	-	-	-	170.3	-	-	-
25	2.26	s	-	21.0	CH ₃	21, 24	-
26	3.81	s	-	55.4	CH ₃	4'	-

The ^1H - ^1H correlation spectroscopy (COSY) indicated ^1H - ^1H correlations between H-2',6'/H-3',5', and the HMBC correlation between H-26 and C-4', suggested the methoxyl group was located at C-4'. The ^1H - ^1H correlations between H-2',6'/H-3',5', H-10/H-3 and H-11, the long range COSY cross peaks appeared between the following pairs: H-2',6'/H-10 (7.08-2.61, 7.08-2.79) and the heteronuclear multiple bond correlation (HMBC) between H-10 and C-1', C-3, C-4, suggested the *para*-substituted benzene ring was linked to C-10. The long range ^1H - ^1H correlation between H-19/H-23 (5.57-1.36), and the HMBC correlation between H-19 and C-23, indicated the tertiary methyl group to C-18 was adjacent to C-19. Moreover, there is no proton signal found at C-18, suggesting the hydroxyl group was also linked to C-18. The ^1H - ^1H correlations between H-11/H-10, and the HMBC correlation between H-11 to C-4, C-5, C-6, suggested one secondary methyl group was linked to C-5. The ^1H - ^1H correlations between H-22/H-15, and the HMBC correlation between H-22 to C-15, C-16, C-17, suggested the other secondary methyl group was linked to C-16.¹²⁸

The two hydrogens linked to C-12 showed typical broad singlets in the ^1H NMR and typical olefinic signals from heteronuclear single quantum correlation (HSQC, $\delta_{\text{H}} - \delta_{\text{C}}$, 5.12/5.36-113.9). Three methylene groups: 10 ($\delta_{\text{H}} - \delta_{\text{C}}$, 2.61/2.88-44.8), 15 (1.83/2.05-42.8), and 17 (1.56/1.88-53.7), also showed clear olefinic signals from HSQC. The HMBC correlation from H-25 to C-24 and C-21 revealed the link of the acetyl group to C-21.¹²⁹

The chemical shifts of the carbons from C-1 to C-23 of **64** were almost identical values to the respective carbon chemical shifts of cytochalasin H **174**. The comparison of the proton-proton coupling constants for cytochalasin H **174** and **65** indicates that the relative stereochemistry of both compounds are the same. Moreover, the full NMR data of pyrichalasin H was elucidated and published in 1987.¹⁰⁴ The data of **65** is almost identical to that previously reported for pyrichalasin H. Taking all this evidence together, we can confirm that compound **65** is pyrichalasin H (Table 2.1).

2.3.1.2 Minor Compounds

We also obtained pure compounds **65a** ($t_R = 6.5$ min, 4.8 mg/L) and **65b** ($t_R = 7.3$ min, 2.6 mg/L) as white powders. The UV and mass spectra for both compounds looks identical to each other and very similar to that for pyrichalasin H (Figure 2.3 A-C). HRMS of **65a** showed a molecular formula of $C_{31}H_{41}NO_6$ ($[M+Na]^+$ calculated 546.2832, found 546.2836), while **65b** also showed an identical molecular formula of $C_{31}H_{41}NO_6$ ($[M+Na]^+$ calculated 546.2832, found 546.2829). These results could suggest that **65a** and **65b** might be isomers of **65**. Next, the full NMR data of **65a** and **65b** (Appendix, Table 6.8 & 6.9) were obtained. The proton, carbon, H-H COSY, HMBC and HSQC data of **65a** and **65b** were fully elucidated. The two sets of data between **65a** and **65b** are almost identical. Then we individually compared the data of **65a** and **65b** to pyrichalasin H. Again, these three sets of NMR data are identical to each other. Moreover, we mixed the three compounds and dissolved in MeOH and re-injected the sample into LCMS, and only a single peak was observed (Figure 2.3 D). This result indicates that these three compounds are likely to be slowly interconverting tautomers.

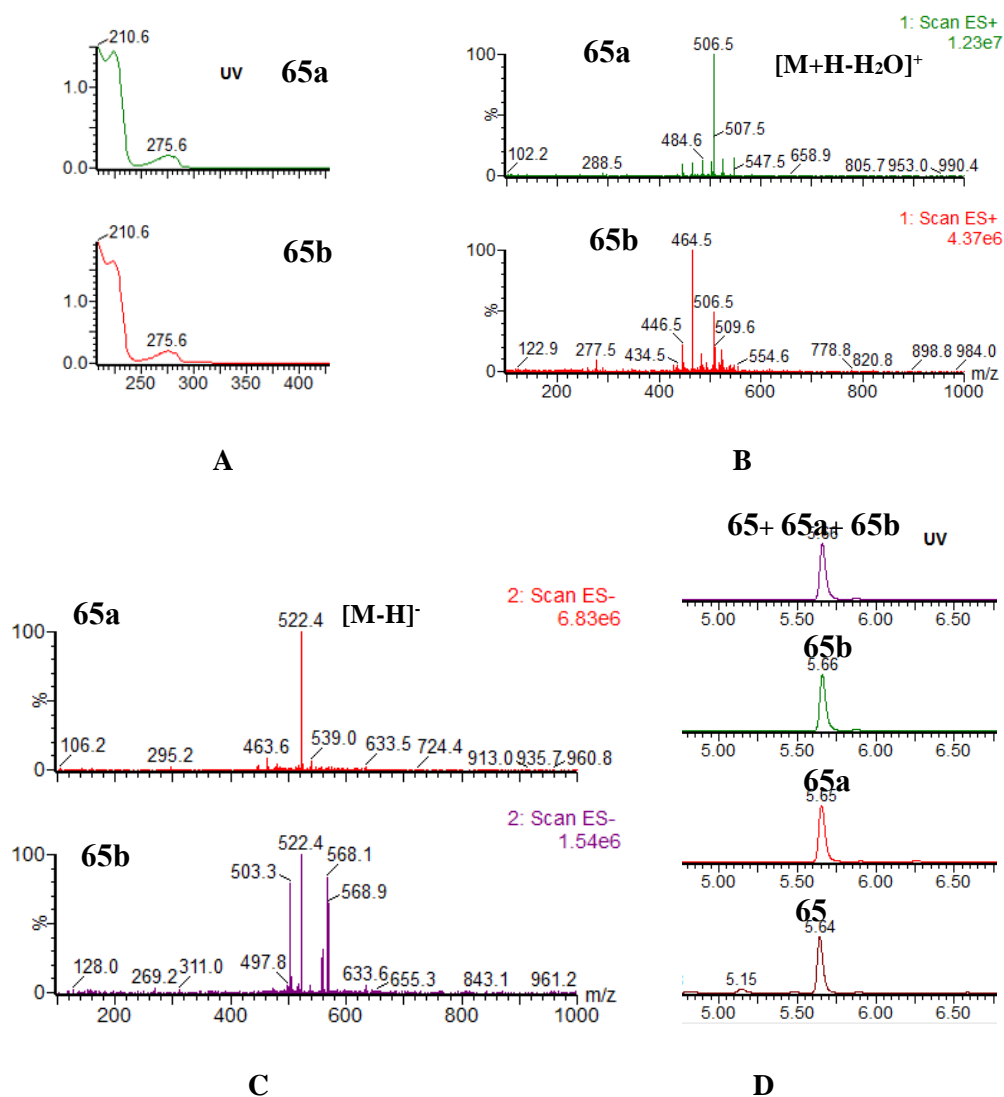


Figure 2.3 UV and mass spectrum of compound **65a** and **65b**.

Compound **156** ($t_R = 5.2$ min, 2.1 mg/L) was purified as a white powder. The UV spectra showed the maximum absorption at 276 and 224 nm (Figure 2.4), which is similar to pyrichalasin H. HRMS of **156** confirmed a molecular formula of $C_{29}H_{39}NO_5$ ($[M+Na]^+$ calculated 504.2726, found 504.2725).

Full NMR was acquired and analysed. 1H and ^{13}C NMR data of **156** identified 29 carbons and 39 protons.¹⁰⁹ The signal of H-25 was not observed in proton NMR and HSQC spectra, also the chemical shift of H-21 moved downfield due to the effect of the new hydroxyl group, the remaining signals of both carbon and hydrogen chemical shifts were similar to pyrichalasin H. On the basis of the above evidence the structure was confirmed as pyrichalasin J **156** (Figure 2.5).

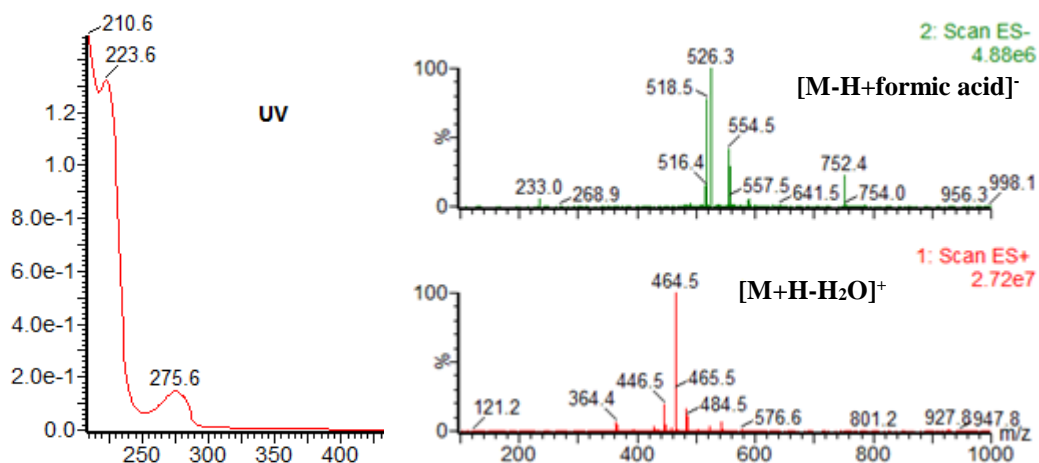


Figure 2.4 UV and mass spectrum of compound **156**.

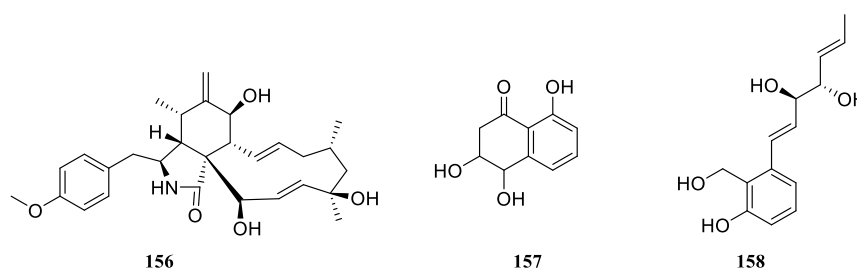


Figure 2.5 Chemical structure of minor compounds isolated from *M. grisea* NI980 wild type (WT) strain.

Compound **157** ($t_R = 3.1$ min, 10.4 mg/L) was purified as yellow powder. The UV spectra showed the maximum absorption at 333 and 260 nm (Figure 2.6), which is different from pyrichalasin H. HRMS of **157** confirmed a molecular formula of $C_{10}H_{10}O_4$ ($[M-H]^-$ calculated 193.0501, found 193.0497).

Full NMR was acquired and analysis of 1H and ^{13}C NMR data of **157** identified 10 carbons and 10 protons (Appendix, Table 6.6). Combined with 2D NMR, 1H - 1H COSY, HMBC and HSQC, compound **157** was confirmed as known compound 3,4,8-trihydroxy-3,4-dihydronaphthalen-1(2H)-one (Figure 2.5).¹³⁴

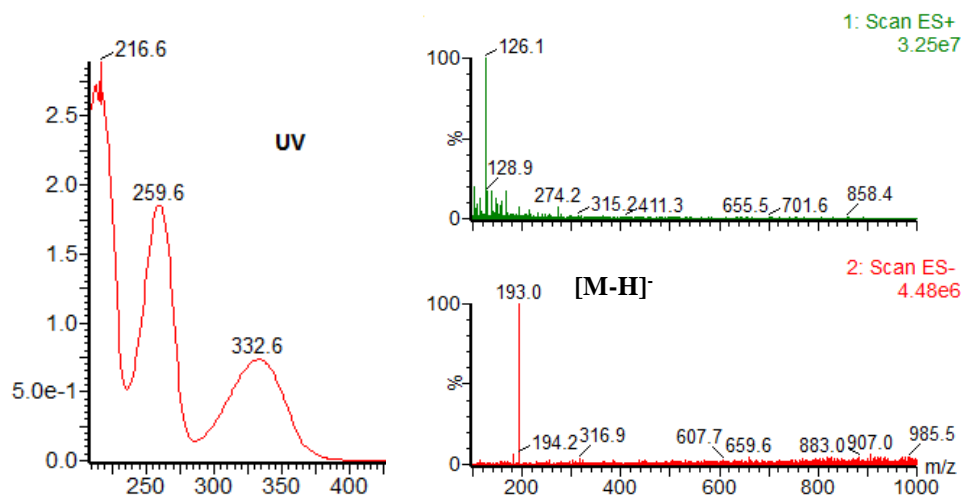


Figure 2.6 UV and mass spectrum of compound **157**.

Compound **158** ($t_R = 3.5$ min, 13.7 mg/L) was purified as a yellow powder. The UV spectra showed a maximum absorption at 280 nm (Figure 2.7), which is different from pyrichalasin H. HRMS of **158** confirmed a molecular formula of $C_{14}H_{18}O_4$ ($[M+Na]^+$ calculated 273.1103, found 273.1105).

Full NMR was acquired and analysis of 1H and ^{13}C NMR data of **158** identified 14 carbons and 18 protons (Appendix, Table 6.7). Combined with 2D NMR, 1H - 1H COSY, HMBC and HSQC, compound **158** was confirmed as dihydropyriculol (Figure 2.5).¹³¹

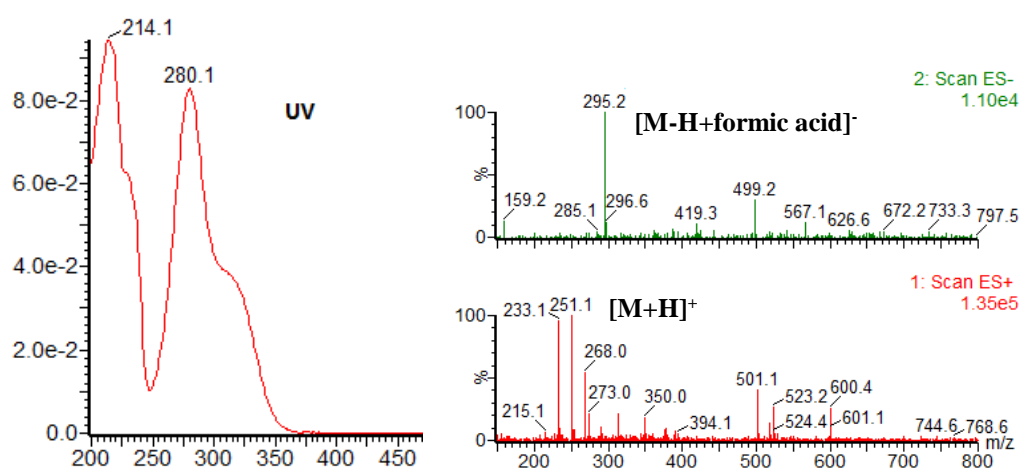


Figure 2.7 UV and mass spectrum of compound **158**.

2.3.2 *pyiS* Gene Knockout

2.3.2.1 Preparation of Deletion Strain

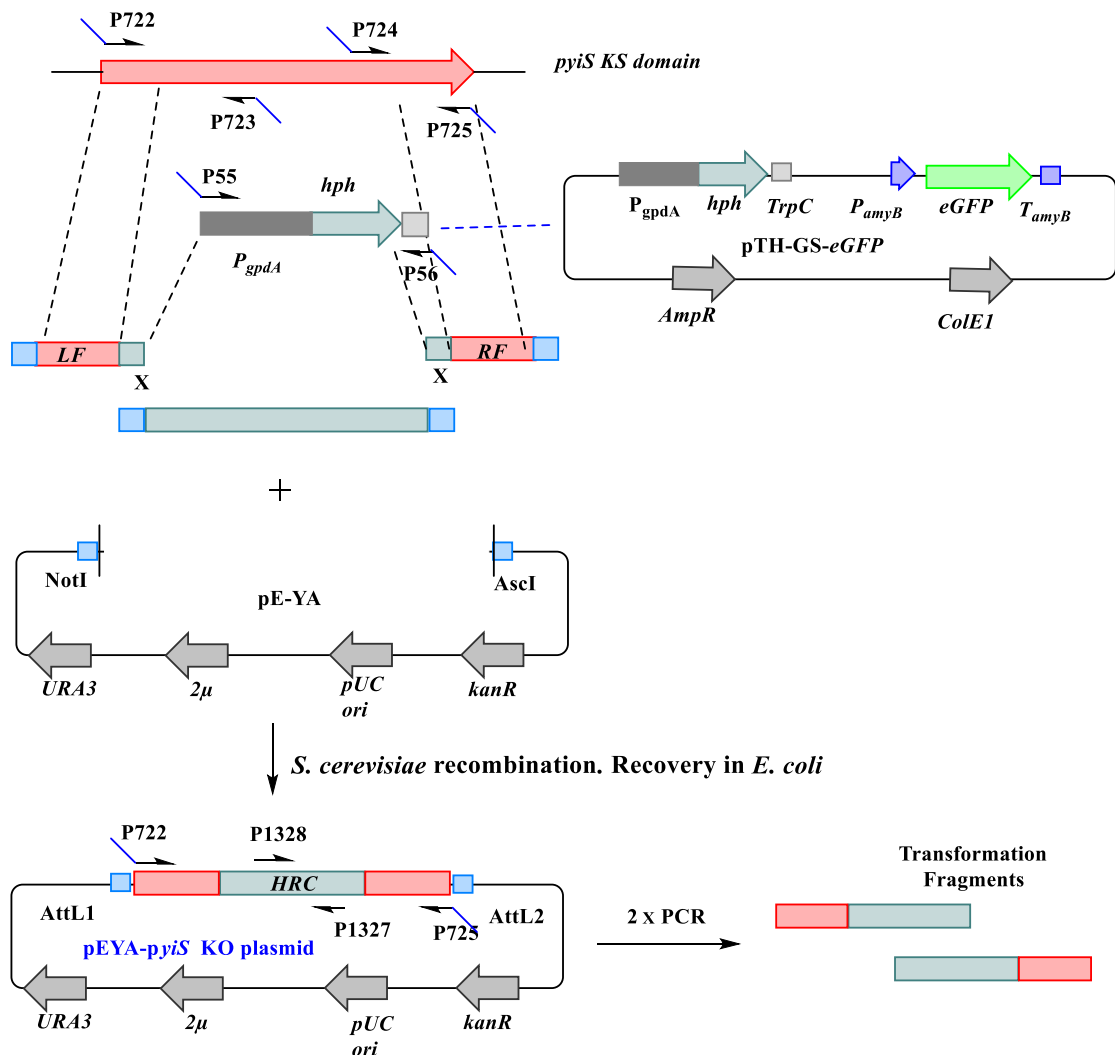
Bioinformatic analysis of the genome of *M. grisea* NI980 carried out by Dr. Elizabeth Skellam (Chapter 1.4.2) showed that eight PKS-NRPS BGC are present. Detailed analysis suggested that the *pyi* cluster could be responsible for pyrichalasin biosynthesis. In order to prove this hypothesis we set out to delete *pyiS* encoding the central PKS-NRPS. For targeted gene disruption, a KO vector consisting of a selection marker Hygromycin B resistance cassette flanked by arms homologous to the target gene (TG) has to be assembled. DNA fragments can be recombined in *S. cerevisiae* by homologous recombination with an overlap sequence of 30 bp. This method has been used extensively to build up vector constructs through PEG mediated co-transformation of individual DNA fragments (Scheme 2.4).¹³²

In this study pE-YA was used as the vector for the assembly of all KO constructs. This vector contains the 2μ origin of replication (*ori*) and *ura3* gene (encoding an orotidine 5'-phosphate decarboxylase) to select uracil auxotroph *S. cerevisiae* in uracil and uridine free medium. All DNA fragments for yeast recombination were amplified by PCR using gDNA of *M. grisea* as the template. Oligonucleotides P722-P725 (Chapter 6.1.5, Cox group ID) were used together with Q5 High-Fidelity DNA Polymerase (*New England, Biolabs*) to precisely amplify the *pyiS* gene (Scheme 2.4). The pTH-GS-*egfp* vector was used as a PCR template for the amplification of a fungal selection marker, in this case hygromycin B under the control of the *gdpA* promoter (*P_{gdpA}*) from *Aspergillus. sp.* The primer pair P55- P56 were used to clone the hygromycin resistant cassette (HRC) (Scheme 2.4, Chapter 6.1.5). The necessary 30 bp sequence overlap for homologous recombination of the individual DNA fragments was introduced by PCR through tails on the designed oligonucleotides. The 5' and 3' bipartite substrates for *pyiS* were amplified using oligonucleotides P722+ P1327 and P725+ P1328 from the corresponding template vector plasmid (Scheme 2.4, Chapter 6.1.5).

The vector pE-YA was then linearized by restriction hydrolysis with *AscI* and *NotI* enzymes prior to PEG mediated co-transformation with the PCR amplified DNA fragments. The constructed plasmid DNA was isolated from *S. cerevisiae* and directly used to transform competent *E. coli*. For propagation in *E. coli*, there is an additional *ori*

(pUC) and the *nptII* gene, encoding the neomycin phosphotransferase II, which also confers resistance to kanamycin (*kanR*).¹³³ Obtained colonies were screened by PCR and confirmed by sequencing (*Eurofins, Ebersberg*).

The obtained plamid was then used as a template for two final PCR to produce the two bipartite transformation fragments (Scheme 2.4). These two PCR products were purified and directly used for PEG/CaCl₂ mediated protoplast transformation of *M. grisea*. Transformation mixtures were selected on hygromycin plates, and picked colonies sub-cloned on 2-3 further selection plates.¹³⁴



Scheme 2.4 General method for assembly of KO cassettes targeting *pyiS* KS domain in pE-YA vector by yeast recombination (HR).¹³⁴

2.3.2.2 Chemical and Genetic Analysis of *pyiS* KO

In total, over 30 colonies were obtained from the initial transformation recovery plates (hygromycin B concentration 240 $\mu\text{g}/\text{mL}$, Figure 2.8 A); 20 colonies were obtained from the second round selection (hygromycin B concentration 120 $\mu\text{g}/\text{mL}$, 2nd selection plates, Figure 2.8 B); 15 transformants were obtained from the third selection (Figure 2.8 C). 15 transformants were inoculated into DPY liquid medium at 25 °C, 110 rpm for 7 days before supernatant was filtered to be free from cell material and extracted twice with ethyl acetate (Figure 2.8 D).

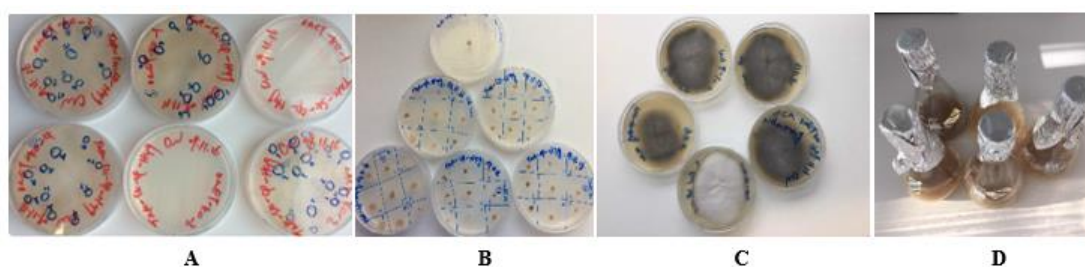


Figure 2.8 Transformants obtained from three rounds of selection.

The organic extracts from 15 transformants were analysed by LCMS. The results showed 4 out of 15 mutants no longer produced pyrichalasin H **65**, no other interesting peaks were detected, peak ($t_R = 5.40$) is not relevant (Figure 2.9).

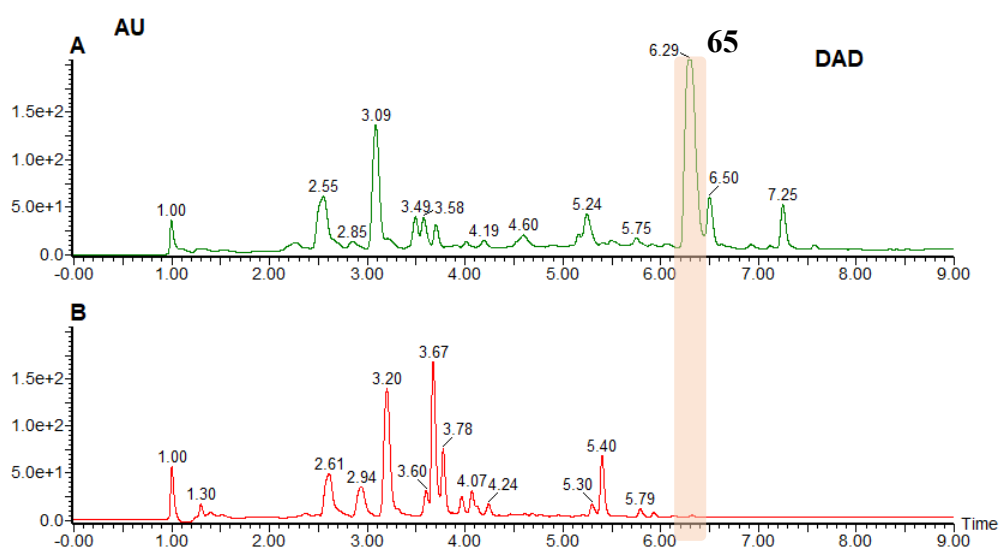
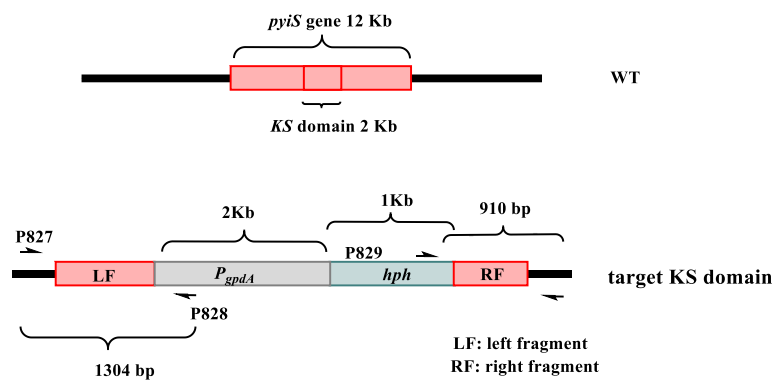


Figure 2.9 LCMS chromatogram (DAD trace) of liquid extracts from *M. grisea* *pyiS* KO experiments. **A**, wild type control; **B**, *pyiS* KS domain KO strain.

For genetic testing of the 4 putative positive transformants obtained from *pyiS* KO transformation, genomic DNA (gDNA) was extracted and used as the PCR template. Primers were designed to bind to the region outside the target gene, and inside the resistant cassette for both targeting fragments. The disruption of *pyiS* was analysed with oligonucleotides P827-P830 which could differential both a disrupted *pyiS* and an intact *pyiS* (Figure 2.10, Chapter 6.1.5). As shown clearly in the gel picture (Figure 2.10 B) of the PCR products that bipartite substrates binding precisely to the target gene in all positive transformants.

A



B

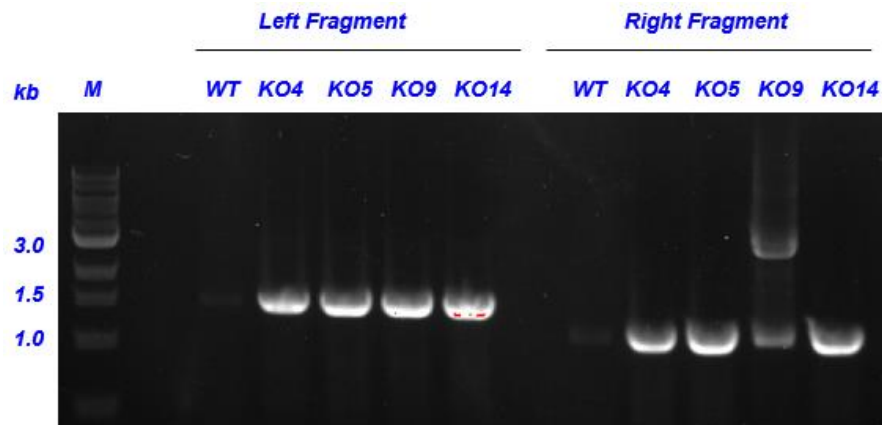


Figure 2.10 A, Genetic analysis of transformants obtained with bipartite marker strategy by PCR; **B**, PCR analysis for confirmation of target gene replacement events at the *pyiS* locus. Expected fragment sizes: left fragment = 1304 bp, and right fragment = 910 bp. M, DNA ladder marker.

2.3.3 Targeted Inactivation of Tailoring Genes in Pyrichalasin BGC

2.3.3.1 Preparation of *pyiC*, *pyiB*, *pyiH*, *pyiD*, *pyiG*, *pyiA* Deletion Strains

Next, we targeted all the putative tailoring genes (*pyiA*, *pyiB*, *pyiD*, *pyiG*, and *pyiH*) as well as the *pyiC* gene which is assumed to encode a *trans*-ER protein. Using the same methodology described in section 2.3.1, the required plasmids were constructed (Figure 2.11).

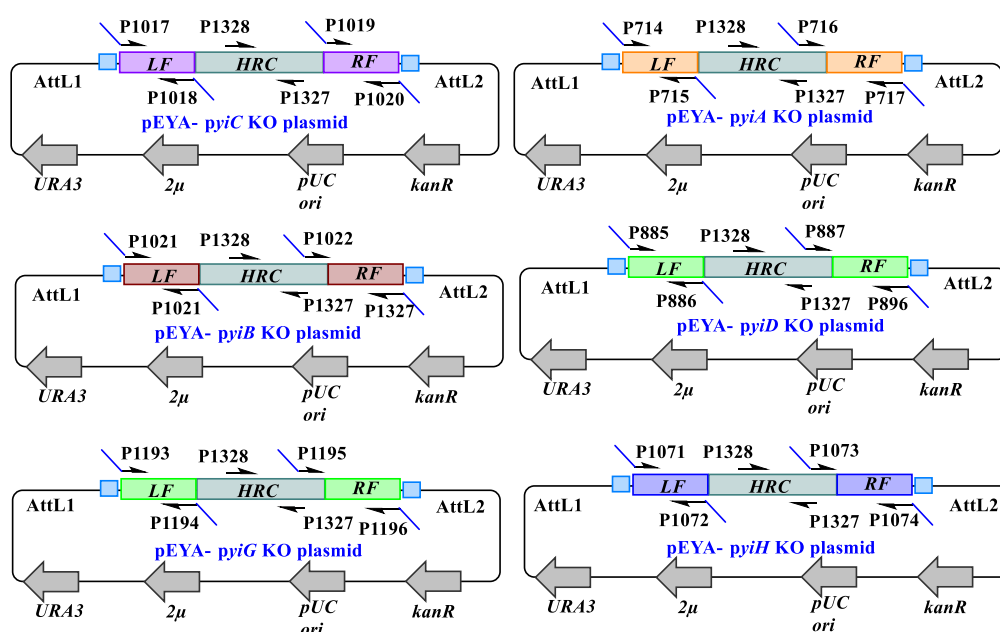


Figure 2.11 Overview of constructed KO vectors in this work.

2.3.3.2 Chemical and Genetic Analysis of *pyiC* KO

The transformation process was performed following the same protocol described in section 2.3.1. The number of transformants generated per experiment and the number of true KOs obtained per strain were screened by PCR and summarized (Table 2.2).¹⁰⁹

Table 2.2 Transformation efficiency using the bipartite method in *M. grisea* NI980.¹⁰⁹

Gene Disrupted	Number of transformants screened	Number of disrupted genes (confirmed by PCR)	Success rate (%)
<i>PyiS</i>	15	4	26.7
<i>PyiC</i>	20	4	20
<i>PyiB</i>	92	1	1.1
<i>PyiH</i>	24	1	4.1
<i>PyiG</i>	53	7	13.2
<i>PyiD</i>	18	3	16.7
<i>PyiA</i>	57	5	8.8

2.3.3.2 Chemical Analysis of *pyiC* KO

The LCMS data of *pyiC* KO (encoding the *trans*-ER) showed that the abolition of pyrichalasin H **65**, and no other interesting peaks were detected (Figure 2.12).

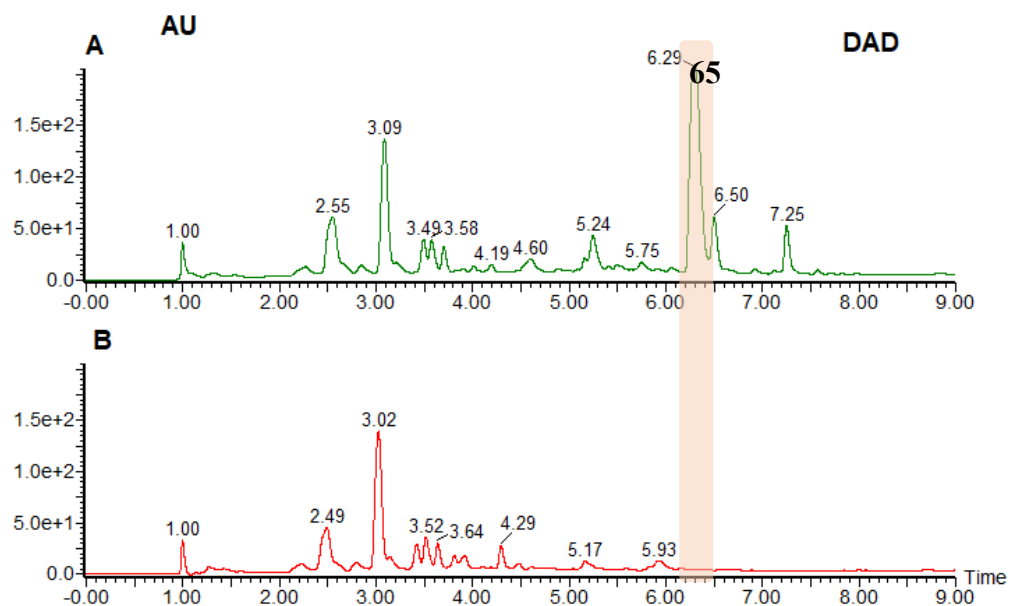
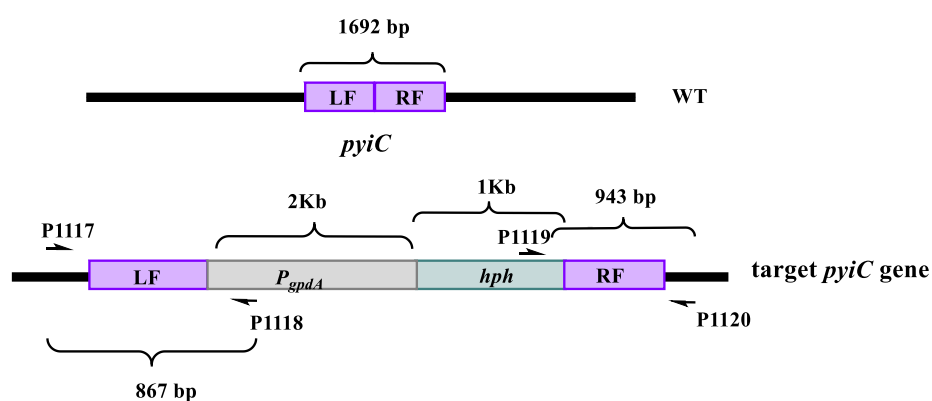


Figure 2.12 LCMS chromatograms (DAD trace) of organic extracts from *pyiC* KO experiments in *M. grisea*; **A**, wild type control; **B**, positive KO transformant.

The same strategy described in section 2.2.2 was adopted for the genetic testing of *pyiC* KO transformants. The agarose gel electrophoresis shown the precise binding of bipartite fragments to the target gene in all transformants.

A



B

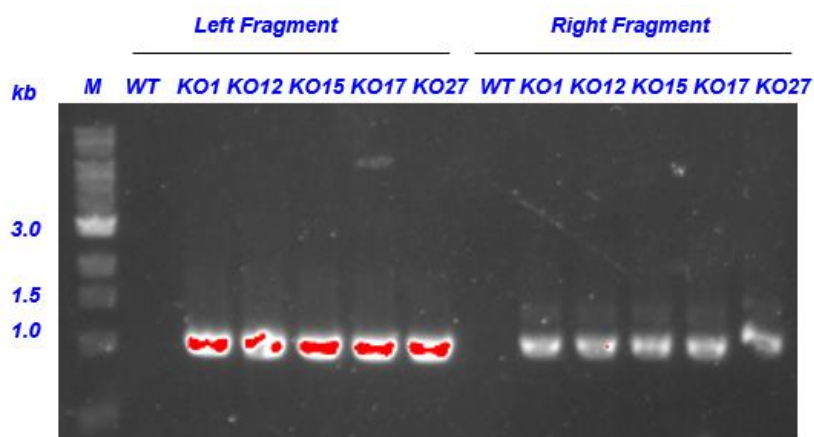


Figure 2.13 PCR analysis for confirmation of target gene replacement events at the *pyiC* locus. Expected fragment sizes, left fragment = 867 bp, and right fragment = 943 bp. M, DNA ladder marker.

2.3.3.3 Chemical and Genetic Analysis of *pyiB* KO

The LCMS chromatogram of *pyiB* KO showed the complete loss of pyrichalasin H **65**, and a peak corresponding to pyrichalasin J **156**, was detected ($t_R = 5.3$ min, Figure 2.14), compound **159** and **160** are unrelated metabolites.

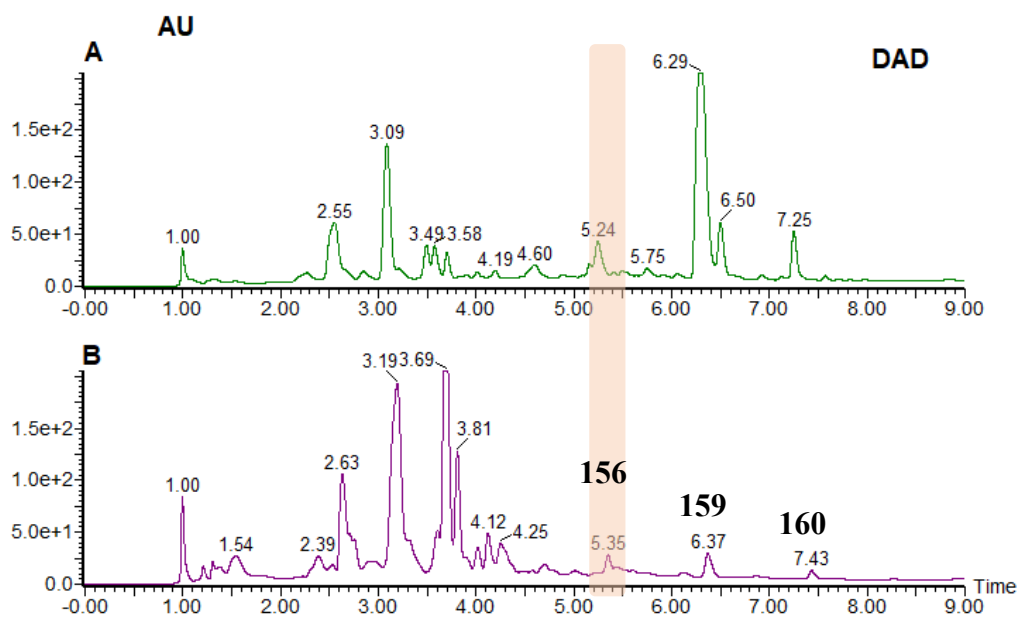
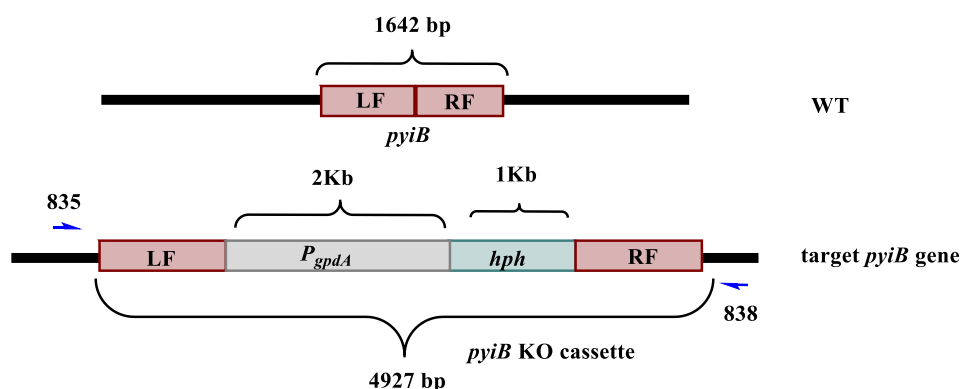


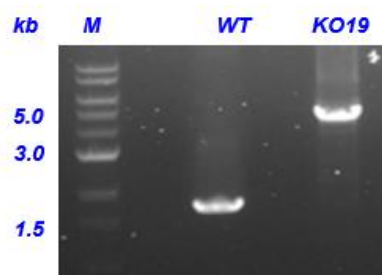
Figure 2.14 LCMS chromatograms (DAD trace) of organic extracts from *pyiB* KO experiments in *M. grisea*. **A**, wild type control; **B**, KO-19. Compound **159** and **160** are unrelated metabolites.

The genetic testing of *pyiB* KO transformation was performed using the same method as above (Figure 2.15 A). However, for some unknown reasons, we could not generate the expected PCR fragments when using one primer outside of the target gene and another primer binding within the hygromycin resistance cassette (HRC) region. In contrast, the predicted size of undisrupted *pyiB* appeared from wild type control by using the same pair of primers (Figure 2.15 B, Table 6.4). This result clearly indicated that the hygromycin resistance gene correctly recombined at the desired position within the target gene.

A



B



C

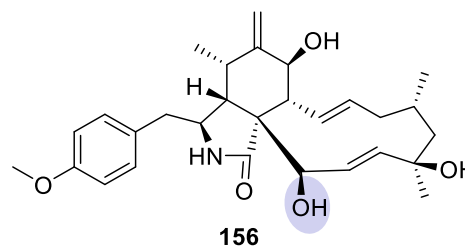


Figure 2.15 A, PCR analysis for confirming targeted gene replacement events at the *pyiB* locus; B, Expected fragment sizes: 4927 bp. M, DNA ladder marker kb; C, chemical structure of **156**.

Compound **156** ($t_R = 5.3$ min, 2.1 mg / L) was purified as white powder. The UV spectra (methanol) showed the maximum absorption at 276 and 228 nm, which is different from pyrichalasin H. HRMS of **156** confirmed a molecular formula of $C_{29}H_{39}NO_5$ ($[M+Na]^+$ calculated 504.2726, found 504.2725). HRMS and full NMR data confirmed this compound is the same as pyrichalasin J **156** (Appendix, Figure 2.15 C).¹⁰⁹

2.3.3.4 Chemical and Genetic Analysis of *pyiH* KO

Chemical analysis of transformants obtained after introducing the *pyiH* KO (encoding an oxidoreductase) fragments revealed that pyrichalasin H **65** was completely abolished

from the LCMS profile of the *pyiH* KO extract. However, three new interesting peaks were detected **161** ($t_R = 5.7$ min), **162** ($t_R = 7.0$ min) and **163** ($t_R = 8.2$ min, Figure 2.16).

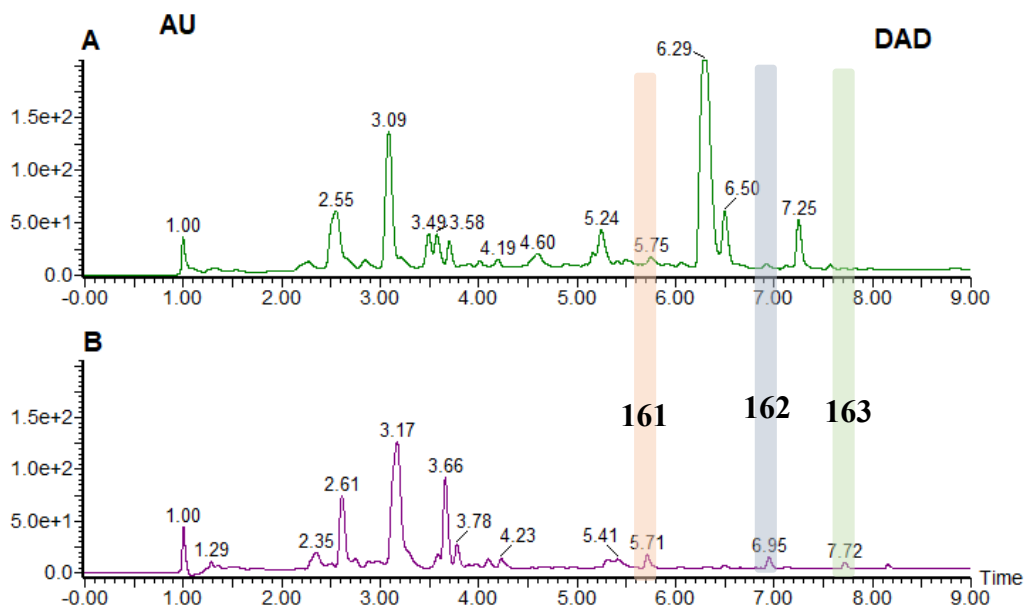
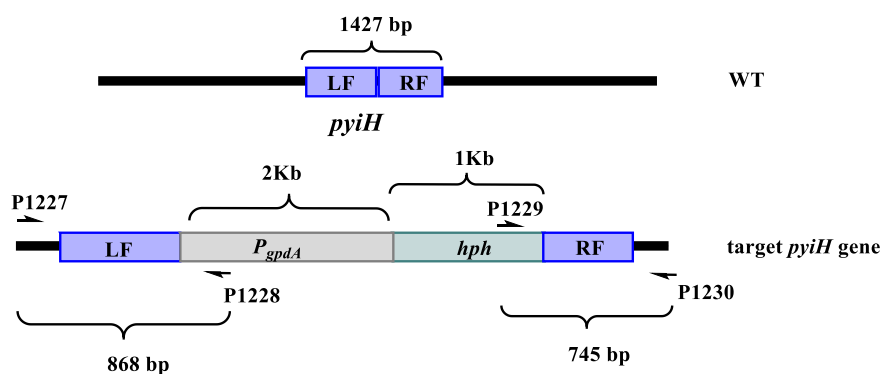


Figure 2.16 LCMS chromatograms (DAD trace) of organic extracts from *pyiH* KO experiments in *M. grisea*. **A**, wild type control; **B**, KO-5.

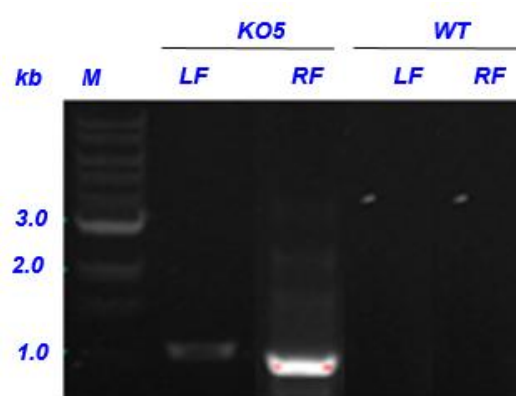
The same strategy described in section 2.2.2 was used for the genetic testing of *pyiH* KO transformants (Figure 2.16 A). The agarose gel electrophoresis shows the precise integrity of both left and right bipartite fragments to the target gene in the only transformant obtained from transformation. In contrast, there is no bands amplified from the WT gDNA, which also confirms of bipartite the target gene (Figure 2.16 B).

Compound **161**, **162** and **163** were purified as white powders, the compound physical data were measured and summerized in Table 2.3.

A



B



C

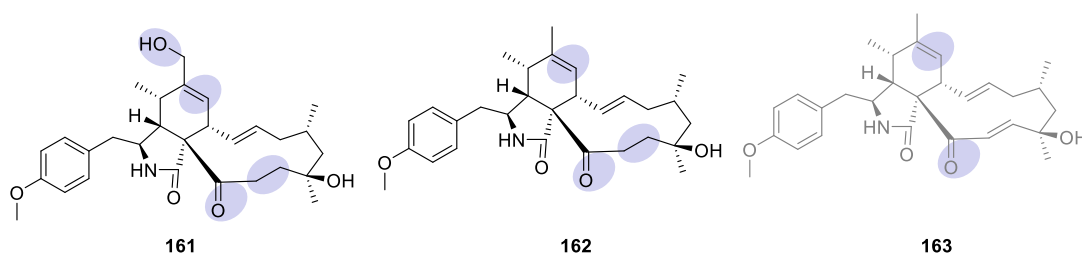


Figure 2.17 **A**, Genetic analysis of transformants obtained with bipartite marker strategy by PCR; **B**, PCR analysis for confirmation of target gene replacement events at the *pyiH* locus. Expected fragment sizes: left fragment = 868 bp, and right fragment = 745 bp, M, DNA ladder marker; **C**, chemical structure of **161**, **162** and **163**.

Table 2.3 Compound physical data from *pyiH* KO experiment.¹⁰⁹

Compound Nr.	t _R (min)	UV (nm)	HRMS (calculated /found)	Molecular Formula	Titre (mg / L)	Appearance
161	5.7	276, 224	504.2726 /504.2724	C ₂₉ H ₃₉ NO ₅	2.8	white
162	7.0	276, 224	488.2777 /488.2775	C ₂₉ H ₃₉ NO ₄	1.9	white
163	8.2	276, 224	464.2801 / 464.2802	C ₂₉ H ₃₇ NO ₄	1.0	white

Full NMR data was acquired, and analysis of ¹H and ¹³C NMR spectra of **161** identified 29 carbons and 39 protons. The signal of H-25 of pyrichalasin H **65** was not found from proton NMR and HSQC, also the chemical shift of H-21 moves to the lower field due to the attachment of hydroxyl group. The signal of olefin H-6 and H-12 were not found from proton NMR and HSQC, the ¹H-¹H correlations between H-12 / H-4 and H-7 (3.93-2.41, 3.93-5.49), and the HMBC correlation between H-12 to C-5, C-6, C-7, suggesting that a C-12 methyl group added to C-6. In the meantime, the double bond migrated from C-6 and C-12 to C-6 and C-7, proved by the drastic increase of carbon chemical shift of C-6 (143.8) and C-7 (124.9). New olefinic signal appeared from HSQC ($\delta_H - \delta_C$, 3.93, 61.7), which indicated a methylene group connected with a hydroxyl group linked to the C-6. Moreover, the olefin signal between C-19 and C-20 disappeared. The rest signals of both carbon and hydrogen chemical shifts were similar to pyrichalasin H **65**. Based on the above evidence, the structure of compound **161** was confirmed (Figure 2.17 C).¹⁰⁹

Full NMR data of **162** was also achieved and analysis of the data revealed, 29 carbons and 39 protons. The signal of H-25 of pyrichalasin H **65** was again not found from proton NMR and HSQC, also the chemical shift of H-21 move to the lower field due to the presence of a hydroxyl group, the signal of double bond H-6 and H-12 were not found from proton NMR and HSQC, the ¹H-¹H correlations between H-12/H-4 and H-7(3.93-2.41, 3.93-5.49), and the HMBC correlation between H-12 to C-5, C-6, C-7, suggesting that C-6 and C-12 olefin was replaced by a C-12 methyl group linked to C-6. The rest signals of both carbon and hydrogen chemical shifts were similar to **161**. Based

on the above evidence, the structure of compound **162** was confirmed (Figure 2.17 C).¹⁰⁹

Full NMR data was also acquired for **163**. Analysis of its ¹H and ¹³C NMR identified 29 carbons and 37 protons. The signal of H-25 of pyrichalasin H **65** not found from proton NMR and HSQC, also the chemical shift of H-21 move to the lower field due to the presence of the hydroxyl group, the ¹H-¹H correlations between H-12/H-4 and H-7(3.93-2.41, 3.93-5.49), and the HMBC correlation between H-12 to C-5, C-6, C-7, suggesting that the C-6 and C-12 double bond was replaced by a C-12 methyl group linked to C-6. The rest of the signals of both carbon and hydrogen chemical shifts were similar to **162**. Based on the above evidence, the structure of compound **163** was confirmed (Figure 2.17 C).¹⁰⁹

2.3.3.5 Chemical and Genetic Analysis of *pyiD* KO

The liquid extraction of three *pyiD* KO (encoding a P450 vtychromo monooxygenase) mutants were analysed chemically. The result showed the complete abolition of pyrichalasin H **65** from the LCMS chromatogram, and four new peaks were detected **164** (*t_R* = 5.3 min), **165** (*t_R* = 5.7 min), **166** (*t_R* = 6.5 min) and **167** (*t_R* = 7.6 min, Figure 2.18).

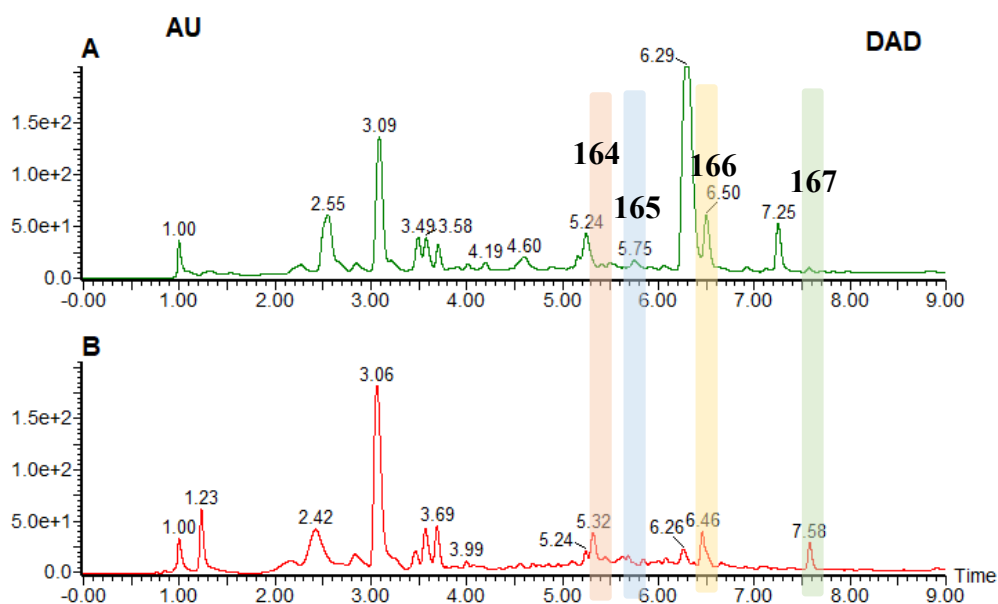
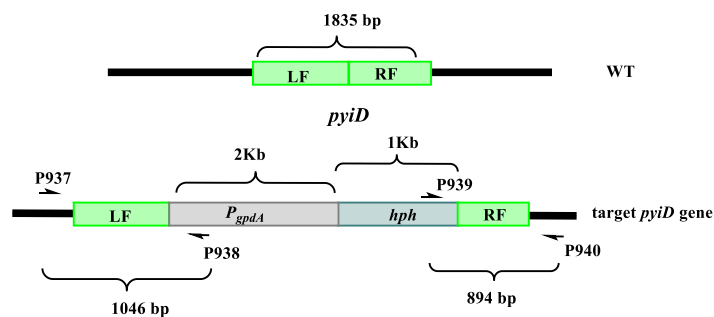


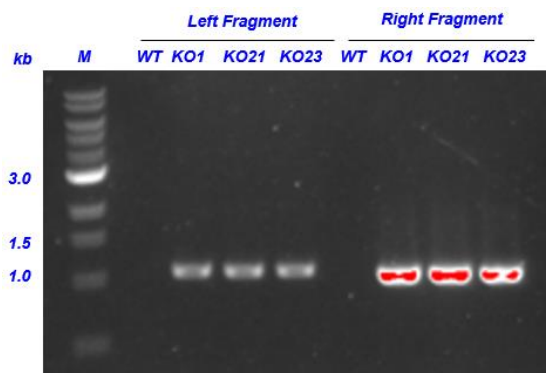
Figure 2.18 LCMS chromatograms (DAD trace) of organic extracts from *pyiD* KO experiments in *M. grisea*.
A, wild type control; **B**, KO strain.

Genetic analysis of the genomic DNA extracted from the *pyiD* transformants was repeated as (Figure 2.19 A, Chapter 6.1.5). The gel picture clearly showed that both the LF and RF were integrated correctly into the genome of transformants (Figure 2.19 B).

A



B



C

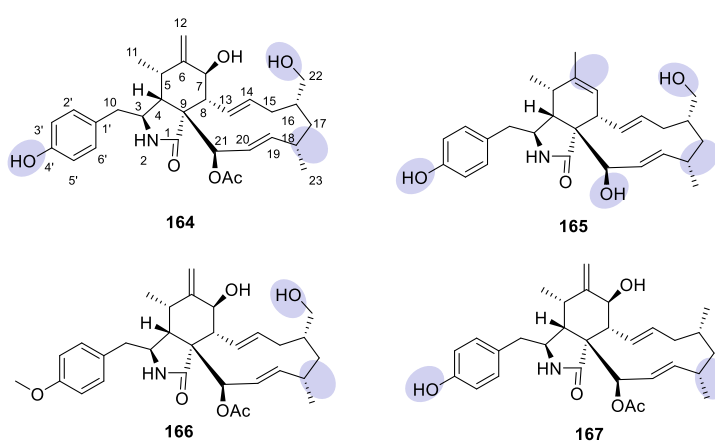


Figure 2.19 A, Genetic analysis of transformants obtained with bipartite marker strategy by PCR; **B**, PCR analysis for confirmation of target gene replacement events at the *pyiD* locus. Expected fragment sizes: left fragment = 1046 bp, and right fragment = 894 bp, M, DNA ladder marker; **C**, structure of isolated compounds.

Compounds **164**, **165**, **166** and **167** were purified, the compound physical data were measured (Table 2.4).

Table 2.4 Compound physical data from *pyiD* KO experiment.¹⁰⁹

Compound Nr.	tR (min)	UV (nm)	HRMS (calculated /found)	Molecular Formula	Titre (mg / L)	Appearance
164	5.3	277, 224	532.2675 /532.2676	C ₃₀ H ₃₉ NO ₆	2.5	white
165	5.7	277	474.2620 /474.2621	C ₂₈ H ₃₇ NO ₄	1.8	white
166	6.5	276, 224	546.2832 / 546.2833	C ₃₁ H ₄₁ NO ₆	3.8	white
167	7.6	278, 211	494.2906 / 494.2905	C ₃₀ H ₄₀ NO ₅	3.1	white

Full NMR data was acquired and analysis of ¹H and ¹³C NMR spectra of **164** identified 30 carbons and 39 protons. The signal of H-22 and H-26 of pyrichalasin H **65** were not found from proton NMR and HSQC, there are clear olefinic signal showed in HSQC ($\delta_H - \delta_C$, 3.26/3.38-67.1), indicating that a methylene attached. The ¹H-¹H correlations between H-22/H-15, and the HMBC correlation between H-22 to C-15, C-16, C-17, suggested that the C-22 methyl group was replaced by methylene connected with a hydroxyl group, but still linked to C-16. The rest fo the signals of both carbon and hydrogen chemical shifts were similar to pyrichalasin H. Therefore, the structure of compound **164** was confirmed (Figure 2.19 C).¹⁰⁹

Full NMR data was acquired and analysis of ¹H and ¹³C NMR spectra of **165** identified 28 carbons and 37 protons. Compared to compound **164**, the signal of H-25 was not found from proton and HSQC spectra of **165**, also the chemical shift of H-21 moved to lower field due to the link of the hydroxyl group. This demonstrated the lack of the acetyl group. The typical methyl signal from HSQC and the HMBC correlation from H-12 to C-5, C-6, C-7, suggested a methyl group was linked to C-6. The rest signals of both carbon and hydrogen chemical shifts were similar to **164**. Putting all above evidence together, the structure of compound **165** was confirmed (Figure 2.19 C).¹⁰⁹

Similarly, the full NMR data of **166** were acquired and summarized, then compared to pyrichalasin H **65**). The ^1H - ^1H correlation spectroscopy (COSY) indicated ^1H - ^1H correlations between H-2',6'/H-3',5', and the HMBC correlation between H-26 and C-4', suggesting the methoxyl group was located at C-4'. The rest signals of both carbon and hydrogen chemical shifts were similar to **65**. Therefore, the structure of compound **166** was confirmed (Figure 2.19 C).¹⁰⁹

The full NMR data was acquired and analysis of ^1H and ^{13}C NMR spectra of **167** identified 30 carbons and 40 protons. Compared to pyrichalasin H **65**, the HMBC spectrum of **167** did not show the correlation between H-26 and C-4', suggesting the cleavage of methoxyl group. Moreover, there is H-18 to C-17 and C-19 from HMBC correlation, suggesting the cleavage of hydroxyl group at C-18. Hence, the structure of compound **167** was confirmed (Figure 2.19 C).¹⁰⁹

2.3.3.6 Chemical and Genetic Analysis of *pyiG* KO

The LCMS results showed 5 mutants from *pyiG* KO (encoding a second P450 monooxygenase) did not produce pyrichalasin H **65**, but five new interesting peaks were detected **168** ($t_{\text{R}} = 6.3$ min), **169** ($t_{\text{R}} = 7.0$ min), **170** ($t_{\text{R}} = 7.5$ min), **171** ($t_{\text{R}} = 7.9$ min) and **172** ($t_{\text{R}} = 8.7$ min, Figure 2.20).

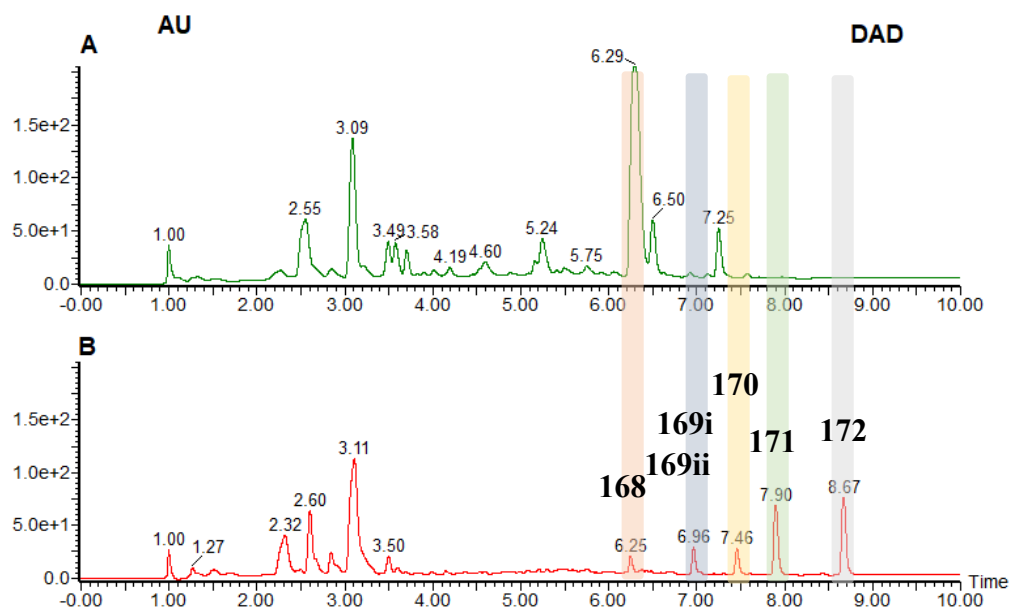


Figure 2.20 LCMS chromatograms (DAD trace) of organic extracts from *pyiG* KO experiments in *M. grisea*. **A**, wild type control; **B**, KO strain.

Genetic analysis of the genomic DNA extracted from *pyiG* KO transformants was done (Figure 2.21 A, Chapter 6.1.5). The agarose gel electrophoresis results showed that both the LF and RF of bipartite substrates were integrated correctly into the genome of *pyiG* transformants (Figure 2.21 B).

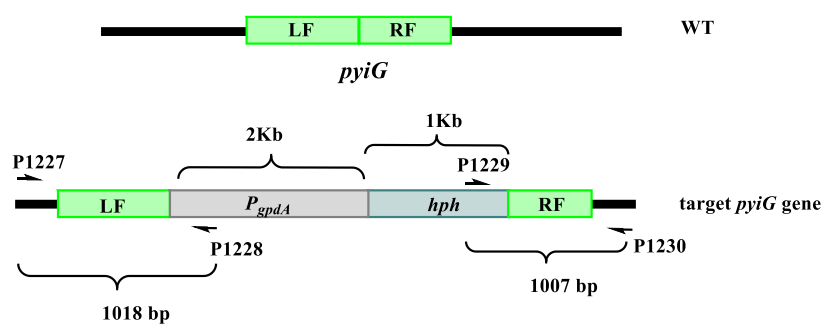
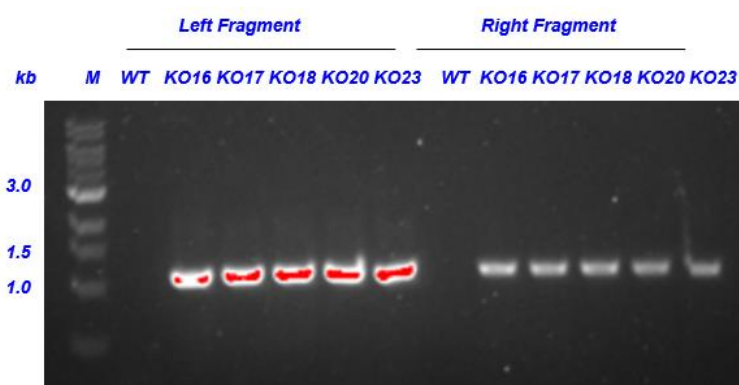
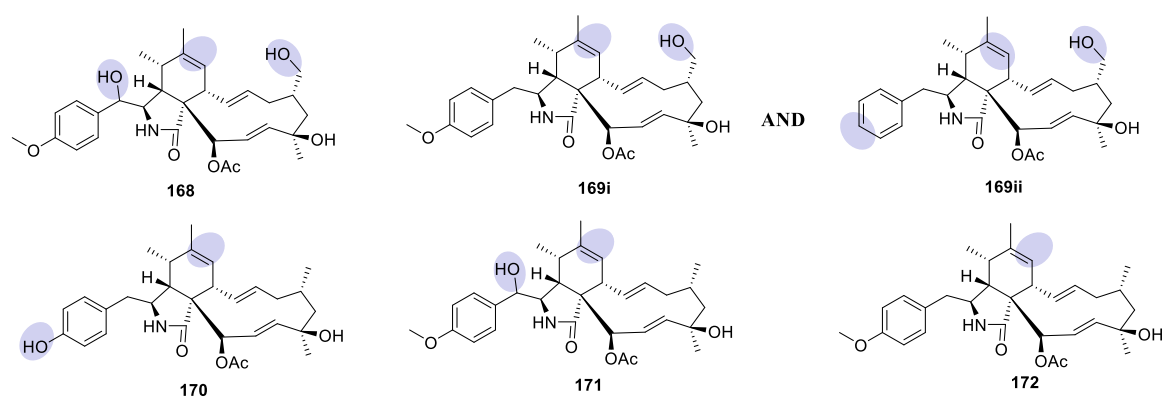
A**B****C**

Figure 2.21 **A**, Genetic analysis of transformants obtained with bipartite marker strategy by PCR; **B**, PCR analysis for confirmation of target gene replacement events at the *pyiG* locus. Expected fragment sizes: left fragment = 1018 bp, and right fragment = 1007 bp, M, DNA ladder marker; **C**, chemical structures of new metabolites isolated from *pyiG* KO experiment.

Compounds **168 -172** were purified, the compound physical data were measured and summarized in Table 2.5.

Table 2.5 Compound physical data from *pyiG* KO experiment.¹⁰⁹

Compound Nr.	tR (min)	UV (nm)	HRMS (calculated /found)	Molecular formula	Titre (mg / L)	Appearance
168	6.3	275, 226	532.2675 /532.2676	C ₃₁ H ₄₁ NO ₇	2.5	white
169i	6.7	276, 211	546.2832 /546.2839	C ₃₁ H ₄₁ NO ₆	3.7	white
169ii	6.7	276, 211	516.2726 / 516.2727	C ₃₀ H ₃₉ NO ₅	3.7	white
170	7.5	276, 227	530.2882 / 530.2876	C ₃₁ H ₄₁ NO ₅	3.9	white
171	7.9	278, 211	546.2832 / 546.2825	C ₃₁ H ₄₁ NO ₆	11.2	white
172	8.7	276, 227	516.2726 / 516.2725	C ₃₀ H ₃₉ NO ₅	23.2	white

Full NMR data of **168** was obtained and after analysis of ¹H and ¹³C NMR spectra 31 carbons and 41 protons were identified. Compared to pyrichalasin H **65**, the signals of alkene carbons H-6 and H-12 were not found from proton and HSQC spectrum, a broad singlet appeared in proton NMR (δ_{H} 1.65) and HSQC ($\delta_{\text{H}} - \delta_{\text{C}}$, 1.65-19.6), the ¹H-¹H correlations between H-12/H-8 (3.19-1.65), and the HMBC correlation between H-12 to C-5, C-6, C-7, suggested that a C-12 methyl group is linked to C-6. In the meantime, the double bond migrated from C-6 and C-12 to C-6 and C-7, proved by the increase of carbon chemical shift of C-6 (137.7) and C-7 (127.4). However, the signal of H-10 methylene group was not observed from proton NMR, instead by the observation of the correlation of ($\delta_{\text{H}} - \delta_{\text{C}}$, 4.48-77.0) from HSQC, combined with the ¹H-¹H correlations between H-10/H-3 (4.48-3.16), and the HMBC correlation between H-10 to C-1', C-3,

suggesting that a hydroxyl group linked to C-10. The ^1H - ^1H correlations between H-22/H-17, and the HMBC correlation between H-22 to C-16, C-17, suggesting that a hydroxyl group was linked to C-22. The rest signals of both carbon and hydrogen chemical shifts were similar to pyrichalasin H. Based on the above evidence, the structure of compound **168** was confirmed (Figure 2.21 C).¹⁰⁹

NMR analysis of **169** revealed that it is actually a mixture of two co-eluting compounds, designated as compounds **169i** and **169ii**. Full NMR data of **169i** was acquired. Compared to **168**, the only difference came from the HMBC correlation from H-10 to C-1' and C-3, which indicated the methylene group at C-10. Therefore, the structure of compound **169i** was confirmed (Figure 2.21 C).

Furthermore, full NMR data of **169ii** was also obtained. The only difference between **169i** and **169ii** is the HMBC correlation from H-4' to C-3', C-4' and C-5', indicating that the cleavage of methoxyl group from C-4'. The structure of **169ii** was elucidated (Figure 2.21 C).

The full NMR of **170** was also fully assigned. Compared to compound **169i**, the signal of C-26 methyl was not found from proton NMR and HSQC, while without the observation of the correlation of H-4' to C-3', C-4' and C-5' from proton and HMBC spectra, suggested the cleavage of C-26 methyl and the hydroxyl group attached to C-4'. The COSY correlations between H-22/H-15, and the HMBC correlation between H-22 to C-15, C-16 and C-17, suggested the methyl group is linked to C-16. Therefore, the structure of compound **170** was confirmed (Figure 2.21 C).

Full NMR spectra of compound **171** was obtained, ^1H and ^{13}C NMR spectra were closely elucidated and identified 31 carbons and 41 protons. Compound **168** was used as template to elucidate the structure of **171**. The ^1H - ^1H correlation spectroscopy (COSY) indicated ^1H - ^1H correlations between H-2',6'/H-3',5', and the HMBC correlation between H-26 and C-4', suggested the methoxyl group was located at C-4'. Meanwhile, the signal of H-10 methylene group not observed from proton NMR, instead by the observation of the correlation of ($\delta_{\text{H}} - \delta_{\text{C}}$, 4.48-77.0) from HSQC, yet the ^1H - ^1H correlations between H-10/H-3(4.48-3.16), and the HMBC correlation between

H-10 to C-1', C-3, suggested that a hydroxyl group was linked to C-10. The remaining signals of both carbon and hydrogen chemical shifts were similar to **168**. Based on the above evidence, the structure of compound **171** was elucidated. (Figure 2.21 C).

Full NMR data of **172** were acquired and analysis of ^1H and ^{13}C NMR spectra, identified 31 carbons and 41 protons. Compared to **171**, the ^1H - ^1H correlation spectroscopy (COSY) showed the ^1H - ^1H correlations between H-2',6'/H-3',5', and the HMBC correlation between H-26 and C-4', suggested the methoxyl group was linked at C-4'. The rest signals of both compound **171** and **172** were similar to each other. Taken all together, the evidence confirmed structure of compound **172** (Figure 2.21 C).¹⁰⁹

2.3.3.7 Chemical and Genetic Analysis of *pyiA* KO

The liquid extracts from *pyiA* KO (encoding the *O*-methyltransferase) transformants showed 5 mutants no longer produced pyrichalasin H **65**, instead two interesting peaks were detected **173** ($t_R = 5.2$ min) and **174** ($t_R = 6.3$ min, Figure 2.22).

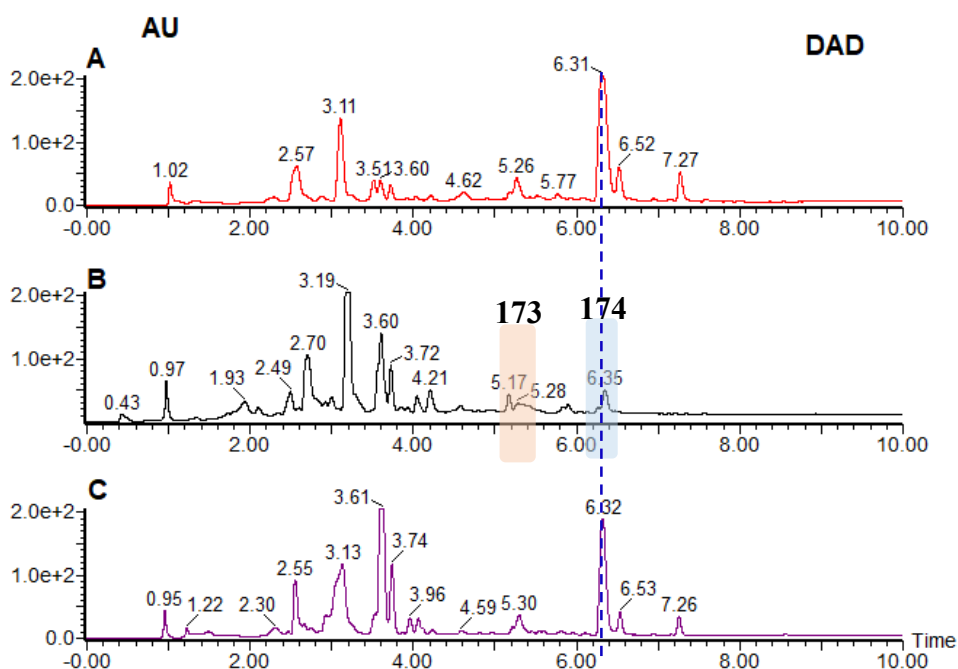
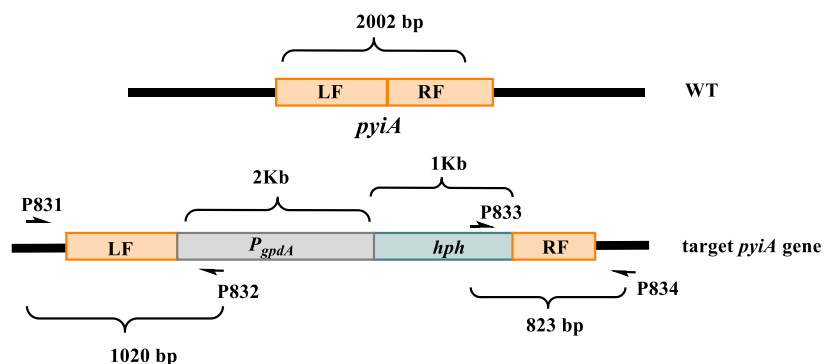


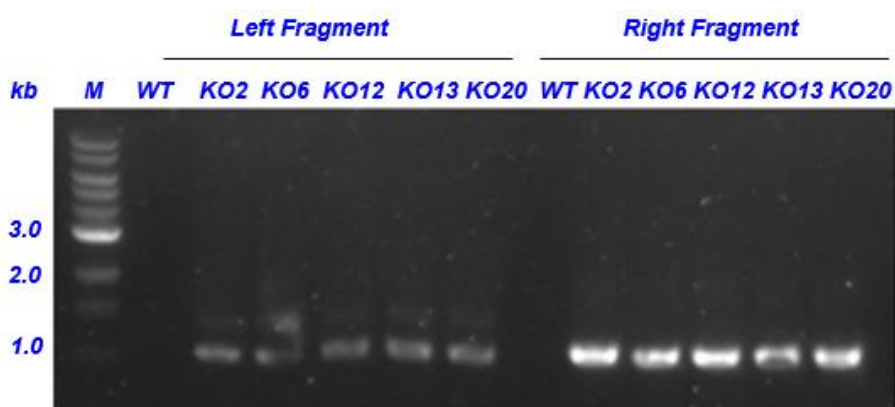
Figure 2.22 LCMS chromatograms (DAD trace) of organic extracts from *pyiA* KO experiments in *M. grisea*. **A**, wild type control; **B**, KO strain; **C**, feeding *O*-methyltyrosine to KO strain.

Genetic analysis of the genomic DNA extracted from the $\Delta pyiA$ transformants was done (Figure 2.23 A, Chapter 6.1.5). The agarose gel electrophoresis results showed that both the LF and RF of bipartite substrates were integrated correctly into the genome of *pyiG* transformants (Figure 2.23 B).

A



B



C

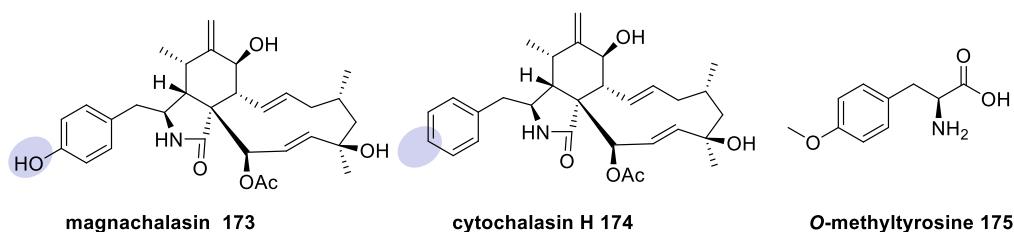


Figure 2.23 A, PCR analysis for confirmation of target gene replacement events at the *pyiA* locus. **B**, expected fragment sizes: left fragment = 1020 bp, and right fragment = 823 bp M: DNA ladder marker; **C**, chemical structures of metabolites isolated from *pyiA* KO experiment.

Compound **173** - **174** were purified, the compound physical data were measured and summarized in Table 2.6.

Table 2.6 Compound physical data from *pyiH* KO experiment.¹⁰⁹

Compound Nr.	tR (min)	UV (nm)	HRMS (calculated /found)	Molecular Formula	Titre (mg /L)	Appearance
173	5.2	277, 211	508.2699 /508.2696	C ₃₀ H ₃₉ NO ₆	2.8	white
174	6.3	218	492.2750 / 492.2753	C ₃₀ H ₃₉ NO ₅	1.0	white

Compound **173** was purified and full NMR data was recorded. This revealed 30 carbons and 39 protons. The signal of the C-26 methyl group not found from proton NMR and HSQC. In the meantime, the lack of the correlation of H-4' to C-3', C-4' and C-5' from proton and HMBC spectra, suggested the loss of the C-26 methyl and the hydroxyl group attached to C-4'. That is the major difference between **173** and **65**. Based on these evidences, we confirmed that **173** is magnachalasin (Figure 2.23 C).

Full NMR data of compound **174** was also acquired. The HMBC correlation from H-4' to C-3', C-4' and C-5', indicated that the cleavage of methoxyl group from C-4'. In the meantime, with the observation of the correlation of H-4' to C-3', C-4' and C-5' from proton and HMBC spectra, suggested the cleavage of hydroxyl group from C-4'. The rest signals of both carbon and hydrogen chemical shifts were similar to pyrichalasin H. Based on these evidence, we confirmed the structure of **174** is cytochalasin H (Figure 2.23 C).

Compound **173** and **174** were fully elucidated by both HRMS and NMR. **173** is the expected de-methyl product. However, the discovery of cytochalasin H **174** is surprising, since it is a known compound derived from phenylalanine and has not previously been detected in *M. grisea* WT culture. Pyrichalasin H is not postulated to derive from phenylalanine, and none of the KO experiments described above indicate that phenylalanine is incorporated, hydroxylated at the para-position and then methylated,

although, several minor isolated compounds do contain a phenyl moiety. An alternative explanation may be the true precursor for PyiS is *O*-methyltyrosine. When PyiA is not functional, *O*-methyltyrosine cannot be synthesized and in its absence, the A-domain of PyiS can select tyrosine and/or phenylalanine. This hypothesis fits with the lower titres of both compounds and a number of intermediates characterized in the KO experiments, *e.g.* **164**, **167**, **169ii**, **170**, **173** and **174** also in low titres.

In order to confirm our hypothesis, *O*-methyltyrosine **175** was fed to a *pyiA* KO strain. *O*-Methyltyrosine (200 mg) was dissolved into double distilled water (10 mg / mL) and filter sterilized. 100 µl of this solution was fed to the Δ *pyiA* knock-out strain inoculated into 500 mL Erlenmeyer flasks containing 100 mL DPY. The feeding was repeated at 24 hour intervals four times. On the 7th day the cultures were extracted.

The feeding result showed the pyrichalasin H production was restored (Figure 2.22 C). This is a convincing experiment to confirm that *O*-methyltyrosine **175** is the real precursor involved in the biosynthesis of pyrichalasin H.

2.4 Discussion & Conclusion

In order to confirm that the *pyi* BGC is responsible for pyrichalasin H biosynthesis, we first targeted the *pyiS* gene by using the bipartite gene knockout (KO) strategy. Functional disruption of the PKS-NRPS resulted in the total disappearance of **65** and **156**. Next, *pyiC* was targeted. This gene encodes a *trans*-ER protein. Production of compounds **65** and **156** was completely abolished, and no new metabolites were detected. These experiments confirmed that pyrichalasin H was synthesized by the enzymes encoded by the *pyi* BGC.

Moreover, all genetically tested transformants possessed a disrupted target gene, while the wild type control showed a non-disrupted result. This indicated that the bipartite substrate cassette combined with protoplast-mediated transformation is a reliable and effective method to disrupt genes in the *M. grisea* strain.

With the purpose of understanding the full biosynthetic pathway to pyrichalasin H and generating novel cytochalasans, we targeted all the tailoring genes individually. These genes were believed to encode enzymes involved in modifying the backbone of pyrichalasin H. Inactivation of *pyiB*, encoding a putative acetyltransferase, led to the

abolition of **65**. The de-acetyl product **156** still exist, but its titre was not greatly increased (Scheme 2.5). Therefore, *pyiB* involved in the biosynthesis of **156** by encoding the *O*-acetyltransferase.

Then, the *pyiA* gene encoding an *O*-methyltransferase, was disrupted. The result showed the total abolition of **65**, and two new metabolites **173** and **174** were obtained in low yield. Both compounds were fully identified by HRMS and NMR. Compound **173** is a tyrosine derived and compound **174** is a phenylalanine derived analogues of **65**. Metabolite **173** is the expected de-methyl product, which confirmed the function of PyiA. However, the appearance of phenylalanine derived cytochalasin H **174** is unexpected. This result also shows that the downstream enzymes are not sensitive to the change in structure of the aromatic ring.

Literature investigation around the engineering of NRPS was done to provide evidences to our novel findings. In the biosynthesis of cyclosporine, various natural amino acids (*e.g.*, tryptophan, tyrosine, phenylalanine) can be incorporated by the NRPS domain to produce novel cyclosporine analogues in *Tolypocladium inflatum*.^{135,136} Moreover, the NRPS adenylation (A) domain is flexible enough to allow incorporation of the modified precursors into the final peptide.

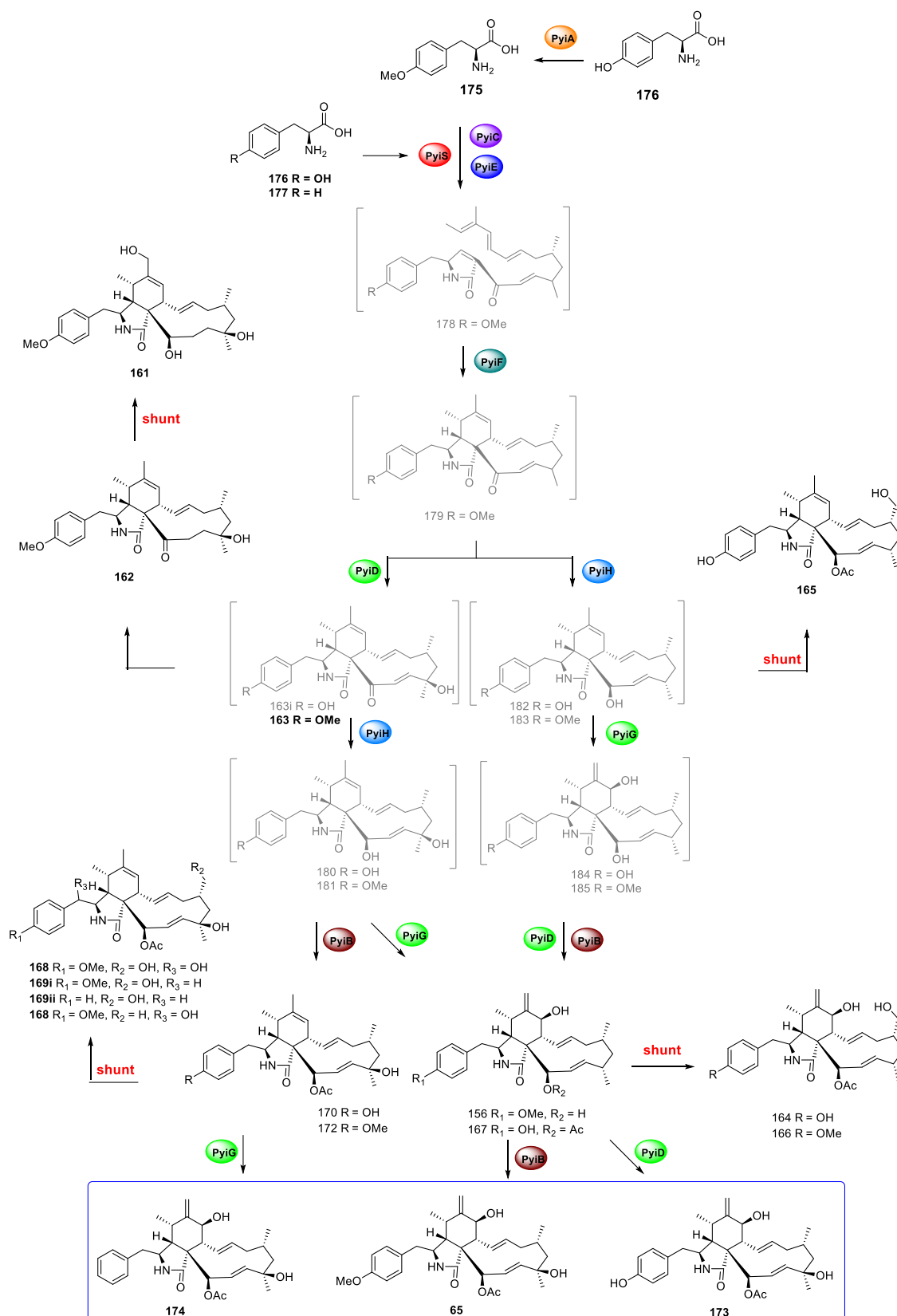
With the support of this evidence, one possible explanation to the *pyiA* KO results is that the A domain of PKS-NRPS prefers to incorporate *O*-methyltyrosine **175**. It can also weakly accept tyrosine and phenylalanine in the absence of **175**. Therefore, *O*-methyltyrosine **175** is the true precursor for the pyrivalasin H biosynthesis. PyiA is involved in the very first step of biosynthetic pathway, rather than the previous assumption that it will methylate the pyrivalasin scaffold in the late stage biosynthesis. To test whether **175** is the true substrate for PyiS, **175** was fed to the *pyiA* KO strain. Pyrivalasin H **65** was restored in a similar titre compared to the WT strain, while compound **173** and **174** were not detected any more. This shows that **175** is the true precursor for the NRPS A domain. Therefore, PyiA methylates tyrosine **176** into *O*-methyltyrosine **175**, then **175** serves as a precursor in the **65** biosynthesis.

Next, *pyiH* encoding an oxireductase was disrupted, resulting in the loss of **65** and production of three novel compounds **161** – **163**. All three compounds were fully elucidated by NMR and HRMS (Figure 2.17 C). The olefin between C-19 and C-20 was

reduced in both **161** and **162**. There is an unusual hydroxyl group at C-12 in **161**, indicating other cryptic enzymes involved, therefore **161** is produced as a shunt metabolite. **163** was obtained in a very low yield, result in some signal missing from NMR spectra, but the key functional groups can be identified. All three compounds contain the C-21 carbonyl group, which confirmed that the function of PyiH is to reduce the carbonyl group into a hydroxyl group, followed by the PyiB transfer of an acetyl group to it.

Disruption of the P450 monooxygenase encoded by *pyiD*, led to the complete abolition of **65** and production of four new compounds **164** - **167**. Structure elucidation was done and described in section 2.3.2 (Figure 2.19 C). All compounds lack a hydroxyl group at C-18, indicating PyiD introduces a hydroxyl group at C-18, therefore, it is a C-18 hydroxylase. Compound **164**, **165** and **166** all contain a C-22 hydroxyl group, this result can be explained by the modification of unknown enzymes, these three compounds can be regarded as shunt products.

The second P450 monooxygenase encoded by *pyiG*, was disrupted, causing the loss of **65**, and production of five new compounds **168** – **172**. Structure elucidation (described in section 2.3.2, Figure 2.21), showed that all compounds lacked a hydroxyl group at C-7, indicating PyiG is a C-7 hydroxylase. Compound **169** turned to be **169i** and **169ii** based on the NMR analysis. Compound **168**, **171**, **169i** and **169ii** are shunt products as they all contain a C-22 hydroxyl group, which was assumed to be modified by cryptic enzymes. Especially, compound **168** and **171** has another hydroxyl group at C-10.



Scheme 2.5 Putative late-stage Biosynthetic Pathway of Pyrichalasin H **65** and Isolated Intermediates.¹⁰⁹

Taken together, these results reveal the overall biosynthetic pathway of pyrlichalasin H (Scheme 2.5). In the early step, PylA transfers a methyl group from SAM **36** to tyrosine to generate *O*-methyltyrosine **175**, which is then the preferred substrate of the PylS A-domain. Compound **178** is then probably released as an intermediate before a Knoevenagel condensation, possibly catalysed by PylE, then followed by a putative Diels-Alder cyclization, possible catalysed by PylF to form the pyrlichalasin backbone **179** as a putative middle stage product. All compounds isolated featured the tricycle core typical of the cytochalasans showing that this is formed before the late-stage enzymes investigated here, and after the activity of PylS / PylC.

Then the biosynthetic route branches into two directions. On the first branch, PylD is one of the first tailoring enzyme to act due to the observation of **161** and **162** in the PylH KO. The PylH KO intermediate **163** went off the pathway to give the shunt products **161** and **162**. Both PylB and PylG can modify the intermediate **180** and **181** which has already been decorated by PylH, to give **156**, **170** and **171** in parallel. These compounds will be further substrates of PylB and PylG to give the final products **65** and **174** (shown in green rectangle, Scheme 2.5). Compound **170** and **172** will further leave the pathway by the formation of shunt compounds **168** - **171**.

On the second branch, PylH first acts on the Diels-Alder product **179**, to give **182** and **183**. Then PylG catalyses a hydroxylation reaction on **182** and **183** to produce **184** and **185**. The compound **184** and **185** were modified by PylB and PylD at the same time to give **156** and **167**. Again, catalysis happened on both **156** and **167** to generate compounds **65** and **73** (shown in green rectangle, Scheme 2.5). Compound **164** and **166** were released as shunt products.

The tailoring enzymes which are all able to act on more than one substrate lead to the complexity of this pathway. In addition, when PylA is absent, the PylS A-domain is able to select phenylalanine and/or tyrosine, this can be explained by the observation of **164**, **165**, **167**, **169ii**, **170**, **173** and **174**. PylB, PylD and PylG can modify many different substrates. This can be observed by the discovery of **156**, **163**, **167** and **172**. The three tailoring enzymes also participated in the production of the final compounds **65**, **173** and **174**.

There are several reported cases regarding the pathway investigation of cytochalasans. Watanabe and co-workers elucidated the function of redox enzymes during the

biosynthesis of Chaetoglobosin A **63** (Chapter 1.3.1).¹³⁷ Tang and co-workers investigated the regulator gene *ccsR* in the *A. clavatus* BGC.¹³⁸ They also determined the function of Baeyer–Villiger monooxygenase (BVMO) during the biosynthesis of cytochalasins E **64** and K **82** (Chapter 1.2.2).⁶⁹ However, no one fully elucidated the complete pathway for cytochalasin biosynthesis. To the best of our knowledge, this is the most comprehensive study of cytochalasin biosynthesis to date.

3 Combinatorial Biosynthesis of Late Stage Cytochalasan Tailoring Cytochrome P450 Monooxygenases

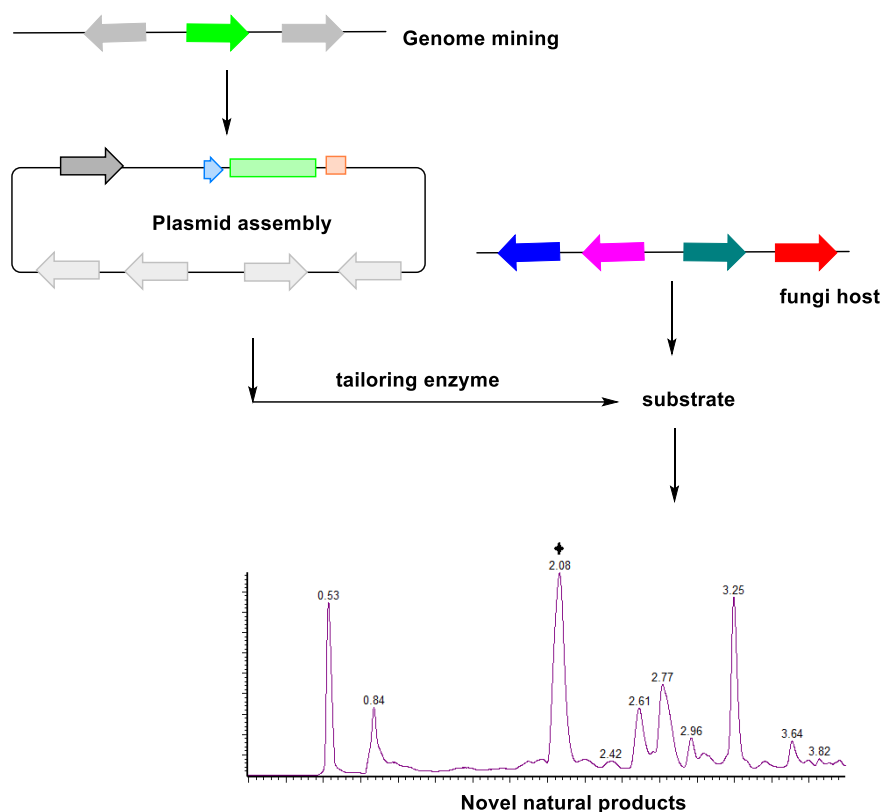
Partial results of the presented work have been published in *Org. Lett*, 2019, 21, 8756 – 8760.¹³⁹

3.1 Introduction

Combinatorial biosynthesis can be defined as the application of genetic engineering to modify biosynthetic pathways encoding natural products in order to generate novel and decorated architectures using nature's biosynthetic machinery. Heterologous expression techniques play an important role in this strategy.¹⁴⁰

3.1.1 Heterologous Expression

Heterologous expression has been used as a major tool in the study of fungal synthetic biology, it can not only allow us to study fungal enzymes/pathways in different hosts, but also shows the capability of fungi to be the heterologous host. Heterologous expression of fungal natural product (NP) gene or gene cluster that use a host from the same species lead to positive results in most cases. Moreover, the chances of success will also be improved by using a host that already exhibits the ability of producing NP. Heterologous expression can also be used as an effective method in the discovery of novel NP (Scheme 3.1).¹⁴¹



Scheme 3.1 Structures of synthetic biology strategy for natural product production in filamentous fungi.¹⁴¹

Moreover, successful NP production needs not only a good host, but also the involvement of different enzymes. Understanding their biosynthesis requires expression of several genes simultaneously. Plasmids which contain one or more expression genes have been designed to provide high-level expression in filamentous fungi.¹⁴¹

Lazarus and co-workers developed the multigene expression vector pTYGS-bar, which has the herbicide glufosinate ammonium (*bar*) as a selection marker, contains four fungal promoters/terminators (*P/T_{amyB}*, *P/T_{adh}*, *P/T_{gpdA}*, *P/T_{eno}*). The shuttle vector contains the 2 μ origin of replication and the *URA3* gene for plasmid maintenance and the selection in *ura3* mutant strains of yeast.¹⁴² For selection and propagation in *E. coli* the vector contains an appropriate ori (*colE1*) and confers resistance to chloramphenicol (*camR*) as well as ampicillin (*ampR*). The plasmid was designed with *attR1* and *attR2* recombination sites adjacent to *P_{amyB}* and *T_{amyB}*, respectively. A Gateway destination cassette, comprising a kanamycin (*kanR*) resistance gene and the toxic *ccdB* gene flanked by *attR1* and *attR2* sites was inserted into the expression vector (Figure 3.1).¹³⁴

Three of these cloning sites include an *AscI* restriction sequence (P/T_{adh} , P/T_{gpdA} , P/T_{eno}) and are designed for *in vivo* homologous recombination in *S. cerevisiae*. The general process of assembling the multigene expression vector starts from the digestion of the plasmid with *AscI*. Then the tailoring enzyme coding regions are amplified from genomic DNA, and the amplified fragments and restriction digest are examined by agarose gel electrophoresis. Finally, the target vector is assembled by co-transformation of DNA fragments and the digested plasmid in yeast.¹⁴³

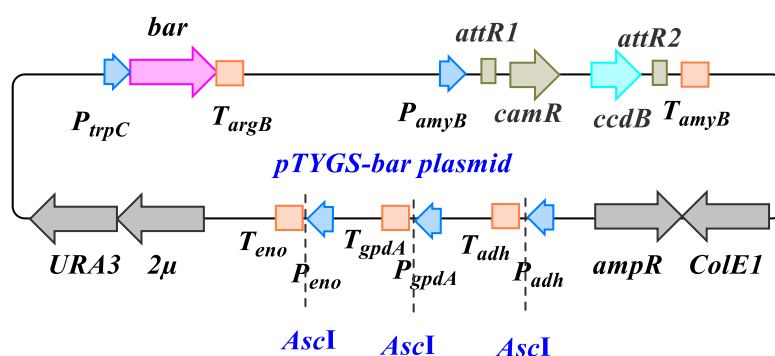


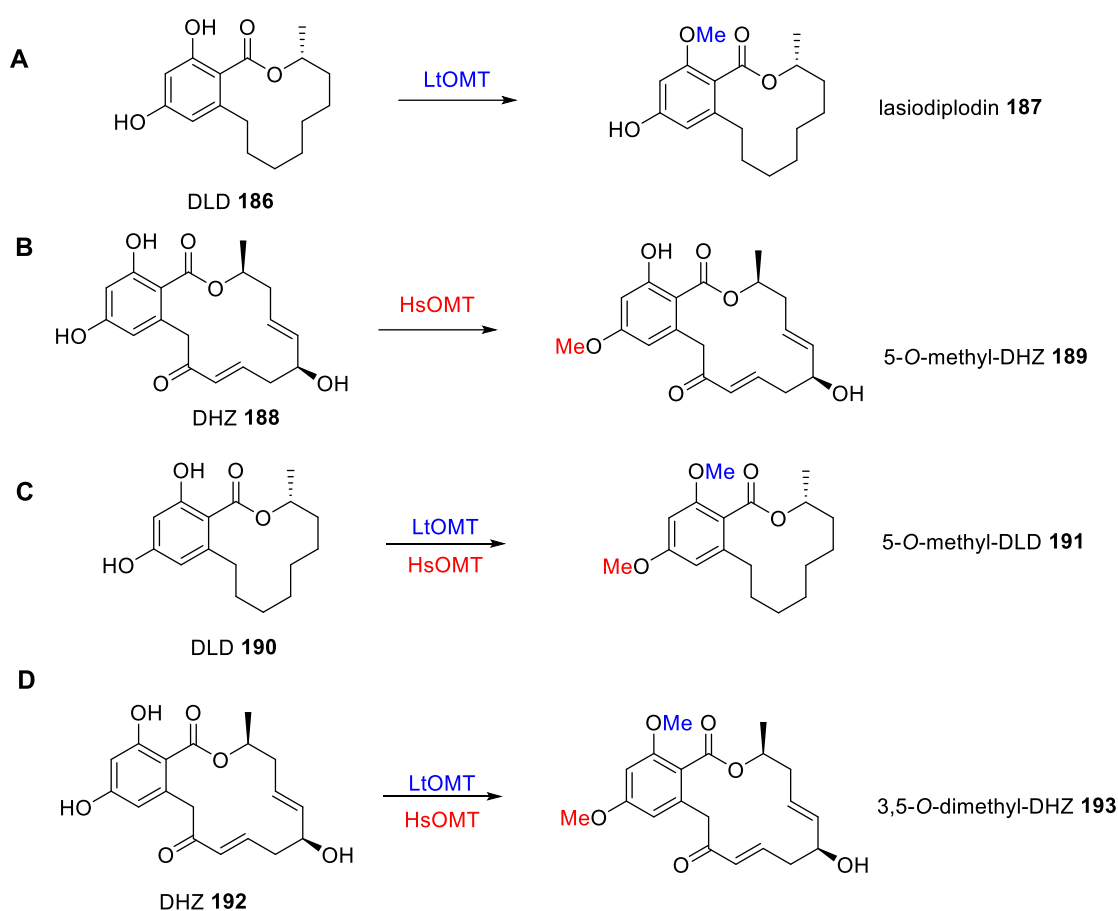
Figure 3.1 Structures of multigene expression vector pTYGS-bar.¹³⁴

3.1.2 Benzenediol Lactone Engineering

Fungal benzenediol lactone (BDL) polyketides exhibit many of bioactivities, including immune system modulatory effects and heat shock response, serving as an important pharmacophore. BDL backbones are biosynthesized by pairs of collaborating, sequentially acting iterative polyketide synthases (iPKSs), forming quasi-modular BDL synthases (BDLSs).¹⁴⁰

O-methylation has been engineered in natural product biosynthetic pathways by disrupting the genes encoding native *O*-methyltransferase (*O*-MeT) enzymes or augmenting the pathways with genes for heterologous *O*-MeT. Molnar and co-workers have described a combinatorial biosynthesis strategy to modulate the BDL scaffolds. They identified two orthologous *O*-MeT, LtOMT and HsOMT involved in the biosynthesis of two fungal benzenediol lactones.^{144,145} LtOMT obtained from *Lasiodiplodia theobromae* methylates the C-3 phenolic hydroxyl of the demethylasiodiplodin (DLD) **186** to produce lasiodiplodin **187** (Scheme 3.2 A).

HsOMT from *Hypomyces subiculosus* methylates the C-5 phenolic hydroxyl of dehydrozearalenol (DHZ) **188** to afford 5-*O*-methyl-DHZ **189** (Scheme 3.2 B), an intermediate of hypothemycin. To investigate whether these regiospecific enzymes can modify different substrates, Molnar and co-workers used *S. cerevisiae* as a host to co-express LtOMT and HsOMT with the DLD-producing iPKS pair and DHZ-synthesizing pair, separately. Luckily, both *O*-MeTs recognise the BDL substrates offered by the non-cognate iPKS pairs to produce the desired double *O*-methylated product (Scheme 3.2 C&D).¹⁴⁴



Scheme 3.2 Combinatorial biosynthesis of *O*-methylated BDLs using LtOMT and HsOMT.¹⁴⁴

This example confirms that combinatorial biosynthesis can be a good strategy for pathway engineering and generate novel compounds.

3.2 Aims

Previous knockout (KO) experiment targeting pyrichalasin H **65** produced by *Magnaporthe grisea* showed that the tailoring enzymes are promiscuous and can modify a range of cytochalasan intermediates. However, the tailoring modifications are highly regio-selective, they can only recognize part of the cytochalasan molecule. For example, P*yi*D can only catalyses a hydroxylation reaction at C-18 and P*yi*G can only catalyses a hydroxylation reaction at C-7. The differences between different cytochalasan skeletons away from the reaction region are not important enough to disrupt the enzyme functions.

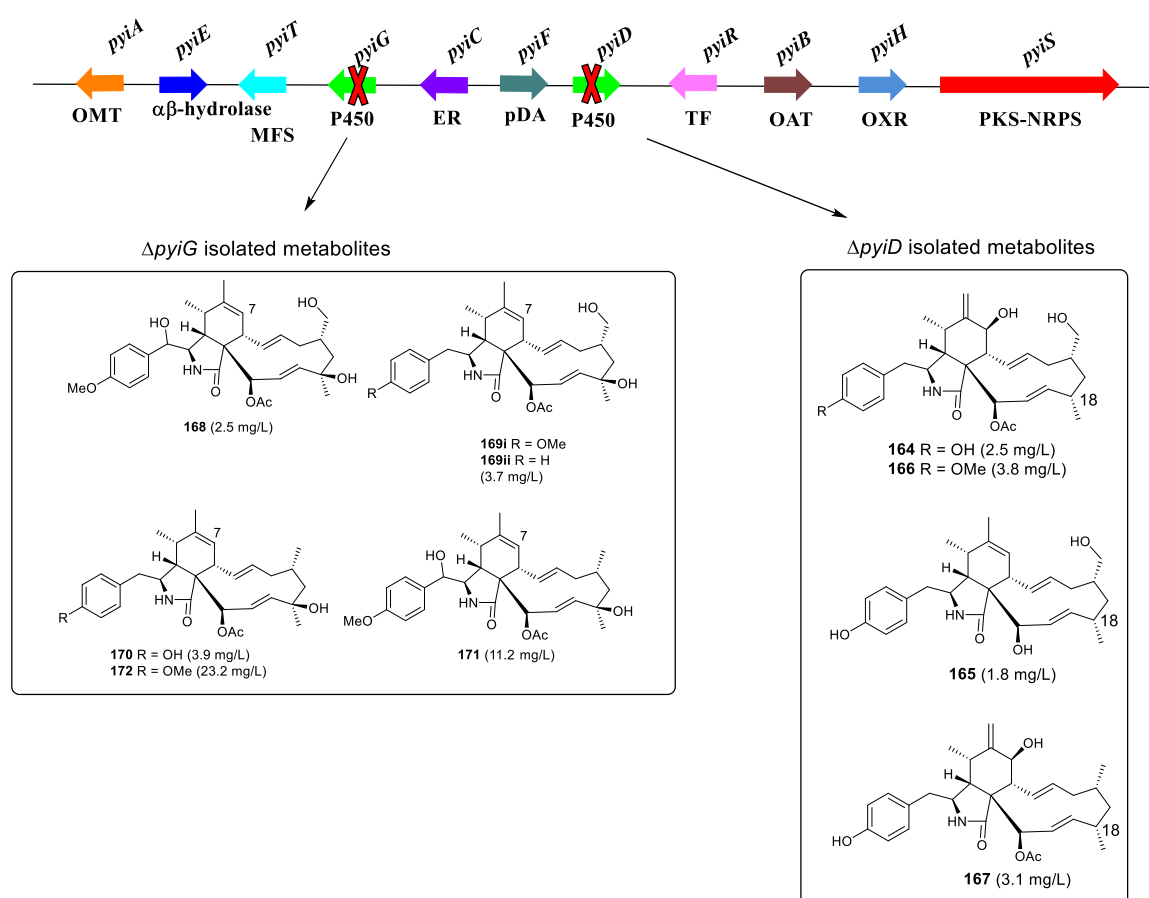


Figure 3.2 Structures of metabolites isolated from *M. grisea* NI980 P450 mutant strain.

To investigate the range of the promiscuity of the tailoring genes during cytochalasan biosynthesis, we decided to use the P450 disruption strain (Δ *pyiD* and Δ *pyiG*) as a bioengineering platform and use the combinatorial biosynthesis approach to heterologously express modification genes (such as P450s, BVMO and *O*-MeT) from other putative cytochalasan biosynthetic gene clusters (BGC). The result would achieve

two goals: firstly, to elucidate the biological role of cryptic enzymes, and secondly, to generate novel cytochalasins by introducing tailoring genes from other BGC.

3.3 Results

3.3.1 Combinatorial Biosynthesis with *ccsB* into *Magnaporthe grisea* NI980 *pyiH* Disruption Strain

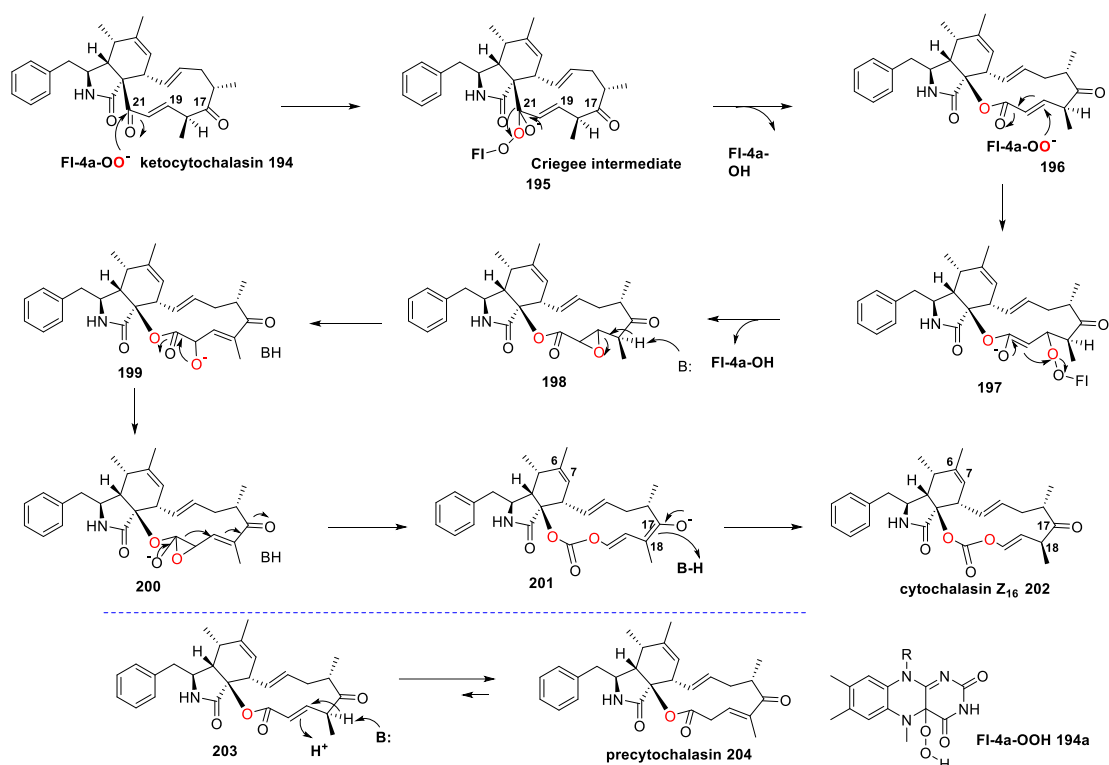
3.3.1.1 Introduction

The *ccsB* gene (ACLA_078650) comes from the cytochalasin E BGC of *Aspergillus clavatus* NRRL1. The size of *ccsB* is 1967 bp with only one intron. Tang and co-workers have already elucidated the function of *ccsB*. It is the first reported carbonate-forming Baeyer-Villiger monooxygenase in fungi.⁶⁹

CcsB has been confirmed to catalyse the formation of an in-line carbonate in the macrocyclic portion of cytochalasin E.⁶⁹ The beginning step is a classic BVMO mechanism of oxygen insertion, FI-4a-OO⁻ **194a** on C-21 of **194** forms the intermediate **195** (Scheme 3.3). Expected migration of tertiary C-9 to the distal oxygen on FI-4a-OO⁻ leads to release of FI-4a-OH and formation of ester **196**. Release of ester **196** into an aqueous environment can generate the observed shunt product **204**. In another way, **196** can remain in the active site of CcsB or be recaptured by CcsB and undergo further oxidation to yield **202**.^{146,147} After reduction and regeneration of FI-4a-OO⁻, it was supposed the nucleophilic FI-4a-OO⁻ complex performs a 1,4-conjugate Michael addition at C-19 to yield adduct **197**, which leads to the formation of epoxide **198**. Epoxidation of the $\alpha\beta$ -unsaturated ester is observed in the cytochalasin family, such as in the epoxycytochalasin compounds.

Subsequently, base-catalysed abstraction of the acidic α -proton leads to formation of the vinylogous C-17 ketone and the alcoholate anion species **199**. Attack at the neighbouring carbonyl group affords an epoxy alkoxide **200**, which can readily rearrange with aid of the distal vinylogous ketone to yield the enolate **201**. Moreover, ketonization of C-17 followed by proton abstracting from the protonated general base

affords the carbonate **202**. Unlike **204**, **202** does not undergo double bond migration, possibly due to resonance stabilization through the carbonate oxygen. Examples of the rearrangement of the α -hydroxyl, β -diketones into esters have been reported in literature,¹⁴⁸ and can proceed under thermal or basic conditions *via* the proposed epoxy-tetrahedral intermediate such as shown in **200**. Furthermore, an example of Lewis-acid-promoted conversion of an α -hydroxyl, β -dicarbonyl compound to a carbonate rearrangement has been reported (Scheme 3.3).¹⁴⁹



Scheme 3.3 Proposed reaction mechanism of *ccsB* in converting **194** to **202** and **204**.⁶⁹

3.3.1.2 Aim

The *ccsB* gene from *A. clavatus* has been confirmed to encode the BMVO and catalyse the insertion of two oxygen atoms between carbonyl in the macrocycle of cytochalasin E. Previous knockout (KO) experiment targeting *pyiH*, resulted in the isolation of three novel compounds **161** - **163** (details are described in chapter 2.3.1, Figure 3.3). All three compounds contain the carbonyl group in the macrocycle. They are similar to **194**, but lack the keto function at C-17, and hydroxylation at C-16 would prevent the second

oxidation, but the first oxidation could work. The purpose of heterologous express *ccsB* into Δ *pyiH* strain is try to determine if CcsB can catalyse the oxygen insertion into the KO substrates **161-163**. Moreover, we want to generate some novel carbonate pyrichalans by combinatorial biosynthesis of *ccsB*.

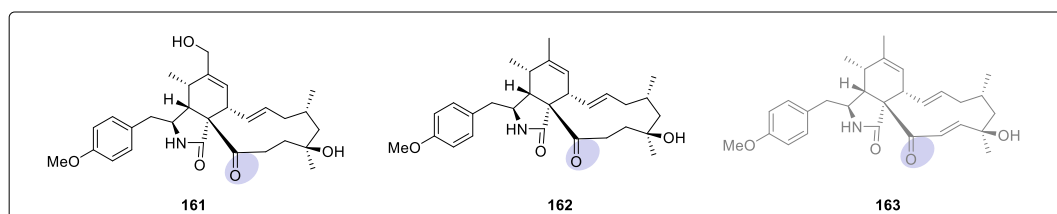
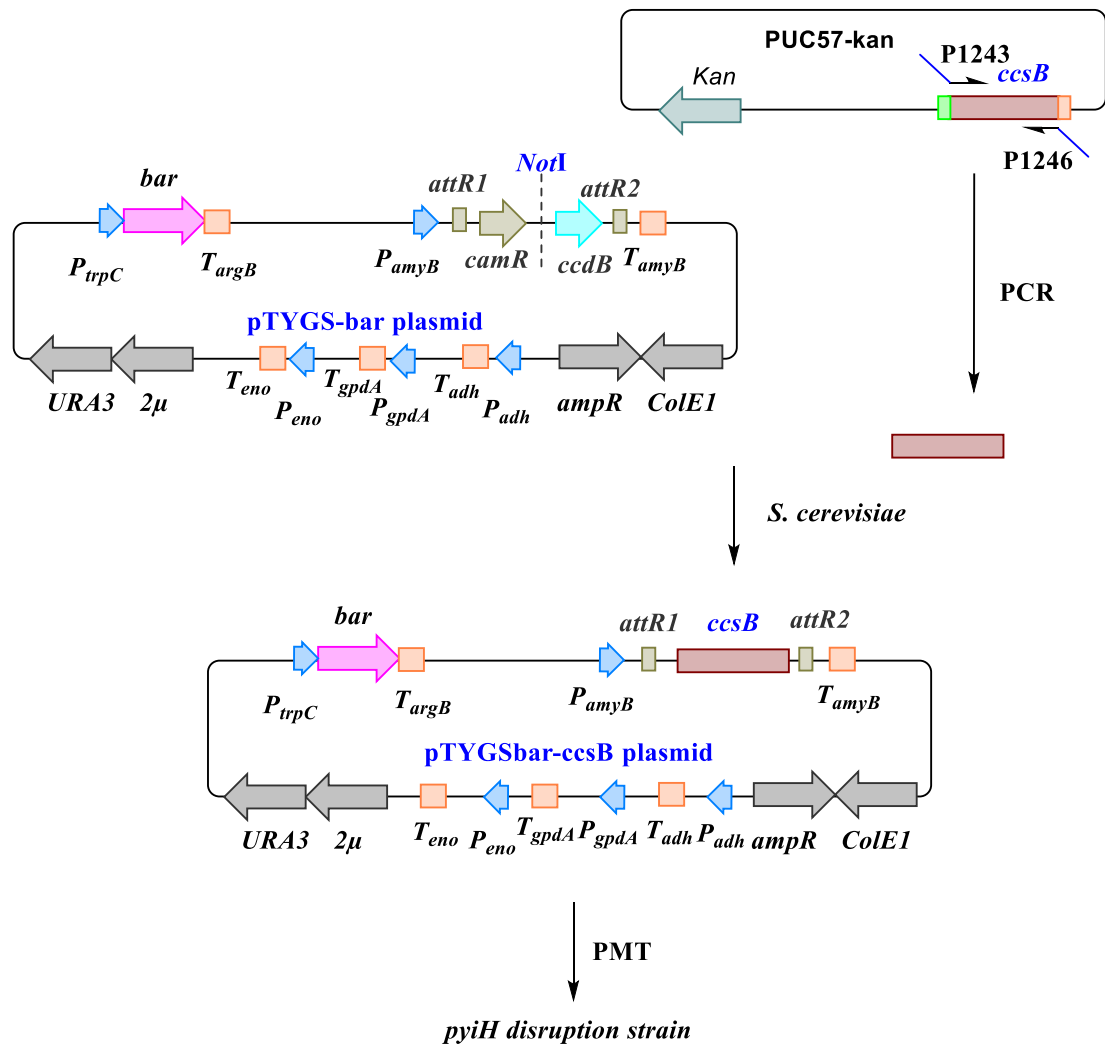


Figure 3.3 Structures of metabolites isolated from *M. grisea* NI980 *pyiH* mutant strain.

3.3.1.3 Vector Construction and Gene Transformation

The detailed information of pTYGS-bar plasmid has been described in section 3.1.1.¹⁴² There is a *NotI* restriction sequence between the *P/T_{amyB}* positions. The pTYGS-bar plasmid was first digested by *NotI*. The *ccsB* fragments were amplified from plasmid PUC57-kan vector (*ccsB* gene was codon optimized before synthesis, purchased from BASECLEAR). *S. cerevisiae* was then used to assemble the vector and gene by homologous recombination (LR) in the desired order as the DNA fragments include 30 bp unique homologous overlap sequence. These were introduced by PCR through tails at the designed oligonucleotides. The desired pTYGSbar-*ccsB* vector was purified from *S. cerevisiae* and propagated in *E. coli* TOP10. The verified vector was transformed into *pyiH* disruption protoplaste by PMT. Hygromycin B was used as the selection marker for KO experiment, previously. *M. grisea* is also sensitive to glufosinate ammonium (basta). So it can be used as the second selection marker for heterologous expression *ccsB* gene into *pyiH* KO strain (Scheme 3.4).



Scheme 3.4 General procedure for assembly of heterologous expression vector for *ccsB* gene in pTYGSbar by yeast homologous recombination (HR) and protoplast-mediated transformation (PMT).¹⁴²

3.3.1.4 PCR Analysis of pTYGSbar – *ccsB*

The pTYGSbar-*ccsB* plasmids were analysed by PCR (Chapter 6.1.5). Twenty transformants were obtained from three rounds of selection with basta as a second selection marker, 4 out of 20 transformants were confirmed as positive by PCR (Figure 3.4).

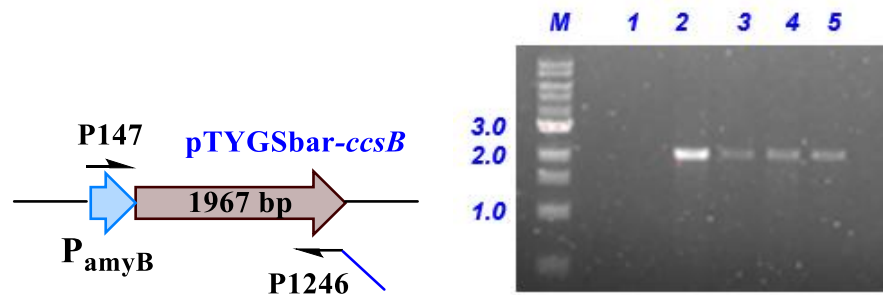


Figure 3.4 Agarose gel electrophoresis analysis for confirmation of *ccsB* genes fused into the genome of *M. grisea* Δ *pyiH*; M, DNA ladder marker (kb), different colonies are represented by numbers.

3.3.1.5 Chemical Analysis

Liquid extraction from the *ccsB* heterologous expression strain led to no observed change in the metabolite profiles compared to the *pyiH* KO metabolites (Figure 3.5).

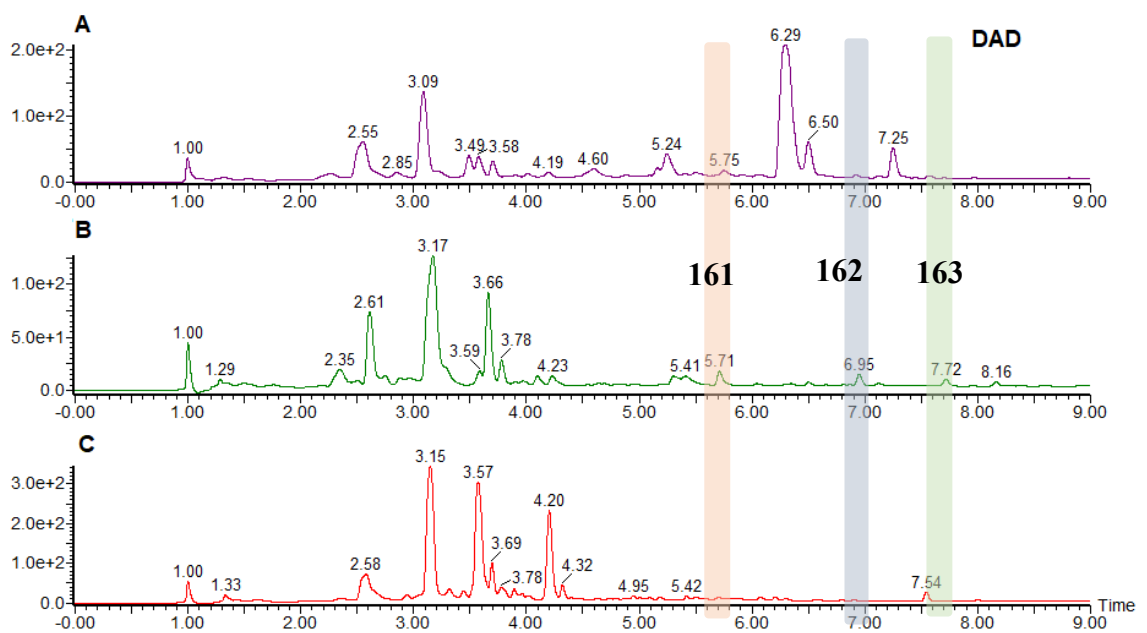


Figure 3.5 LCMS chromatogram (DAD trace) of *ccsB* heterologous expression into *M. grisea* Δ *pyiH* extracted on the 7th day from DPY medium. **A**, *M. grisea* WT; **B**, *M. grisea* Δ *pyiH*; **C**, *ccsB* heterologous expression into *M. grisea* Δ *pyiH*.

According to the catalytic mechanism of BVMO mentioned above, the catalytic substrates for CcsB are ketones in the macrocyclic portion of cytochalasans.¹⁴² In the *ΔpyiH* strain, compound **161**, **162** and **163** all contains a ketone group, make them good substrates participate in the oxidation reaction. However, there were no any carbonate products found in the *ccsB* expression experiment. One possible reason would be the extremely low yield of the ketone metabolites, CcsB cannot functionalise in low concentration. Secondly, although the *ccsB* gene from *A. clavatus* have already been codon optimised in order to fit in *M. grisea*, for some un-known reasons, it is still difficult for *ccsB* to express properly in another different fungal species. Also we know PamyB is relatively weak promoter in *M. grisea*.

3.3.2 Heterologous Expression of Cryptic Cytochalasan P450s into *Magnaporthe grisea* NI980 P450 Disruption Strain

3.3.2.1 Bioinformatic Analysis of P450s from *Hypoxylon fragiforme* Gene Cluster

Hypoxylon fragiforme MUCL 51264 was proved to be responsible for the biosynthesis of cytochalasin H **174**, deacetylcytochalasin H **205**, epoxycytochalasin H **206**, fragiformin E **207**, L-694,474 **208**, and L-687,318 **209** (Figure 3.6).¹²⁸ Cytochalasin H **174** has an almost identical structure to **65**, the only difference is the 4'-*O*-methyl of pyrivalasin H. Methyltyrosine is a precursor of **65**, while **174** incorporates phenylalanine.¹²⁹ Compounds **205** and **208** are precursors of **174**, while compounds **206**, **207** and **209** appeared to be various derivatives.

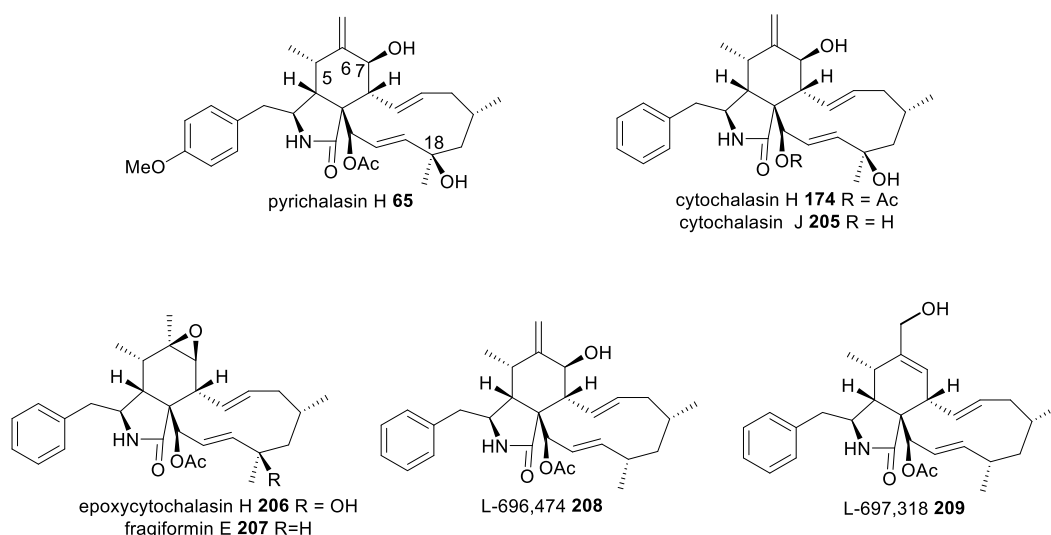


Figure 3.6 Structures of metabolites isolated from *Hypoxylon fragiforme* MUCL 51264.^{14,129}

Genome sequencing of *H. fragiforme* MUCL 51264 was achieved and analysed by Dr Eric Kuhnert. Only two BGC contained PKS-NRPS genes, and only one of them contained genes encoding an α,β -hydrolase and a putative Diels-Alderase (pDA) which are indicative of cytochalasan BGC.¹⁵⁰ This putative cytochalasan BGC was assigned as the *hff* nomenclature (Table 3.1, GenBank accession no. MN477016). Gene annotation were executed by using fungiSMASH,¹⁰⁸ GenDBE, and FGENESH.¹⁵¹ In total ten genes were identified in the *hff* gene cluster: a PKS-NRPS (*hffS*); a trans-ER (*hffC*); a putative Diels-Alderase (*hffF*); an oxidoreductase (*hffH*); an acetyltransferase (*hffB*); a transporter (*hffT*); an $\alpha\beta$ -hydrolase (*hffE*); two P450s (*hffD* and *hffG*); and a transcription factor (*hffR*).¹³⁹

Table 3.1 Gene annotation of the putative cytochalasan BGC of *H. fragiforme* MUCL 51264.¹³⁹

<i>Gene</i>	<i>Trivial name</i>	Putative Function	Homology	Nucleotide identity (%)
<i>H.fragiforme_g4342.t1</i>	<i>hffH</i>	Oxidoreductase	PyiH	80.2
<i>H.fragiforme_g4344.t1</i>	<i>hffB</i>	Acetyltransferase	PyiB	68.8
<i>H.fragiforme_g4345.t1</i>	<i>hffR</i>	Transcriptional regulator	PyiR	50.0
<i>H.fragiforme_g4346.t1</i>	<i>hffE</i>	$\alpha\beta$ -Hydrolase	PyiE	77.4
<i>H.fragiforme_g4347.t1</i>	<i>hffT</i>	MFS transporter	PyiT	74.1
<i>H.fragiforme_g4348.t1</i>	<i>hffS</i>	PKS-NRPS	PyiS	75.0
<i>H.fragiforme_g4349.t1</i>	<i>hffD</i>	Cytochrome P450	PyiD	80.9
<i>H.fragiforme_g4350.t1</i>	<i>hffF</i>	Putative Diels-Alderase	PyiF	80.6
<i>H.fragiforme_g4351.t1</i>	<i>hffC</i>	<i>Trans</i> -enoyl reductase	PyiC	85.0
<i>H.fragiforme_g4352.t1</i>	<i>hffG</i>	Cytochrome P450	PyiG	76.3

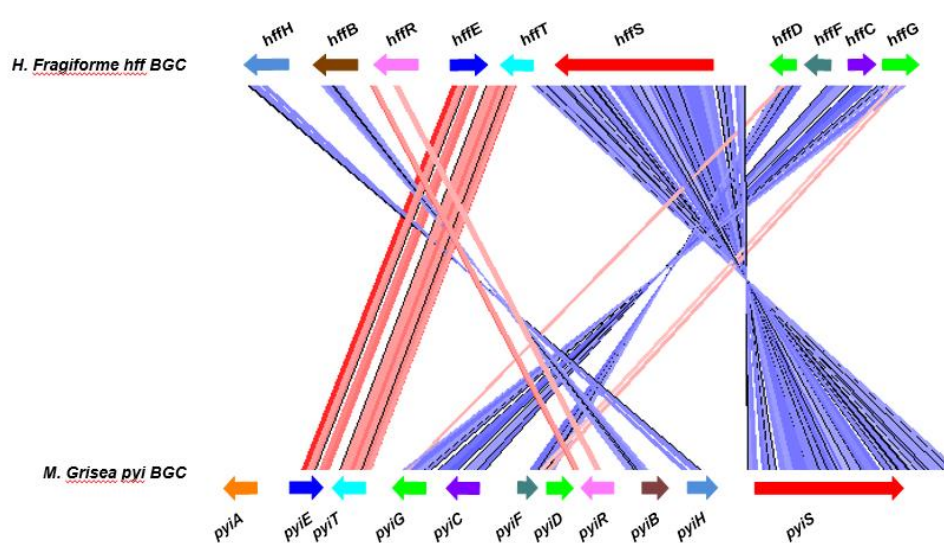


Figure 3.7 Artemis comparison of cytochalasan BGC identified in *Magnaporthe* sp. *M. grisea* NI980 BGC (bottom) and *H. fragiforme* *hff* BGC (top).

Artemis comparison between *M. grisea* NI980 and *H. fragiforme* were executed. This showed two differences between the clusters. First, compared to *M. grisea* NI980, the BGC identified in *H. fragiforme* MUCL 51264 does not encode an *O*-methyltransferase, which is expected since **207** does not require *O*-methyltyrosine for its biosynthesis. Second, the gene order and the orientation of the homologues are not conserved (Figure 3.7). Similar comparison between *M. grisea* NI980 and *P. oryzae* Guy11 were done and described in chapter 1.4.3. Sequence alignment showed *hffD*, a gene encoding a P450 has 80% sequence similarity with *pyiD*. Next, *hffG* has 75% sequence similarity to *pyiG*, while only 20% identity with *pyiD* (Table 3.2).

There are four P450 genes *CYP1-4* in the *P. oryzae* ACE1 BGC (Chapter 1.4.3). Alignment showed that *pyiD* shares more sequence similarity to *CYP4* (49% identity) and *pyiG* shares more similarity to *CYP3* (40% identity). *CYP1* has 38% similarity with *pyiD* and *CYP2* shares 34% identity with *pyiG* (Table 3.2). However, these similarities were not recognised by the Artemis comparison tool. One possible reason might be that the bioinformatics predictions create a confusion between *pyiD* and *pyiG*.¹⁵⁰

Table 3.2 Sequence % similarity analysis of the P450s used in this study.¹³⁹

	<u>PviD</u>	<u>HffD</u>	<u>PviG</u>	<u>HffG</u>	CYP1	CYP2	CYP3	CYP4
<u>PviD</u>		80.8%	19.7%	20.3%	37.9%	16.5%	16.9%	49.4%
<u>HffD</u>	80.8%		19.7%	20.3%	38.3%	16.2%	16.7%	49.4%
<u>PviG</u>	19.7%	19.7%		75.4%	19.0%	33.9%	40.2%	17.3%
<u>HffG</u>	20.3%	20.3%	75.4%		18.8%	32.7%	40.7%	18.0%
CYP1	37.9%	38.3%	19.0%	18.8%		17.2%	18.5%	34.5%
CYP2	16.5%	16.2%	33.9%	32.7%	17.2%		28.5%	17.7%
CYP3	16.9%	16.7%	40.2%	40.7%	18.5%	28.5%		14.1%
CYP4	49.4%	49.4%	17.3%	18.0%	34.5%	17.7%	14.1%	

3.3.2.2 Aim

Cytochrome P450 (CYP) monooxygenases are one of the most versatile biological catalysts which have the ability to oxidase a wide range of substrates. The CYP enzymes play important roles in various fungal metabolisms. To investigate the range of the promiscuity of the cytochrome P450 monooxygenases during cytochalasan biosynthesis, the P450 disruption strain ($\Delta pyiD$ and $\Delta pyiG$) obtained from previous KO experiments were designed as a bioengineering platform and use the combinatorial biosynthesis approach to heterologous express P450 encoding genes from other putative cytochalasan biosynthetic gene cluster (BGC). We aim to elucidate the biocatalytic properties of different fungal CYPs. In the meantime, we hope to generate novel cytochalasans modified by different functional CYPs.

3.3.2.3 Vector Construction and Gene Transformation

The detailed information of pTYGS-bar plasmid has been described in section 3.1.1. There is a *NotI* restriction sequence between the *P/T_{amyB}* cloning sites. The pTYGSbar-*P450* plasmids used for heterologous expression in *pyiD/pyiH* disruption strain was constructed in the same way described in section 3.3.1.3 (Scheme 3.4). P450 heterologous expression experiment were follow the same protocol as we used in the transformation in *pyiH* KO strain.

Six P450 genes (*hffD* and *hffG* from *H. fragiforme*, and *CYP1-4* from *P. oryzae*) were cloned and the corresponding pTYGSbar – P450 plasmid were constructed using above method (Scheme 3.4, Figure 3.8).

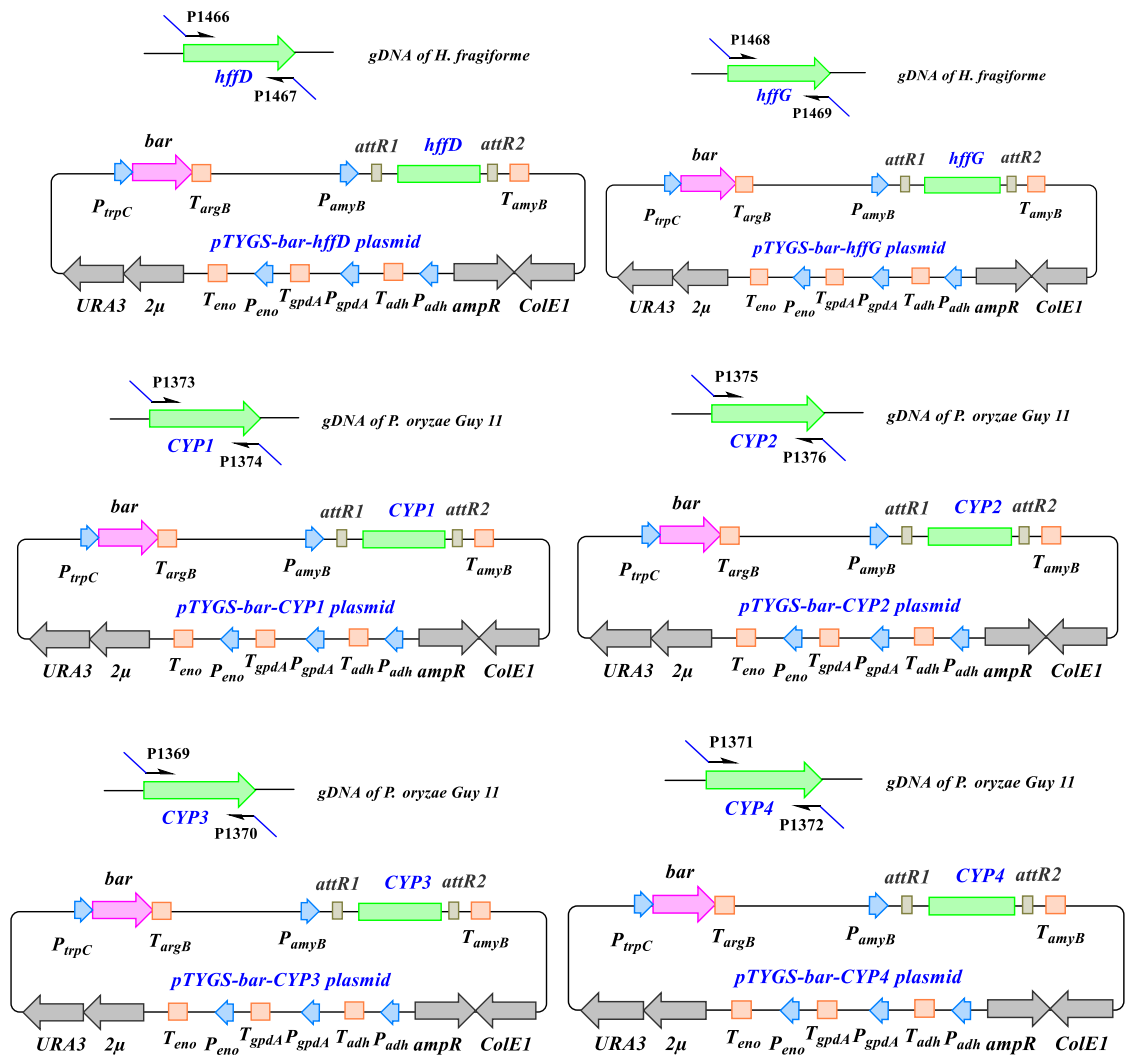


Figure 3.8 Overview of constructed heterologous expression plasmids in this work.¹³⁹

3.3.2.4 PCR analysis of pTYGSbar – P450s

Around 5 μ g of purified pTYGSbar-P450 plasmids were used in the fungal transformation. Transformants were obtained from three rounds of selection with basta and screened for genetic testing before being inoculated into liquid culture. Genomic DNA was extracted and used as the PCR template. Target genes were analysed with oligonucleotides specific for the targeted P450 gene region and as well as *M. grisea* Δ PyiD gDNA (Figure 3.9, Chapter 6.1.5). Forward primer binding with the region of *P_amyB*, while the reverse primer binding in the 3' end of each P450 gene. All the the PCR results were analysed by agarose gel electrophoresis (Figure 3.9).

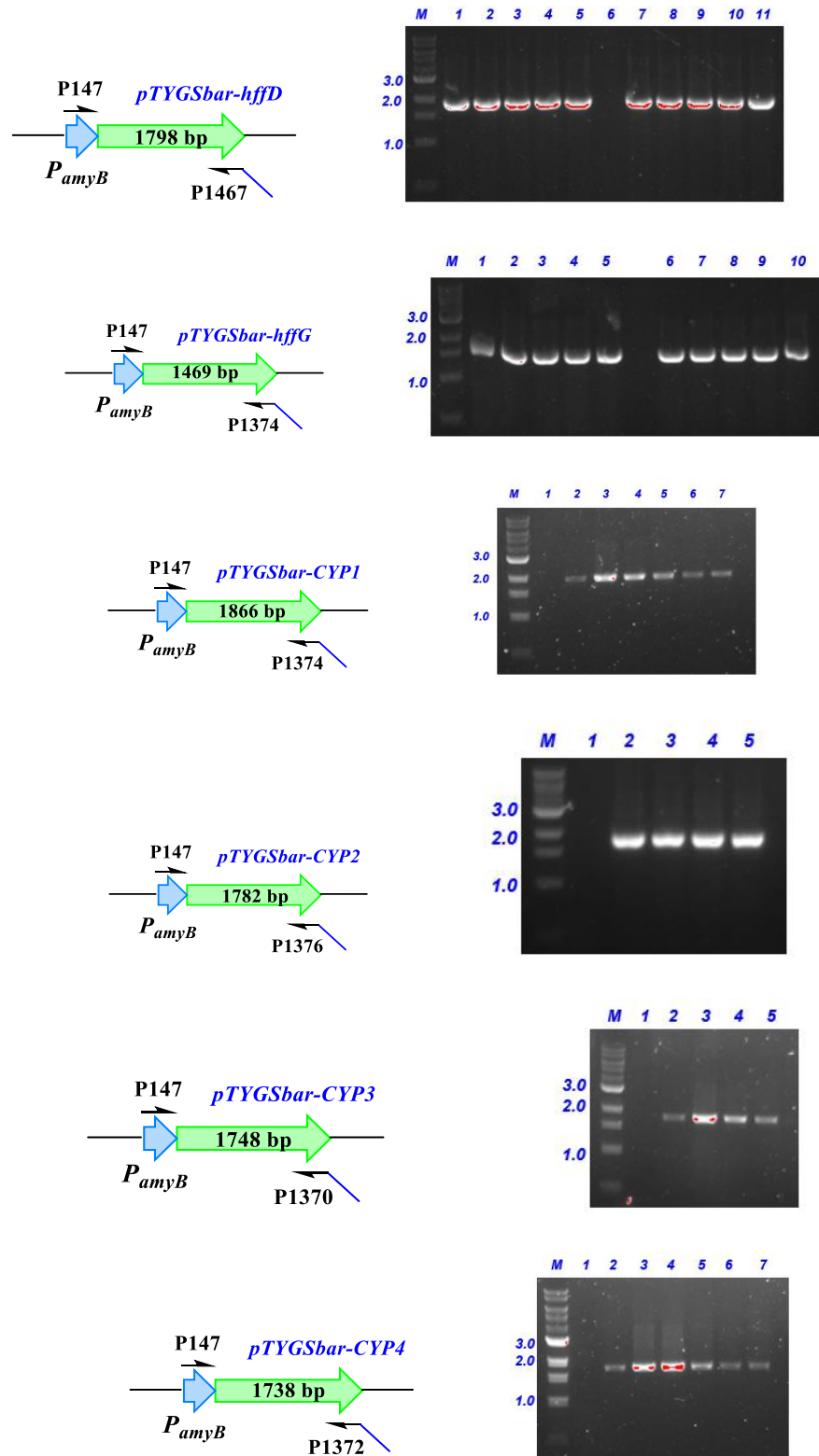


Figure 3.9 Oligonucleotide strategy of PCR analysis for confirmation of *P450* genes fused into the genome of *M. grisea* Δ *PyiD*; M: DNA ladder marker (Kb), different colonies are represented by numbers.

3.3.2.5 Chemical Analysis

The heterologous expression process was done following the same protocol described in section 3.3.1.4. The number of positive transformants confirmed by PCR, and the transformation efficiency of P450 genes into *M. grisea* Δ *pyiD* strain were summarized (Table 3.3).¹³⁹

Table 3.3 Heterologous expression efficiency in *M. grisea* *pyiD* KO strains.¹³⁹

Gene heterologously expressed	Number of transformants generated	Confirmed by PCR / Number of transformants screened	Efficiency (%)
<i>hffD</i>	30	8/10	80
<i>hffG</i>	30	10/10	100
<i>CYP1</i>	41	7/20	35
<i>CYP2</i>	50	5/20	25
<i>CYP3</i>	51	5/10	50
<i>CYP4</i>	18	6/10	60

Selected positive transformants were inoculated into DPY liquid medium at 25 °C, 110 rpm for 7 days before the filtration were extracted with ethyl acetate. Liquid extraction was dissolved in methanol and analysed by LCMS.

3.3.2.6 Heterologous Expression of *hffD* into Δ *pyiD* Strain

The *hffD* heterologous expression transformants were extracted and analysed by LCMS. The result showed a new peak appeared at the same RT as **65** (Figure 3.10 C).¹³⁹

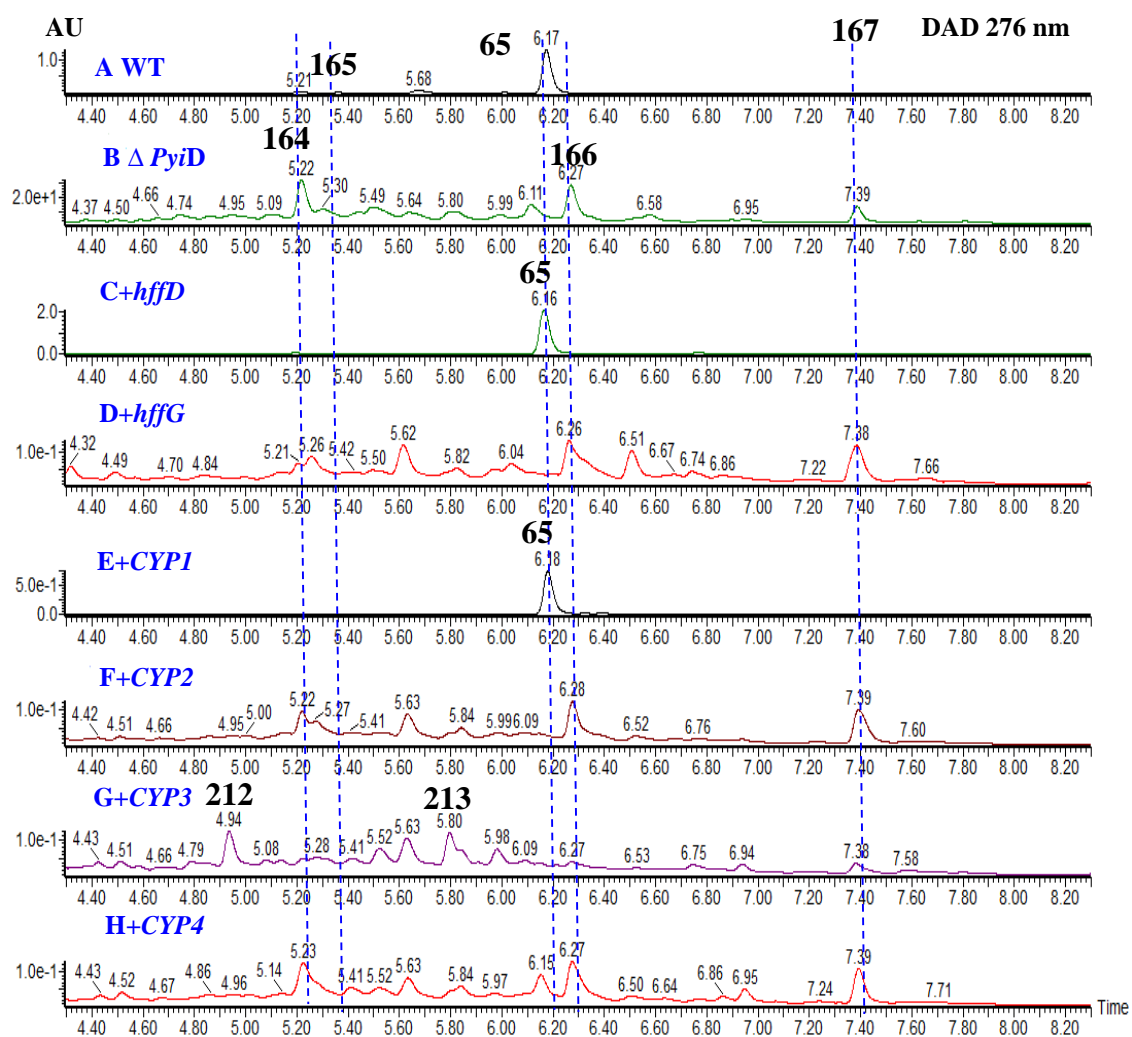


Figure 3.10 LCMS chromatogram (DAD trace) of mycelia extracts derived from *M. grisea* Δ *pyiD* strains transformed with crytic P450 genes. Chromatograms were monitored using a diode array detector scanning at 276 nm. **A**, *M. grisea* WT; **B**, *M. grisea* Δ *pyiD*; ; **C – H** indicated heterologous complementation experiments.¹³⁹

The new compound ($t_R = 6.2$ min, 21.7 mg/L) was purified as white powder. The UV spectra (methanol) showed the maximum absorption at 275 and 223 nm (Figure 3.10), which is similar to pyrichalasin H **65**. HRMS of the new compound confirmed a molecular formula of $C_{31}H_{41}NO_6$ ($[M-H]^-$ calculated 522.2856, found 522.2852), identical to **65**.

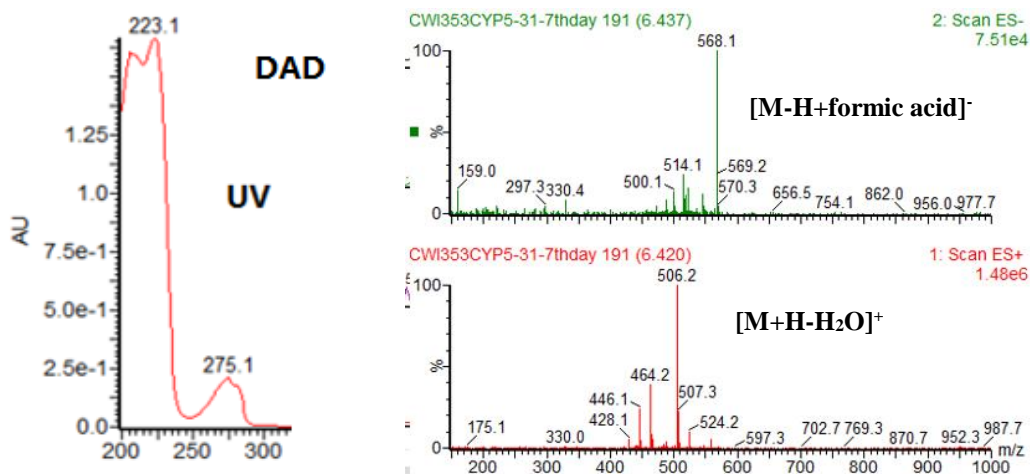


Figure 3.11 UV spectrum (left) and mass spectra (right) of **210** isolated from *hffD* heterologous expression into *M. grisea* Δ *PyiD*.

Full NMR was acquired and analysis of ^1H and ^{13}C NMR data of the new compound identified 31 carbons and 41 protons.¹³⁹ Both carbon and proton spectra were almost identical to pyrichalasin H **65**. Furthermore, 2D NMR, such as, H-H COSY, HMBC and HSQC were also investigated. The 2D signals of the new compound were also identical to the data from **65**. Based on those evidence, we elucidated that the new compound is pyrichalasin H **65**. As compounds **164** - **167** all lack a hydroxyl group at C-18, the production of **65** was restored when *hffD* was transformed into *M. grisea* Δ *pyiD* strain. This indicates that *hffD* encodes the C-18 hydroxylase and is functionally equivalent to *pyiD*.

3.3.2.7 Heterologous Expression of *CYP1* into Δ *pyiD* Strain

The *CYP1* heterologous expression transformants were extracted and analysed by LCMS. The result showed a new peak appeared (Figure 3.10 E), also at a RT corresponding to **65**.

The new compound ($t_{\text{R}} = 6.2$ min, 15.3 mg/L) was purified as a white powder. The UV spectra showed the maximum absorption at 276 nm (Figure 3.12), which is similar to **65**. HRMS of the new compound confirmed a molecular formula of $\text{C}_{31}\text{H}_{41}\text{NO}_6$ ($[\text{M}+\text{Na}]^+$ calculated 546.2832, found 546.2829), also identical to **65**.

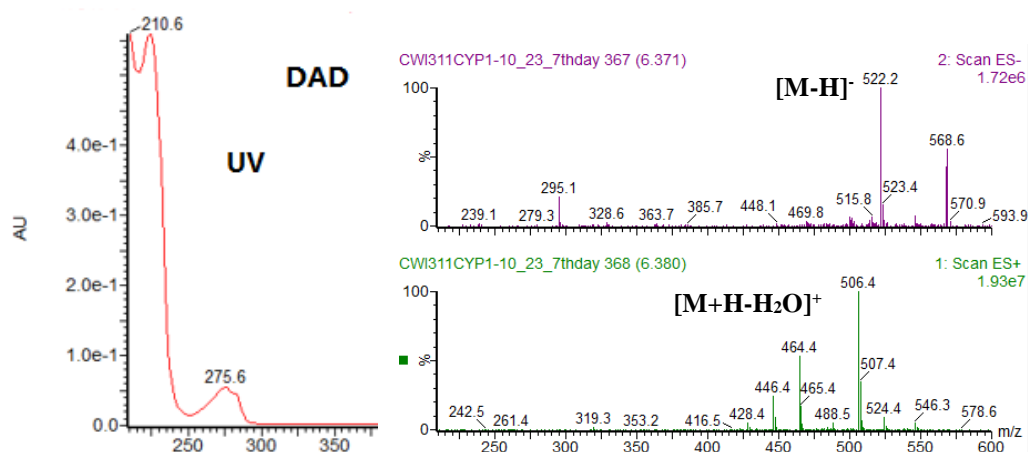


Figure 3.12 UV spectrum (left) and mass spectra (right) of **211** isolated after heterologous expression of CYP1 into *M. grisea* Δ PyiD.

Full NMR was acquired and analysed of ^1H and ^{13}C NMR data of the new compound identified 31 carbons and 41 protons. Both carbon and proton spectrum were almost identical to pyrichalasin H. Furthermore, 2D NMR, such as, H-H COSY, HMBC and HSQC were also investigated. The 2D signals of the new compound also identical to the data from **65**. Based on those evidence, we elucidated that the new compound is pyrichalasin H **65**. As compounds **164-167** all lack a hydroxyl group at C-18, the production of **211** was restored when CYP1 was transformed into *M. grisea* Δ pyiD strain. This indicates that CYP1 also encodes a C-18 hydroxylase.

3.3.2.8 Heterologous Expression of CYP3 into Δ pyiD Strain

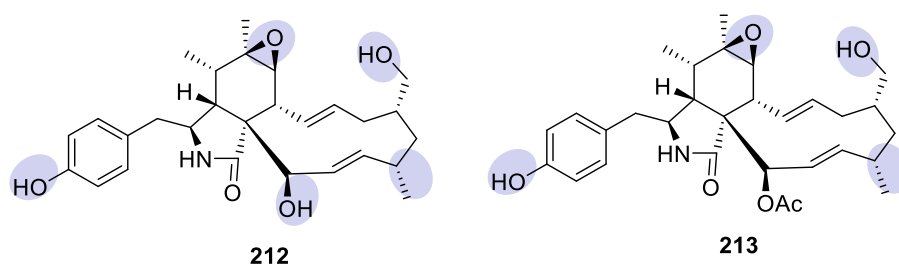
The CYP3 heterologous expression transformants were extracted and analysed by LCMS. Two new peaks **212** and **213** appeared from the LCMS profile (Figure 3.10 G). These had RT which did not correspond to **65**.

Compound **212** and **213** were purified as white powders, the compound physical data were measured (Table 3.4).

Table 3.4 Compound physic data from CYP3 heterologous expression experiment.¹³⁹

Compound Nr.	t _R (min)	UV (nm)	HRMS (calculated /found)	Molecular Formula	Titre (mg / L)	Appearance
212	5.3	275	490.2569 /490.2569	C ₂₈ H ₃₇ NO ₅	2.0	white
213	5.9	275, 224	532.2672 / 532.2672	C ₃₀ H ₃₉ NO ₆	1.5	white

Full NMR was acquired and analysis of ¹H and ¹³C NMR data of **212** identified 28 carbons and 37 protons compound to **65**. The signal of H-22 and H-26 of **65** were not found from proton NMR and HSQC. There are two obvious correlations observed by HSQC ($\delta_H - \delta_C$, 3.26/3.38-67.1), indicating that there is a new methylene formed. The ¹H-¹H correlations between H-22/H-15, and the HMBC correlation between H-22 to C-15, C-16, C-17, suggest that a hydroxyl group is linked at C-22. The signal of methyl group at C-24 is not found in the proton NMR, confirming the lack of the acetyl group. The chemical shift of C-5, C-6 and C-7 changed dramatically compared to pyrichalasin H, which is in accordance with an epoxide between C-6 and C-7, in the new compound. The remaining signals of both carbon and hydrogen chemical shifts were similar to pyrichalasin H. Therefore, the structure of compound **212** was confirmed (Figure 3.13).

**Figure 3.13** Chemical structure of **212** and **213**.

Full NMR data of **213** were acquired, and analysis of ^1H and ^{13}C NMR data identified 30 carbons and 39 protons. Compared to **212**, the signal of H-25 was found from proton and HSQC spectra, indicating the acetyl group attached to the C-21 hydroxyl group. The remaining signals of **213** are similar to **212**, therefore the structure of compound **213** was confirmed (Figure 3.13).

3.3.2.9 Heterologous Expression of *hffG*, *CYP2* and *CYP4* into Δ *pyiD* Strain

The same transformation method was used to generate transformants for the heterologous expression of *hffG*, *CYP2* and *CYP4* into *M. grisea* *pyiD* KO strain. However, liquid extraction from *hffG*, *CYP2* and *CYP4* containing strains led to no observed change in the metabolite profiles compared to the KO metabolites (Figure 3.10 D, F and H). The plasmids used for heterologous expression in *pyiG* disruption strain are the same as we used in the *pyiD* disruption strain (Figure 3.8). All P450 genes heterologous expression experiments follow the same protocol as we used in the transformation in *pyiD* KO strain. The heterologous expression process was done following the same steps described in section 3.3.1.4, the number of positive transformants were confirmed by PCR, the transformation efficiency of P450 genes into *M. grisea* Δ *pyiG* strain are summarized (Table 3.5).

Table 3.5 Heterologous expression efficiency in *M. grisea* *pyiG* KO strains.¹³⁹

Gene heterologously expressed	Number of transformants generated	confirmed by PCR / Number of transformants screened	Efficiency (%)
<i>hffG</i>	30	9/10	90
<i>CYP1</i>	32	5/10	50
<i>CYP2</i>	37	5/18	27.8
<i>CYP3</i>	10	2/10	20
<i>CYP4</i>	36	6/12	50

All pTYGSbar-*P450* plasmids were analysed with the same oligonucleotides and the same methods described in section 3.3.1.4. All the agarose gel electrophoresis analyse results are summarized (Figure 3.14).

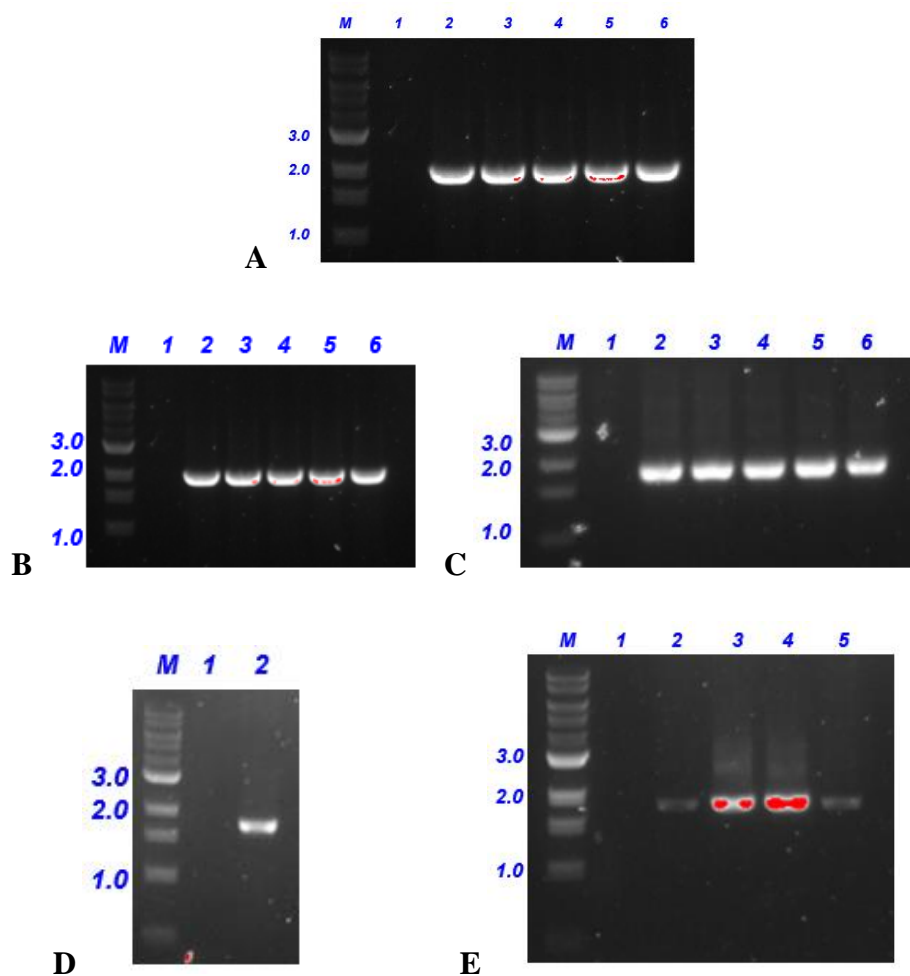


Figure 3.14 Agarose gel electrophoresis analysis for confirmation of *P450* genes fused into the genome of *M. grisea* Δ *pyiG*; M, DNA ladder marker (Kb), different colonies are represented by numbers. **A-E**: Colony PCR results of *hffG*, *CYP1*, *CYP2*, *CYP3*, *CYP4* heterologous expression transformants.

3.3.2.10 Heterologous Expression of *hffG* into Δ *pyiG* Strain

All positive *hffG* containing transformants were extracted and analysed by LCMS. The result showed a new peak appeared which corresponded with **65**(Figure 3.15 C).

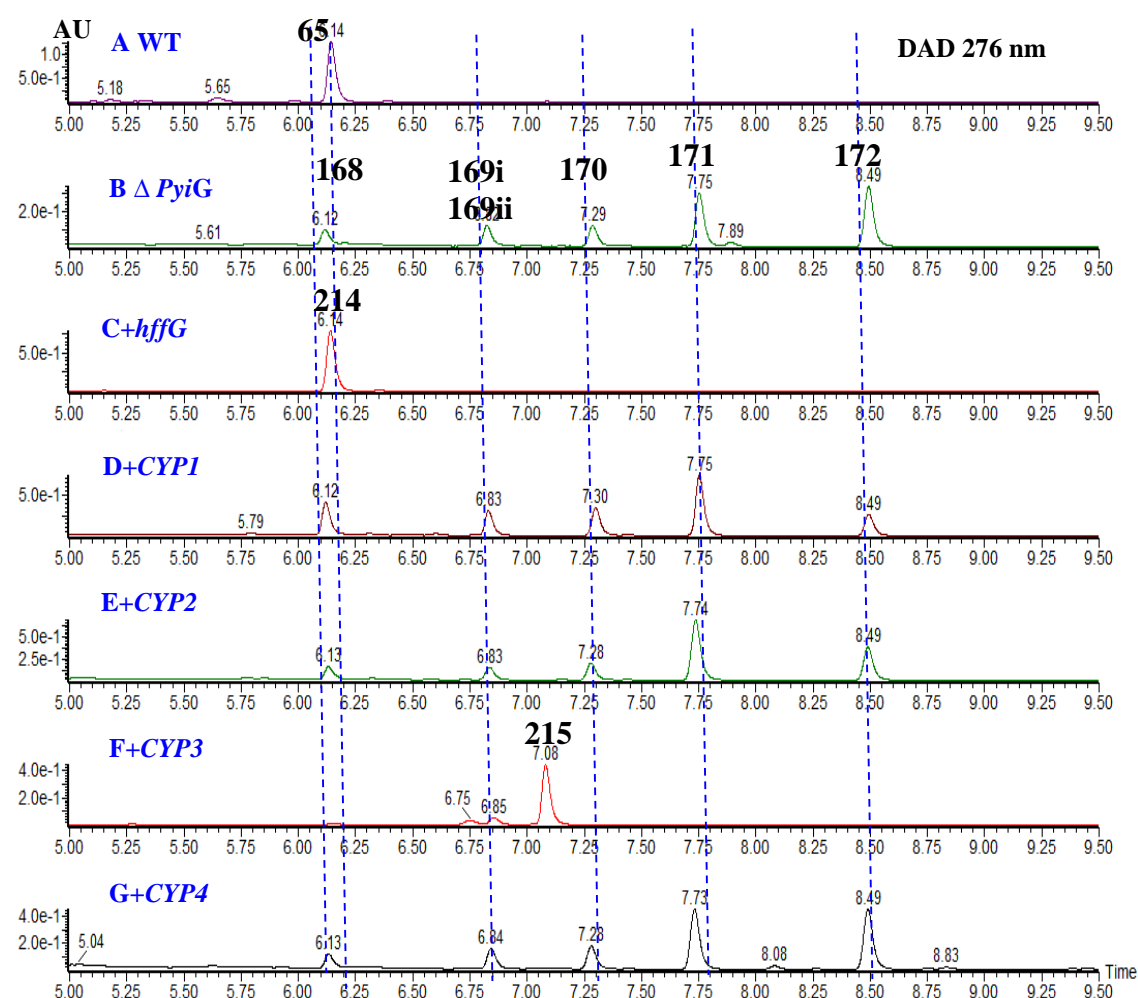


Figure 3.15 LCMS chromatogram (DAD trace) of mycelia extracts derived from *M. grisea* Δ *pyiG* strains transformed with crytic P450 genes. Chromatograms were monitored using a diode array detector scanning at 276 nm. **A**, *M. grisea* WT; **B**, *M. grisea* Δ *pyiG*; **C – G** indicated complementation experiments.¹³⁹

Compound **214** was purified as white powder the compounds physical data were measured (Table 3.15).

Table 3.6 Compound physical data from *hffG* and *CYP3* heterologous expression experiment.¹³⁹

Compound Nr.	t _R (min)	UV (nm)	HRMS (calculated /found)	Molecular Formula	Titre (mg / L)	Appearance
214	6.3	276, 221	546.2832 /546.2835	C ₃₁ H ₄₁ NO ₆	13.8	white
215	7.1	275, 223	532.2672 / 532.2672	C ₃₁ H ₄₁ NO ₆	28.6	white

Full NMR was acquired and analysis of ¹H and ¹³C NMR data of **214** identified 31 carbons and 41 protons. Both carbon and proton spectra were almost identical to pyrichalasin H. Furthermore, 2D NMR, such as, H-H COSY, HMBC and HSQC were also investigated. The 2D signals of **214** were also identical to the data from **65**. Based on these evidence, we elucidated that compound **214** is pyrichalasin H **65**. As compounds **168** - **172** all lack a hydroxyl group at C-7, the production of **65** was restored when *hffG* was transformed into *M. grisea ΔpyiG*. This indicates that *hffG* encodes the C-7 hydroxylase.

3.3.2.11 Heterologous Expression of *CYP3* into Δ *pyiG* Strain

The *CYP3* heterologous expression transformants were extracted analysed by LCMS. The result showed one new peak **215** appeared (Figure 3.15 F). The physical data of **215** is listed in Table 3.6.

Full NMR data was acquired and analysis of ^1H and ^{13}C NMR spectra of **215** identified 31 carbons and 41 protons. The chemical shift of C-5, C-6 and C-7 changed dramatically compared to pyrichalasin H, which is in accordance with the presence of an epoxide between C-6 and C-7 in the new compound. The remaining signals of both carbon and hydrogen chemical shifts were similar to pyrichalasin H **65**. Therefore, the structure of compound **215** was confirmed (Figure 3.16).

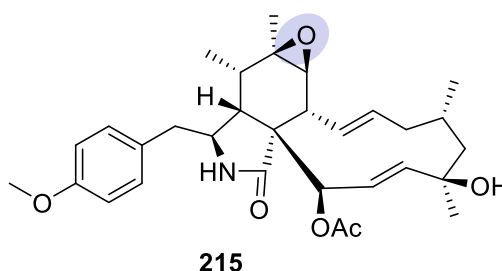


Figure 3.16 Chemical structure of **215**.

3.3.2.12 Heterologous Expression of *CYP1*, *CYP2* and *CYP4* into Δ *pyiG* Strain

Liquid extraction from the *CYP1* heterologous expression strain led to no observed change in the metabolite profiles compared to the *pyiG* KO metabolites (Figure 3.15 D). This result is not beyond our expectation, since we have elucidated that *CYP1* catalyses a C-18 hydroxylation in *pyiD* KO strain.

Liquid extraction from either CYP2 or CYP4 containing strains also led to no observed change in the metabolite profiles compared to the *pyiG* KO metabolites (Figure 3.15 E, Figure 3.15 G).

3.4 Discussion & Outlook

Heterologous expression experiments indicated that HffD and HffG site-selectively add a hydroxyl group to C-18 and C-7 of metabolites from the P450 disruption strain separately. Both HffD and HffG perform a single hydroxylation at the desired position. These results connect the production of compounds **205** - **209** in *H. fragiforme* with the *hff* gene cluster. Moreover, cryptic P450s from other synthetic pathway were proved to be functional in our P450 disruption strain. This synthetic biology platform can be used to systematically investigate the function and scope of different cryptic tailoring enzymes.

Subsequently, we systematically investigated four putative p450s (*CYP1-4*) from *Pyricularia oryzae* Guy 11 *ACE1/SYN2* BGC in this platform. First, we expressed CYP1-4 into the *M. grisea* Δ *pyiD* strain and investigated the resulting extracts by LCMS. Expressing *CYP1* restored the production of **65** with a low titer of 15.3 mg/L, the structure of compound **65** was confirmed by HRMS and NMR. Therefore, the function of the putative *CYP1* is uncovered as a site-selective C-18 hydroxylase (Table 3.7). The decreased yield is likely caused by the use of a non-native gene under the control of a non-native promoter. We already know that PamyB is not a strong promoter in *M. grisea*.

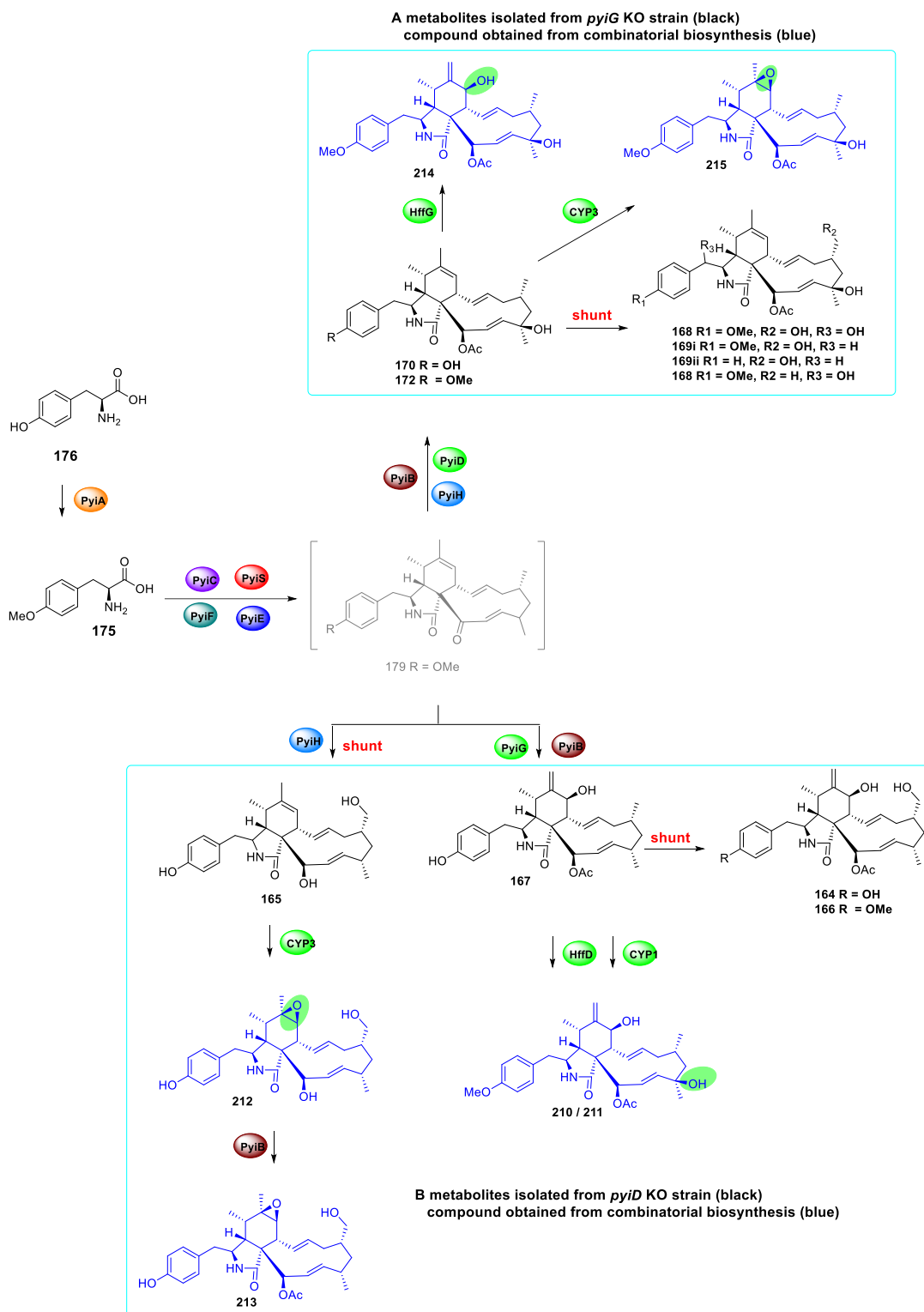
Table 3.7 Summary of heterologous expression experiment.¹³⁹

Gene added	Compounds produced (mg / L)		Deduced function of cryptic P450
	<i>M. grisea</i> Δ <i>pyiD</i>	<i>M. grisea</i> Δ <i>pyiG</i>	
hffD	65 (21.7)	-	C-18 hydroxylase
hffG	-	65 (13.8)	C-7 hydroxylase
<i>CYP1</i>	65 (15.3)	-	C-18 hydroxylase
<i>CYP2</i>	-	-	-
<i>CYP3</i>	212 (2.0) 213 (1.5)	215 (28.6)	C-6/C-7 epoxidase
<i>CYP4</i>	-	-	-

The introduction of CYP3 resulted in two new compounds **212** and **213** in small amounts. The NMR of **212** and **213** shown to have typical epoxide resonances at C-6, C-7 and H-7. The production of **212** and **213** can be explained as derivatives from the epoxidation of compound **165** by CYP3 (Scheme 3.5 B). Compound **165** comes from the off-pathway shunt in the biosynthesis of **65**. Compound **213** is the acetylated product of compound **212** catalysed by acetyltransferase PyiB. Compounds **164**, **166**, and **167** already have a hydroxyl group at C-7 introduced by the native P450 PyiG, and therefore cannot act as substrates for CYP3. Only when compound **165** is present can CYP3 perform its function as a site-selective epoxidase of the C-6/C-7 olefin. However, introduction of either CYP2 or CYP4, led to no observable changes in the metabolite profiles.

Then, we expressed *CYP1-4* P450s into *M. grisea* Δ *pyiG* host and the liquid extractions of transformants were analysed by LCMS. Expression of either *CYP1*, *CYP2*, or *CYP4* did not result in any observed metabolites. It is not surprising that CYP1 did nothing in *M. grisea* Δ *pyiG* host, as we have previously confirmed that CYP1 is a site-selective C-18 hydroxylase in *M. grisea* Δ *pyiD* strain and compounds **168** - **172** from *M. grisea* Δ *pyiG* host already possess a hydroxyl group at C-18 (Scheme 3.5 A, Table 3.7).

The introduction of CYP3 lead to the production of the new compound **215** (28.6 mg/L). Compound **215** was purified and fully elucidated by HRMS and NMR. The production of **215** can be explained from the epoxidation of on-pathway intermediate **172** catalysed by CYP3 (Scheme 3.5 A). Combined with new epoxide metabolites **212** and **213** isolated from CYP3 heterologous expression into *M. grisea* Δ *pyiD* strain. The function of CYP3 as a C-6/C-7 regio-selective P450 is confirmed (Table 3.7).¹³⁹



Scheme 3.5 Network of tailoring modifications observed during the biosynthesis of **65** and summary of the functionality introduced by the heterologous expression of P450s, *HffD*, *HffG*, *CYP1*, and *CYP3* into *M. grisea* P450 mutant strains. Compounds in blue are found *via* combinatorial biosynthesis.¹³⁹

There are different functional P450 enzymes known in cytochalasan biosynthesis, for example, P450s catalyse hydroxylation reaction in cytochalasin K **82** at C-7 and epoxychoylochalasin H **206** at C-18, epoxidation P450s at C-6 and C-7 in epoxychoylochalasin H and chaetoglobosin A **63** and also iterative hydroxylation P450s in cytochalasin K **82** at C-17 and C-18, epoxychoylochalasin H at C-19 and C-20 (Figure 3.17).^{129,138, 76} In our case, neither CYP1 nor CYP3 operate iteratively, even though neither of them react with their native substrates.

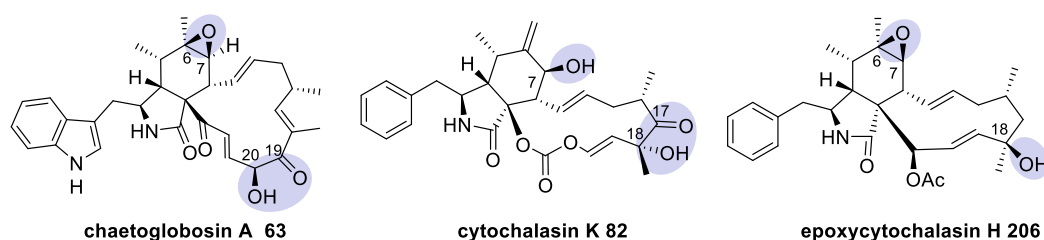
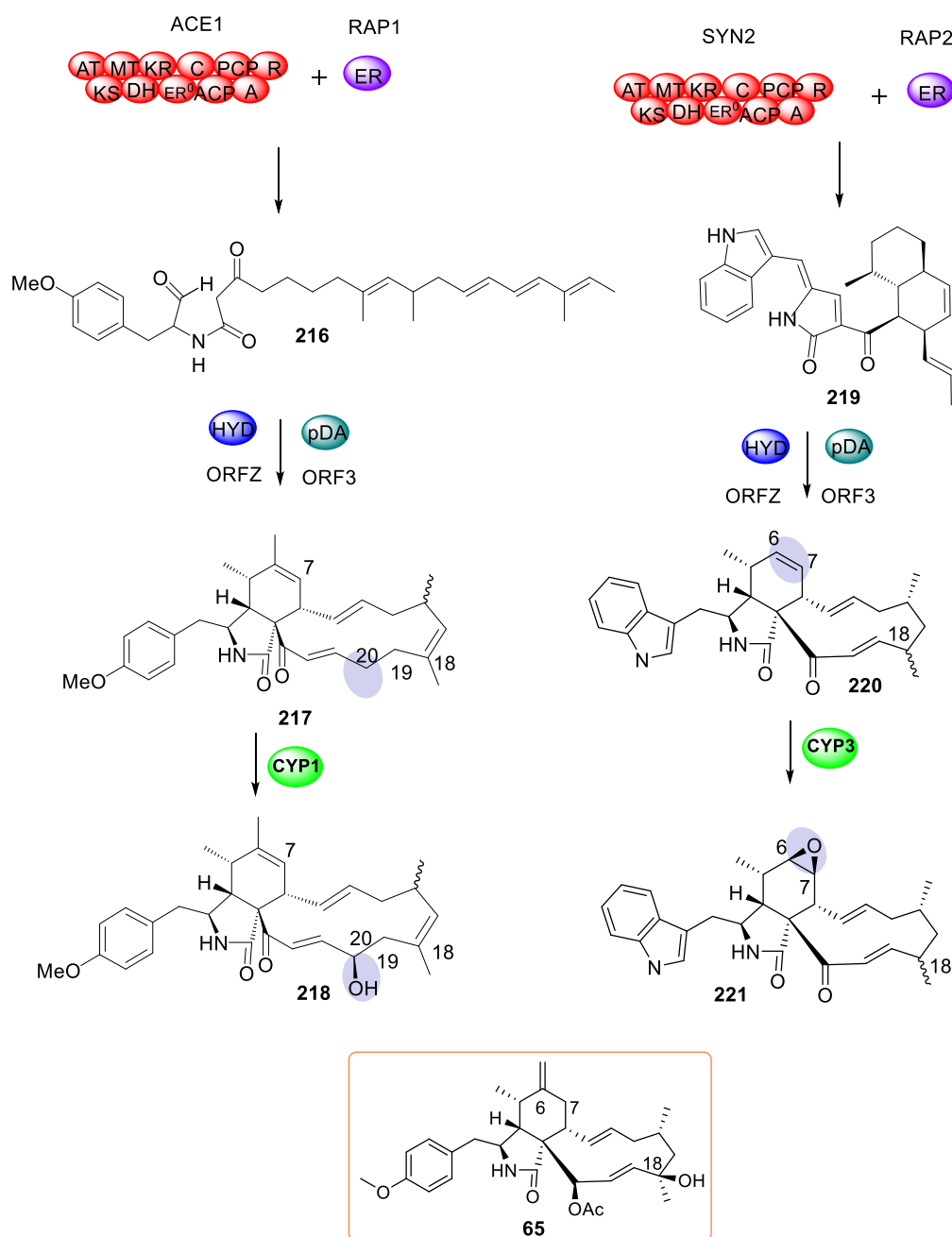


Figure 3.17 Structures of cytochalasan derived from the action of P450s.^{129,138, 76}

The proposed polyketide backbone **217** synthesised by the ACE1 PKS-NRPS is two carbons longer than the pyrichalasin H **65** skeleton. (Scheme 3.6). The *CYP1* gene originates from ACE1 gene cluster, encoding CYP1 that catalyzes a regioselective hydroxylation at C-18 of pyrichalasin H intermediate.¹¹³ However, there is a methyl group at the corresponding position of putative ACE1 intermediate **217**, it is impossible for CYP1 to catalyse a hydroxylation reaction at C-18 of **217**. Therefore, it is likely that the hydroxylation happens at C-20 to produce **218**, since both of these two carbons are next to olefin.

Larsen and co-workers obtained compound **219** from expression of SYN2 and RAP2.¹⁵² Epoxidation usually happen at C-6 / C-7 olefin generating compound **221**, no matter if there is a methyl group at C-6 position (Scheme 3.6).



Scheme 3.6 Putative structures for the cryptic cytochalasins encoded by the *P. oryzae* Guy11 ACE1/SYN2 BGC and catalysed by P450 enzymes.¹³⁹

Systematic investigation of cryptic P450 genes CYP1-2 from ACE1 cluster, and CYP3-4 from the SYN2 cluster, resulted in changes to the observed metabolites from three out of eight experiments. But, heterologous expression CYP2 and CYP4 into *ΔpyiD / ΔpyiG* strains, no metabolite profile change, making it difficult to predict the function of CYP2 and CYP4. Böhnert and co-workers reported that CYP2 gene is split in ACE1 gene cluster,¹⁵⁰ maybe that is the reason we did not find any chemical changes from CYP2 expression. However, it is surprising that we did not observe any metabolite change in

CYP4 expression experiment. Especially as bioinformatic analyse indicates that CYP4 shares higher sequence similarity with PylD as (49%), while CYP1 which shares less than 38% similarity with PylG, but still catalyses a hydroxylation reaction at C-18 (Table 3.2). CYP4 may not recognise the cytochalasin P450 metabolites and this could be one of the possible reasons.

To sum up, for the first time, we demonstrated the possibility of using a combinatorial biosynthesis strategy between different cytochalasan BGC. The functions of four cryptic P450 enzymes were elucidated. It is an effective strategy to decorate the cytochalasan backbone by introducing functional P450 genes. In the meantime, these experiments uncover the selectivity and versatility of cytochalasan P450 enzymes. Moreover, this bioengineering platform can be developed into a cell factory to design and generate novel cytochalasans by introducing different tailoring enzymes using combinatorial biosynthesis.

Outlook

We have developed the P450 disruption strain as a synthetic platform. In future, multifunction cryptic P450s from different pathways could be introduced into this platform to generate more structural complicated cytochalasans. Moreover, P450s from different fungal species or from different microorganisms can also be heterologous expressed into the platform to further elucidate the actual function of those mysterious P450s. Except for P450s, other functional tailoring enzymes, for example, halogenase, methyltransferase *etc*, could be tested in this cell factory, these enzymes will furthermore decorate the backbone of pyrlichalasin H to produce more new functionalised cytochalasans.

4. Generating New Pyrichalasin by Mutasynthesis

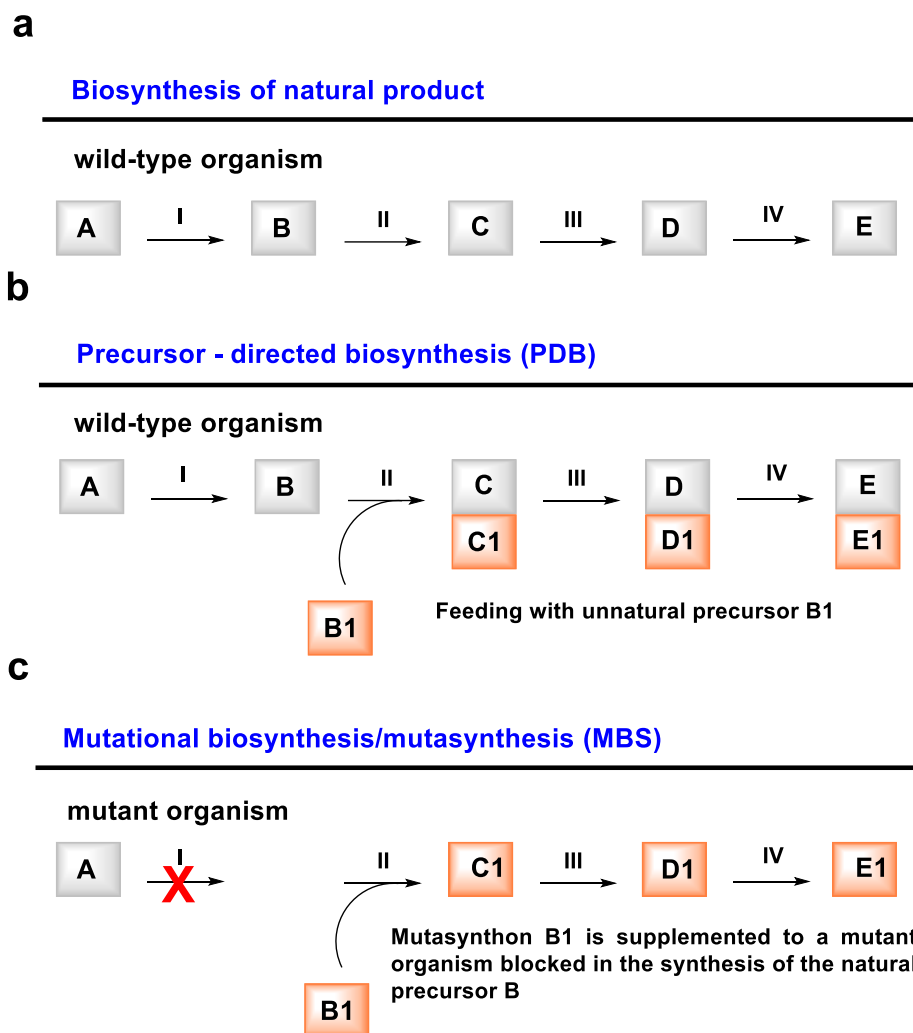
4.1 Introduction to Mutasynthesis and Other Methods of Pathway Engineering

Natural products play an essential role in many industries, in particular pharmaceuticals. However, the implementation of many promising biologically active compounds as pharmaceuticals is limited by natural product isolation. Many of these compounds are produced in very limited amounts by their natural source, and isolation of these compounds from their host organisms consumes natural supply. Historically, chemists have attempted to solve this problem through organic synthesis. However, while organic synthesis has allowed affordable access to some natural products, total synthesis of many natural products is still not economically feasible for mass production.^{1,153}

Recent trends in the synthesis and production of bioactive molecules have shown increased interest in green synthetic processes. Particularly, there has been a movement toward implementation of fermentation to solve problems commonly encountered in organic synthesis. This technology can be expanded to produce advanced intermediates in the synthetic process. Microorganisms such as yeast, bacteria, and filamentous fungi can convert simple starting materials into stereochemically complex natural products. Fermentation reduces the use of organic solvents and organic reagents. Natural products obtained by fermentation can be efficiently converted into new structures that would be difficult to obtain synthetically.¹⁵⁴

Using the respective wild-type (WT) strain to generate novel structural diversity of microbially produced secondary metabolites is one of the oldest strategies (Scheme 4.1 a). Precursor-directed biosynthesis (PDB) is performed by supplementing biosynthetic precursor-analogues to the fermentation of WT strains (Scheme 4.1 b). Based on the fact that WT producers are used, PDB is a straightforward way for exploiting the biosynthetic machinery of secondary metabolites, compared to the time-consuming genetic manipulations using methods of modern molecular biology. However, there is usually an internal competition of natural and unnatural precursors, and yields of the desired analogues can be low, and this problem is consequently accompanied by

difficulties in separation of these compounds in the presence of the natural metabolites.¹⁵³

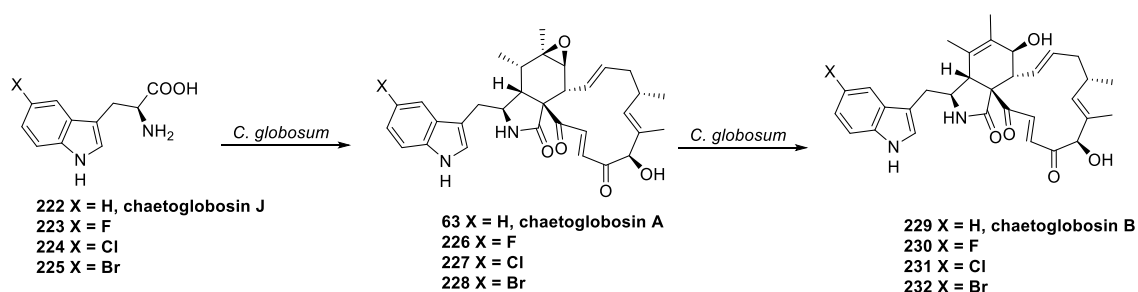


Scheme 4.1 Biosynthetic conceptions for natural product synthesis and derivatives (I-IV = enzymes; A = starter building block; B-D = biosynthetic intermediates; E = natural product or derivative).¹⁵³

Chaetoglobosins are structurally intriguing fungal cytochalasans with an isoindole moiety fused to a macrocycle.^{155,156} They are well known for their specific binding to actin filaments, making them important chemical tools in cell and molecular biology.^{157,158} Halogenated derivatives as biosynthetic precursors are particularly useful in the producing of modified chaetoglobosins, since they are structurally very similar to the natural substrates. The introduction of halogen atoms such as fluorine can often

improve the bioavailability, bioactivity and stability of the starting compounds in numerous ways.

A comprehensive example of PDB was applied by Tan and co-workers who generated new analogues of chaetoglobosins by feeding halogenated precursors to *Chaetomium globosum*. Chaetoglobosins A **63**, B **229** and J **222** (Scheme 4.2),¹⁵⁹ were isolated with high yields from *Chaetomium globosum* (strain no. 1C51). Halogenated precursors **223** - **225** were fed to the organism, and novel halogenated chaetoglobosins **226** - **228** and **230** - **232** were isolated (Scheme 4.2). All isolated compounds were tested and found to be immunosuppressive in a mouse model.¹⁶⁰

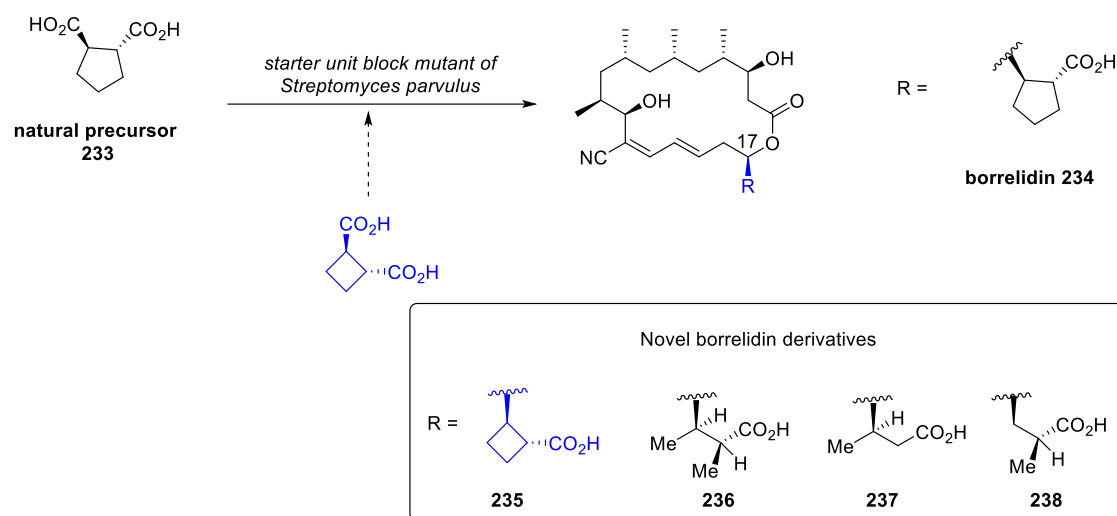


Scheme 4.2 Precursor-directed biosynthesis of chaetoglobosin.¹⁶⁰

Another interesting strategy which combines chemical and biosynthesis, is the use of genetically engineered microorganisms. This strategy has been termed as mutational biosynthesis (MBS), or in short mutasynthesis.^{161,162} According to Rinehart,¹⁶³ mutasynthesis involves the generation of biosynthetic blocked mutants, feeding of mutasynthons to these mutants and their integration into novel metabolites, followed by isolation of the unnatural products for evaluation of their biological activities (Scheme 4.1 c). More recently, mutasynthesis has experienced a rapid development because the number of fully sequenced biosynthetic gene clusters coding for pharmaceutically important natural products has substantially increased, accelerating the stage for easier creation of specific blocked mutants and therefore efficient access to modified drug candidates.

An impressive application of MBS for lead optimisation was reported by Wilkinson and co-workers. They dealt with the polyketide derived angiogenesis inhibitor borrelidin **234** (Scheme 4.3).¹⁶⁴ Using a non-producing strain disrupted in the biosynthesis of the

starter unit dicarboxylic acid **233**, supplementation with various analogues resulted in a set of novel borrelidins **235** – **238** differing in the C-17 side chain. Biological evaluation of their anti-proliferative activity indicated a significantly improved selectivity of the C-17 cyclobutyl analogue **235** for *in vitro* angiogenesis inhibition over cytotoxicity. These results demonstrate that MBS can be successfully applied for lead optimisation, while total- or semisynthetic approaches towards such compounds would be difficult.¹⁶⁵



Scheme 4.3 Mutational biosynthesis of borrelidins **234** - **238**.¹⁶⁵

4.2 Aims

Targeted disruption of the *pyiA* *O*-MeT (Chapter 2.3.1) led to the discovery of the unexpected phenylalanine-derived cytochalasin H **174**. Previous *O*-MeT KO result suggested that the true precursor for the A-domain might be *O*-methyltyrosine **175**.¹⁰⁹ This hypothesis will be investigated by observing whether pyrichalasin H **65** is restored after feeding **175** to *pyiA* KO strain.

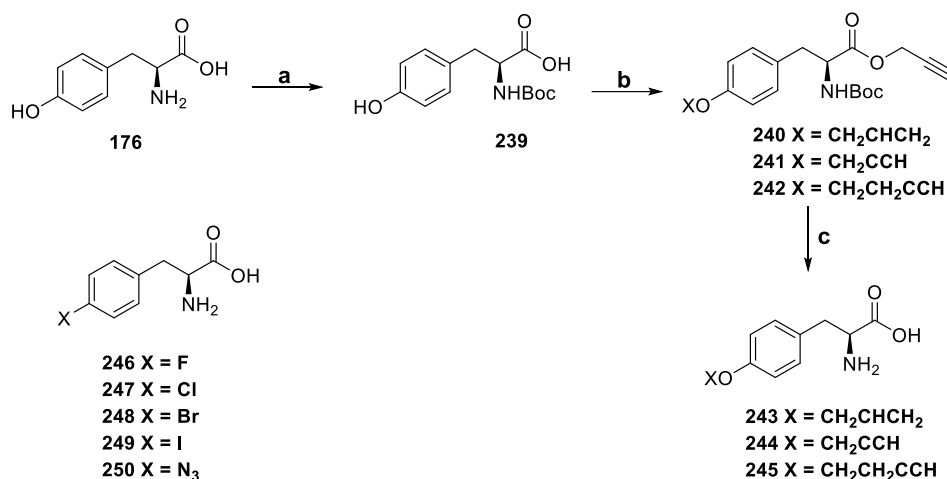
Next, we will investigate whether halogenated pyrichalasans can be made: 4'-halogenated phenylalanines will be fed to the Δ *pyiA* strain to confirm this idea. As copper catalysed azide alkyne cycloaddition (click) reactions are widely used in generating new compounds, we will also feed 4'-azido and 4'-alkyne phenylalanines to determine whether a clickable system can be built. Furthermore, we will feed the Δ *pyiA* strain more complex alkyne and azide substrates, to see if we can build an even more

complex system. Eventually, a library of un-natural 4'-substitute pyrichalasan will be built, followed by the bioevaluation those novel cytochalasans.

4.3 Results

4.3.1 Synthesis of Substrates

O-Propargyl phenylalanine was synthesized in three steps from L-tyrosine **176**.^{166,167} Treatment of **176** with di-*tert*-butyl pyrocarbonate in a mixture of dioxane and water gave the amine protected **239**. Allyl bromide was added into the solution of **239** with potassium carbonate under reflux conditions overnight. The obtained crude product **240** was directly dissolved in a solution of TFA and DCM to cleave the BOC protecting group to give the desired feeding precursor **243** (Scheme 4.4). *O*-Propargyl-tyrosine **244** and *O*-but-3-ynyl tyrosine **245** were synthesized by the same method. All other feeding precursors **246** - **250** were purchased from Sigma-Aldrich.¹⁶⁰



Scheme 4.4 Chemical synthesis of **243** - **245**. Reagents and conditions: **a**, (Boc)₂O, dioxane, H₂O, Et₃N, RT, 1 h; **b**, 1-bromobut-3-yne, K₂CO₃, THF, reflux, 12 h; **c**, TFA, CH₂Cl₂, RT, 2 h.

M. grisea WT strain produces **65** at 60 mg/L (Figure 4.1 A), but the KO strain produces much less of **173** (2.8 mg/L) and **174** (19.5 mg/L, Figure 4.1 B). After addition of *O*-

methyltyrosine **175** (10 mg/mL) to the *pyiA* KO strain over 7 days, the crude extract was dissolved in MeOH and analysed by LCMS ((Figure 4.1 C, Chapter 2.3.3).¹⁰⁹

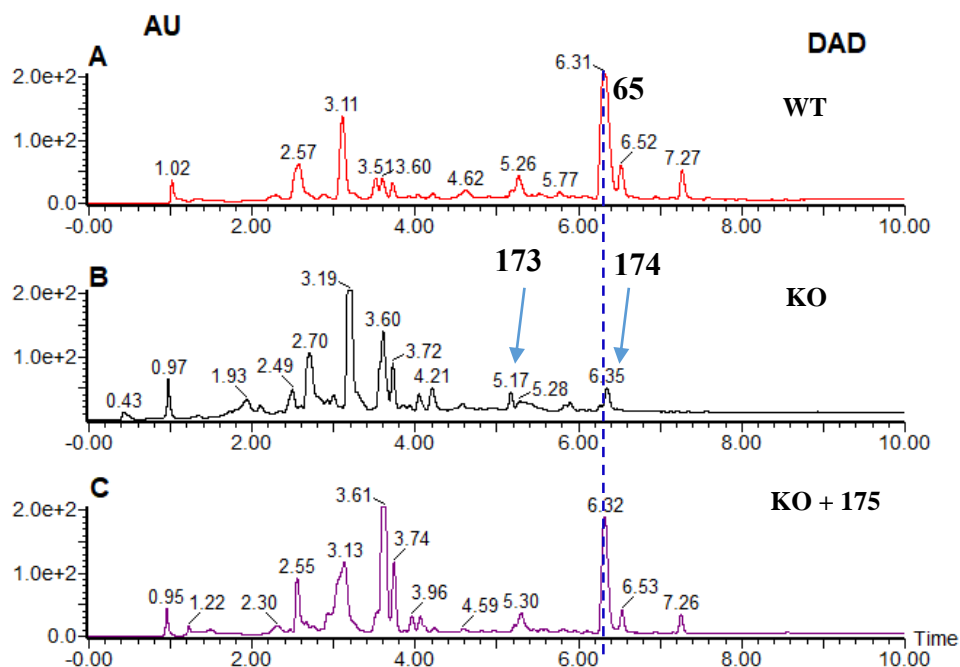
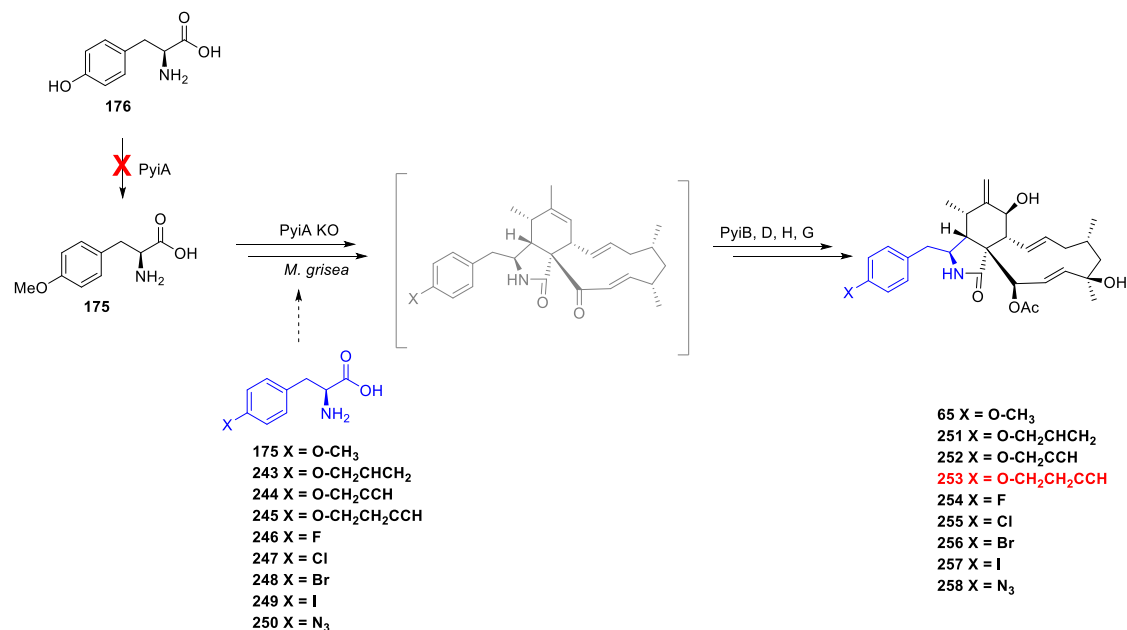


Figure 4.1. LCMS chromatograms (DAD trace) of organic extracts from *pyiA* KO experiments in *M. grisea*: **A**, wild type control; **B**, *pyiA* KO strain; **C**, feeding *O*-methyltyrosine **175** to *pyiA* KO strain.¹⁰⁹

The result showed the restoration of **65** with a yield of 61.6 mg/L (Table 4.1), almost equal titers compared to the WT strain. Compound **173** and **174** could no longer be detected under these conditions clarifying that **175** is the preferred substrate of the PyiS NRPS A-domain.

In order to explore the tolerance of the PyiS NRPS A-domain, 4'-fluoro- / chloro- /bromo- /iodo-/azido-phenylalanine, 4'-*O*-allyl-tyrosine and 4'-*O*-propargyl-tyrosine **243 - 250** were fed using the same method as feeding 4'-*O*-methyltyrosine. Surprisingly, all 7 substrates were incorporated to give the corresponding 4'-functionalised pyrivalasins **251 -258** in purified yields from 26 to 60 mg/L (Scheme 4.5, Table 4.1,). However, we did not obtain the 4'-*O*-butynyl pyrivalasin **253**. All new pyrivalasins were fully characterised by NMR, HRMS and IR spectroscopy (Appendix, compound

252 and 257 were synthesized by Maurice, compound 253 and 258 were synthesized by Adrian).



Scheme 4.5 Precursor-directed biosynthesis of 4-substituted pyrichalasin.

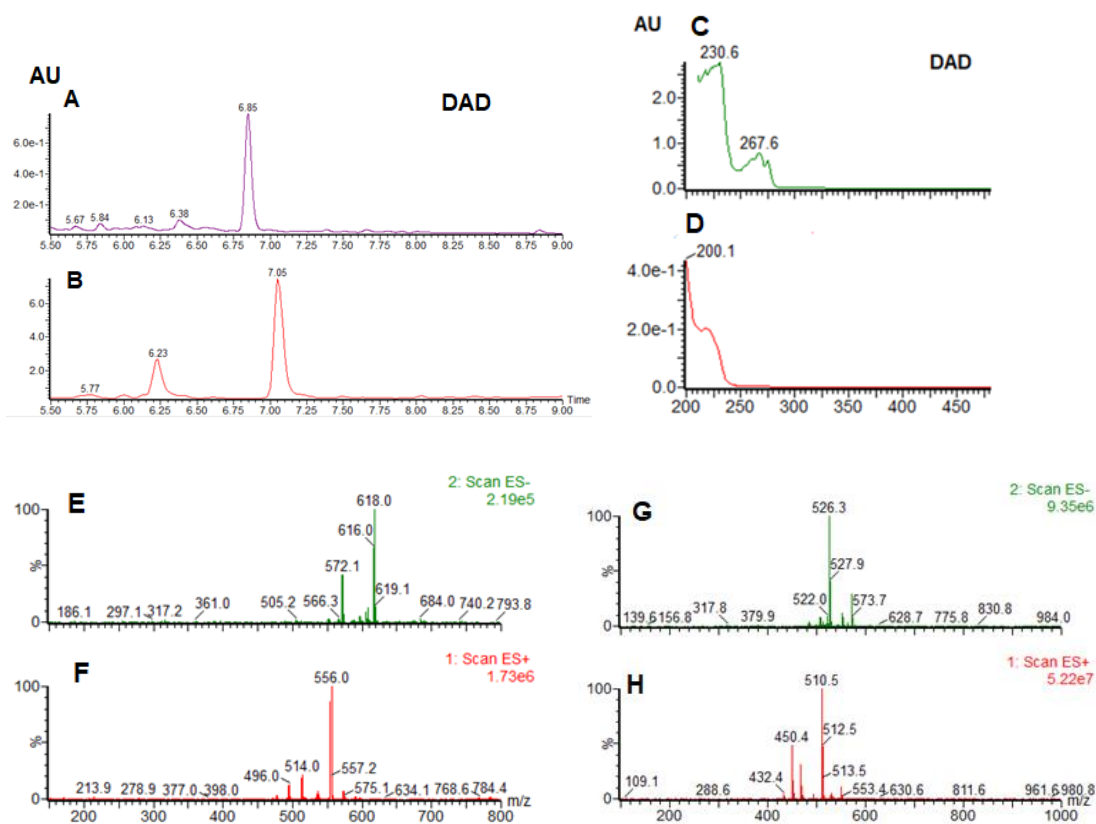


Figure 4.2. LCMS and mass chromatograms (DAD trace) of 254 and 255 feeding studies. A, C, E, F: compound 254 LCMS chromatogram, UV absorbance, mass spectra of 254; B, D, G, H: compound 255 LCMS chromatogram, UV absorbance, mass spectra of 255.

Table 4.1 Yield of the new pyrichalasin obtained from feeding study.

Entry	Feeding substrates (10 mg/mL)	Molecular Formula	Appearance (powder)	Titer (mg/L)
1	4'- <i>O</i> -Methyl-L-tyrosine 175	C ₃₁ H ₄₁ NO ₆	white	61.6
2	4'- <i>O</i> -allyl-tyrosine 243	C ₃₃ H ₄₃ NO ₆	light yellow	32.2
3	4'- <i>O</i> -propargyl-tyrosine 244	C ₃₃ H ₄₁ NO ₆	white	44.6
4	4'-fluoro phenylalanine 246	C ₃₀ H ₃₈ FNO ₅	light yellow	26.8
5	4'-chloro phenylalanine 247	C ₃₀ H ₃₈ ClNO ₅	white	55.7
6	4'-bromo phenylalanine 248	C ₃₀ H ₃₈ BrNO ₅	white	41.3
7	4'-iodo phenylalanine 249	C ₃₀ H ₃₈ INO ₅	white	52.5
8	4'-azido phenylalanine 250	C ₃₀ H ₃₈ N ₄ O ₅	light yellow	38.9

4.4 Discussion & Conclusion

In order to investigate the tolerance of the A-domain of PyiS, we then fed 4 different 4'-halogenated phenylalanines (**246** - **249**) to Δ *pyiA* KO strain. To our surprise, all 4 substrates were incorporated by PyiS to give the corresponding new 4'-halogenated pyrichalasin (**254** - **257**).

Compound **252** and **258** were obtained, after feeding 4'-azido phenylalanine and *O*-propargyl tyrosine to the *pyiA* deficient strain. Subsequently, a more complex system was tested by feeding 4'-*O*-allyl-tyrosine **243** and *O*-butynyl phenylalanine **245** to the KO strain in parallel, we obtained the desired 4'-*O*-allyl pyrichalasin **251**, while no 4'-*O*-butynyl pyrichalasin **253** was detected.

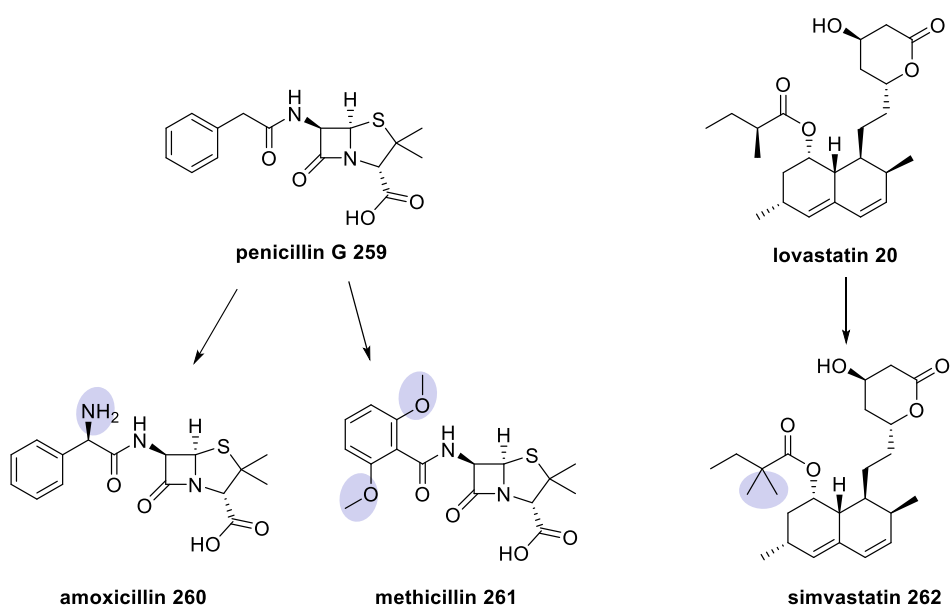
From the above feeding experiments, we can draw the conclusion that the A-domain of PyiS can recognise different 4'-substituted phenylalanines. The A-domain is therefore tolerant to different substrates. It can process small (*e.g.* 4'-F) and medium (*e.g.* 4'-O-allyl) substrates but larger (*e.g.* 4'-O-butynyl) substrates are not used.

5. Chemical Modification of Mutasyntetic Pyrichalasangans

5.1 Introduction

Natural products are an important source of lead compounds for drug development, these compounds often exhibit great potency when tested against specific targets, however, other properties of these compounds, such as solubility, bioavailability, exposure, stability, and metabolism, many need to be improved. Several approaches have been used to diversify natural products.¹⁶⁸

There is a long history of the use of synthetic chemistry to modify natural products to generate compounds with improved pharmacological properties. For example, amoxicillin **260**, a β -lactam antibiotic produced by semisynthesis has a broader spectrum than penicillin G **259**, while methicillin **261** has a greater resistance to penicillinase.¹⁶⁹ Similarly, the semisynthetic simvastatin **262** is more potent than the fungal polyketide natural product lovastatin **20** (Scheme 5.1).¹⁷⁰ This semisynthetic approach has been widely used to diversifying the structural complexity of many natural product drug candidates.

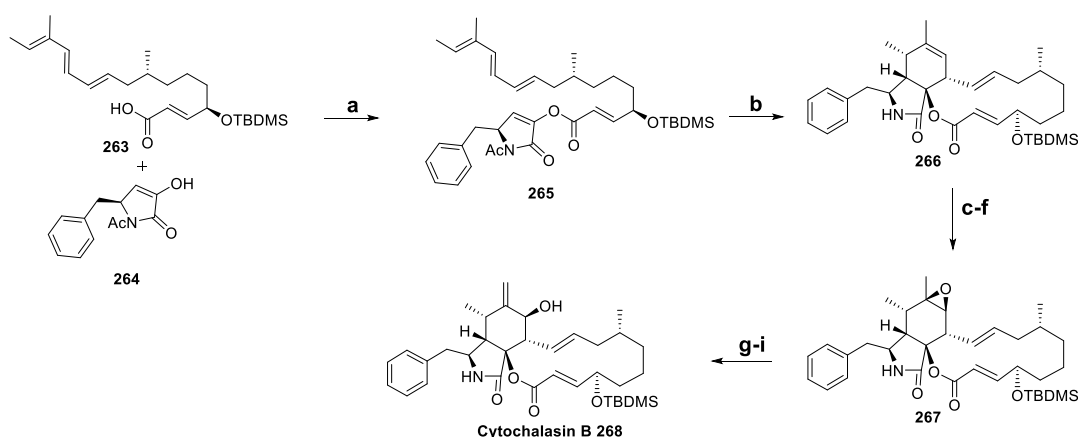


Scheme 5.1 Chemical modification of derivatives of penicillin G **259** and lovastatin **20**.¹⁷⁰

Mutasynthesis experiment by feeding 4'-substituted phenylalanines **243** - **250** to Δ *pyiA* strain, gave the corresponding 4'-functionalised pyrichalasin **251** - **258** in titres around 30-60 mg / L similar to the pyrichalasin H **65** production in wild type strains (Chapter 4.3). These compounds themselves may have new properties. Alternatively the introduced functional groups could be used in further chemical derivatisation reactions.

5.1.1 Total synthesis of Cytochalasin B

Total synthesis of several cytochalasins has been reported. For example, the first total synthesis of cytochalasin B **268** was done by Stork and co-workers (Scheme 5.2).^{171,172} A triene **263** was esterified with *N*-acetylhydroxypyrrolone **264** to form the precursor **265** for the key intramolecular [4+2] cycloaddition. The Diels-Alder reaction required harsh conditions (180 - 190 °C, 6 d) and provided the macrocycle **266** in low yield (30%). Subsequently, compound **266** undergoes several more steps to form epoxide **267**, then two more steps were carried out to produce the final product cytochalasin B **268**. Therefore, the scope and practicality of total synthesis are limited, and the syntheses have not been extended to the production of functionalised analogues.^{173,174}

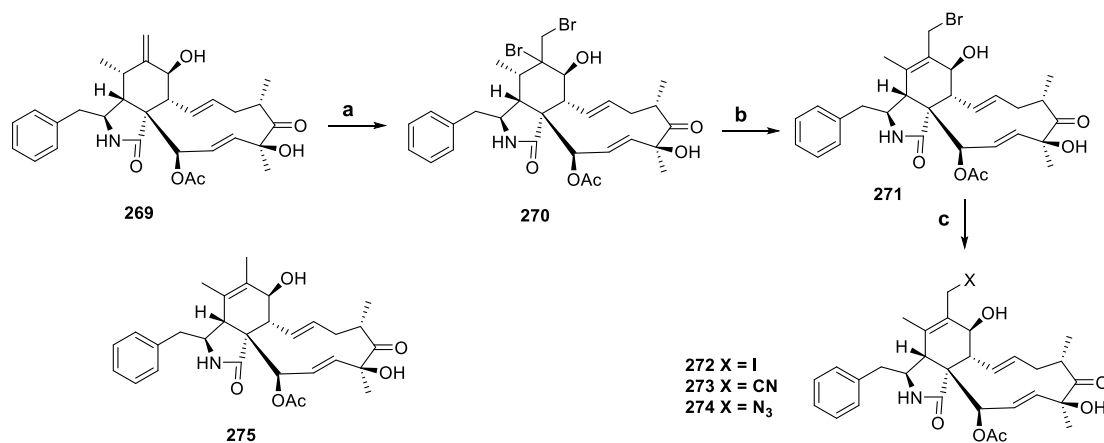


Scheme 5.2 Total synthesis of cytochalasin B **268**. Reagents and conditions: a, 2-chloropyridine methiodide, 20 mol% DMAP, NEt₃, RT, CH₂Cl₂, 69%; b, 180-190 °C, 6 d, 30%; c, 3 equiv. LDA, -78 °C, THF; d, 3 equiv. PhSeCl, H₂O₂, pyridine, CH₂Cl₂ 76% trans-selective; e, Ac₂O, DMAP, NEt₃ 88%; f, 1 equiv. *t*-BuOOH, 2.5 mol% Mo(CO)₆, 0.7 M in benzene, 75 °C, 1.5 h, 89%; g, Al(O*i*Pr)₃, Δ, xylene, 8 h, 74%; h, K₂CO₃, MeOH, 86%; i, Bu₄NF, THF 75%.¹⁷¹

5.1.2 Chemical Modification of Cytochalasin D

Considering the vast knowledge on the backbone of natural cytochalasins and their biological activities, it is surprising to find that very few investigations have been reported on the chemical modification of cytochalasins, or attempts to functionalise them for more targeted use in chemical biology.

Tanenbaum and co-workers examined the synthesis and biological activities of cytochalasin D derivatives (Scheme 5.3).¹⁷³ Cytochalasin D **269** was reacted with phenyltrimethylammonium perbromide to give 6,12-dibromocytochalasin D **270** (stereochemistry not given). **270** was then selectively monodehydrohalogenated with lithium chloride. Nucleophilic substitution reactions with sodium iodide, cyanide and azide gave three novel cytochalasin derivatives **272** - **274**. Cytochalasin C **275** and D **269** caused almost identical biological responses to tumor cell lines, while derivatives with iodo **272** or azido **274** functions significantly reduced the effectiveness (30-50%). The dibromo derivative **270** exhibit even lower potencies, which may be rationalized by steric hinderance, or the high electronegativity of **273** likely due to the C-12 nitrile.¹⁷¹



Scheme 5.3 Derivatization of cytochalasin D **269**. Reagents and conditions: a, PhNMe₃Br₃, THF; b, LiCl, DMF; c, NaI, X = I; NaCN, X = CN; NaN₃, X = N₃.¹⁷¹

In our case the 4'-functionalised pyrichalasins **251** - **258** obtained from feeding experiment, should allow us to do some chemical modifications targeting these functional pyrichalasins to generate new unnatural functionalised cytochalasins.

5.2 Aims

A library of different 4'-substituted pyrivalasans was created by mutasynthesis (Chapter 4). These pyrivalasins can be used as substrates to further generate different functional molecules by various chemical reactions. More and more novel cytochalasan have been reported, while few dimeric cytochalasan have been found. Generating dimeric pyrivalasins would be worth trying by chemical modification. For example, 4'-bromo pyrivalasin **256** could be used to generate dimeric pyrivalasins by Suzuki reaction; triazole containing pyrivalasins could be synthesized by click chemistry using azide and alkyne substrates; fluorescent dyes could also be linked to pyrivalasin by Huisgen cycloaddition. Furthermore, these synthesized functional pyrivalasins will be tested on microorganisms, tumor cell lines and in the cell biology area. Our target is to develop some anti-fungal or anti-tumor drug candidates, or to generate new cell imaging tools for actin visualization.

5.3 Results

5.3.1 Generating New Hybrid Molecular Pyrivalasans by Copper-Catalyzed Azide-Alkyne Huisgen Cycloaddition (CuAAC)

The concept of click chemistry (CC), first introduced by K. B. Sharpless, has been widely adopted for use in drug discovery. For a decade, CC has provided the ability to rapidly and reliably synthesize novel materials. The use of CC is likely to significantly advance drug discovery and bioconjugation development.¹⁷⁵ The copper-catalyzed Huisgen azide-alkyne cycloaddition (CuAAC) is the leading method of the "click chemistry" group.^{176,177} Because of the straightforward procedures, the high functional group tolerance, and the usually high yields. CuAAC has affected all fields of chemistry from materials to life science.^{178,179}

An alkyne-azide cycloaddition occurs between an organic azide and a terminal alkyne in the presence of Cu(I) to form a 1,4 disubstituted 1,2,3 triazole. The rate of this reaction is fast, which means that it proceeds efficiently at room temperature. However, the mechanism of the alkyne - azide click reaction mediated by copper (CuAAC) remains

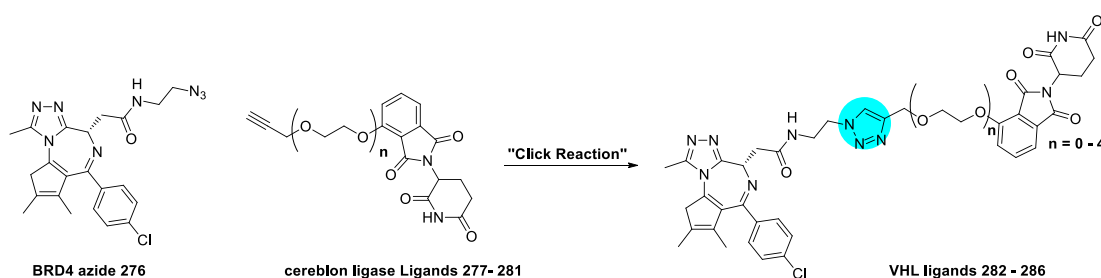
difficult to establish owing to the involvement of several reaction intermediates and the widespread use of copper-catalyzed cycloaddition reaction.¹⁸⁰

5.3.2 Application of Huisgen Cycloaddition

Targeted protein degradation, using bifunctional small molecules (Protacs) to remove specific proteins from cells, has emerged as a powerful new modality of chemical biology and drug discovery. Protacs composed of a ligand for a target protein of interest, and a ligand for an E3 ubiquitin ligase, combined by a flexible linker.¹⁸¹ This approach “hijacks” the function of a ligase to transfer ubiquitin subunits to the target protein, thereby tagging it for recognition by the proteasome and coding its destruction.^{182,183}

There is little literature insight into the ideal linker and suggested experience in protac design. A comprehensive study of ligase ligand/linker length activity relationship with a bromodomain and extraterminal domain-4 (BRD4) targeting protac been investigated to understand of the structure active relationship (SAR) of these bispecific molecules.¹⁸⁴ A reliable linking strategy to couple ligase ligand-containing motifs and target protein ligands, which led to the Huisgen 1,3-dipolar cycloaddition reaction. A new triazole ring was formed by using the azides and alkynes as substrates and catalyzed by copper. This reaction was referred as “click chemistry” due to its ease of use.¹⁸⁵ This reaction is high yielding, requiring stoichiometric quantities of each component and shows excellent functional group compatibility under mild reaction conditions.

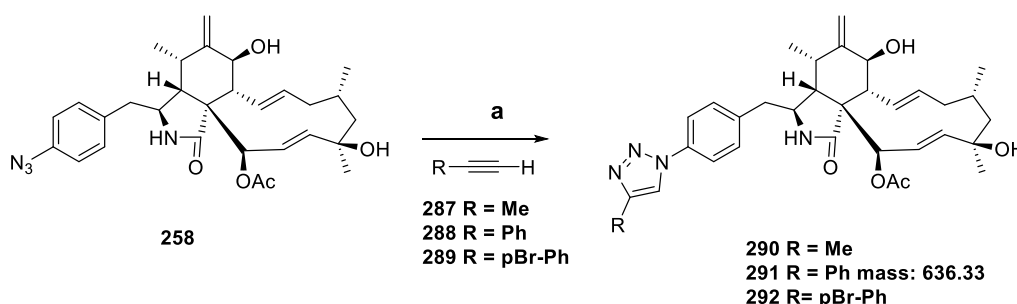
With BRD4 azide **276** and alkyne cereblon ligase ligands **277 – 281** in hand, then undergoes the typical conditions for a click reaction to generate the library of Von Hippel-Lindau (VHL) ligands **282 – 286** (Scheme 5.4).¹⁸⁶



Scheme 5.4 Protac synthesis using the “Click Reaction”.¹⁸²

5.3.3 Result

10 mg of 4'-Azido pyrichalasin **258** was reacted with a series of alkynes (prop-1-yne **287**, phenylacetylene **288**, 4-bromo-1-ethynylbenzene **289**) and shown to be a good substrate for alkyne-azide Huisgen cycloaddition reaction.¹⁸⁷ The reaction mixture was checked by analytical LCMS. The correct mass pattern of the target compounds was found. The starting material in each case was totally consumed (Scheme 5.5). The solvent was removed *in vacuo*. The residue was dissolved in ethyl acetate and washed with water, organic phase was dried over MgSO₄, filtered and characterized to dryness *in vacuo*. The crude product was dissolved in MeOH and purified by LCMS to give the expected triazole products **290** - **292** in good yield, those compounds were fully characterized by HRMS and 2D NMR. The typical methyl group resonance from the triazole ring can be found from heteronuclear single quantum correlation spectra (HSQC, $\delta_H - \delta_C$, 7.73/118.9, Scheme 5.5, Appendix).¹⁸⁷



Scheme 5.5 Synthesis of functionalised pyrichalasins. Reagents and conditions: a, DIPEA, DMF, CuI, RT, 12 h.¹⁸⁷

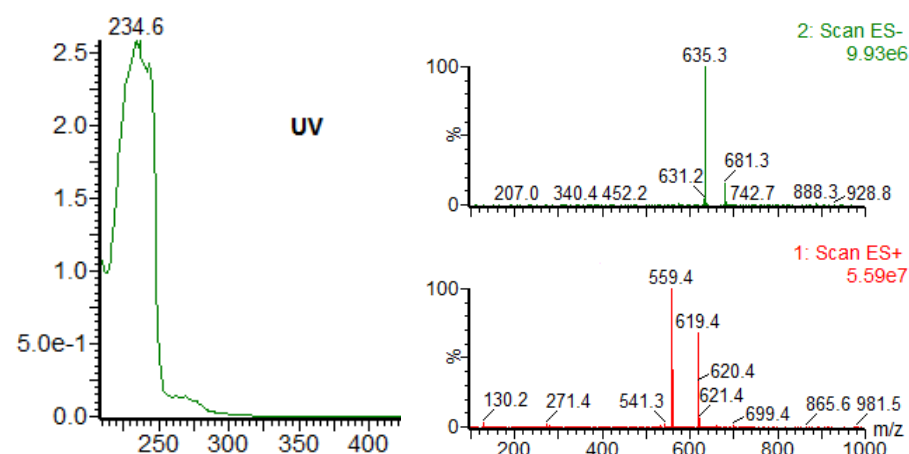


Figure 5.1 UV and mass spectra of compound **291**.

Synthesis of Hybrid Pyrichalasin

Biotin is a water soluble vitamin which forms excellent stable complexes with avidin and streptavidin.¹⁸⁸ It has been investigated in a wide range of applications from molecular labelling and bio-interfaces to nanostructure assembly.¹⁹⁰ 23-hydroxyl-CODD-Me **293** and related compounds are potential anti-inflammatory, cancer chemotherapeutic agents. Biotinylated CDDO was used as an effective method of selectively identifying their protein targets within the proteome of a cell because streptavidin has a very high affinity for biotin.¹⁸⁹ For example, the C-23 biotin conjugate of CDDO-Me **294**, was used as a good affinity probe for the identification of cellular radicicol-binding proteins.¹⁹⁰

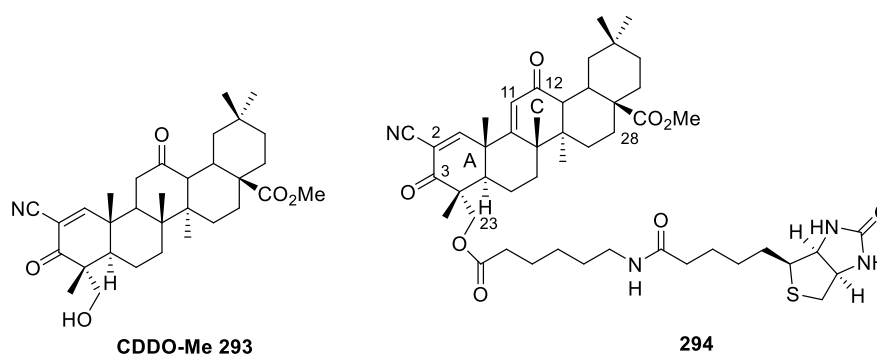
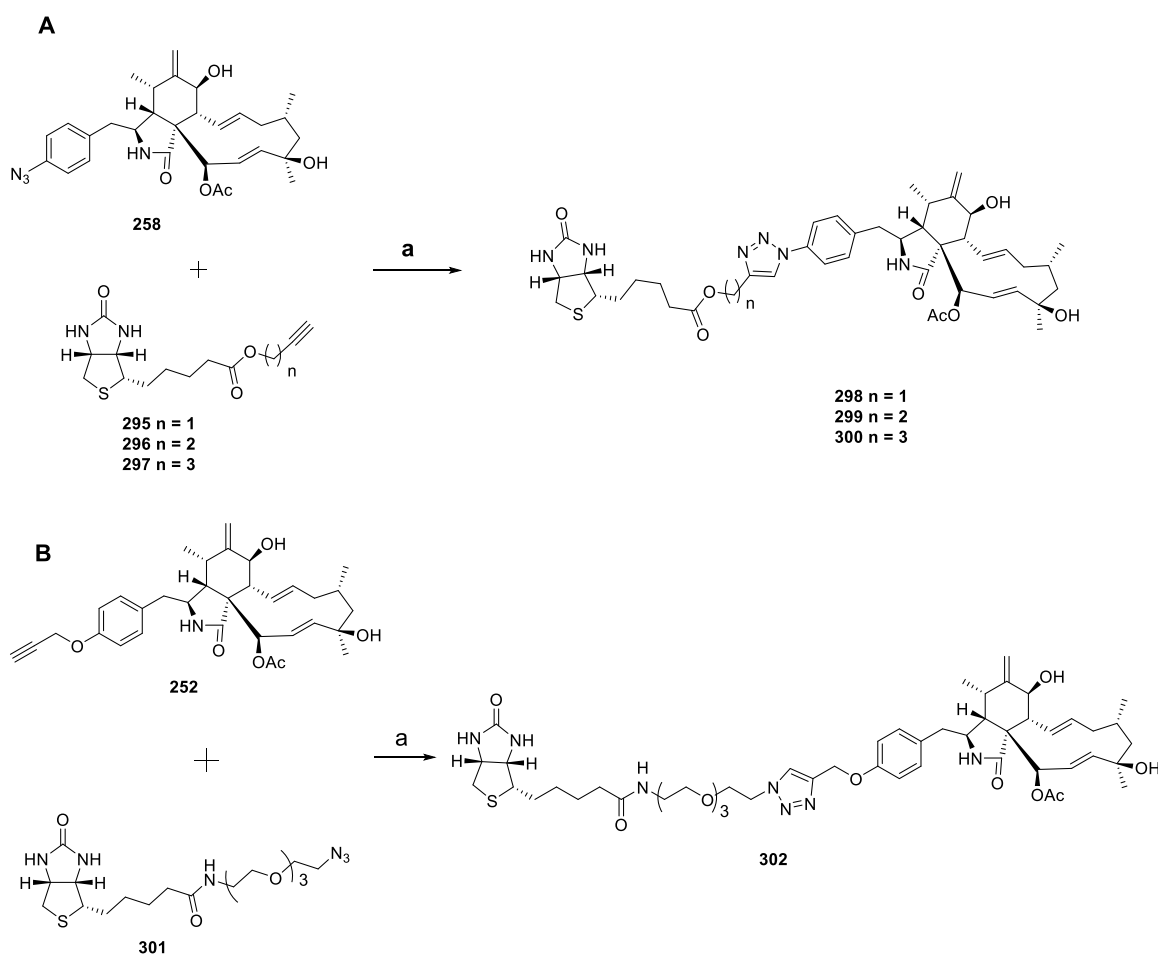


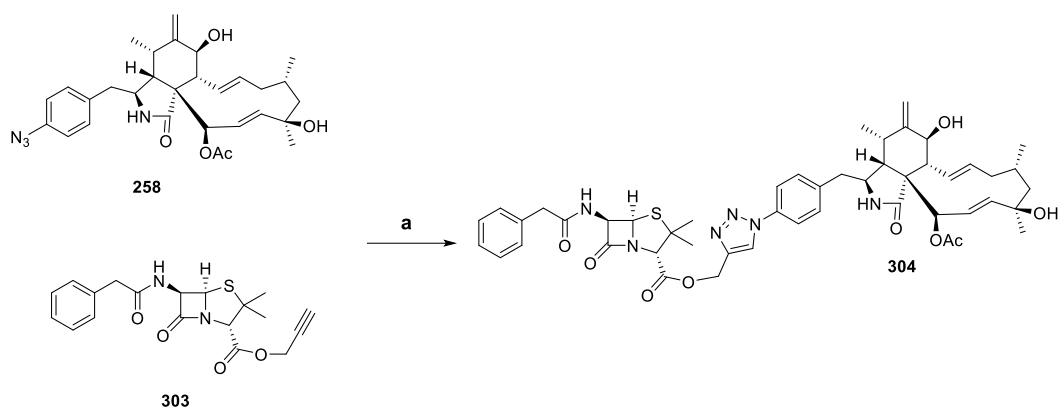
Figure 5.2 C-23 biotin conjugate of CDDO-Me **294**.¹⁹⁰

Based on the successful Huisgen cycloaddition reaction described in the previous section, the biotin-propargyl ester **295**, biotin-homopropargyl ester **296** and biotin-pent-4-ynyl ester **297** (synthetic details were described in chapter 6.2.7) were tested and showed that the expected pyrichalasin-biotin products **298** - **300** were formed as expected (Scheme 5.6 A). Similar chemistry was achieved by coupling the biotin-PEG-azide **301** (synthetic details was described in chapter 6.2.7) with 4'-*O*-propargyl pyrichalasin **252** to create **302** containing a longer and more hydrophilic PEG linker (Scheme 5.6 B).¹⁹⁰ All compounds were synthesised in 10 mg scale using standard procedures, purified and fully characterised as mentioned above (Appendix).



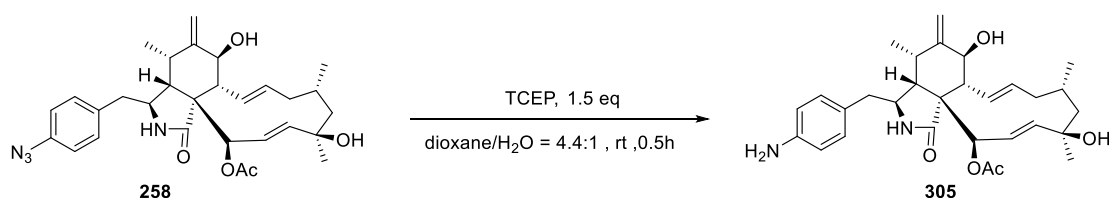
Scheme 5.6 Synthesis of hybrid pyrichalasin. Reagents and conditions: a, DIPEA, DMF, CuI, RT, 12 h.¹⁹¹

Hybrid molecules, obtained by the combination of structural features of two differently active moieties, is one of the most popular chemical entities for developing modified backbones often with improved properties in the area of biology and medicinal science. Penicillin G **259** features a thiazolidine ring, which is fused to a highly labile β -lactam ring carbonyl. It is one of the most widely used antibiotics in a range of agricultural and medicinal applications. We also experimented with the production of hybrid metabolites. For example, 10 mg of propargyl ester of penicillin G **303** (synthetic details were described in chapter 6.2.7) reacted smoothly with **258** to give the conjugate **304** as white powder in a yield of 88.6%. (Scheme 5.7).¹⁹¹



Scheme 5.7 Synthesis of hybrid pyrichalasin. Reagents and conditions: a, DIPEA, DMF, CuI, RT, 12h.¹⁹¹

10 mg of 4'-Azido pyrichalasin **258** was reduced (Staudinger reaction) to 4'-amino pyrichalasin **305** in good yield, by using triscarboxyethylphosphine (TCEP) as a reductive reagent. The highly unusual amino cytochalasin product **305** was purified by preparative LCMS and confirmed by HRMS and full NMR characterization (Scheme 5.8, Appendix).¹⁹²



Scheme 5.8 Preparation of 4'-amino pyrichalasin **305**. Reagents and conditions: dioxane, H₂O, TCEP, RT, 0.5 h.¹⁹²

5.3.4 Synthesis, Bioevaluation and Application of Fluorescent Dye Linked Pyrichalasans in Cell Visualization

Actin is one of the most abundant proteins in eukaryotic cells and its amino acid sequence is very highly conserved from yeast to man. The concentration of actin in eukaryotic cells is relatively high and reaches the micromolar range.¹⁹³ Actin fulfills a multitude of cellular functions, such as intracellular transport, adhesion and concentration, membrane dynamics and migration, cytokinesis and cell-cell contact

regulation, polarity and cell shape control, as well as gene regulation and other less well explored functions in the nucleus.¹⁹⁴

Although methods for the visualization of single tissues have been well established for decades,¹⁹⁵ it has still been a challenge to visualize specific actin structures and their related functions, in particular under real-time conditions in living cells and organisms.

Phalloidin **45** is a bicyclic heptapeptide, which is isolated from the mushroom *Amanita phalloides*. Phalloidin binds to filamentous actin (F-actin) in high affinity and lowers the critical concentration of actin polymerization in solution. It has been widely used to study actin dynamics *in vitro*, and dye linked analogues of phalloidin serve as highly specific reagents for microscopic visualization of the actin cytoskeleton (Figure 5.3).^{196,197}

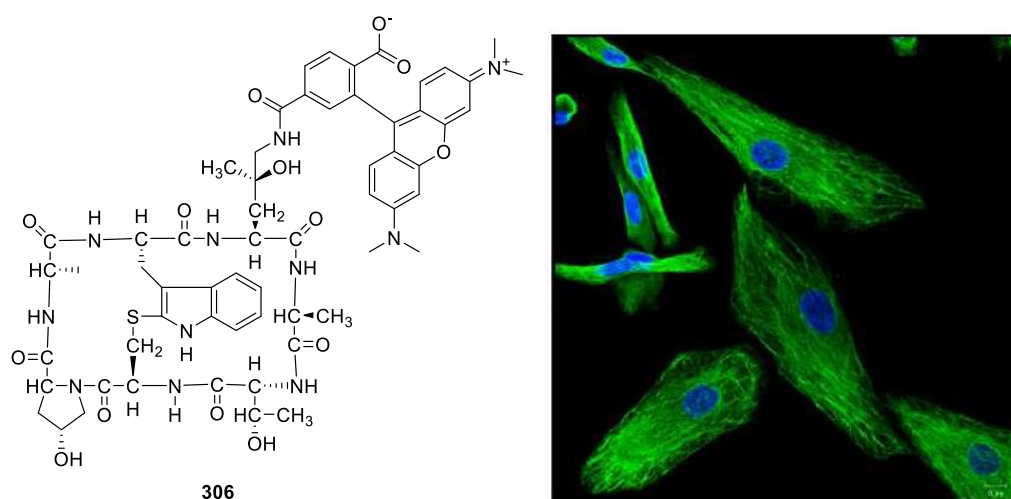
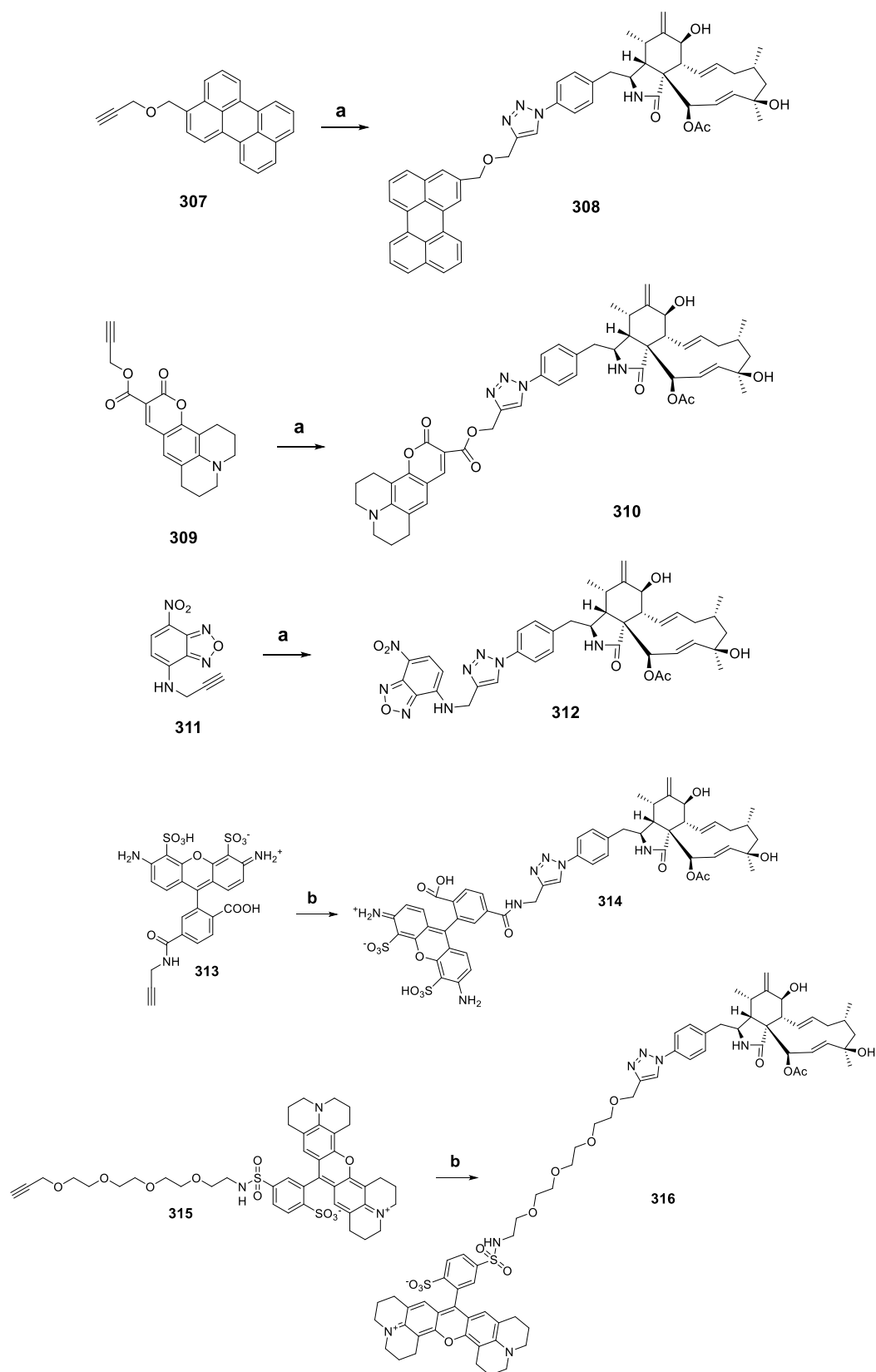


Figure 5.3 F-actin stained with Phalloidin - Rhodamine Conjugate **306**.¹⁹⁸

Cytochalasins bind to the barbed end of actin filaments, which inhibits both the association and dissociation of subunits at that end. The binding between actin⁴³ and cytochalasin causes inhibition of polymerization.¹⁹⁹ Cytochalasin linked with a fluorescent dye tail would allow the intracellular locations of actin barbed end to be tracked as well as observation of the actin disruption properties.

5.3.5 Results

Several well-known commercially available fluorescent tags were easily added to the pyrichalasin scaffold using click chemistry. For example, 4'-azidopyrichalasin **258** was reacted with the perylene-linked acetylene **307** to give the expected product **308** in high yield. Similarly, the acetylene-linked coumarin dye **309** also coupled smoothly to give the expected **310**. The 7-nitro-4-(prop-2-ynylamino) benzofuran (NBD) dye **311** was added to **258** to form the expected **312**. Finally, Texas Red- **313** and AF-488- **315** were also linked using the same methodology to afford **314** and **315** individually. All compounds were synthesised in 5-10 mg scale using standard procedures, purified and fully characterised by HRMS and NMR (Scheme 5.9, Appendix, Compound **307**, **309** and **311** were provided by Prof. Mark Brönstrup's group).^{191,200}

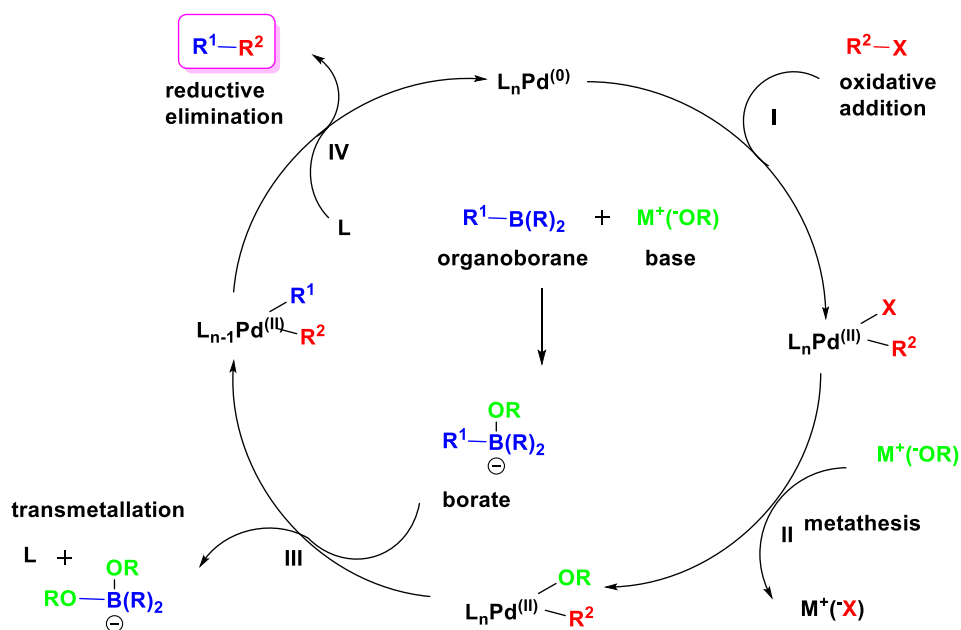


Scheme 5.9 Synthesis of dye-linked pyrchalasans. Reagents and conditions: a, **258**, DIPEA, DMF, CuI, RT, 12 h; b, **258**, CuSO₄, sodium ascorbate, DMF/H₂O = 4:1.^{191,200}

5.3.6 Generating Dimeric Pyrrochalsans with Different Chain Length Linkers

The importance of transition metal catalysed carbon-carbon bond forming reactions is well studied in the literature.²⁰¹ Suzuki-Miyaura cross-coupling reactions, along with numerous others in this general field, has sparked great interest in C-C bond formation reactions. The palladium-catalysed cross-coupling reaction between organoboron compounds and organic halides or triflates provides a powerful and general method for the formation of carbon-carbon bonds. There are several advantages to this method: first, mild reaction conditions; second, commercial availability of many boronic acids; and third, the inorganic by-products are environmentally safer and much less toxic than organostannanes *etc.*^{202,203}

The mechanism of the Suzuki cross-coupling is analogous to the catalytic cycle for the other cross-coupling reactions and has four distinct steps. The cycle is initiated by the oxidative addition of the organic halide to the stabilized Pd⁽⁰⁾ species to form Pd^(II) (Step I, Scheme 5.10). Followed by the exchange of the anion attached to the palladium for the anion of the base (metathesis, Step II, Scheme 5.10). The transmetalation step transfers the R¹ group from the metal boron to the metal palladium to generate an intermediate containing R¹, R² and ligand in the coordination sphere of palladium (Step III, Scheme 5.10). Two reductive eliminations from this intermediate produce the coupling R¹-R² product and regeneration of Pd⁽⁰⁾ (Step IV, Scheme 5.10). Although organoboronic acids do not transmetallate to the Pd(II)-complexes, the corresponding ate-complexes readily undergo transmetalation. The quaternization of the boron atom with an anion increases the nucleophilicity of the alkyl group and it accelerates its transfer to the palladium in the transmetalation step. Very bulky and electron-rich ligands (*e.g.*, P(*t*-Bu)₃) increase the reactivity of otherwise unreactive aryl chlorides by accelerating the rate of the oxidative addition step (Scheme 5.10).²⁰⁴



Scheme 5.10 Catalytic cycle for the Suzuki-Miyaura cross coupling.¹⁷⁵

5.3.7 Results

20 mg of 4'-bromo-pyrichalasin **256** was used to synthesis the 4'-borolated pyrichalasin **317** by using *bis*(pinacolato)diboron, in the presence of Pd(dppf)Cl₂ under reflux conditions. After 8 hours, the mass of target boronic ester intermediate **317** was detected by analytic LCMS. The product was then purified by preparative LCMS. The target intermediate **317** (mass = 619.4) was obtained as a white solid and confirmed by full NMR characterization (Figure 5.4, Appendix).

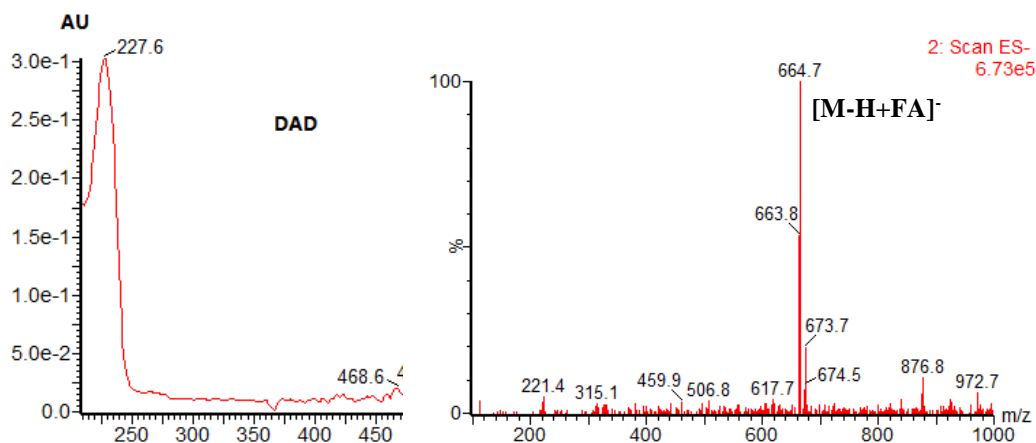
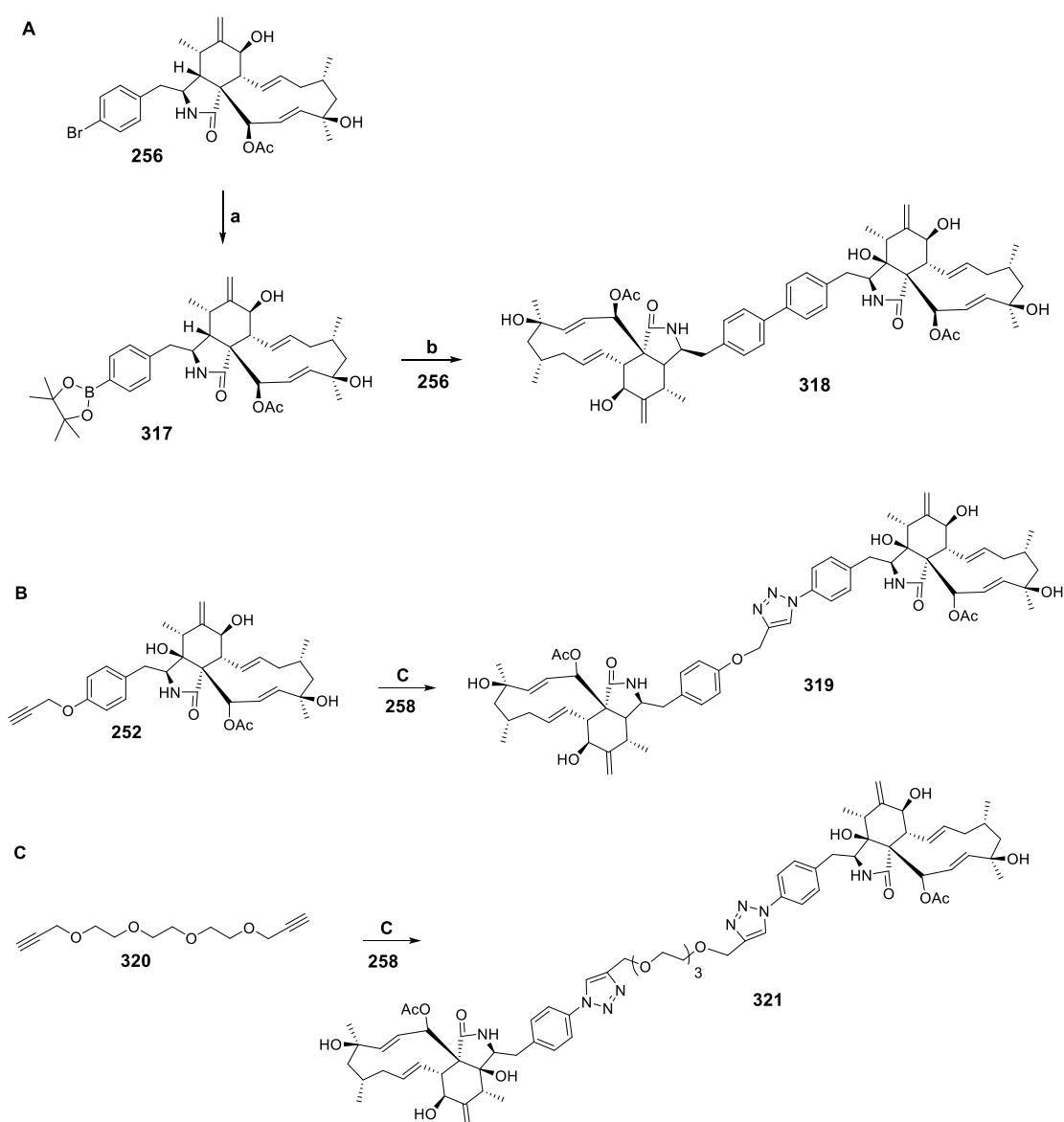


Figure 5.4 UV and mass spectra of compound **317**.

Subsequent reaction of **317** with 10 mg 4'-bromo-pyrichalasin **256** in a separate reaction catalysed by Pd(PPh₃)₄ in the presence of X-phos as a ligand,²⁰⁵ then produced the unprecedented 4'-4' cytochalasin H symmetrical dimer **318** (Scheme 5.11 A).^{205,206}

Then the unsymmetrical dimer **319** with a simple hydroxymethyl triazole linker was formed by the direct coupling of **252** and **258** through click chemistry (Scheme 5.11 B). Moreover, a longer and more polar linker was introduced into the dimer by Huisgen coupling between the bis-propargyl-PEG linker **320** and **258** to produce **321** (Scheme 5.11 C). All these compounds were synthesised in 10 mg scale, and their structures were confirmed by HRMS and full NMR characterization (Appendix).



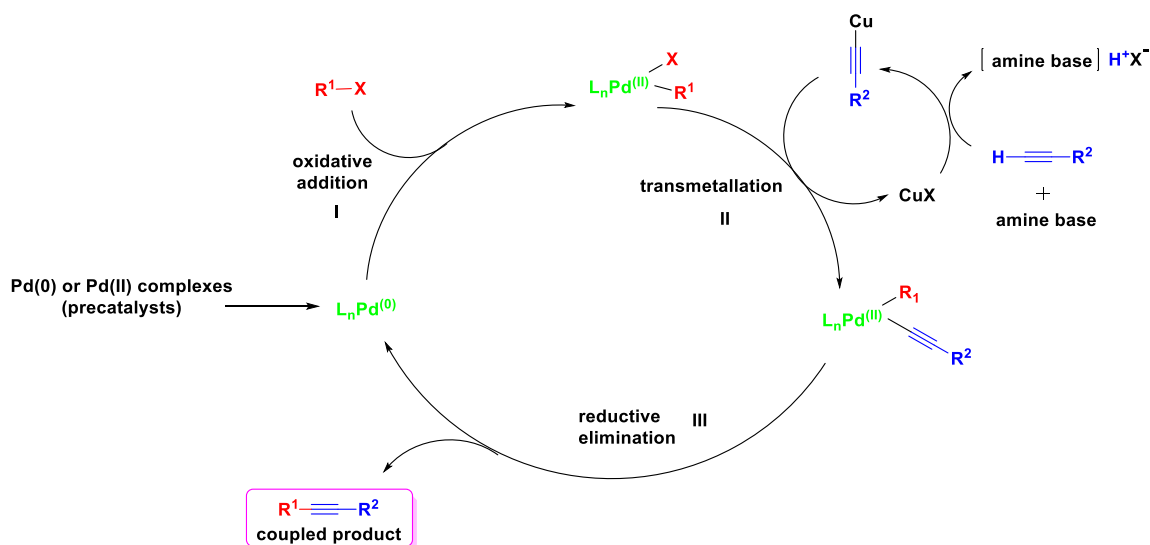
Scheme 5.11 Synthesis of dimeric pyrichalasin. Reagents and conditions: a, Pd(dppf)Cl₂, CH₃CO₂K, Dioxane, 110 °C, 8h; b, Pd(PPh₃)₄, X-Phos, Dioxane, H₂O, 110 °C, 2 h; c, DIPEA, DMF, CuI, RT, 12

h.^{187,191}

5.3.8 Generating New Pyrichalasin by Sonogashira Reaction

In 1975, K. Sonogashira and co-workers reported that symmetrically substituted alkynes could be prepared under mild conditions by reacting acetylene gas with aryl iodides or vinyl bromides in the presence of catalytic amounts of $\text{Pd}(\text{PPh}_3)\text{Cl}_2$ and cuprous iodide (CuI).¹⁷⁰ The copper-palladium catalysed coupling of terminal alkynes with aryl and vinyl halides to give enynes is known as the Sonogashira cross-coupling.¹⁷⁵

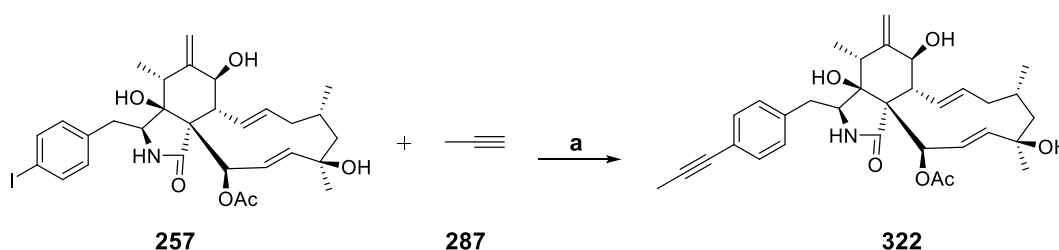
The mechanism of the Sonogashira cross-coupling follows the expected oxidative addition-reductive elimination pathway. However, the structure of the catalytically active species and the precise role of the CuI catalyst is unknown. The reaction commences with the generation of a coordinatively unsaturated $\text{Pd}(0)$ species from a $\text{Pd}(\text{II})$ complex by reduction with the alkyne substrates or with an added phosphine ligand. The $\text{Pd}(0)$ then undergoes oxidative addition with the aryl or vinyl halide followed by transmetalation by the copper(I)-acetylide (Step I-II, Scheme 5.12). Reductive elimination affords the coupled product and the regeneration of the catalyst completes the catalytic cycle (Step III, Scheme 5.12).¹⁷⁵



Scheme 5.12 Mechanism of the Sonogashira cross-coupling reaction.¹⁷⁵

5.3.9 Result

5 mg 4'-bromo **256** and the alkyne of prop-1-yne **287** were tested as substrates in Palladium-catalysed cross-coupling reactions. The brominated derivative **256** did not react smoothly in the first attempt of Sonogashira cross-coupling reactions. However, the 4'-iodo substrates **257** reacted cleanly, to give the desired product 4'-acetylene **322**, this compound was also confirmed by HRMS and NMR (Scheme 5.13, Appendix).^{207,208}



Scheme 5.13 Sonogashira reaction of 4'-iodopyrichalasin **257**. Reagents and conditions: (a) Pd(dppf)Cl₂, CH₃CO₂K, dioxane, 110 °C, 8 h.^{207,208}

5.4 Discussion & Outlook

Functional pyrichalasin **251** - **258** were generated by mutasynthesis (Chapter 4). Many interesting and unprecedented functionalised cytochalasins were generated based on the above substrates. All compounds were synthesised in around 5 - 10 mg scale using standard procedures (experimental details are summarized in chapter 6.2.7) and easily purified by HPLC. For example, 4'-bromo pyrichalasin **256** can be used as the starting material to generate dimeric pyrichalasin **318** by Suzuki cross coupling reaction. 4'-Iodo pyrichalasin **257** is the starting reagent for Sonogashira reaction.

Both 4'-azidophenylalanine **258** and *O*-propargyl phenylalanine **252** are very popular substrates for click chemistry (CC). Dimeric pyrichalasins **319** were synthesized *via* Huisgen chemistry. Subsequently, several functional hybrid pyrichalasins were also generated by CC. For example, the bioactive molecule biotins were coupled to pyrichalasin H to give the corresponding different chain length conjugates **298** - **300**, so as the penicillin G was linked and produce **304**. Cytochalasins can bind to actin protein in high affinity, several commonly used fluorescent dyes were linked to pyrichalasin to

form the molecular probe **308** - **316**, these molecules can be used to track actin protein in eukaryotic cell.

All compounds were sent to our collaborator Prof. Marc Stadler and co-workers and tested for their antifungal activities, cytotoxicity and actin-disruption properties. First, the compounds were tested in a standard minimal inhibitory concentration (MIC) assay towards *Schizosaccharomyces pombe*, *Pichia anomala*, *Mucor hiemalis*, *Candida albicans*, and *Rhodotorula glutinis*, no candidates showed significant antifungal activity. 4'-Amino-pyrichalasin **305** had no activity to the microorganisms, weak activity was observed from compounds **287**, **295**, **302**, **304**, **308**, coumarin-linked **310** showed moderate activity vs *S. pombe* only.

Standard cytotoxicity assays were tested on L929, KB3.1, PC3, A549, MCF-7, A431 and SKOV-3 tumor cell lines. 4'-amino pyrichalasin **305** was significantly less cytotoxic (0.2 - 30 µg/ml), large hybrid compounds such as biotins (**295** - **297**), penicillin **304** and perylene **308** were also much less cytotoxic (0.5 - 37 µg/ml). To our surprise, dimeric compounds **318** and **319** showed unexpected cytotoxicity (0.1 - 8.0 µg/ml), while acetylene **322** showed good potency (0.2 - 3.2 µg/ml).

Selected compounds were investigated for their actin-disruption activity *in vivo*. SKOV-3 cells were immobilised and the nucleus were stained with DAPI, and phalloidin-atto594 can selectively stains filamentous actin. Cytochalasin B **268** serves as a standard compound and clearly collapses actin at 10 µg/ml compared with DMSO control (Figure 5.5). Pyrichalasin H **65** and dimeric pyrichalsin **318** shows the same activity at this concentration (Figure 5.5, this experiment was done by M. Sc Christopher Lambert).

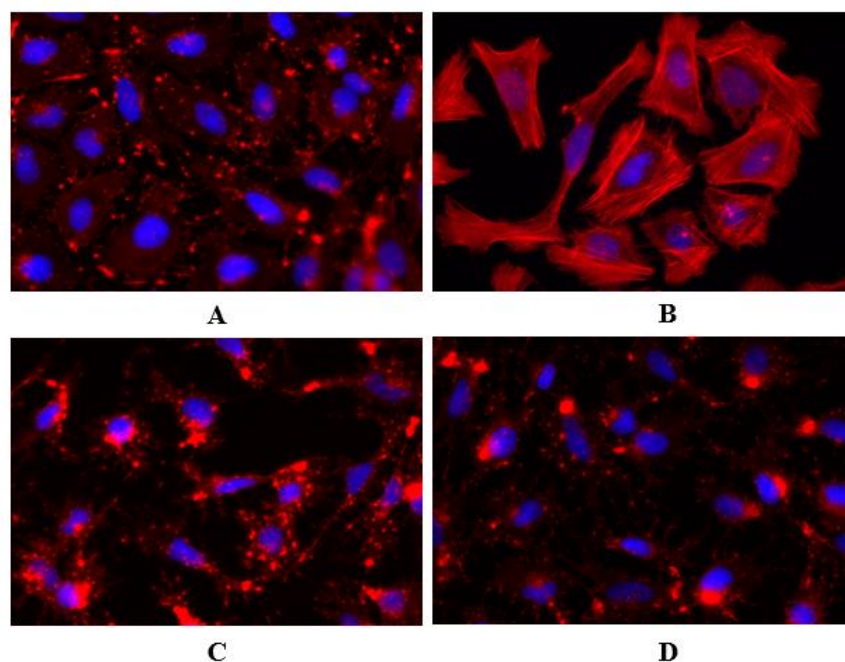


Figure 5.5 Actin disruption assay. **A**, Cytochalasin B; **B**, DMSO control; **C**, Pyrichalsin H; **D**, Dimeric pyrichalsin. All sample concentration: 5 $\mu\text{g}/\text{ml}$, red signal from Phalloidin-ATTO 594 bound to actin, Blue signal from DAPI stain in the nucleus.

U2OS cells were stained with fluorescent dye linked pyrichalans and observed under fluorescent microscope. Coumarin-linked **310** shows collapse of depolymerization of actin at 10 $\mu\text{g}/\text{ml}$ (phalloidin red channel). Observation of the blue-green fluorescence from coumarin indicating the molecule collocated with actin at lower concentration (2 $\mu\text{g}/\text{ml}$). In contrast, the perylene-linked compound **308** showed much more diffuse location within cells and no significant collocation with actin. A possible explanation would be the high hydrophobicity of the perylene molecule (Figure 5.6, this experiment was done by M. Sc Christopher Lambert). More hydrophilic dyes Texas Red linked pyrichalans **314** and AF-488 linked **316** have been created and are under testing.

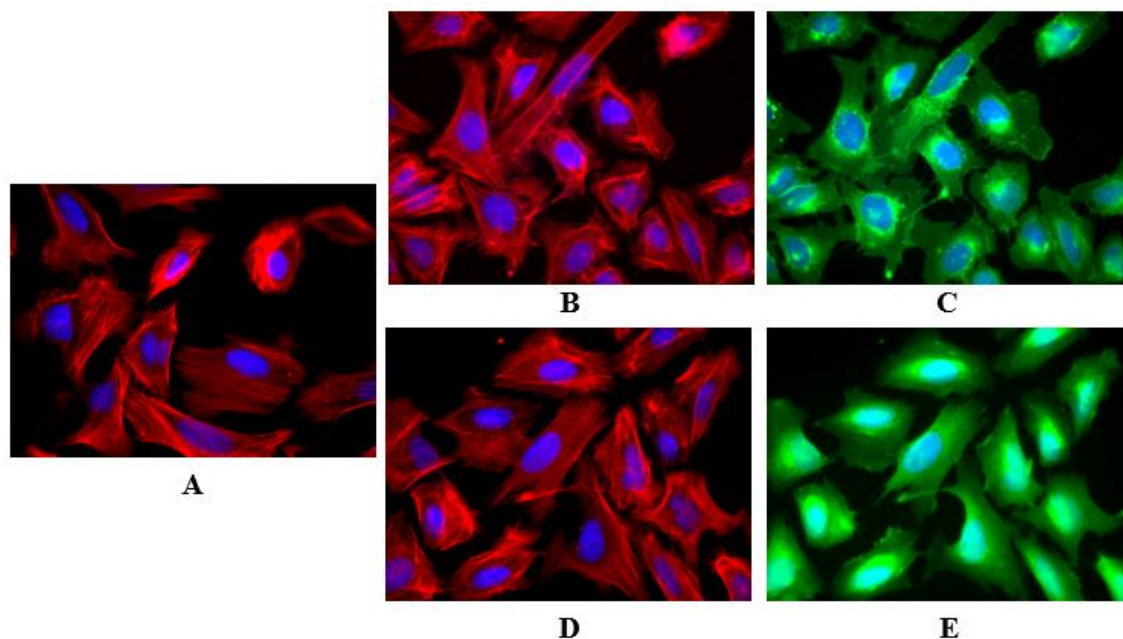


Figure 5.6 Actin localisation assay: **A**, Phalloidin-ATTO 594 stain cells (control); **B**, **308** co-stain with phalloidin (10 $\mu\text{g/ml}$, red channel); **C**, **310** co-stain with phalloidin (10 $\mu\text{g/ml}$, green channel); **D**, **310** co-stain with phalloidin (2 $\mu\text{g/ml}$, red channel); **E**, **310** co-stain with phalloidin (2 $\mu\text{g/ml}$, green channel).

In total, 18 novel functionalised cytochalasans were generated by chemical modification. Their bioactivities were confirmed by our collaborators. Based on the library we built, some more interesting reactions could be done in future. For example, Staudinger ligation, Buchwald-Hartwig Cross-Coupling reaction and so on. However, these are all the first attempts to determine the biological activities of the newly synthesized pyrichalasans. In future, more targeted cytochalasans will be synthesized, more logical and specific biotests will be executed, to explore the possible application of our compounds in both chemistry and biology areas.

6 Overall Conclusion and Outlook

Overall, the combination of gene knockout (KO) experiment, combinatorial biosynthesis was confirmed to be a powerful strategy to understanding and engineering the biosynthesis of fungal polyketide – nonribosomal peptide hybrid pyrichalasin H **65**. Mutasythesis and Semisynthesis were effective methods to generate functional cytochalasan. Moreover, biotest results showed some of novel cytochalasan have the potential to be actin protein imaging tool, some of them exhibit actin disruption ability and also showed antimicrobial activity.

First of all, we start to elucidate pyrichalasin H **65** biosynthetic pathway by knockout experiment target on *pyi* BGC. The function of seven genes was investigated individually. Thirteen novel cytochalasan were generated. For the first time, we confirmed that *O*-methyltyrosine **175** is the true precursor for compound **65** biosynthesis. Targeting KO *pyiS* gene, resulting the abolition of **65**, this experiment confirmed that the *pyi* BGC responsible for the biosynthesis of **65**. The function of two P450 genes were also investigated, *pyiD* was confirmed encoding C-18 hydrolase due to all the isolated metabolites all lack of a C-18 hydroxyl group, while *pyiG* was confirmed to encode C-7 hydrolase because all the C-7 hydroxyl group were missing from the purified compounds. All the isolated metabolites were confirmed by both HRMS and NMR. The *O*-methyltransferase encoding gene *pyiA* was also disrupted, the desired demethyl product magnachalasin **173** was obtained. However, the phenylalanine fused cytochalasin H **174** was also obtained in lower titre. This result reminds us the true precursor might be *O*-methyltyrosine **175**. It was confirmed by the restoration of pyrichalasin H **65** by feeding *O*-methyltyrosine **175** to *pyiA* mutant strain. Targeting *pyiB* gene KO, which encodes *O*-acetyltransferase, the de-acetyl product pyrichalasin J **156** was obtained. By KO the oxidoreductase encoding gene *pyiH*, three carbonyl cytochalasans **161** - **163** were isolated. Put all this results together, the late stage biosynthetic pathway of pyrichalasin H was fully elucidated (detailed conclusion in chapter 2.4).¹⁰⁹

Several mutant strains were generated by KO experiment, including two P450 disruption stains. We developed the two P450 mutant strains as the cell factory for generating novel cytochalasan by heterologous expression cryptic P450 genes from other biosynthetic pathway. In total, six P450 genes were investigated including *hffD* and *hffG* from *Hypoxylone fragiforme* BGC and *CYP1-4* from *P. oryzae* Guy 11 BGC. Three novel epoxide cytochalasan were isolated. The function of CYP1, HffD and HffG were confirmed as hydroxylase, and the CYP3 was confirmed as epoxidase. The function of CYP2 and CYP4 remain unknown, due to the several possible reasons.¹³⁹ These results from pathway engineering by combinatorial biosynthesis proved that the mutant P450 strain can be a good bioengineer platform to investigate unknown P450s as well as other tailoring gene (detailed conclusion in chapter 3.4).

Previous *pyiA* KO result confirmed the *O*-methyl tyrosine **175** is the true precursor for pyrichalsin H **65** biosynthesis, when **175** is absent, the KO strain can weakly select tyrosine and phenylalanine. Therefore, we fed different functional group substituted amino acid **243 – 250** to Δ *pyiA* strain, and seven novel cytochalasan **251 – 258** were obtained.

With the novel cytochalasan **251 – 258** generated by mutasynthesis, we further did some chemical modification based on these compounds. Eighteen functional pyrichalasin were synthesized various kind of chemical reactions. For example, compound **256** can be substrate for Suzuki cross coupling reaction to generate dimeric pyrichalasin **318**. Compound **252** and **258** can be the reagent for the copper catalyzed alkyne azide cycloaddition (CuAAC) reaction. Moreover, five dye linked fluorescent pyrichalasin **308 – 316** were generated by click chemistry (detailed conclusion in chapter 5.3.3).

All the generated compounds were sent to our collaborators in HZI for biotest. The fluorescent pyrichalasin shown the ability to localize and visualize the actin cell. Some of them showed the inhibition of actin polymerization. Our compounds also showed the inhibition on microorganisms (detailed conclusion in chapter 5.4).

Base on the result we obtained from above experiments. There are interesting projects we can do in the near future. For the newly developed bioengineering platform, different tailoring enzymes will be investigated, such as, BVMO, *O*-MeT. For mutasynthesis, different position substituted un-natural amino acids will be feed to the $\Delta pyiA$ strain. The tolerance of adenylation domain will be investigated. Furthermore, several more different chemical reactions can be carried out to synthesize more novel functional cytochalasan. Therefore, more biotests will be done to explore the potential biological activities of cytochalasan.

7. Experimental

7.1 Biology Parts

7.1.1 General

Chemical biology methods were carried out according to guidelines of Cox group, as well as kit manufacturers. All chemicals and media ingredients used in this work were purchased from the following companies: Bio-Rad, Sigma-Aldrich, Acros, Alfa Aesar, abcr, Baseclear and Carbosynth. All solutions and media used throughout the research as well as all glassware used for microbial cultures were sterilized by autoclaving. Solutions affected by heating were sterilized by filtration through disposable syringe filter 0.22 μm and 0.45 μm filters. These heat sensitive solutions used in the study were antibiotics solutions, polyethylene glycol (PEG) solutions used in yeast and fungal transformations. All microbiological experiments were carried out in a Bio class II microbiological safety cabinet.

7.1.2 Enzymes

Restriction endonucleases, DNA polymerases, reverse transcriptase and LR-clonase were purchased from New England Biolabs, Thermo Scientific and Invitrogen. Enzymes were used according to manufacturer's instructions with the appropriate supplied buffers.

Table 7.1 Enzymes used in this study.

Enzyme	Manufacturer
<i>AscI</i>	NEW ENGLAND BioLabs (Ipswich, MA, USA)
<i>EcoRI</i>	NEW ENGLAND BioLabs (Ipswich, MA, USA)
<i>HindIII</i>	NEW ENGLAND BioLabs (Ipswich, MA, USA)
<i>NotI</i>	NEW ENGLAND BioLabs (Ipswich, MA, USA)
RNase A	NEW ENGLAND BioLabs (Ipswich, MA, USA)
LR-clonase	Invitrogen (Waltham, MA, USA)
Taq DNA polymerase	NEW ENGLAND BioLabs (Ipswich, MA, USA)
Q5 HiFi DNA Polymerase	NEW ENGLAND BioLabs (Ipswich, MA, USA)

7.1.3 Antibiotics

The antibiotics were purchased from Roth (Karlsruhe, Germany) and amresco (Solon, USA). All antibiotics stock solutions were prepared in distilled water. They were then filter sterilized through 0.22 μm syringe filters and stored at $-20\text{ }^{\circ}\text{C}$. Stock and working concentrations are listed in the Table below.

Table 7.2 Antibiotics used in this study.

Antibiotic	Stock Solution (mg / mL)	Final Concentration (μg / mL)
Carbenicillin	50 in H ₂ O	50
Kanamycin	50 in H ₂ O	50
Hygromycin B	50 in H ₂ O	120 - 240
Glufosinat-ammonium (Basta)	50 in H ₂ O	50 - 200

7.1.4 plasmids and Vectors

Plasmids provided to be used in this study with their description and sources.

Table 7.3 Plasmid used in this study.^{109,139}

Plasmid	Brief Description	Supplier
pEYA	<i>Saccharomyces cerevisiae</i> – <i>E. coli</i> shuttle and Gateway entry vector	Dr. Colin Lazarus
pUC18-hygB-pgpdA-GS	<i>Magnaporthe grisea</i> expression vector, <i>E. coli</i> -fungal Gateway destination vector with hygromycin B cassette	Dr. Rozida M. Khalid
pTHGS-eGFP	Template for cloning the hph gene and gdpA promoter	Dr. Colin Lazarus
pTYGS-bar	Template for heterologous expression with basta cassette	Dr. Colin Lazarus
pE-YA-PKS-KO	Targeting <i>pyiS</i> gene knockout vector with Hygromycin B cassette	Dr. Elizabeth J. Skellam
pE-YA-OMET-KO	Targeting <i>pyiS</i> gene knockout vector with Hygromycin B cassette	Dr. Elizabeth J. Skellam
pE-YA-OACT-KO	Targeting <i>pyiS</i> gene knockout vector with Hygromycin B cassette	Chongqing Wang

pE-YA-OXR-KO	Targeting <i>pyiS</i> gene knockout vector with Hygromycin B cassette	Chongqing Wang
pE-YA-P450-1-KO	Targeting <i>pyiS</i> gene knockout vector with Hygromycin B cassette	Chongqing Wang
pE-YA-P450-2-KO	Targeting <i>pyiS</i> gene knockout vector with Hygromycin B cassette	Chongqing Wang
pUC57-ccsB-Kan	Template for cloning the <i>ccsB</i> gene	Baseclear
pTYGS-bar-ccsB	Template for <i>ccsB</i> heterologous expression with basta cassette	Chongqing Wang
pTYGS-bar-CYP1	pTYGSbar containing the <i>M. oryzae</i> Guy11 CYP1 gene under the control of the <i>amyB</i> promoter	Chongqing Wang
pTYGS-bar-CYP2	pTYGSbar containing the <i>M. oryzae</i> Guy11 CYP2 gene under the control of the <i>amyB</i> promoter	Chongqing Wang
pTYGS-bar-CYP3	pTYGSbar containing the <i>M. oryzae</i> Guy11 CYP3 gene under the control of the <i>amyB</i> promoter	Chongqing Wang
pTYGS-bar-CYP4	pTYGSbar containing the <i>M. oryzae</i> Guy11 CYP4 gene under the control of the <i>amyB</i> promoter	Chongqing Wang
pTYGS-bar-hffD	pTYGSbar containing the <i>M. oryzae</i> Guy11 hffD gene under the control of the <i>amyB</i> promoter	Chongqing Wang
pTYGS-bar-hffG	pTYGSbar containing the <i>M. oryzae</i> Guy11 hffG gene under the control of the <i>amyB</i> promoter	Chongqing Wang

7.1.5 Primers and Their Sequences

Oligonucleotides synthesized and used as PCR or RT-PCR primers were purchased from Sigma-Aldrich. They are listed in the Table below.

Table 7.4 Primers used in this study.

Cox group ID	Sequence (5' to 3')
55	CATGATGGGGATCCTCTAGTG

56 CAGGTCGAGTGGAGATGTG
87 CTTCTTAAATATCGTTGTAAGTTCCTGA
88 CGAAGTATATTGGGAGACTATAGCTACTAG
89 ATTCACCACTATTATTCCCACCCTATAATA
90 GAGACGAAACAGACTTTTTTCATCGCTAAAA
91 CTTTTCTTTCTCTTTCTTTTCCCATCTTC
92 TACGACAATGTCCATATCATCAATCATGACTGACCTCCTAAAACCCCAGTG
147 TGCTTGGAGGATAGCAACCG
148 GGGGATGACAGCAGTAACGA
714 TAATGCCAACTTTGTACAAAAAAGCAGGCTCATTTCGATTTTGGCCACCCC
715 ACGTATTTTCAGTGTCGAAAGATCCACTAGA CTCCTTCCCTCCGCAAAGTT
716 CCCAGCACTCGTCCGAGGGCAAAGGAATAGCGGGCGACTTCATTATACACC
717 TATAATGCCAACTTTGTACAAGAAAGCTGGGCCTCCCAAGATGGTACCAC
722 TAATGCCAACTTTGTACAAAAAAGCAGGCTGGCGGCAACTTTTAGTGAGC
723 ACGTATTTTCAGTGTCGAAAGATCCACTAGACAGGATCAGGTTTCGATCCGG
724 CCCAGCACTCGTCCGAGGGCAAAGGAATAGTAGAGGTGAAGGCGTTGCAG
725 TATAATGCCAACTTTGTACAAGAAAGCTGGGCTGGCAGATGTTTCGTTGG
781 GGTTTTTATCTGCCGGTGG
782 CCTCCCAAGATGGTACCAC
783 CTGGCAGATGTTTCGTTG
784 ATGTGCTGCTGTGTCTGTC
785 CATTTCGATTTTGGCCACC
786 GCGGCAACTTTTAGTGAGC
827 CACATCTGGCCTCAACACCA
828 GGACCCTCTATGCTCCAAGC
829 AGAGCTTGGTTGACGGCAAT
830 AGAATACGGGGTCTTGTGCC
831 CACTTGTTACTCCCCACCC
832 GACTCCTTCCCTCCCTCCTT
833 AGAGCTTGGTTGACGGCAAT
834 ACGTTGACCTGGTCTGCATT
835 CCACGTCTGCTGGTCTTTCT
836 GATGCTTTGGGCCGAGGAC

837 AGTACAGATGCATGACGGCC
838 GCAACAACGTGTGGAGCTTT
885 ATGCCAACTTTGTACAAAAAAGCAGGCTCCTGGTGATACGGCAGAGCTTG
886 CGAAAGATCCACTAGAGGATCCCCATCATGCGTGTGAGATCCCATCGGTT
887 CCCAGCACTCGTCCGAGGGCAAAGGAATAGTCGCTCCGTTCTGAAGAAG
896 AATGCCAACTTTGTACAAGAAAGCTGGGTCTGTCGTAGTTGCGAAGGAAG
937 CACATTTTTGTTAGAGCCACAAATTGT
938 CCTTATCGTACTCCATGTTGGT
939 GGCTGTGTAGAAGTACTCGC
940 TTGGTTTTCAGCGGCAGGC
1017 ATGCCAACTTTGTACAAAAAAGCAGGCTCCTATTTATATGTAATCGGCAT
1018 CGAAAGATCCACTAGAGGATCCCCATCATGGCCTATACCAAAAACACACT
1019 CCCAGCACTCGTCCGAGGGCAAAGGAATAGCTTGATGGCTGCGGCGCAGT
1020 AATGCCAACTTTGTACAAGAAAGCTGGGTCCATGCAAACATCAAACATG
1021 ATGCCAACTTTGTACAAAAAAGCAGGCTCCATCATCACTCGTCTGAACAT
1022 CGAAAGATCCACTAGAGGATCCCCATCATGCTGGTGAAGCGAAAAGCAGG
1023 CCCAGCACTCGTCCGAGGGCAAAGGAATAGTTACTTGGCACTCACCAAGA
1024 AATGCCAACTTTGTACAAGAAAGCTGGGTCTTTACACAAAAAGTCGCGA
1071 ATGCCAACTTTGTACAAAAAAGCAGGCTCCATGGCGTCATGGCATCACAA
1072 CGAAAGATCCACTAGAGGATCCCCATCATGCGCCTTGGCTTTTCTTGCCT
1073 CCCAGCACTCGTCCGAGGGCAAAGGAATAGTCGACACGGTATATTTGCAC
1074 AATGCCAACTTTGTACAAGAAAGCTGGGTCCACGTCGGTTGACGCATCAT
1117 ACGCTGACTGGGGCTTGA
1118 GAGCGTTGGTGTACTTGAAGT
1119 TGGTTGACGGCAATTTGATG
1120 CAGTGCCATCTGCGTCTCTA
1127 CCTTCCTGTTTTTGTACACC
1128 ACTCCTCCTTGACACCACC

1129 GAAGTACTCGCCGATAGTGGAA
1130 TCACTATAGGGGATATCAGCTGG
1193 ATGCCAACTTTGTACAAAAAAGCAGGCTCCGAGCTCTTCTTTATATCCAG
1194 CGAAAGATCCACTAGAGGATCCCCATCATGCGATACTATCTTCTGGACGA
1195 CCCAGCACTCGTCCGAGGGCAAAGGAATAGCGGAATTGGCCACTGTCATC
1196 AATGCCAACTTTGTACAAGAAAGCTGGGTCCACCTGTGCTGCGATGAAAC
1227 ACGCCCTTAGGCAACTAGGA
1228 TAATGAGCTGGCGGAACTGG
1229 GGGCGTACACAAATCGCC
1230 CTCGCGACTGCATGTGGAAA
1243 TCTGAACAATAAACCCACAGCAAGCTCCGATGGGCTCGCTCCTGAGCAT
1246 CTCTCCACCCTTCACGAGCTACTACAGATCTCAGCGCTTGCCATGCCCT
1327 CGTCAGGACATTGTTGGAG
1328 GCTTTCAGCTTCGATGTAGG
1369 TCTGAACAATAAACCCACAGCAAGCTCCG ATGTTAGATATGTCCCAACC
1370 CTCTCCACCCTTCACGAGCTACTACAGATCAGCATTGTTTCGAGGTTCCAT
1371 TCTGAACAATAAACCCACAGCAAGCTCCG ATGTTGTCTCTTTTGGAAAC
1372 CTCTCCACCCTTCACGAGCTACTACAGATC CTAACATTCTGACT
1373 TCTGAACAATAAACCCACAGCAAGCTCCGATGATGACTCCAACCGAACTT
1374 CTCTCCACCCTTCACGAGCTACTACAGATC CTATTTCTTCCCCTCGTTCAG
1375 TCTGAACAATAAACCCACAGCAAGCTCCG ATGACGACAGTCCAGAAAGA
1376 CTCTCCACCCTTCACGAGCTACTACAGATC CTATAACCTCCTTTCTCGAA
1466 TCTGAACAATAAACCCACAGCAAGCTCCGATGTTTTTCGAGCATCCAGAC
1467 CTCTCCACCCTTCACGAGCTACTACAGATC CTAATACCTCGCCCTCACC

1468 CTCTCCACCCTTCACGAGCTACTACAGATC CTAGGCACGAGCCTTTAGAT

1469 TCTGAACAATAAACCCACAGCAAGCTCCG ATGCTGAATTCGTCCGCCAT

7.1.6 Media, Buffers and Solutions

All media, buffers and solutions were prepared with distilled water. Growth media and transformation solutions were sterilised at 121 °C for 15 or by disposable sterile filter (0.45 µm pore size, Roth).

Buffers

50x TAE (tris-acetate-EDTA) buffer stock (DNA agarose gel running buffer)

242 g of Tris acetate in 700 ml distilled water, then 57.2 ml glacial acetic acid and 100 ml 0.5 M EDTA pH 8.0 were added and mixed. Distilled water was added to bring the volume to 1 liter. The agarose was dissolved in 0.5x final concentration of the TAE.

DEPC-treated water

Dissolved diethylpyrocarbonate (DEPC, Sigma-Aldrich) was in distilled water to a final concentration of 0.1 %. It was then incubated at 37 °C for 24 hours and sterilized by autoclaving.

STC buffer

200g/l sucrose, 50mM Tris-HCl, 50mM CaCl₂ (Sigma-Aldrich) were dissolved in 1 L distilled water and sterilised by autoclave. The final PH is around 7.5.

PTC buffer

60% PEG 3350, 1 M Sorbito, 50mM Tris-HCl, 50mM CaCl₂ (Sigma-Aldrich) were dissolved in 1 L distilled water and sterilised by autoclave. The final PH is around 7.5.

TB4 buffer

200g/l sucrose (Sigma-Aldrich), 3g/l yeast extract were dissolved in 1 L distilled water and sterilised by autoclave.

TE buffer

10 mM Tris-HCl [pH 7.5] and 1 mM EDTA were added together to make the final volume to 1 liter, pH 8.0.

Trace elements

7.9 mg ZnSO₄·7H₂O, 0.6 mg CuSO₄, 0.1 mg H₃BO₃, 0.2 mg MnSO₄·H₂O, 0.14 mg NaMoO₄ and ddH₂O were added together to make the final volume to 1 liter.

Vitamin solution

1.0 mg thiamine and 5 µg biotin were added together with ddH₂O to make the final volume to 1 liter.

Media

LB agar

0.5 % (w/v) NaCl, 1 % (w/v) Tryptone, 0.5 % (w/v) Yeast extract and 1.5 % (w/v) Agar were added together, ddH₂O was added to make the final volume to 1 liter.

SM-URA agar

0.17 % (w/v) Yeast nitrogen base, 0.5 % (w/v) (NH₄)₂SO₄, 2 % (w/v) D-(+)-Glucose Monohydrate, 0.077 % (w/v) Complete supplement mixture minus uracil, 1.5 % (w/v) Agar were added together, ddH₂O was added to make the final volume to 1 liter.

CM agar²⁰⁹

The CM agar was prepared by dissolving 10 g glucose, 2 g peptone, 1 g yeast extract, 1 g casamino acids, 6 g NaNO₃, 0.5 g KCl, 0.5 g MgSO₄, 1.5 g KH₂PO₄ and 15 g agar in 1 litre of the final volume solution. This is followed by autoclaving at 121 °C for 15 minutes at 15 psi.

YPAD agar

20 g tryptone, 10 g yeast extract, and 0.3 g adenine, 20 g D-(+)-Glucose monohydrate and 15 g agar were dissolved in distilled water to make the final solution up to 1 liter. The medium was autoclaved at 121 °C for 15 minutes at 15 psi.

DPY agar²¹⁰

20 g dextrin, 10 g polypeptone, 5 g yeast extract, 5 g KH₂PO₄, 0.5 g MgSO₄, and 15 g agar were dissolved in 1 liter of distilled water and sterilized by autoclaving at 121 °C for 15 minutes at 15 psi.

TNK-CP agar²¹¹

10 g glucose, 2 g yeast extract, 2 g NaNO₃, 0.5 g MgSO₄·7H₂O, 0.1 g CaCl₂·2H₂O, 4 mg FeSO₄·7H₂O, 2 g KH₂PO₄ and 15 g agar were dissolved in distilled water to make the final solution up to 1 liter. The medium was autoclaved at 121 °C for 15 minutes at 15 psi.

TNK-SU-CP agar²¹¹

10 g glucose, 200 g sucrose, 2 g yeast extract, 2 g NaNO₃, 0.5 g MgSO₄·7H₂O, 0.1 g CaCl₂·2H₂O, 4 mg FeSO₄·7H₂O, 2 g KH₂PO₄ and 15 g agar were dissolved in distilled water to make the final solution up to 1 liter. The medium was autoclaved at 121 °C for 15 minutes at 15 psi.

S.O.C (post-transformation recovery medium)²¹²

5 g yeast extract, 0.2 g KCl and 20 g tryptone were dissolved in distilled water and the pH was adjusted to 7.0 using 2 M NaOH solution. The volume is brought to 1 litre with distilled water. Then sterilized by autoclaving at 121 °C for 15 minutes at 15 psi.

Yeast Extract Peptone Dextrose Medium (YPAD)

20 g tryptone, 10 g yeast extract, and 0.3 g adenine, 20 g D-(+)-Glucose monohydrate were dissolved in distilled water to make the final solution up to 1 liter. The medium was autoclaved at 121 °C for 15 minutes at 15 psi.

Complete medium (CM)²⁰⁹

The CM medium was prepared by dissolving 20 g cottonseed flour, 10 g lactose monohydrate in 1 litre distilled water, followed by autoclaving at 121 °C for 15 minutes at 15 psi.

TNK-CP medium²¹¹

10 g glucose, 2 g yeast extract, 2 g NaNO₃, 0.5 g MgSO₄·7H₂O, 0.1 g CaCl₂·2H₂O, 4 mg FeSO₄·7H₂O and 2 g KH₂PO₄ were dissolved in distilled water to make the final solution up to 1 liter. The medium was autoclaved at 121 °C for 15 minutes at 15 psi.

TNK-CP-Su-Hyg medium²¹¹

TNK-CP-Su-Hyg has the same components and prepared in the same way as TNK-CP medium with the addition of 200 g sucrose before autoclaving and addition of hygromycin B in a final concentration of 240 mg/l before use.

TNK-CP-Hyg medium²¹¹

TNK-CP-Hyg has the same components and prepared in the same way as TNK-CP medium with the addition of hygromycin B in a final concentration of 120 mg/l before use.

DPY medium²¹⁰

20 g dextrin, 10 g polypeptone, 5 g yeast extract, 5 g KH₂PO₄ and 0.5 g MgSO₄ were dissolved in 1 liter of distilled water and sterilized by autoclaving at 121 °C for 15 minutes at 15 psi.

7.1.7 Growth and Storage Conditions for Microorganisms

Escherichia coli

***ccdB* strain**

Chemically competent of *E. coli* ccsB strain (Thermo Fisher Scientific) has a genotype F-mcrA Δ(mrr-hsdRMS-mcrBC) Φ80lacZΔM15 ΔlacX74 recA1 araΔ139 Δ(ara-leu)7697 galU galK rpsL (StrR) endA1 nupG fhuA::IS2.

TOP10 strain

Chemically competent *E. coli* top 10 strain (Thermo Fisher Scientific) has a genotype F-mcrA, Δ(mrr-hsdRMS-mcrBC), φ80lacZΔM15, ΔlacX74, recA1, araD139, Δ(araleu)7697, galU, galK, rpsL, (StrR), endA1, nupG.79.

Fungal Strains

Saccharomyces cerevisiae

(Stratagene) YPH499 strain auxotrophic to uracil was kindly provided by Dr. Colin Lazarus. Its genotype is MATa, ura3-52, lys2-801amber, ade2-101ochre, trp1- Δ 63, his3- Δ 200, leu2- Δ 1.247.

Magnaporthe grisea NI980 strain

M. grisea NI980 is a *Digitaria smutsii* isolate obtained from our collaborators Marc-Henri Lebrun and co-workers and was used as the wild-type strain in this study.

Fermentation and extraction protocols

Strains were cultivated on Oatmeal Agar (OMA) (4% w/v oat meal, 0.5% w/v sucrose, 2% agar) or Complete Medium (CM) agar at 25 °C. For cytochalasan production strains were cultivated in Soy Sauce Sucrose (SSS) medium (5% v/v soy sauce, 5% w/v sucrose, in autoclaved tap water) or DPY liquid medium (2% w/v dextrin from potato starch, 1% w/v polypeptone, 0.5% w/v yeast extract, 0.5% w/v monopotassium phosphate, 0.05% w/v magnesium sulfate, 2.5% w/v agar) for 7 days at 25 °C, 110 rpm.

For extraction, *M. grisea* spores were collected from MG agar plates incubated for 7 days and inoculated into 500mL Erlenmeyer flasks containing 100 mL DPY. The spores were allowed to grow in the liquid culture for 7-8 days on shakers at 110 rpm at 25 °C. The cells were blended in the fermentation broth, filtered to remove the mycelium, and transferred into a separating funnel. An equal volume of EtOAc was added into the separating funnel and the aqueous layer was extracted twice. The organic solvent from the two extractions was combined and dried with MgSO₄, filtered and evaporated to dryness. The crude extract was dissolved into 1 mL HPLC grade MeOH.

7.1.8 Feeding Studies

Compound **246** – **249** were purchased from Sigma-Aldrich, compound **243** – **245** were synthesized by three steps chemical reaction (Chapter 4.3.1).

200 mg of 4'-*O*-methyl-tyrosine **175** was dissolved into double distilled water (10 mg/mL) and filter sterilized. 200 μ l of this solution was fed to the Δ *pyiA* knock-out strain inoculated into 500 mL Erlenmeyer flasks containing 100 mL DPY. The feeding

was repeated at 24 hour intervals four times. On the 7th day the cultures were extracted using the method described above.

200 mg of 4'-*O*-allyl-tyrosine **243** was dissolved into double distilled water (10 mg/mL) and filter sterilized. 200 µl of this solution was fed to the Δ *pyiA* knock-out strain inoculated into 500 mL Erlenmeyer flasks containing 100 mL DPY. The feeding was repeated at 24 hour intervals four times. On the 7th day the cultures were extracted using the method described above.

200 mg of 4'-*O*-propargyl-tyrosine **244** was dissolved into double distilled water (10 mg/mL) and filter sterilized. 200 µl of this solution was fed to the Δ *pyiA* knock-out strain inoculated into 500 mL Erlenmeyer flasks containing 100 mL DPY. The feeding was repeated at 24 hour intervals four times. On the 7th day the cultures were extracted using the method described above.

200 mg of 4'-fluoro- / chloro- /bromo- /iodo-phenylalanine **246 - 249** were dissolved into double distilled water (10 mg/mL), stirred at 60 °C until dissolved completely and filter sterilized. 200 µl of this solution was fed to the Δ *pyiA* knock-out strain inoculated into 500 mL Erlenmeyer flasks containing 100 mL DPY. The feeding was repeated at 24 hour intervals four times. On the 7th day the cultures were extracted using the method described above.

200 mg of para-azido-phenylalanine was dissolved into double distilled water (10 mg/mL) and filter sterilized. 200 µl of this solution was fed to the Δ *pyiA* knock-out strain inoculated into 500 mL Erlenmeyer flasks containing 100 mL DPY. The feeding was repeated at 24 hour intervals four times. On the 7th day the cultures were extracted using the method described above.

7.1.9 DNA and RNA Visualization, Isolation and Purification

Agarose Gel Electrophoresis

DNA electrophoreses were achieved in 1 % agarose (w/v, containing Roti – Safe Gel Stain, Roth) gels dissolved in 0.5 x TAE buffer The moulded gels were immersed in the same buffer contained in a horizontal electrophoresis apparatus (Sigma-Aldrich). 5 µl of

each of the samples mixtures with loading buffer and 1 kb DNA Ladder (Thermo Scientific) were loaded onto the gel to run parallel to each other at 130 V, 400 mA, and for 0.5 hour. This allowed identification of DNA bands appeared on the samples run as DNA ladder provided band sizes range from 500 bp to 10000 bp. DNA bands separated on the gel were visualized by the Molecular Imager Gel doc XR + (Bio-Rad) system under UV light (312 nm). Digital images recorded using the Software Image Lab (Bio-Rad). Fresh RNA samples were run in the same manner as DNA samples and visualized similarly.

DNA purification from gel or PCR

Fragments were isolated and DNA was purified using NucleoSpin[®] Gel and PCR Clean-up kit (Macherey-Nagel) according to the manufacturer's instructions.

Plasmid DNA isolation from *E. coli*

E. coli transformants that contained the plasmid were inoculated in 5 ml of LB medium containing the selection antibiotic. The cultures were incubated overnight in the shaker incubator at 37 °C with shaking at 250 rpm. The cells were collected by centrifugation and the plasmid was obtained according to the method of the NucleoSpin[®] Plasmid kit (Machery-Nagel).

Plasmid DNA isolation from *Saccharomyces cerevisiae* (yeast)

Colonies of yeast recombination appeared on SM-URA plates after incubation at 30 °C for 3 or more days were used for plasmids isolation. They were collected and processed according to the method described by the Zymoprep II[™] Yeast Plasmid Miniprep Kit (ZYMO RESEARCH).

Genomic DNA isolation from *M. grisea*

Spores of *M. grisea* transformants were inoculated in DPY medium. They were incubated at 25 °C with shaking at 110 rpm around 4-5 days. Grown mycelia were

collected by filtration under vacuum and washed with water. Collected mycelia were then ground under liquid nitrogen to a very fine powder. 50 mg of the powdered mycelia were processed according to instructions of GenElute Plant DNA Isolation Kit (Sigma-Aldrich) for genomic DNA preparation.

RNA extraction from *M. grisea*

All equipment used in handling mycelia were washed with DEPC-treated water overnight at 37 °C and autoclaved. Grown mycelia were collected by filtration under vacuum and washed with DEPC-treated water. Collected mycelia were then ground under liquid nitrogen to a very fine powder. 50 mg of the powdered mycelia were processed according to instructions of ZR Fungal/Bacteria RNA Miniprep Kit (ZYMO RESEARCH). A digestion step for removal of any DNA contaminations was conducted by the DNase according to manufacturer instructions.

7.1.10 DNA Amplification from DNA and RNA Templates

High fidelity DNA polymerase chain reaction (PCR)

Polymerase chain reactions were conducted by amplification of DNA from plasmid or genomic DNA or RNA templates with Q5 high fidelity 2X Master Mix (New England Biolabs), follow the manufacturers' instructions.

Analytical PCR

PCR analysis performed on *E. coli* colonies is called colony-PCR. In which a part of single or several colonies (tested individually) was transferred via toothpick into 10 µl TE buffer placed in eppendorf tubes. The tubes were heated at 55 °C for 5 minutes and then 80 °C for 5 minutes then cooled to room temperature. OneTaq® 2X Master Mix (New England Biolabs) with standard buffer was used, following the manufacturers' instructions, for screening purposes. The solution was used as DNA source for analysis. PCR performed on either DNA sample or DNA extracted from *E. coli*. The analytical PCR run the same programme mentioned under high fidelity PCR with omitting of the

final extension step. DNA sequences were checked by DNA sequencing (Mix2Seq kit, Eurofins).

7.1.11 Fungal Transformations

Saccharomyces cerevisiae transformation for DNA recombination²⁰⁹

Two criteria are required for yeast recombination: first, all DNA fragments should be in similar concentrations. This was achieved by running gel electrophoresis of DNA fragments and the densities of their corresponding bands appeared upon UV illumination relative to the marker were used as indicators for their concentrations. The concentration of DNA fragments can also be measured by DeNovix DS-11+ spectrophotometer. The second criterion was that one of DNA fragments was a *S. cerevisiae* – *E. coli* shuttle vector with selection markers suitable for both organisms.

The process of yeast transformation started by growing yeast cells in 10-20 ml YPAD medium overnight at 30 °C with shaking at 200 rpm. Solution of SS-DNA (Single-Strand Carrier DNA or salmon sperm DNA) (2 mg/ml) was boiled for 5 minutes and was then chilled on ice. For each transformation the following components were added to the 50 µl yeast suspension aliquot in the following order with mixing by vortex after each step:

- 1- 40 µl DNA in water (with equimolar concentrations of fragments).
- 2- 50 µl SS-DNA. (2 mg/ml)
- 3- 240 µl PEG solution (50% w/v polyethylene-glycol [PEG] 3350).
- 4- 36 µl 1 M Li-acetate (sterilized by filtration).
- 5- 50 µl digested vector

The mixture was incubated at 30 °C for 30 minutes and then incubated at 42 °C for another 30 minutes. The cells were precipitated by centrifugation at 6000 rpm for 15 seconds and resuspended in 1 mL fresh water to give final suspension, 200 µl aliquots

were spread on SM-URA plates and incubated at 30 °C for 4-5 days or until the appearance of colonies of transformants.

***E. coli* transformation**

E. coli cells (TOP10) were provided as frozen chemically competent cells in small 1.5 ml centrifuge tubes. Cells tubes were thawed on ice and 5-10 µl of the plasmid solution was immediately added into the cell suspension followed by gentle tapping of the tube and incubation on ice for 30 minutes. The cells were then heat-shocked in 42 °C water bath for exactly 30-45 seconds and returned immediately into ice to be left for additional 2 minutes.

250-300 µl SOC medium was added to the cell suspension and then incubated on shaking incubator for 1 hour at 37 °C. 200 µl of the resulted suspension were spread on the pre-warmed LB agar plates containing an antibiotic corresponding to the selection marker present in the plasmid transformed and plates were eventually incubated inverted in a 37 °C incubator overnight. On the next day, transformants colonies appeared and used for further experiments.

***Magnaporthe grisea* transformation**

M. grisea strain used in this research was the NI980 strain known to be sensitive to both hygromycin B as well as Basta antibiotics. Constructs used for transformation and expression in *M. grisea* NI980 were containing hygB. Fungus was grown on CM plates for 7-10 days. A plug of the medium with fungal mycelia was transferred to 100 ml sterilized CM broth medium in 500 ml Erlenmeyer conical flask. The flask was incubated at 25 °C for 3-4 days with shaking at 150 rpm. Mycelia were homogenised using glass beads and transferred to a new CM broth medium followed by incubation at the same latter conditions for 1-2 days. Mycelia were collected by filtration, and protoplasting was performed using *Trichoderma harzianum* lysing enzymes (20 mg/ml) and Driselase enzyme (10 mg/ml) in NaCl (0.9 M) with gentle shaking at room temperature for 2-3 h. Protoplasts were filtered through miracloth and centrifuged at 2000 rpm for 10 min. Protoplasts were then resuspended (washed) in sterilized STC

buffer (200 g/l sucrose, 50 mM Tris-HCl, 50 mM CaCl₂·2H₂O, pH 7.5) and stored at -80 frizer.

Protoplasts were diluted to 3x10⁷/ml in STC buffer and approximately 5 µg (20 µl) of appropriate plasmid was added to 200 ml protoplast solution. The mixture was incubated on ice for 30 min, 1 ml of filter sterilized PTC buffer (60 % PEG 3350, 1 M sorbitol, 50 mM Tris-HCl, 50 mM CaCl₂·2H₂O, pH 7.5) was then added and the mixture was incubated at room temperature for a further 30 min. 4 – 5 ml of sterilized TB3 recovery medium (200 g/l sucrose, 3 g/l yeast extract) was added to the concentrate and left to be shaken very gently overnight. The mixture was centrifuged at 3000 rpm for 5 minutes and supernatant was reduced to 1 ml for concentration. The concentrate was then mixed with 19 ml of molten TNK-SU-CP-Hyg containing 240 µg/ml hygromycin B at 45-50 °C and mixed well then poured in plates. Plates were incubated at 25 °C for 5-7 days with daily observation until most or all colonies of transformants appeared. Transformants were then further selected on TNK-CP-Hyg plates (2ndry transformation plates) containing 120 µg/ml hygromycin B. Finally, clones grown on 2ndry plates were purified to single spores and used or stored at -80°C freezer.

7.2 Chemistry parts

7.2.1 General

All chemical extractions with organic solvents, evaporations and concentrations of various organic extracts were performed within the chemical hoods. Evaporations *in vacuo* were aided by rotary BOSCH or HEIDOLPH evaporator. All chemicals and reagents used in microbiology were analytical or molecular biology grade. They were purchased from Sigma-Aldrich, Fischer, Alfa Aesar and carbosynth or borrowed from OCI labs. Chemicals used in extraction and analysis of the secondary metabolites from fungi were analytical or HPLC grade.

7.2.2 Analytical LCMS

LCMS data were obtained using a Waters LCMS system comprising of a Waters 2767 autosampler, Waters 2545 pump system and a Phenomenex Kinetex column (2.6 µ, C18,

100 Å, 4.6 × 100 mm) equipped with a Phenomenex Security Guard precolumn (Luna C₅ 300 Å) eluted at 1 mL/min. Detection was performed by Waters 2998 diode array detector between 200 and 600 nm; Waters 2424 ELSD and Waters SQD-2 mass detector operating simultaneously in ES+ and ES- modes between 100 *m/z* and 1500 *m/z*. Solvents were **A**, HPLC-grade H₂O containing 0.05% formic acid; and **B**, HPLC-grade CH₃CN containing 0.045% formic acid. Gradients were as follows: Method 1 (optimised for non-polar compounds): 0 min, 10% **B**; 10 min 90% **B**; 12 min, 90% **B**; 13 min, 10% **B** and 15 min, 10% **B**. Method 2 (optimised for polar compounds): 0 min, 10% **B**; 10 min 40% **B**; 12 min, 90% **B**; 13 min, 10% **B** and 15 min, 10% **B**.

7.2.3 Preparative LCMS

Compounds were purified using a Waters massdirected autopurification system consisting of a Waters 2545 pump and Waters 2767 autosampler. The chromatography column was a Phenomenex Kinetex Axia column (5µ, C₁₈, 100 Å, 21.2 × 250 mm) fitted with a Luna C₅ 300 Å Phenomenex Security Guard precolumn. The column was eluted at 20 mL/min at 22 °C. Solvents used were **A**, H₂O + 0.05% formic acid; and **B**, CH₃CN + 0.045% formic acid. All solvents were HPLC grade. The column outlet was split (100:1) and the minority flow was supplemented with HPLC-grade MeOH + 0.045% formic acid to 1000 µL/min and diverted for interrogation by diode array (Waters 2998) and evaporative light-scattering (Waters 2424) detectors. The flow was also analysed by mass spectrometry (Waters SQD-2 in ES+ and ES- modes). Desired compounds were collected into glass test tubes. Combined fractions were evaporated *in vacuo*, weighed and dissolved directly in NMR solvent for analysis.

7.2.4 High Resolution Mass Spectrometry (HRMS) Analysis

HRMS was obtained using a UPLC system (Waters Acquity Ultraperformance, running the same method and column as above) connected to a Q-TOF Premier mass spectrometer.

7.2.5 Infrared Spectrum (IR) Analysis

Infrared Spectra were recorded using a Shimadzu IR Affinity-1S fourier transform infrared spectrophotometer and quest at diamond extended range accessory (black).

7.2.6 Nuclear Magnetic Resonance (NMR) Analysis

A Bruker Avance 500 instrument equipped with a cryo-cooled probe at 500 MHz (^1H)/125 MHz (^{13}C) and 600 MHz (^1H)/150 MHz (^{13}C) were used for all NMR analysis. Standard parameters were used for the collection of 2D spectra (^1H , ^1H -correlation spectroscopy (COSY), heteronuclear single-quantum coherence (HSQC) and HMBC) in the indicated solvents. ^1H and ^{13}C spectra are referenced relative to residual protonated solvents. All δ values are quoted in ppm and all J values in Hz.

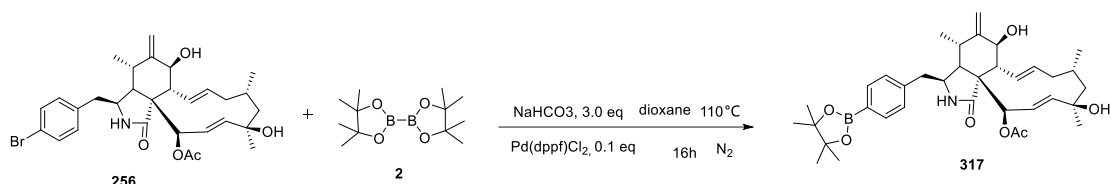
7.2.6 Software

Table 7.5 All softwares used in this study.

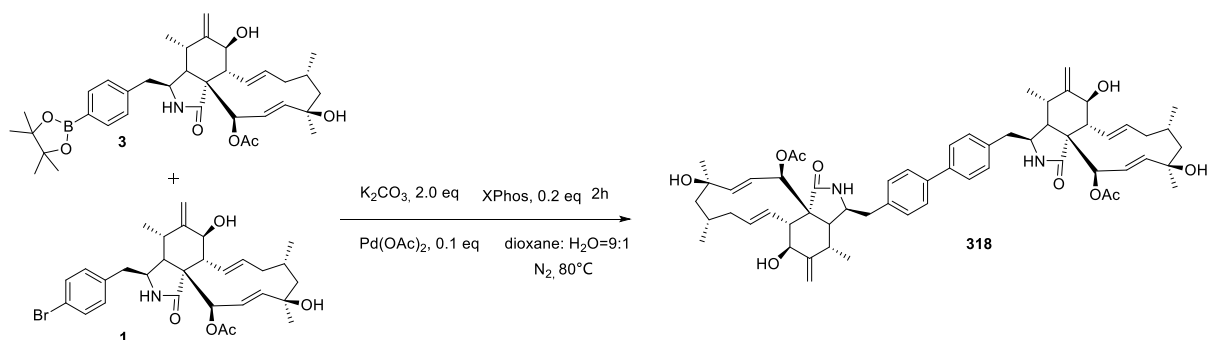
Software	Manufacturer
antiSMASH	Open online database
BLAST [®]	basic local alignment search tool of the National Center for Biotechnological Information
Geneious 7.1.9	Biomatters (Auckland 1010, New Zealand)
Image Lab	Bio-Rad Laboratories Ltd., Informatics Division (München, Germany)
Leica DM 4000 B LED	Leica microsystems Ltd. (Wetzlar, Germany)
MassLynx	Waters, Milford, MA, USA
MestReNova	Mestrelab Research, S.L. (Santiago de Compostela, ES)
Molecular Imager Gel doc XR+	Bio-Rad Laboratories, Inc. (München, Germany)

7.2.7 Synthetic Procedures

Synthesis of 318



To a stirred solution of **256** (20 mg, 0.035 mmol, 1.0 eq) and **2** (17.8 mg, 0.07 mmol, 2.0 eq) in dioxane (3 mL) was added Pd(dppf)Cl_2 (2.6 mg, 0.0035 mmol, 0.1 eq), NaHCO_3 (10.2 mg, 0.11 mmol, 3.0 eq). The mixture was stirred at 110 °C for 8 hours under nitrogen and the solvent was removed *in vacuo*. The residue was dissolved in EtOAc (2 mL) and washed with water (2 mL x 2). The organic phase was dried over MgSO_4 , filtered and evaporated to dryness *in vacuo*. The residue was dissolved in MeOH and purified by LCMS to afford 12.6 mg of desired product (yield: 58.3%) as a white solid.²⁰⁵



To a stirred solution of **317** (7.6 mg, 0.012 mmol, 1.5 eq) and **256** (7 mg, 8 μmol , 1.0 eq) in dioxane (4 mL) was added Pd(OAc)_2 (0.12 mg, 0.8 μmol , 0.1 eq) and XPhos (0.76 mg, 1.6 μmol , 0.2 eq) and K_2CO_3 (2.2 mg, 16 μmol , 2.0 eq). The mixture was stirred at 80 °C for 2 hours under nitrogen and the solvent was removed *in vacuo*. The residue was dissolved in EtOAc (4 mL) and washed with water (3 mL x 2). The organic phase was dried over MgSO_4 , filtered and evaporated to dryness *in vacuo*. The residue was

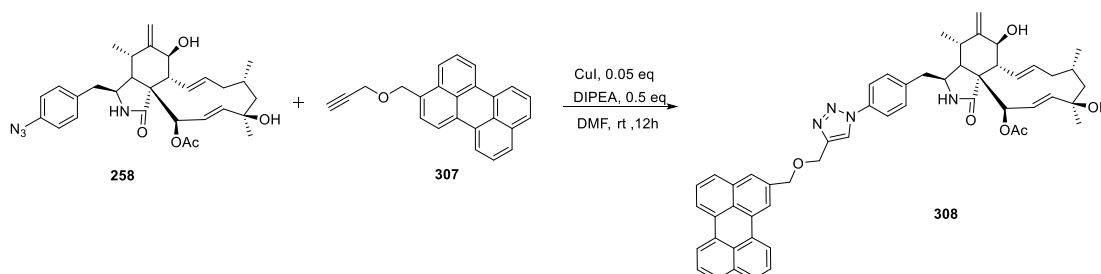
dissolved in MeOH and purified by LCMS to afford 5.1 mg of desired product (yield: 42.6%) as a white solid.²⁰⁶

¹H NMR (500 MHz, CDCl₃): δ (Hz) = 7.51 (d, J = 8.1 Hz, 2H), 7.22 (d, J = 8.1 Hz, 2H), 5.89 (dd, J = 2.7 and 16.6 Hz, 1H), 5.75 (ddd, J = 1.3, 9.7 and 15.5 Hz, 1H), 5.58 (dd, J = 2.5 and 2.7 Hz, 1H), 5.57 (dd, J = 2.4 and 16.6 Hz, 1H), 5.41 (ddd, J = 4.7, 10.0 and 15.5 Hz, 1H), 5.37 (brs, 1H), 5.13 (brs, 1H), 3.84 (dd, J = 1.3 and 10.8 Hz, 1H), 3.29 (ddd, J = 0.9, 4.6 and 9.6 Hz, 1H), 2.95 (dd, J = 9.8 and 10.8 Hz, 1H), 2.92 (dd, J = 4.4 and 13.5 Hz, 1H), 2.81 (m, 1H), 2.68 (dd, J = 9.9 and 13.5 Hz, 1H), 2.26 (s, 3H), 2.16 (dd, J = 4.6 and 8.9 Hz, 1H), 2.04 (m, 1H), 1.88 (m, 1H), 1.80 (m, 1H), 1.79 (m, 1H), 1.56 (m, 1H), 1.37 (s, 3H), 1.06 (d, J = 8.6 Hz, 3H), 0.99 (d, J = 6.7 Hz, 3H).

¹³C NMR (125 MHz, CDCl₃): δ = 174.3, 170.3, 148.1, 139.6, 138.4, 137.8, 129.7, 129.1, 127.1, 126.7, 125.6, 113.4, 77.1, 74.6, 69.3, 53.5, 53.4, 51.7, 50.3, 46.9, 44.9, 42.5, 32.5, 30.8, 28.2, 26.2, 20.6, 13.9.

HRMS (m/z): calculated for [C₆₀H₇₆N₂O₁₀ + Na]: 1007.5398, found: 1007.5402.

Synthesis of 308



To a stirred solution of **258** (10 mg, 0.019 mmol, 1.0 eq) and **307** (12.2 mg, 0.038 mmol, 2.0 eq) in DMF (2 mL) was added CuI (0.2 mg, 0.95 μ mol, 0.05 eq) and DIPEA (1.2 mg, 9.5 μ mol, 0.5 eq). The mixture was stirred at room temperature for 12 hours under nitrogen and the solvent was removed *in vacuo*. The residue was dissolved in EtOAc (2 mL) and washed with water (2 mL x 2). The organic phase was dried over MgSO₄, filtered and evaporated to dryness *in vacuo*. The residue was dissolved in MeOH and purified by LCMS to afford 8.0 mg of desired product (yield: 72.5%) as a yellow solid.¹⁸⁷

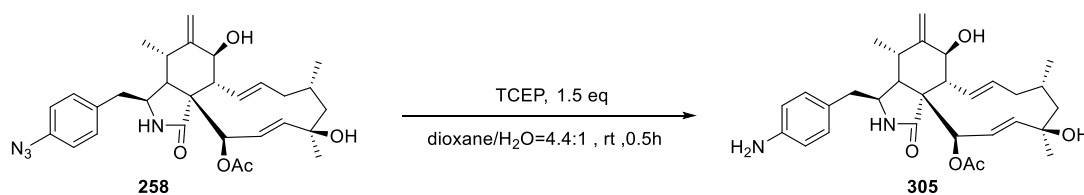
¹H NMR (500 MHz, CDCl₃): δ (Hz) = 8.23 (dd, J = 1.0 and 7.6 Hz, 2H), 8.18 (s, 1H), 8.00 (dd, J = 0.9 and 8.3 Hz, 2H), 7.87 (s, 1H), 7.72 (d, J = 8.2 Hz, 1H), 7.65 (d, J = 8.5 Hz, 1H), 7.56 (m, 1H), 7.52 (dd, J = 1.6 and 7.8 Hz, 2H), 7.27 (d, J = 8.5 Hz, 2H), 5.85 (dd, J = 2.2 and 17.0 Hz, 1H), 5.76 (ddd, J = 1.4, 9.7 and 15.4 Hz, 1H), 5.58 (brs, 1H), 5.56 (brs, 1H), 5.42 (ddd, J = 4.8, 10.1 and 15.4 Hz, 1H), 5.39 (brs, 1H), 5.14 (brs, 1H), 5.09 (s, 2H), 4.90 (s, 2H), 3.88 (dd, J = 1.3 and 10.8 Hz, 1H), 3.29 (m, 1H), 2.98 (m, 1H), 2.90 (m, 1H), 2.81 (m, 1H), 2.74 (m, 1H), 2.28 (s, 3H), 2.16 (dd, J = 3.7 and 5.0 Hz, 1H), 2.06 (m, 1H), 1.90 (m, 1H), 1.83 (m, 1H), 1.82 (m, 1H), 1.61 (m, 1H), 1.38 (s, 3H), 1.07 (d, J = 6.4 Hz, 3H), 0.99 (d, J = 6.6 Hz, 3H).

¹³C NMR (125 MHz, CDCl₃): δ = 174.3, 170.2, 147.7, 146.1, 138.4, 138.0, 137.9, 136.0, 135.1, 134.7, 133.0, 132.8, 132.0, 131.1, 130.3, 129.1, 128.5, 128.3, 127.6, 127.3, 126.7, 126.2, 125.4, 123.2, 120.6, 120.4, 120.0, 119.2, 113.8, 76.8, 74.4, 71.1, 69.4, 63.4, 53.3, 52.9, 51.6, 49.9, 46.8, 44.7, 42.3, 32.4, 30.8, 28.1, 26.1, 20.6, 13.7.

HRMS (m/z): calculated for [C₅₄H₅₄N₄O₆ + Na]: 877.3941, found: 877.3940.

IR (powder, cm⁻¹): 2922, 1735, 1693, 1519, 1369, 1228, 1043, 1014, 962, 812, 767, 542.

Synthesis of 305



To a stirred solution of **258** (10 mg, 0.019 mmol, 1.0 eq) in 2.0 mL dioxane-water mixture (4.4:1, v/v) was added TCEP (7.0mg, 0.028 mmol, 1.5 eq). The mixture was stirred at room temperature for 1 hour and the solvent was removed *in vacuo*. The residue was dissolved in EtOAc (2 mL) and washed with water (2 mL x 2). The organic phase was dried over MgSO₄, filtered and evaporated to dryness *in vacuo*. The residue was dissolved in MeOH and purified by LCMS to afford 6.7 mg of desired product (yield: 70.2%) as a white solid.¹⁹²

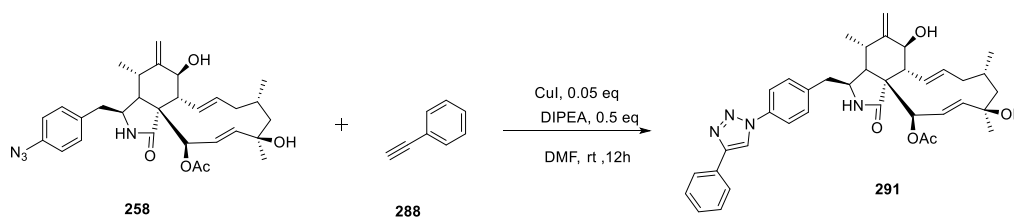
¹H NMR (500 MHz, CDCl₃): δ (Hz) = 6.95 (d, J = 8.3 Hz, 2H), 6.65 (d, J = 8.3 Hz, 2H), 5.89 (dd, J = 2.1 and 17.2 Hz, 1H), 5.76 (ddd, J = 1.3, 9.6 and 15.4 Hz, 1H), 5.58

(m, 1H), 5.53 (dd, $J = 2.3$ and 17.2 Hz, 1H), 5.40 (ddd, $J = 4.9$, 10.2 and 15.4 Hz, 1H), 5.37 (brs, 1H), 5.13 (brs, 1H), 3.86 (dd, $J = 1.4$ and 10.8 Hz, 1H), 3.20 (ddd, $J = 1.1$, 4.7 and 9.4 Hz, 1H), 2.96 (dd, $J = 9.8$ and 10.8 Hz, 1H), 2.80 (m, 1H), 2.75 (dd, $J = 4.6$ and 13.7 Hz, 1H), 2.56 (dd, $J = 9.8$ and 13.7 Hz, 1H), 2.25 (s, 3H), 2.11 (dd, $J = 4.4$ and 4.7 Hz, 1H), 2.06 (m, 1H), 1.87 (m, 1H), 1.82 (m, 1H), 1.79 (m, 1H), 1.58 (dd, $J = 3.1$ and 14.3 Hz 1H), 1.35 (s, 3H), 1.05 (d, $J = 6.4$ Hz, 3H), 0.96 (d, $J = 6.7$ Hz, 3H).

^{13}C NMR (125 MHz, CDCl_3): $\delta = 174.1, 170.1, 148.1, 145.3, 138.7, 138.0, 133.8, 130.0, 129.8, 127.1, 126.0, 115.3, 113.9, 77.2, 74.4, 69.6, 53.8, 51.8, 50.2, 47.2, 44.8, 42.6, 32.9, 31.2, 28.4, 26.5, 20.9, 14.1$.

HRMS (m/z): calculated for $[\text{C}_{60}\text{H}_{76}\text{N}_2\text{O}_{10} + \text{Na}]$: 531.2835, found: 531.2830.

Synthesis of 291



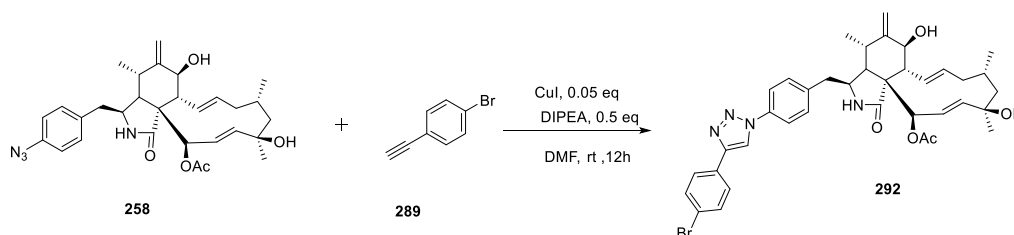
To a stirred solution of **258** (10 mg, 0.019 mmol, 1.0 eq) and **288** (4 mg, 0.038 mmol, 2.0 eq) in DMF (2 mL) was added CuI (0.2 mg, 0.95 μmol , 0.05 eq) and DIPEA (1.2 mg, 9.5 μmol , 0.5 eq). The mixture was stirred at room temperature for 12 hours under nitrogen and the solvent was removed *in vacuo*. The residue was dissolved in EtOAc (2 mL) and washed with water (2 mL x 2). The organic phase was dried over MgSO_4 , filtered and evaporated to dryness *in vacuo*. The residue was dissolved in MeOH and purified by LCMS to afford 7.4 mg of desired product (yield: 61.8%) as a white solid.¹⁸⁷

^1H NMR (500 MHz, CDCl_3): δ (Hz) = 8.18 (s, 1H), 7.92 (dd, $J = 1.4$ and 8.4 Hz, 2H), 7.78 (d, $J = 8.5$ Hz, 2H), 7.47 (dd, $J = 7.4$ and 8.4 Hz, 2H), 7.40 (dd, $J = 8.4$ and 18.6 Hz, 1H), 7.34 (d, $J = 8.5$ Hz, 2H), 5.87 (dd, $J = 3.0$ and 16.2 Hz, 1H), 5.74 (ddd, $J = 1.4, 9.7$ and 15.4 Hz, 1H), 5.59 (brs, 1H), 5.58 (brs, 1H), 5.44 (ddd, $J = 4.8, 10.1$ and 15.4 Hz, 1H), 5.37 (brs, 1H), 5.13 (brs, 1H), 3.85 (dd, $J = 1.6$ and 10.7 Hz, 1H), 3.32 (m, 1H), 2.95 (m, 1H), 2.81 (m, 1H), 2.80 (m, 1H), 2.65 (m, 1H), 2.26 (s, 3H), 2.17 (dd, $J = 3.8$ and 5.0 Hz, 1H), 2.05 (m, 1H), 1.89 (m, 1H), 1.82 (m, 1H), 1.79 (m, 1H), 1.58 (dd, $J = 2.9$ and 14.4 Hz 1H), 1.35 (s, 3H), 1.06 (d, $J = 6.5$ Hz, 3H), 0.99 (d, $J = 6.7$ Hz, 3H).

¹³C NMR (125 MHz, CDCl₃): δ = 174.2, 170.2, 148.5, 147.7, 138.6, 138.1, 138.1, 136.3, 130.3, 129.6, 128.7, 128.5, 126.9, 125.6, 117.0, 114.2, 77.0, 74.4, 69.7, 53.9, 53.3, 51.6, 50.2, 47.1, 44.9, 42.8, 32.7, 31.1, 28.3, 26.5, 20.9, 13.9.

HRMS (*m/z*): calculated for [C₄₀H₄₆N₁O₆ + Na]: 659.3223, found: 659.3218.

Synthesis of 292



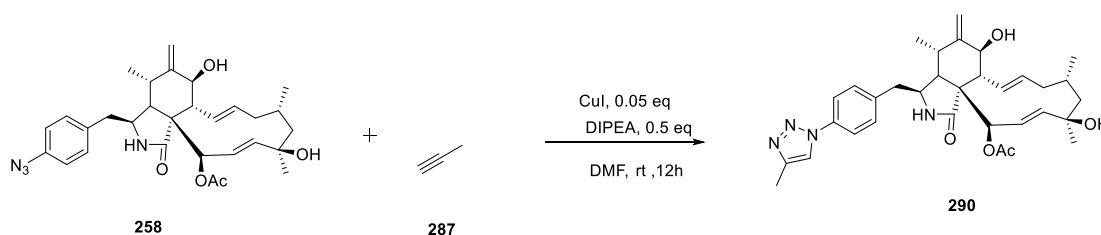
To a stirred solution of **258** (10 mg, 0.019 mmol, 1.0 eq) and **289** (6.8 mg, 0.038 mmol, 2.0 eq) in DMF (2 mL) was added CuI (0.2 mg, 0.95 μ mol, 0.05 eq) and DIPEA (1.2 mg, 9.5 μ mol, 0.5 eq). The mixture was stirred at 80 °C for 12 hours under nitrogen and the solvent was removed *in vacuo*. The residue was dissolved in EtOAc (2 mL) and washed with water (2 mL x 2). The organic phase was dried over MgSO₄, filtered and evaporated to dryness *in vacuo*. The residue was dissolved in MeOH and purified by LCMS to afford 8.1 mg of desired product (yield: 60.6%) as a white solid.¹⁸⁷

¹H NMR (500 MHz, CDCl₃): δ (Hz) = 8.20 (s, 1H), 7.82 (dd, *J* = 1.4 and 8.4 Hz, 2H), 7.78 (d, *J* = 8.5 Hz, 2H), 7.61 (dd, *J* = 7.4 and 8.4 Hz, 2H), 7.38 (dd, *J* = 8.5 and 18.6 Hz, 1H), 5.88 (dd, *J* = 3.0 and 16.2 Hz, 1H), 5.76 (ddd, *J* = 1.4, 9.7 and 15.4 Hz, 1H), 5.58 (brs, 1H), 5.58 (brs, 1H), 5.41 (ddd, *J* = 4.8, 10.1 and 15.4 Hz, 1H), 5.39 (brs, 1H), 5.15 (brs, 1H), 3.88 (dd, *J* = 1.6 and 10.7 Hz, 1H), 3.33 (m, 1H), 2.97 (m, 1H), 2.95 (m, 1H), 2.81 (m, 1H), 2.80 (m, 1H), 2.28 (s, 3H), 2.18 (dd, *J* = 3.8 and 5.0 Hz, 1H), 2.06 (m, 1H), 1.89 (dd, *J* = 3.0 and 14.4 Hz, 1H), 1.83 (m, 1H), 1.81 (m, 1H), 1.61 (dd, *J* = 2.9 and 14.4 Hz, 1H), 1.35 (s, 3H), 1.07 (d, *J* = 6.5 Hz, 3H), 1.02 (d, *J* = 6.7 Hz, 3H).

¹³C NMR (125 MHz, CDCl₃): δ = 174.4, 170.2, 147.6, 147.5, 138.7, 138.3, 136.1, 132.0, 130.5, 129.1, 127.4, 127.0, 126.9, 125.7, 121.0, 120.9, 117.4, 114.3, 77.1, 74.4, 69.9, 53.7, 53.4, 51.7, 50.3, 47.2, 44.9, 42.7, 32.7, 31.2, 28.5, 26.5, 20.9, 14.1.

HRMS (*m/z*): calculated for [C₃₈H₄₃N₄O₅Br + Na]: 737.2315, found: 737.2313.

Synthesis of 290



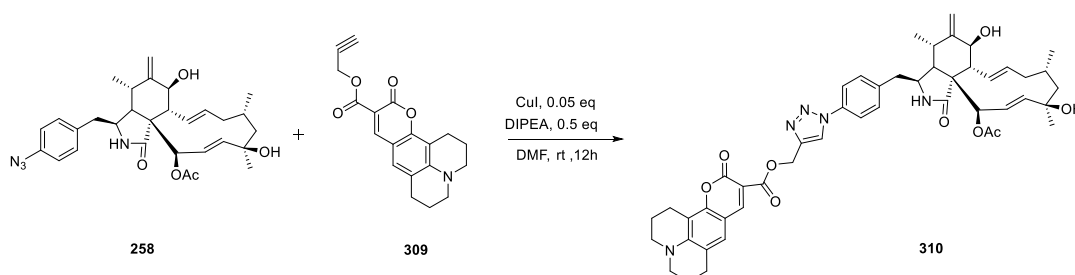
To a stirred solution of **258** (10 mg, 0.019 mmol, 1.0 eq) and **287** (2.0 mg, 0.038 mmol, 2.0 eq) in DMF (2 mL) was added CuI (0.2 mg, 0.95 μmol , 0.05 eq) and DIPEA (1.2 mg, 9.5 μmol , 0.5 eq). The mixture was stirred at room temperature for 12 hours under nitrogen and the solvent was removed *in vacuo*. The residue was dissolved in EtOAc (2 mL) and washed with water (2 mL x 2). The organic phase was dried over MgSO_4 , filtered and evaporated to dryness *in vacuo*. The residue was dissolved in MeOH and purified by LCMS to afford 8.2 mg of desired product (yield: 76.4%) as a white solid.

$^1\text{H NMR}$ (500 MHz, CDCl_3): δ (Hz) = 7.73 (s, 1H), 7.70 (d, $J = 8.5$ Hz, 2H), 7.33 (d, $J = 8.5$ Hz, 1H), 5.85 (dd, $J = 3.0$ and 16.2 Hz, 1H), 5.78 (ddd, $J = 1.4, 9.7$ and 15.4 Hz, 1H), 5.59 (brs, 1H), 5.58 (brs, 1H), 5.43 (ddd, $J = 4.8, 10.1$ and 15.4 Hz, 1H), 5.38 (brs, 1H), 5.14 (brs, 1H), 3.87 (dd, $J = 1.3$ and 10.8 Hz, 1H), 3.31 (m, 1H), 2.97 (m, 1H), 2.95 (m, 1H), 2.80 (m, 1H), 2.77 (m, 1H), 2.28 (s, 3H), 2.18 (dd, $J = 3.8$ and 5.0 Hz, 1H), 2.06 (m, 1H), 1.92 (dd, $J = 3.0$ and 14.4 Hz, 1H), 1.83 (m, 1H), 1.81 (m, 1H), 1.61 (m, 1H), 1.37 (s, 3H), 1.07 (d, $J = 6.5$ Hz, 3H), 1.00 (d, $J = 6.7$ Hz, 3H).

$^{13}\text{C NMR}$ (125 MHz, CDCl_3): $\delta = 174.3, 170.2, 147.7, 144.2, 138.8, 138.2, 137.8, 1, 130.4, 127.0, 125.9, 120.9, 120.8, 118.9, 114.4, 77.2, 74.3, 70.0, 53.8, 53.5, 51.7, 50.2, 47.3, 45.1, 42.7, 32.7, 31.2, 28.6, 26.6, 21.0, 14.1$.

HRMS (m/z): calculated for $[\text{C}_{60}\text{H}_{76}\text{N}_2\text{O}_{10} + \text{Na}]$: 597.3053, found: 597.3061.

Synthesis of 310



To a stirred solution of **258** (5 mg, 0.01 mmol, 1.0 eq) and **309** (3.0 mg, 0.01 mmol, 1.0 eq) in DMF (2 mL) was added CuI (0.1 mg, 0.5 μ mol, 0.05 eq) and DIPEA (0.6 mg, 4.8 μ mol, 0.5 eq). The mixture was stirred at room temperature for 12 hours under nitrogen and the solvent was removed *in vacuo*. The residue was dissolved in EtOAc (2 mL) and washed with water (2 mL x 2). The organic phase was dried over MgSO₄, filtered and evaporated to dryness *in vacuo*. The residue was dissolved in MeOH and purified by LCMS to afford 6.3 mg of desired product (yield: 78.2%) as a deep yellow solid.¹⁸⁷

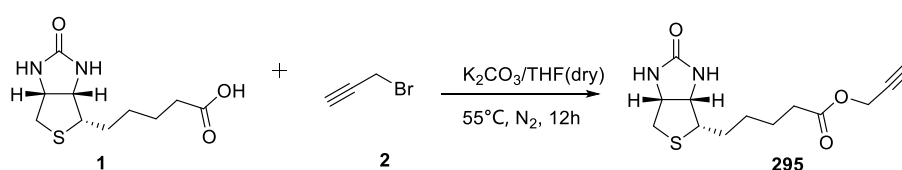
¹H NMR (500 MHz, CDCl₃): δ (Hz) = 8.38 (m, 1H), 8.27 (s, 1H), 7.73 (d, J = 8.5 Hz, 1H), 7.33 (d, J = 8.5 Hz, 1H), 6.94 (s, 1H), 5.85 (dd, J = 2.2 and 17.0 Hz, 1H), 5.76 (ddd, J = 1.4, 9.7 and 15.4 Hz, 1H), 5.59 (brs, 1H), 5.56 (brs, 1H), 5.53 (s, 1H), 5.41 (ddd, J = 4.8, 10.1 and 15.4 Hz, 1H), 5.37 (brs, 1H), 5.13 (brs, 1H), 3.86 (dd, J = 1.3 and 10.8 Hz, 1H), 3.35 (m, 4H), 3.31 (m, 1H), 2.96 (m, 1H), 2.90 (m, 1H), 2.79 (m, 1H), 2.77 (m, 1H), 2.27 (s, 3H), 2.17 (dd, J = 3.7 and 5.0 Hz, 1H), 2.05 (m, 1H), 1.98 (m, 2H), 1.88 (m, 1H), 1.82 (m, 1H), 1.81 (m, 1H), 1.58 (m, 1H), 1.37 (s, 3H), 1.07 (d, J = 6.4 Hz, 3H), 0.94 (d, J = 6.6 Hz, 3H).

¹³C NMR (125 MHz, CDCl₃): δ = 174.3, 170.2, 164.0, 158.7, 153.6, 149.6, 149.0, 148.9, 144.2, 138.6, 138.2, 138.0, 136.0, 130.3, 127.1, 127.0, 125.8, 122.1, 121.0, 119.4, 114.2, 107.3, 105.8, 77.2, 74.4, 69.8, 58.0, 53.8, 53.3, 51.6, 50.1, 49.8, 47.2, 45.0, 42.7, 32.7, 31.2, 28.4, 27.4, 26.5, 20.9, 20.0, 20.4, 14.0.

HRMS (m/z): calculated for [C₄₉H₅₅N₅O₉ + Na]: 880.3897, found: 880.3904.

IR (powder, cm⁻¹): 3419, 2924, 1735, 1685, 1618, 1585, 1560, 1517, 1442, 1369, 1309, 1238, 1197, 1172, 1111, 1045, 962, 792, 439.

Synthesis of **298**



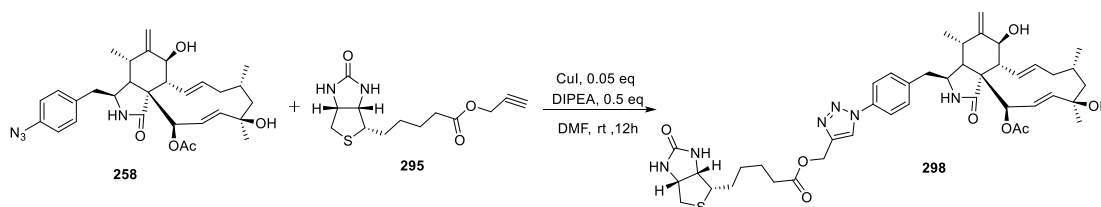
To a stirred solution of **1** (100.0 mg, 0.41 mmol, 1.0 eq) and **2** (0.1 mL, 0.82 mmol, 2.0 eq) in dry THF (4 mL) was added K₂CO₃ (50.0 mg, 0.49 mmol, 1.2 eq). The mixture

was stirred at 55 °C for 12 hours under nitrogen and the solvent was removed *in vacuo*. The residue was dissolved in EtOAc (4 mL) and washed with water (3 mL x 2). The organic phase was dried over MgSO₄, filtered and evaporated to dryness *in vacuo*. The residue was dissolved in MeOH and purified by LCMS to afford 69.0 mg of desired product (yield: 59.7%) as a white solid.¹⁹¹

¹H NMR (500 MHz, CDCl₃): δ (Hz) = 4.70 (d, *J* = 2.5 Hz, 2H), 4.56 (m, 1H), 4.37 (m, 2H), 3.20 (m, 1H), 2.95 (dd, *J* = 5.0 and 12.9 Hz, 1H), 2.77 (d, *J* = 12.9 Hz, 1H), 2.51 (t, *J* = 2.5 Hz, 2H), 2.41 (t, *J* = 7.1 Hz, 2H), 1.73 (m, 2H), 1.50 (m, 2H), 1.27 (m, 2H).

¹³C NMR (125 MHz, CDCl₃): δ = 172.6, 163.1, 79.5, 75.5, 62.0, 60.3, 55.2, 51.9, 40.6, 33.6, 29.8, 28.3, 24.6.

HRMS (*m/z*): calculated for [C₁₃H₁₈N₂O₃S + Na]: 305.0936, found: 305.0936.



To a stirred solution of **258** (10 mg, 0.019 mmol, 1.0 eq) and **295** (10.7 mg, 0.038 mmol, 2.0 eq) in DMF (2 mL) was added CuI (0.2 mg, 0.95 μ mol, 0.05 eq) and DIPEA (1.2 mg, 9.5 μ mol, 0.5 eq). The mixture was stirred at room temperature for 12 hours under nitrogen and the solvent was removed *in vacuo*. The residue was dissolved in EtOAc (2 mL) and washed with water (2 mL x 2). The organic phase was dried over MgSO₄, filtered and evaporated to dryness *in vacuo*. The residue was dissolved in MeOH and purified by LCMS to afford 8.6 mg of desired product (yield: 56.4%) as a light yellow solid.¹⁹¹

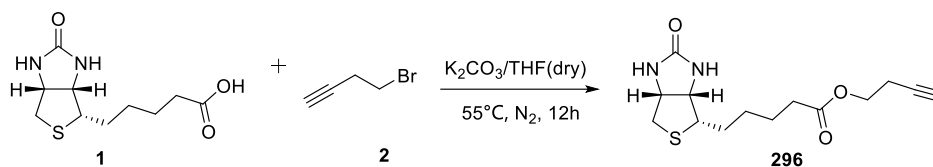
¹H NMR (500 MHz, CDCl₃): δ (Hz) = 8.16 (s, 1H), 7.75 (d, *J* = 8.2 Hz, 2H), 7.33 (d, *J* = 8.2 Hz, 2H), 5.88 (dd, *J* = 2.7 and 16.5 Hz, 1H), 5.74 (ddd, *J* = 1.4, 9.6 and 15.5 Hz, 1H), 5.58 (brs, 1H), 5.52 (brs, 1H), 5.42 (ddd, *J* = 4.8, 10.3 and 15.5 Hz, 1H), 5.39 (brs, 1H), 5.34 (s, 1H), 5.15 (brs, 1H), 4.48 (m, 1H), 4.25 (dd, *J* = 4.4 and 7.8 Hz, 1H), 3.86 (d, *J* = 10.8 Hz, 1H), 3.33 (m, 1H), 3.15 (m, 1H), 2.97 (m, 1H), 2.94 (dd, *J* = 4.8 and 13.5 Hz, 1H), 2.82 (m, 1H), 2.74 (m, 1H), 2.69 (m, 2H), 2.43 (t, *J* = 6.9 Hz, 2H), 2.27 (s, 3H), 2.15 (t, *J* = 4.3 Hz, 1H), 2.06 (m, 1H), 1.91 (m, 1H), 1.82 (m, 1H), 1.73 (m, 2H),

1.67 (m, 2H), 1.48 (m, 2H), 1.35 (s, 3H), 1.07 (d, $J = 6.7$ Hz, 3H), 1.06 (d, $J = 6.5$ Hz, 3H).

^{13}C NMR (125 MHz, CDCl_3): $\delta = 174.8, 173.5, 170.2, 163.3, 147.9, 145.1, 138.8, 138.2, 130.6, 130.3, 127.0, 125.9, 120.9, 119.6, 114.2, 77.4, 74.3, 69.6, 61.6, 60.1, 55.3, 53.8, 53.7, 51.9, 50.5, 47.2, 45.1, 42.8, 40.6, 33.6, 32.9, 31.2, 28.5, 28.3, 28.1, 26.5, 25.5, 24.6, 21.0, 14.4$.

HRMS (m/z): calculated for $[\text{C}_{43}\text{H}_{56}\text{N}_6\text{O}_8\text{S} + \text{Na}]$: 839.3778, found: 839.3773.

Synthesis of 299

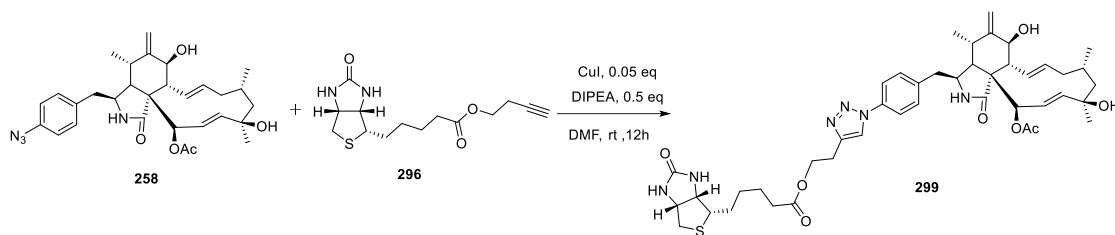


To a stirred solution of **1** (100.0 mg, 0.41 mmol, 1.0 eq) and **2** (80.0 mg, 0.61 mmol, 1.5 eq) in dry THF (4 mL) was added K_2CO_3 (50.0 mg, 0.49 mmol, 1.2 eq). The mixture was stirred at 55°C for 12 hours under nitrogen and the solvent was removed *in vacuo*. The residue was dissolved in EtOAc (4 mL) and washed with water (3 mL x 2). The organic phase was dried over MgSO_4 , filtered and evaporated to dryness *in vacuo*. The residue was dissolved in MeOH and purified by LCMS to afford 100.2 mg of desired product (yield: 82.6%) as a white solid (compound **296** was synthesized by Maurice).¹⁹¹

^1H NMR (500 MHz, CDCl_3): δ (Hz) = 4.54 (m, 1H), 4.35 (m, 1H), 4.21 (t, $J = 6.8$ Hz 2H), 3.19 (m, 1H), 2.96 (dd, $J = 5.1$ and 12.8 Hz, 1H), 2.75 (dd, $J = 1.0$ and 12.8 Hz, 1H), 2.55 (ddd, $J = 2.7, 6.8$ and 13.5 Hz 2H), 2.39 (t, $J = 7.4$ Hz, 2H), 1.73 (m, 2H), 1.71 (m, 1H), 1.46 (m, 1H), 1.28 (m, 2H).

^{13}C NMR (125 MHz, CDCl_3): $\delta = 173.3, 163.1, 80.1, 69.9, 62.0, 61.9, 60.1, 55.2, 40.6, 33.7, 29.7, 28.1, 24.7$.

HRMS (m/z): calculated for $[\text{C}_{14}\text{H}_{20}\text{N}_2\text{O}_3\text{S} + \text{Na}]$: 319.1092, found: 319.1087.



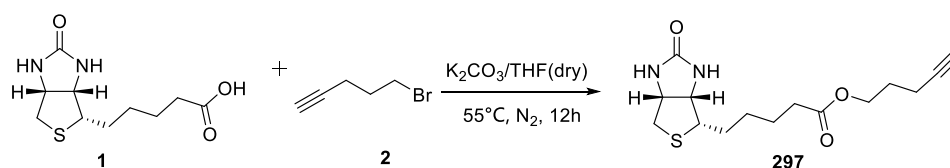
To a stirred solution of **258** (10 mg, 0.019 mmol, 1.0 eq) and **296** (11.2 mg, 0.038 mmol, 2.0 eq) in DMF (2 mL) was added CuI (0.2 mg, 0.95 μ mol, 0.05 eq) and DIPEA (1.2 mg, 9.5 μ mol, 0.5 eq). The mixture was stirred at room temperature for 12 hours under nitrogen and the solvent was removed *in vacuo*. The residue was dissolved in EtOAc (2 mL) and washed with water (2 mL x 2). The organic phase was dried over MgSO₄, filtered and evaporated to dryness *in vacuo*. The residue was dissolved in MeOH and purified by LCMS to afford 9.6 mg of desired product (yield: 61.9%) as a white solid.¹⁹¹

¹H NMR (500 MHz, CDCl₃): δ (Hz) = 7.93 (s, 1H), 7.74 (d, J = 8.2 Hz, 2H), 7.34 (d, J = 8.2 Hz, 2H), 5.87 (dd, J = 2.9 and 16.4 Hz, 1H), 5.74 (m, 1H), 5.55 (brs, 1H), 5.49 (brs, 1H), 5.44 (m, 1H), 5.40 (brs, 1H), 5.15 (brs, 1H), 4.53 (m, 1H), 4.34 (m, 1H), 4.21 (m, 1H), 3.87 (dd, J = 1.7 and 11.0 Hz, 1H), 3.33 (m, 1H), 3.18 (m, 1H), 3.16 (m, 1H), 2.97 (dd, J = 5.0 and 11.0 Hz, 1H), 2.95 (m, 1H), 2.93 (dd, J = 5.0 and 12.9 Hz, 1H), 2.83 (m, 1H), 2.73 (dd, J = 1.1 and 12.9 Hz, 1H), 2.72 (m, 1H), 2.39 (m, 2H), 2.26 (s, 3H), 2.13 (m, 1H), 2.06 (m, 1H), 1.88 (m, 1H), 1.80 (m, 1H), 1.71 (m, 2H), 1.69 (m, 2H), 1.61 (m, 2H), 1.46 (m, 2H), 1.35 (s, 3H), 1.10 (d, J = 6.7 Hz, 3H), 1.07 (d, J = 6.5 Hz, 3H).

¹³C NMR (125 MHz, CDCl₃): δ = 175.2, 173.4, 170.1, 163.2, 147.7, 145.1, 138.8, 138.2, 137.9, 130.7, 130.6, 126.8, 125.7, 120.6, 119.6, 114.1, 77.3, 74.2, 69.5, 61.8, 61.7, 60.0, 55.2, 53.9, 53.6, 52.4, 50.4, 47.1, 45.1, 42.7, 40.5, 33.7, 32.9, 31.2, 28.6, 28.2, 28.1, 26.5, 25.6, 24.6, 20.9, 14.3.

HRMS (m/z): calculated for [C₄₄H₅₈N₆O₈S + Na]: 853.3935, found: 853.3936.

Synthesis of 300

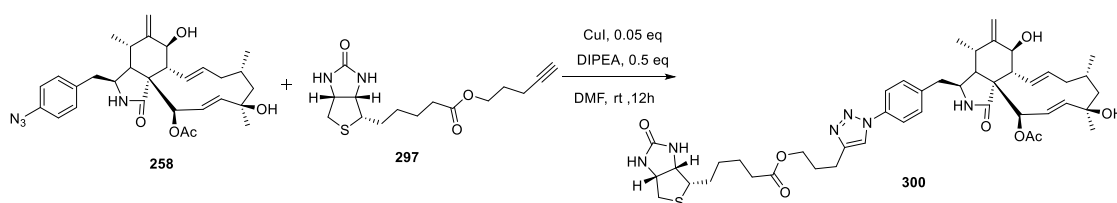


To a stirred solution of **1** (100.0 mg, 0.41 mmol, 1.0 eq) and **2** (90.0 mg, 0.61 mmol, 1.5 eq) in dry THF (4 mL) was added K₂CO₃ (50.0 mg, 0.49 mmol, 1.2 eq). The mixture was stirred at 55 °C for 12 hours under nitrogen and the solvent was removed *in vacuo*. The residue was dissolved in EtOAc (4 mL) and washed with water (3 mL x 2). The organic phase was dried over MgSO₄, filtered and evaporated to dryness *in vacuo*. The residue was dissolved in MeOH and purified by LCMS to afford 96.0 mg of desired product (yield: 75.6%) as a white solid (compound **297** was synthesized by Maurice).¹⁹¹

¹H NMR (500 MHz, CDCl₃): δ (Hz) = 4.53 (m, 1H), 4.33 (m, 1H), 4.19 (t, *J* = 6.3 Hz, 2H), 2.92 (dd, *J* = 5.0 and 12.8 Hz, 1H), 2.78 (d, *J* = 12.8 Hz, 1H), 2.29 (m, 2H), 1.99 (t, *J* = 2.6 Hz, 1H), 1.87 (m, 2H), 1.73 (m, 2H), 1.71 (m, 1H), 1.48 (m, 1H), 1.28 (m, 2H).

¹³C NMR (125 MHz, CDCl₃): δ = 173.6, 163.6, 83.1, 69.5, 62.9, 62.0, 60.1, 40.3, 29.7, 28.6, 27.6, 24.8, 24.7, 15.4.

HRMS (*m/z*): calculated for [C₁₅H₂₂N₂O₃S + Na]: 333.1249, found: 333.1246.



To a stirred solution of **258** (10 mg, 0.019 mmol, 1.0 eq) and **297** (11.7 mg, 0.038 mmol, 2.0 eq) in DMF (2 mL) was added CuI (0.2 mg, 0.95 μmol, 0.05 eq) and DIPEA (1.2 mg, 9.5 μmol, 0.5 eq). The mixture was stirred at room temperature for 12 hours under nitrogen and the solvent was removed *in vacuo*. The residue was dissolved in EtOAc (2 mL) and washed with water (2 mL x 2). The organic phase was dried over MgSO₄, filtered and evaporated to dryness *in vacuo*. The residue was dissolved in MeOH and purified by LCMS to afford 10.1 mg of desired product (yield: 63.8%) as a white yellow solid.¹⁹¹

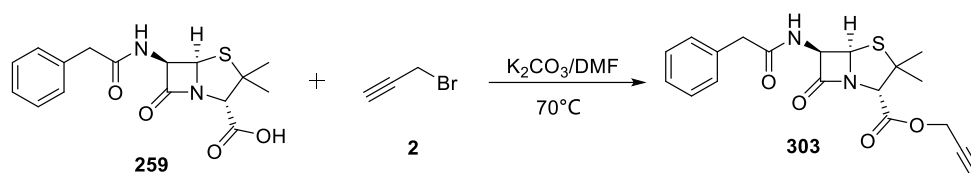
¹H NMR (500 MHz, CDCl₃): δ (Hz) = 7.83 (s, 1H), 7.72 (d, *J* = 8.2 Hz, 2H), 7.33 (d, *J* = 8.2 Hz, 2H), 5.84 (dd, *J* = 2.7 and 16.5 Hz, 1H), 5.74 (ddd, *J* = 1.4, 9.6 and 15.5 Hz, 1H), 5.54 (brs, 1H), 5.52 (brs, 1H), 5.45 (ddd, *J* = 4.8, 10.3 and 15.5 Hz, 1H), 5.39 (brs, 1H), 5.14 (brs, 1H), 4.52 (m, 1H), 4.33 (m, 1H), 4.18 (m, 1H), 3.88 (dd, *J* = 1.5 and 10.8 Hz, 1H), 3.33 (ddd, *J* = 0.9, 4.8 and 9.6 Hz, 1H), 3.19 (m, 1H), 2.94 (m, 1H), 2.93 (m, 1H), 2.81 (m, 1H), 2.75 (m, 1H), 2.74 (m, 1H), 2.37 (m, 2H), 2.27 (s, 3H), 2.13 (m,

2H), 2.06 (m, 1H), 1.91 (m, 1H), 1.89 (m, 2H), 1.82 (m, 2H), 1.80 (m, 1H), 1.70 (m, 2H), 1.69 (m, 1H), 1.61 (m, 1H), 1.48 (m, 2H), 1.36 (s, 3H), 1.06 (d, $J = 6.5$ Hz, 3H), 1.04 (d, $J = 6.6$ Hz, 3H).

^{13}C NMR (125 MHz, CDCl_3): $\delta = 175.2, 173.6, 170.1, 163.3, 147.7, 147.6, 138.7, 138.2, 137.9, 130.7, 130.4, 127.1, 125.8, 120.8, 119.1, 114.2, 77.2, 74.2, 69.7, 63.1, 61.7, 60.0, 55.2, 53.7, 53.6, 52.4, 50.2, 47.2, 45.0, 42.6, 40.6, 33.8, 32.8, 31.3, 28.4, 28.2, 28.1, 27.6, 26.2, 24.7, 21.0, 14.2.$

HRMS (m/z): calculated for $[\text{C}_{45}\text{H}_{60}\text{N}_6\text{O}_8\text{S} + \text{Na}]$: 867.4091, found: 867.4095.

Synthesis of 304

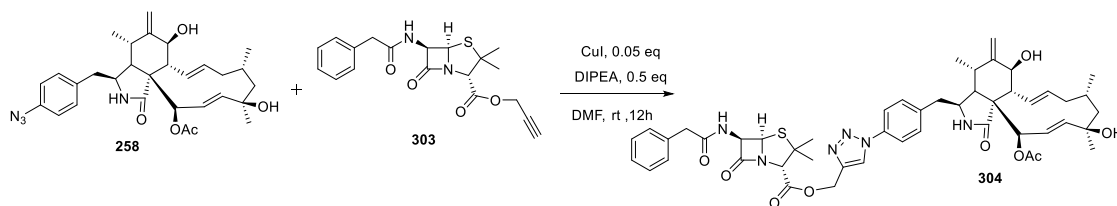


To a stirred solution of **259** (100.0 mg, 0.30 mmol, 1.0 eq) and **2** (0.1 mL, 0.60 mmol, 2.0 eq) in dry DMF (4 mL) was added K_2CO_3 (50.0 mg, 0.49 mmol, 1.2 eq). The mixture was stirred at 70°C for 12 hours under nitrogen and the solvent was removed *in vacuo*. The residue was dissolved in EtOAc (4 mL) and washed with water (3 mL x 2). The organic phase was dried over MgSO_4 , filtered and evaporated to dryness *in vacuo*. The residue was dissolved in MeOH and purified by LCMS to afford 77.3 mg of desired product (yield: 69.4%) as a white solid.¹⁹¹

^1H NMR (500 MHz, CDCl_3): δ (Hz) = 7.38-7.29 (m, 5H), 5.67 (dd, $J = 4.2$ and 9.0 Hz, 1H), 5.53 (d, $J = 4.2$ Hz, 1H), 4.82 (d, $J = 2.5$ Hz, 1H), 4.71 (d, $J = 2.5$ Hz, 1H), 4.42 (s, 1H), 3.65 (s, 2H), 2.53 (t, $J = 2.5$ Hz, 1H), 1.50 (s, 3H), 1.48 (s, 3H).

^{13}C NMR (125 MHz, CDCl_3): $\delta = 173.5, 170.5, 166.8, 133.8, 129.4, 129.0, 127.6, 76.4, 76.2, 70.0, 67.9, 64.7, 58.7, 52.7, 43.6, 26.8.$

HRMS (m/z): calculated for $[\text{C}_{19}\text{H}_{20}\text{N}_2\text{O}_4\text{S} + \text{Na}]$: 395.1041, found: 395.1038.



To a stirred solution of **258** (10 mg, 0.019 mmol, 1.0 eq) and **303** (14.1 mg, 0.038 mmol, 2.0 eq) in DMF (4 mL) was added CuI (0.2 mg, 0.95 μ mol, 0.05 eq) and DIPEA (1.2 mg, 9.5 μ mol, 0.5 eq). The mixture was stirred at room temperature for 12 hours under nitrogen and the solvent was removed *in vacuo*. The residue was dissolved in EtOAc (4 mL) and washed with water (3 mL x 2). The organic phase was dried over MgSO₄, filtered and evaporated to dryness *in vacuo*. The residue was dissolved in MeOH and purified by LCMS to afford 15.0 mg of desired product (yield: 88.6%) as a white yellow solid.¹⁹¹

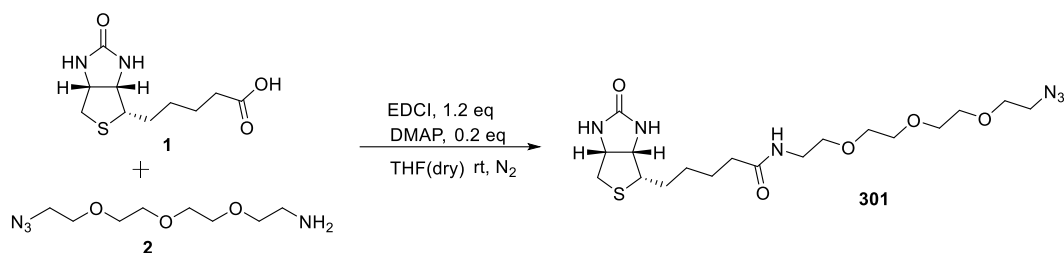
¹H NMR (500 MHz, CDCl₃): δ (Hz) = 8.07 (s, 1H), 7.72 (d, J = 8.5 Hz, 2H), 7.34 (d, J = 8.5 Hz, 2H), 7.39 (m, 2H), 7.30 (m, 2H), 7.28 (m, 2H), 5.86 (dd, J = 2.6 and 16.5 Hz, 1H), 5.75 (m, 1H), 5.69 (dd, J = 4.2 and 9.1 Hz, 1H), 5.55 (brs, 1H), 5.54 (d, J = 4.2 Hz, 1H), 5.52 (brs, 1H), 5.43 (m, 1H), 5.39 (s, 2H), 5.14 (brs, 1H), 4.42 (s, 1H), 3.88 (d, J = 10.6 Hz, 1H), 3.66 (m, 2H), 3.33 (m, 1H), 2.96 (m, 1H), 2.90 (m, 1H), 2.85 (m, 1H), 2.74 (m, 1H), 2.26 (s, 3H), 2.17 (m, 1H), 2.08 (m, 1H), 1.91 (m, 1H), 1.82 (m, 1H), 1.61 (m, 2H), 1.50 (m, 6H), 1.69 (m, 1H), 1.38 (s, 3H), 1.07 (d, J = 6.4 Hz, 3H), 0.98 (d, J = 6.6 Hz, 3H).

¹³C NMR (125 MHz, CDCl₃): δ = 174.6, 173.5, 173.4, 170.3, 170.2, 147.5, 142.4, 138.9, 138.4, 135.7, 133.8, 129.6, 129.5, 129.2, 127.8, 127.6, 127.1, 125.8, 122.2, 121.1, 114.3, 77.1, 74.1, 70.1, 69.7, 67.9, 64.7, 58.5, 58.1, 53.5, 53.2, 51.9, 49.9, 47.0, 44.7, 43.4, 42.6, 40.6, 32.6, 31.4, 28.4, 28.2, 26.9, 26.3, 21.1, 13.8.

HRMS (m/z): calculated for [C₄₉H₅₈N₆O₉S + Na]: 1007.5398, found: 1007.5402.

IR (powder, cm⁻¹): 1784, 1749, 1653, 1521, 1456, 1379, 1300, 1203, 449, 418.

Synthesis of **302**

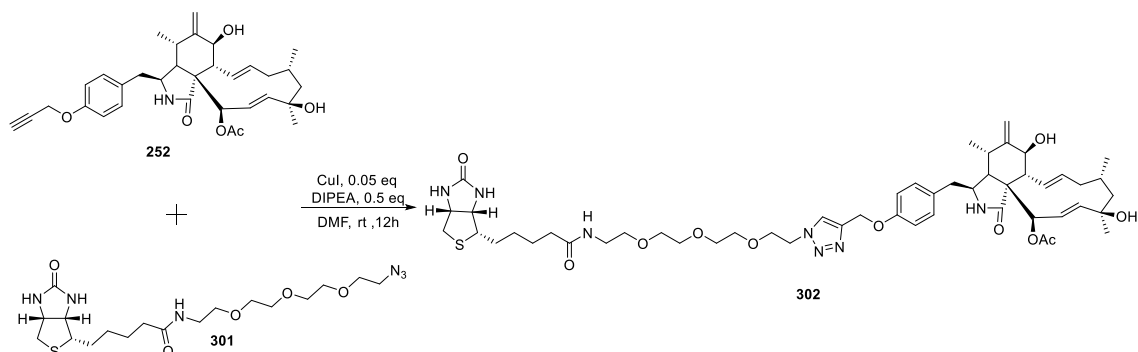


To a stirred solution of **1** (100.0 mg, 0.41 mmol, 1.0 eq) and **2** (98.0 mg, 0.45 mmol, 1.1 eq) in dry THF (4 mL) was added EDCI (94.0 mg, 0.49 mmol, 1.2 eq) and DMAP (10.0 mg, 0.082 mmol, 0.2 eq). The mixture was stirred at room temperature for 12 hours under nitrogen and the solvent was removed *in vacuo*. The residue was dissolved in EtOAc (4mL) and washed with water 3 mL x 2). The organic phase was dried over MgSO₄, filtered and evaporated to dryness *in vacuo*. The residue was dissolved in MeOH and purified by LCMS to afford 111.5 mg of desired product (yield: 61.3%) as a white solid (compound **301** was synthesized by Maurice).²¹³

¹H NMR (500 MHz, CDCl₃): δ (Hz) = 4.46 (m, 1H), 4.27 (m, 2H), 3.65 (m, 2H), 3.62 (m, 2H), 3.59 (m, 2H), 3.50 (m, 2H), 3.40 (t, J = 5.6 Hz, 2H), 3.32 (dd, J = 5.6 and 11.2 Hz 2H), 3.18 (m, 1H), 2.96 (m, 1H), 2.90 (dd, J = 5.0 and 12.7 Hz, 1H), 2.68 (d, J = 12.7 Hz 1H), 2.15 (dd, J = 1.0 and 7.9 Hz, 2H), 1.62 (m, 2H), 1.57 (m, 2H), 1.39 (m, 2H).

¹³C NMR (125 MHz, CDCl₃): δ = 172.8, 163.2, 70.2, 69.8, 69.6, 69.3, 61.4, 59.9, 55.4, 50.5, 40.1, 38.3, 35.4, 28.1, 25.3.

HRMS (m/z): calculated for [C₁₈H₃₂N₆O₅S + Na]: 467.2053, found: 467.2052.



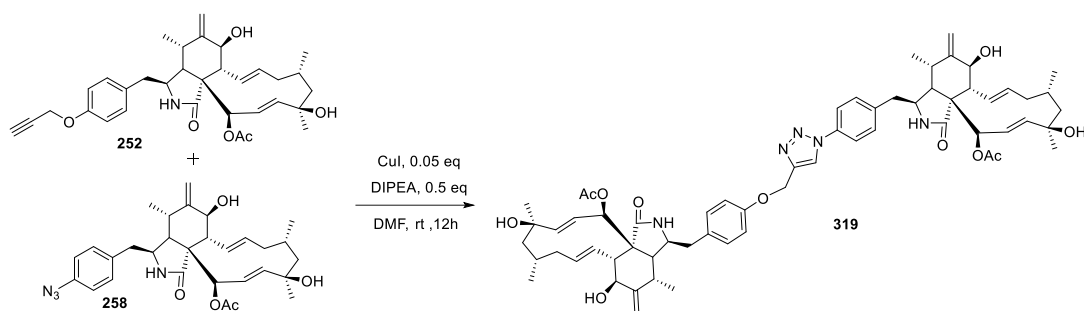
To a stirred solution of **252** (13.0 mg, 0.024 mmol, 1.1 eq) and **301** (10.0 mg, 0.022 mmol, 1.0 eq) in DMF (2 mL) was added CuI (0.23 mg, 1.2 μ mol, 0.05 eq) and DIPEA (1.5 mg, 12 μ mol, 0.5 eq). The mixture was stirred at room temperature for 12 hours under nitrogen and the solvent was removed *in vacuo*. The residue was dissolved in EtOAc (4mL) and washed with water 3 mL x 2). The organic phase was dried over MgSO₄, filtered and evaporated to dryness *in vacuo*. The residue was dissolved in MeOH and purified by LCMS to afford 14.3 mg of desired product (yield: 64.3%) as a white solid.

¹H NMR (500 MHz, CDCl₃): δ (Hz) = 7.86 (s, 1H), 7.10 (d, J = 8.5 Hz, 2H), 6.97 (d, J = 8.5 Hz, 2H), 5.88 (dd, J = 2.6 and 16.6 Hz, 1H), 5.74 (ddd, J = 1.3, 9.7 and 15.3 Hz, 1H), 5.56 (brs, 1H), 5.49 (brs, 1H), 5.41 (ddd, J = 5.1, 10.4 and 15.3 Hz, 1H), 5.37 (brs, 1H), 5.21 (s, 2H), 5.12 (brs, 1H), 4.58 (dd, J = 4.5 and 5.6 Hz 2H), 4.50 (m, 1H), 4.32 (m, 1H), 3.91 (dd, J = 4.5 and 5.5 Hz, 2H), 3.84 (dd, J = 1.3 and 10.8 Hz, 1H), 3.62 (m, 1H), 3.54 (m, 1H), 3.42 (dd, J = 5.3 and 10.5 Hz, 1H), 3.24 (m, 1H), 3.16 (m, 1H), 2.96 (m, 1H), 2.91 (m, 1H), 2.80 (m, 1H), 2.79 (m, 1H), 2.74 (m, 1H), 2.61 (m, 2H), 2.26 (s, 3H), 2.19 (m, 2H), 2.10 (m, 1H), 2.07 (m, 1H), 1.90 (m, 1H), 1.82 (m, 1H), 1.81 (m, 1H), 1.69 (m, 2H), 1.68 (m, 2H), 1.61 (m, 2H), 1.47 (s, 2H), 1.38 (s, 3H), 1.06 (d, J = 6.4 Hz, 3H), 1.00 (d, J = 6.7 Hz, 3H).

¹³C NMR (125 MHz, CDCl₃): δ = 174.6, 173.1, 170.1, 163.6, 157.3, 150.0, 143.9, 138.5, 138.2, 130.3, 130.1, 127.2, 126.0, 124.0, 115.2, 114.0, 77.6, 74.3, 70.4, 70.2, 69.9, 69.8, 69.4, 62.1, 61.8, 60.1, 55.4, 54.0, 53.9, 51.9, 50.3, 50.2, 47.2, 44.5, 43.0, 40.5, 39.2, 35.8, 33.0, 31.2, 28.6, 28.4, 28.2, 26.7, 25.7, 20.9, 14.3.

HRMS (m/z): calculated for [C₅₁H₇₃N₇O₁₁S + Na]: 1014.4986, found: 1014.4977.

Synthesis of **319**



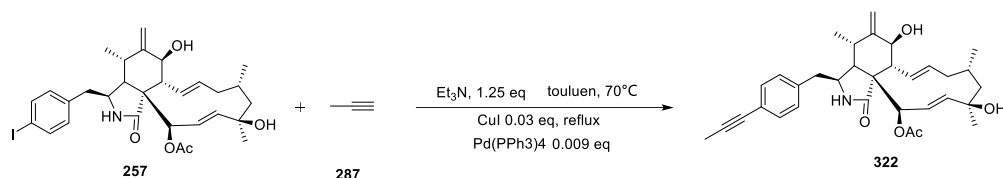
To a stirred solution of **252** (11.0 mg, 0.021 mmol, 1.1 eq) and **258** (10.0 mg, 0.019 mmol, 1.0 eq) in DMF (2 mL) was added CuI (0.2 mg, 0.95 μ mol, 0.05 eq) and DIPEA (1.2 mg, 9.5 μ mol, 0.5 eq). The mixture was stirred at room temperature for 12 hours under nitrogen and the solvent was removed *in vacuo*. The residue was dissolved in EtOAc (2mL) and washed with water 2 mL x 2). The organic phase was dried over MgSO₄, filtered and evaporated to dryness *in vacuo*. The residue was dissolved in MeOH and purified by LCMS to afford 16.5 mg of desired product (yield: 81.5%) as a white solid.¹⁹¹

¹H NMR (500 MHz, CDCl₃): δ (Hz) = 8.08 (s, 1H), 7.71 (d, J = 8.5 Hz, 2H), 7.34 (d, J = 8.5 Hz, 2H), 7.10 (d, J = 8.6 Hz, 2H), 7.00 (d, J = 8.6 Hz, 2H), 5.86 (m, 1H), 5.75 (m, 1H), 5.56 (brs, 1H), 5.52 (brs, 1H), 5.42 (m, 1H), 5.38 (brs, 1H), 5.30 (s, 2H), 5.14 (brs, 1H), 3.86 (dd, J = 2.2 and 11.8 Hz, 1H), 3.25 (m, 1H), 2.96 (m, 1H), 2.80 (m, 1H), 2.26 (s, 3H), 2.16 (dd, J = 3.9 and 5.1 Hz, 1H), 2.05 (m, 1H), 1.91 (m, 1H), 1.82 (m, 1H), 1.81 (m, 1H), 1.58 (m, 1H), 1.36 (s, 3H), 1.07 (d, J = 6.4 Hz, 3H), 1.01 (d, J = 6.6 Hz, 3H).

¹³C NMR (125 MHz, CDCl₃): δ = 174.3, 170.2, 157.3, 147.9, 145.0, 138.8, 138.3, 138.2, 136.0, 130.4, 130.2, 127.9, 125.8, 121.0, 120.5, 115.2, 114.2, 77.5, 74.7, 69.6, 62.0, 53.8, 53.7, 51.8, 50.4, 47.3, 44.9, 42.7, 32.8, 31.3, 28.6, 26.5, 21.0, 14.2.

HRMS (m/z): calculated for [C₆₀H₇₆N₂O₁₀ + Na]: 1104.5674, found: 1104.5688.

Synthesis of 322



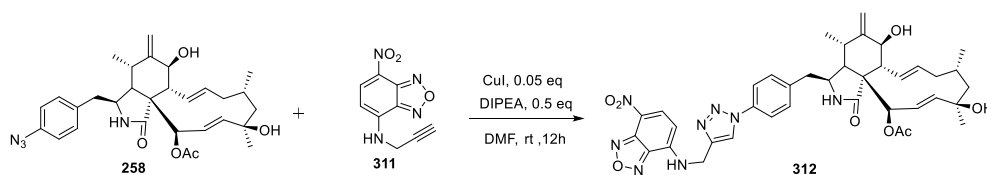
To a stirred solution of **257** (10 mg, 0.019 mmol, 1.0 eq) and **287** (2.0 mg, 0.038 mmol, 2.0 eq) in toluene (2 mL) was added CuI (0.2 mg, 0.95 μmol , 0.05 eq), Et₃N (3.0 mg, 0.03 mmol, 1.5 eq) and Pd(PPh₃)₄ (0.2 mg, 0.1 μmol , 0.009 eq). The mixture was stirred at 80 °C for 12 hours under nitrogen and the solvent was removed *in vacuo*. The residue was dissolved in EtOAc (2 mL) and washed with water (2 mL x 2). The organic phase was dried over MgSO₄, filtered and evaporated to dryness *in vacuo*. The residue was dissolved in MeOH and purified by LCMS to afford 6.7 mg of desired product (yield: 78.2%) as a yellow solid.^{207,208}

¹H NMR (500 MHz, CDCl₃): δ (Hz) = 7.36 (d, J = 8.2 Hz, 2H), 7.09 (d, J = 8.2 Hz, 2H), 5.90 (dd, J = 2.9 and 16.4 Hz, 1H), 5.76 (ddd, J = 1.4, 9.6 and 15.5 Hz, 1H), 5.60 (brs, 1H), 5.54 (brs, 1H), 5.42 (ddd, J = 4.8, 10.3 and 15.5 Hz, 1H), 5.37 (brs, 1H), 5.12 (brs, 1H), 3.85 (d, J = 10.2 Hz, 1H), 3.24 (ddd, J = 1.1, 4.4 and 9.1 Hz, 1H), 2.95 (t, J = 10.2 Hz, 1H), 2.82 (dd, J = 4.8 and 13.5 Hz, 1H), 2.78 (m, 1H), 2.67 (dd, J = 9.5 and 13.5 Hz, 1H), 2.27 (s, 3H), 2.13 (t, J = 4.4 Hz, 1H), 2.05 (m, 1H), 2.04 (s, 3H), 1.82 (m, 1H), 1.80 (m, 1H), 1.57 (m, 1H), 1.37 (s, 3H), 1.06 (d, J = 6.5 Hz, 3H), 0.98 (d, J = 6.7 Hz, 3H).

¹³C NMR (125 MHz, CDCl₃): δ = 174.2, 170.2, 147.9, 138.4, 138.0, 132.0, 131.9, 128.8, 126.9, 126.0, 122.9, 114.2, 86.2, 79.2, 77.5, 74.4, 69.6, 53.7, 53.3, 51.7, 50.6, 47.2, 45.6, 42.7, 32.7, 31.2, 28.7, 26.1, 20.9, 14.1, 4.2.

HRMS (m/z): calculated for [C₃₃H₄₁NO₅ + Na]: 554.2882, found: 554.2889.

Synthesis of 312



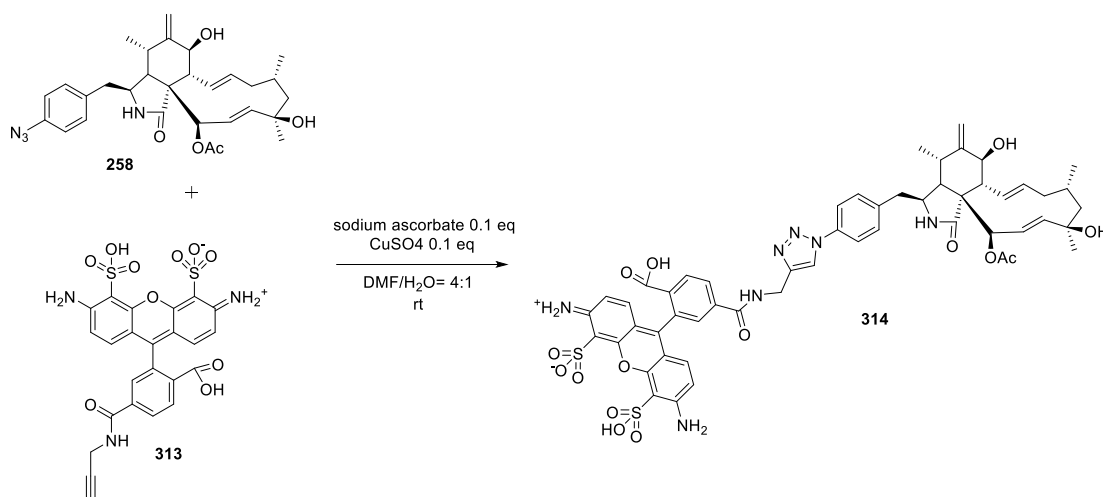
To a stirred solution of **258** (10 mg, 0.019 mmol, 1.0 eq) and **311** (4.5 mg, 0.021 mmol, 1.1 eq) in DMF (2 mL) was added CuI (0.2 mg, 0.95 μ mol, 0.05 eq) and DIPEA (1.2 mg, 9.5 μ mol, 0.5 eq). The mixture was stirred at room temperature for 12 hours under nitrogen and the solvent was removed *in vacuo*. The residue was dissolved in EtOAc (2 mL) and washed with water (2 mL x 2). The organic phase was dried over MgSO₄, filtered and evaporated to dryness *in vacuo*. The residue was dissolved in MeOH and purified by LCMS to afford 8.6 mg of desired product (yield: 61.1%) as a brown solid.¹⁹¹

¹H NMR (500 MHz, CDCl₃): δ (Hz) = 8.54 (d, J = 8.5 Hz, 1H), 8.04 (s, 1H), 7.69 (d, J = 8.5 Hz, 2H), 7.35 (d, J = 8.5 Hz, 1H), 6.44 (d, J = 8.6 Hz, 1H), 5.85 (dd, J = 3.0 and 16.2 Hz, 1H), 5.74 (m, 1H), 5.57 (brs, 1H), 5.46 (brs, 1H), 5.43 (m, 1H), 5.39 (brs, 1H), 5.14 (brs, 1H), 4.93 (s, 2H), 3.86 (dd, J = 1.6 and 10.7 Hz, 1H), 3.35 (m, 1H), 2.98 (m, 1H), 2.96 (m, 1H), 2.81 (m, 1H), 2.78 (m, 1H), 2.26 (s, 3H), 2.17 (dd, J = 3.8 and 5.0 Hz, 1H), 2.06 (m, 1H), 1.88 (m, 1H), 1.82 (m, 1H), 1.81 (m, 1H), 1.60 (m, 1H), 1.37 (s, 3H), 1.07 (d, J = 6.5 Hz, 3H), 1.03 (d, J = 6.7 Hz, 3H).

¹³C NMR (125 MHz, CDCl₃): δ = 174.5, 170.1, 147.8, 144.3, 144.2, 143.1, 138.8, 138.2, 135.9, 135.6, 130.7, 130.6, 126.9, 125.7, 125.2, 121.2, 119.9, 114.3, 99.7, 77.2, 74.4, 69.7, 53.9, 53.3, 51.8, 50.3, 47.3, 44.9, 42.8, 39.4, 32.9, 31.2, 28.4, 26.5, 21.0, 14.3.

HRMS (m/z): calculated for [C₃₉H₄₄N₈O₈ + Na]: 775.3180, found: 775.3179.

Synthesis of 314



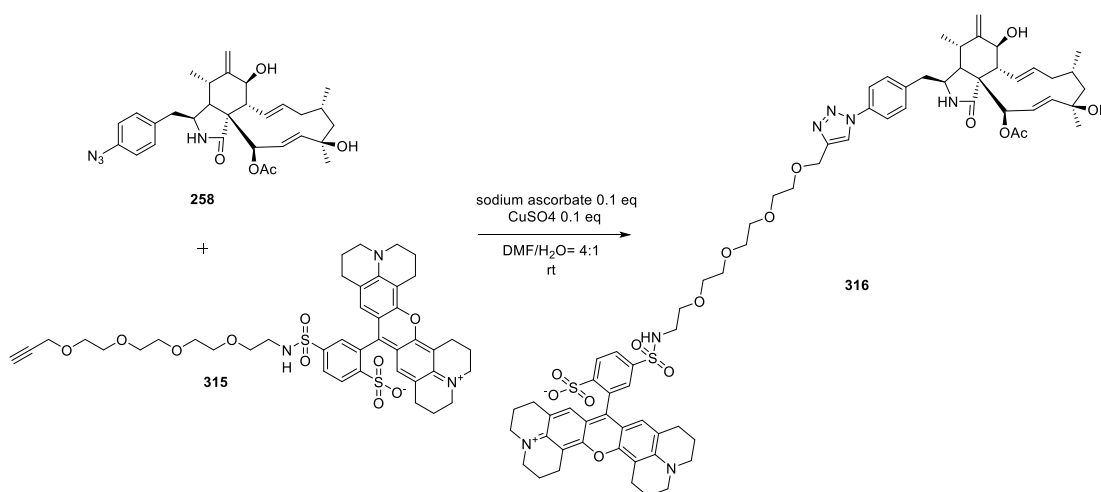
To a stirred solution of **258** (5.6 mg, 0.02 mmol, 2.0 eq) and **313** (3.0 mg, 0.01 mmol, 1.0 eq) in 4.25 mL DMF-water mixture (4:1, v/v) was added sodium ascorbate (0.2 mg, 1 μ mol, 0.1 eq) and copper sulfate (0.12 mg, 1 μ mol, 0.1 eq). The mixture was stirred at room temperature for 12 hours under nitrogen and the solvent was removed *in vacuo*. The residue was dissolved in EtOAc (2 mL) and washed with water (2 mL x 2). The organic phase was dried over MgSO₄, filtered and evaporated to dryness *in vacuo*. The residue was dissolved in MeOH and purified by LCMS to afford 1.7 mg of desired product (yield: 28.5%) as a red solid.²⁰⁰

¹H NMR (500 MHz, CDCl₃): δ (Hz) = 8.65 (s, 1H), 8.19 (d, J = 7.7 Hz 1H), 8.05 (d, J = 7.7 Hz 1H), 7.84 (d, J = 8.5 Hz, 2H), 7.71 (s, 1H), 7.35 (d, J = 8.5 Hz, 1H), 6.47 (d, J = 8.8 Hz, 1H), 6.36 (d, J = 8.8 Hz, 1H), 5.68 (dd, J = 2.2 and 17.0 Hz, 1H), 5.68 (dd, J = 8.8 and 15.5 Hz, 1H), 5.54 (ddd, J = 1.4, 9.7 and 15.4 Hz, 1H), 5.39 (brs, 1H), 5.29 (brs, 1H), 5.09 (ddd, J = 4.8, 10.1 and 15.4 Hz, 1H), 5.06 (m, 2H), 4.84 (brs, 2H), 4.54 (s, 2H), 3.63 (dd, J = 1.3 and 10.8 Hz, 1H), 3.15 (m, 1H), 2.85 (m, 1H), 2.74 (m, 1H), 2.66 (m, 2H), 2.51 (m, 1H), 2.24 (s, 3H), 1.97 (dd, J = 3.7 and 5.0 Hz 1H), 1.90 (m, 1H), 1.69 (m, 1H), 1.62 (m, 2H), 1.60 (m, 1H), 1.39 (s, 2H), 1.14 (s, 3H), 0.48 (d, J = 6.6 Hz, 3H).

¹³C NMR (125 MHz, CDCl₃): δ = 174.6, 170.6, 168.7, 165.5, 151.2, 149.4, 146.1, 146.0, 144.2, 140.4, 138.3, 138.2, 135.6, 134.9, 131.3, 130.3, 130.0, 129.6, 129.5, 129.3, 129.2, 125.8, 125.3, 121.0, 114.7, 114.6, 114.1, 111.8, 105.5, 105.2, 77.0, 72.7, 71.0, 54.3, 53.0, 52.4, 48.3, 46.6, 43.8, 43.5, 35.6, 32.2, 31.4, 28.2, 26.7, 21.1, 13.7.

HRMS (m/z): calculated for [C₅₇H₄₇N₉O₉S₂ + Na]: 1104.3140, found: 1104.3145.

Synthesis of 316



To a stirred solution of **258** (5.6 mg, 0.02 mmol, 2.0 eq) and **315** (4.0 mg, 0.005 mmol, 1.0 eq) in 1.25 mL DMF-water mixture (4:1, v/v) was added sodium ascorbate (0.1 mg, 0.5 μ mol, 0.1 eq) and copper sulfate (0.06 mg, 0.5 μ mol, 0.1 eq). The mixture was stirred at room temperature for 12 hours under nitrogen and the solvent was removed *in vacuo*. The residue was dissolved in EtOAc (2 mL) and washed with water (2 mL x 2). The organic phase was dried over MgSO₄, filtered and evaporated to dryness *in vacuo*. The residue was dissolved in MeOH and purified by LCMS to afford 2.6 mg of desired product (yield: 38.6%) as a purple solid.²⁰⁰

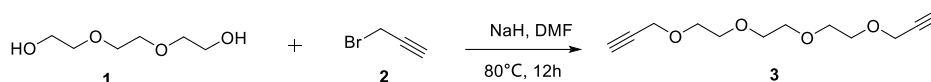
¹H NMR (500 MHz, CDCl₃): δ (Hz) = 8.36 (m, 1H), 8.01 (d, J = 7.9 Hz, 2H), 7.79 (d, J = 8.1 Hz, 2H), 7.36 (d, J = 8.1 Hz, 2H), 7.27 (s, 1H), 6.83 (s, 1H), 5.91 (dd, J = 2.8 and 16.5 Hz, 1H), 5.76 (ddd, J = 1.4, 9.7 and 15.4 Hz, 1H), 5.59 (brs, 1H), 5.45 (m, 1H), 5.38 (brs, 1H), 5.14 (brs, 1H), 4.81 (s, 2H), 3.85 (dd, J = 1.4 and 10.8 Hz, 1H), 3.79 (m, 2H), 3.68 (m, 12H), 3.47 (m, 8H), 3.34 (m, 2H), 3.27 (m, 1H), 2.97 (m, 1H), 2.90 (m, 1H), 2.80 (m, 1H), 2.77 (m, 2H), 2.73 (m, 2H), 2.66 (m, 2H), 2.26 (s, 3H), 2.15 (dd, J = 3.7 and 4.7 Hz, 1H), 2.05 (m, 1H), 1.97 (m, 1H), 1.89 (m, 1H), 1.83 (m, 1H), 1.81 (m, 1H), 1.58 (m, 1H), 1.37 (s, 3H), 1.28 (m, 4H), 1.08 (d, J = 6.5 Hz, 3H), 1.04 (d, J = 6.7 Hz, 3H).

¹³C NMR (125 MHz, CDCl₃): δ = 174.2, 170.1, 152.7, 151.3, 150.0, 148.0, 145.9, 145.7, 138.7, 138.1, 137.7, 137.5, 134.4, 131.5, 129.1, 129.0, 128.8, 128.1, 127.4, 127.1,

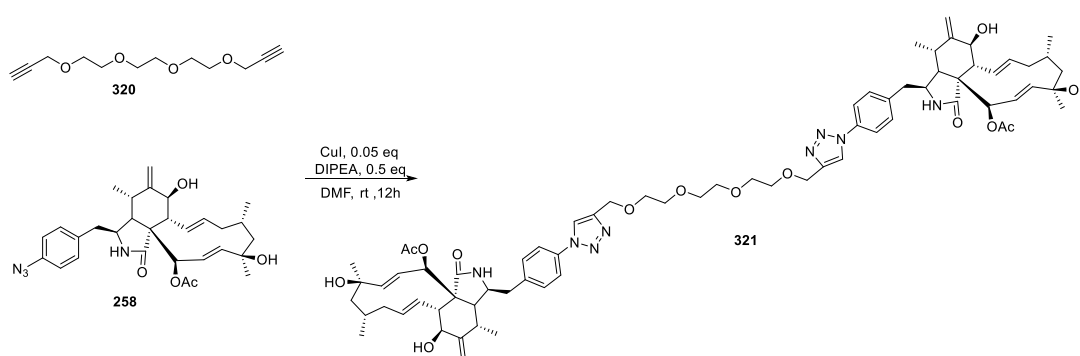
126.8, 126.5, 125.8, 121.2, 120.8, 114.2, 104.6, 77.4, 74.3, 73.6, 70.2, 69.7, 64.3, 53.8, 53.6, 51.7, 50.5, 50.4, 47.2, 45.0, 43.3, 42.7, 32.9, 31.2, 29.6, 28.5, 27.4, 26.5, 20.9, 20.6, 14.2.

HRMS (*m/z*): calculated for [C₇₀H₈₉N₇O₁₅S₂ + H]: 1354.5756, found: 1354.5781.

Synthesis of **321**



To a stirred solution of **1** (100 mg, 0.67 mmol, 1.0 eq) in dry DMF (3 mL) was added sodium hydride (32.2 mg, 1.34 mmol, 2.0 eq). The mixture was stirred at room temperature for 1 hour under nitrogen after which propargyl bromide (0.6 mL, 6.7 mmol, 10.0 eq) was added. The reaction solution was stirred at 80 °C for 12 hours under nitrogen and the solvent was removed *in vacuo*. The residue was diluted with water (10 mL) and then neutralized with 0.1 M HCl (15 mL). The resulting mixture was extracted with EtOAc (15 mL × 2) and the extract was washed with brine (20 mL). The organic phase was dried over MgSO₄, filtered and evaporated to dryness *in vacuo*. The crude light yellow oil (100 mg) was directly used in the next step without further purification.¹⁸⁷



To a stirred solution of **258** (20 mg, 0.038 mmol, 1.0 eq) and **320** (25.8 mg, 0.114 mmol, 3.0 eq) in DMF (4 mL) was added CuI (0.4 mg, 1.90 μmol, 0.05 eq) and DIPEA (2.4 mg, 19.0 μmol, 0.5 eq). The mixture was stirred at room temperature for 12 hours under nitrogen and the solvent was removed *in vacuo*. The residue was dissolved in EtOAc (2 mL) and washed with water (3 mL × 2). The organic phase was dried over MgSO₄,

filtered and evaporated to dryness *in vacuo*. The residue was dissolved in MeOH and purified by LCMS to afford 15.4 mg of desired product (yield: 31.7%) as a brown solid.¹⁹¹

¹H NMR (500 MHz, CDCl₃): δ (Hz) = 8.04 (s, 1H), 7.68 (d, J = 8.5 Hz, 2H), 7.31 (d, J = 8.5 Hz, 1H), 5.88 (dd, J = 2.2 and 17.0 Hz, 1H), 5.75 (ddd, J = 1.4, 9.7 and 15.4 Hz, 1H), 5.56 (brs, 1H), 5.55 (brs, 1H), 5.42 (ddd, J = 4.8, 10.1 and 15.4 Hz, 1H), 5.39 (brs, 1H), 5.14 (brs, 1H), 4.77 (s, 2H), 3.88 (dd, J = 1.3 and 10.8 Hz, 1H), 3.76 (m, 1H), 3.70 (m, 1H), 3.33 (m, 1H), 2.96 (m, 1H), 2.93 (m, 1H), 2.81 (m, 1H), 2.76 (m, 1H), 2.26 (s, 3H), 2.16 (dd, J = 3.8 and 5.1 Hz, 1H), 2.06 (m, 1H), 1.88 (m, 1H), 1.82 (m, 1H), 1.81 (m, 1H), 1.60 (m, 1H), 1.36 (s, 3H), 1.07 (d, J = 6.3 Hz, 3H), 1.02 (d, J = 6.7 Hz, 3H).

¹³C NMR (125 MHz, CDCl₃): δ = 174.3, 170.2, 147.9, 145.0, 138.8, 138.3, 138.2, 136.0, 126.9, 125.7, 120.8, 120.4, 114.2, 77.3, 74.7, 70.6, 69.9, 53.6, 53.5, 51.8, 50.3, 47.3, 45.1, 42.7, 32.8, 31.3, 28.6, 26.5, 21.0, 14.2.

HRMS (m/z): calculated for [C₇₂H₉₄N₈O₁₄ + Na]: 1317.6787, found: 1317.6775.

References

- 1 A. Schueffler and T. Anke, *Nat. Prod. Rep.*, 2014, **31**, 1425–1448.
- 2 S. Bräse, A. Encinas, J. Keck and C. F. Nising, *Chem. Rev.*, 2009, **109**, 3903–3990.
- 3 A. A. Brakhage, *Nat. Rev. Microbiol.*, 2013, **11**, 21–32.
- 4 D. Hoffmeister and N. P. Keller, *Nat. Prod. Rep.*, 2007, **24**, 393–416.
- 5 N. Nagano, M. Umemura, M. Izumikawa, J. Kawano, T. Ishii, M. Kikuchi, K. Tomii, T. Kumagai, A. Yoshimi, M. Machida, K. Abe, K. Shin-ya and K. Asai, *Fungal Genet. Biol.*, 2016, **86**, 58–70.
- 6 N. P. Keller, G. Turner and J. W. Bennett, *Nat. Rev. Microbiol.*, 2005, **3**, 937–947.
- 7 P. G. Arnison, M. J. Bibb, G. Bierbaum, A. A. Bowers, J. M. Willey and W. A. Van Der Donk, *Nat. Prod. Rep.*, 2013, **30**, 108–160.
- 8 U. A. Kshirsagar, *Org. Biomol. Chem.*, 2015, **13**, 9336–9352.
- 9 M. Chudzik, I. Korzonek-Szlacheta and W. Król, *Molecules*, 2015, **20**, 1610–1625.
- 10 R. J. Cox, *Org. Biomol. Chem.*, 2007, **5**, 2010–2026.
- 11 Z. Song, W. Bakeer, J. W. Marshall, A. A. Yakasai, R. M. Khalid, J. Collemare, E. Skellam, D. Tharreau, M.-H. Lebrun, C. M. Lazarus, A. M. Bailey, T. J. Simpson and R. J. Cox, *Chem. Sci.*, 2015, **6**, 4837–4845.
- 12 R. J. Cox, *Org. Biomol. Chem.*, 2007, **5**, 2010.
- 13 D. A. Herbst, C. A. Townsend and T. Maier, *Nat. Prod. Rep.*, 2018, **00**, 1–24.
- 14 B. Shen, *Curr. Opin. Chem. Biol.*, 2003, **7**, 285–295.
- 15 J. Staunton and K. J. Weissman, *Nat. Prod. Rep.*, 2001, **18**, 380–416.
- 16 R. J. Cox, T. S. Hitchman, K. J. Byrom, I. S. C. Findlow, J. Crosby and T. J. Simpson, 1997, **405**, 267–272.
- 17 S. Tropf, *J. Biol. Chem.*, 1995, **270**, 7922–7928.
- 18 B. J. Rawlings, *Nat. Prod. Rep.*, 1999, **16**, 425–484.
- 19 U. Kück and B. Hoff, *Appl. Microbiol. Biotechnol.*, 2010, **86**, 51–62.
- 20 B. J. Dunn and C. Khosla, *J. R. Soc. Interface*, 2013, **10**, 20130297.
- 21 P. Spiteller and W. Steglich, *J. Nat. Prod.*, 2002, **65**, 725–727.
- 22 S. Jenni, M. Leibundgut, T. Maier and N. Ban, *Science*, 2006, **311**, 1263–1268.
- 23 C. Hertweck, *Angew. Chemie Int. Ed.*, 2009, **48**, 4688–4716.

- 24 R. N. Moore, G. Bigam, J. K. Chan, A. M. Hogg, T. T. Nakashima and J. C. Vederas, *J. Am. Chem. Soc.*, 1985, **107**, 3694–3701.
- 25 Y. M. Zheng, F. L. Lin, H. Gao, G. Zou, J. W. Zhang, G. Q. Wang, G. D. Chen, Z. H. Zhou, X. S. Yao and D. Hu, *Sci. Rep.*, 2017, **7**, 1–10.
- 26 A. B. Petersen, M. H. Rønne, T. O. Larsen and M. H. Clausen, *Chem. Rev.*, 2014, **114**, 12088–12107.
- 27 Y. H. Chooi, R. Cacho and Y. Tang, *Chem. Biol.*, 2010, **17**, 483–494.
- 28 R. A. Cacho, Y. H. Chooi, H. Zhou and Y. Tang, *ACS Chem. Biol.*, 2013, **8**, 2322–2330.
- 29 J. Ziegler and P. J. Facchini, *Annu. Rev. Plant Biol.*, 2008, **59**, 735–769.
- 30 T. Dalgleish, J. M. G. Williams, A.-M. J. Golden, N. Perkins, L. F. Barrett, P. J. Barnard, C. Au Yeung, V. Murphy, R. Elward, K. Tchanturia and E. Watkins, *J. Exp. Psychol. Gen.*, 2007, **136**, 23–42.
- 31 J. M. Crawford and C. A. Townsend, *Nat. Rev. Microbiol.*, 2010, **8**, 879–889.
- 32 A. G. Newman, A. L. Vagstad, P. A. Storm and C. A. Townsend, *J. Am. Chem. Soc.*, 2014, **136**, 7348–7362.
- 33 M. E. Ruiz, *Annual Review of Microbiology*, 2004, **58**, 453–488.
- 34 G. L. Challis, J. Ravel and C. A. Townsend, *Chem. Biol.*, 2000, **7**, 211–224.
- 35 G. F. Bills and J. B. Gloer, *Microbiol. Spectr.*, 2016, **6**, 1–2.
- 36 P. Belin, M. Moutiez, S. Lautru, J. Seguin, J. L. Pernodet and M. Gondry, *Nat. Prod. Rep.*, 2012, **29**, 961–979.
- 37 H. L. Conductor and S. D. Bruner, *Nat. Prod. Rep.*, 2012, **29**, 1099–1110.
- 38 L. Du and L. Lou, *Nat. Prod. Rep.*, 2010, **27**, 255–278.
- 39 X. Gao, S. W. Haynes, B. D. Ames, P. Wang, L. P. Vien, C. T. Walsh and Y. Tang, *Nat. Chem. Biol.*, 2012, **8**, 823–830.
- 40 S. Donadio, P. Monciardini and M. Sosio, *Nat. Prod. Rep.*, 2007, **24**, 1073.
- 41 C. T. Walsh, *Nat. Prod. Rep.*, 2016, **33**, 127–135.
- 42 A. W. Goering, J. Li, R. A. McClure, R. J. Thomson, M. C. Jewett and N. L. Kelleher, *ACS Synth. Biol.*, 2017, **6**, 39–44.
- 43 S. C. Tsai, H. Lu, D. E. Cane, C. Khosla and R. M. Stroud, *Biochemistry*, 2002, **41**, 12598–12606.
- 44 H. U. Böhnert, I. Fudal, W. Doh, D. Tharreau, J. L. Notteghem and M. H. Lebrun, *Plant Cell*, 2004, **16**, 2499–2513.

- 45 Z. Song, R. J. Cox, C. M. Lazarus and T. J. Simpson, *ChemBioChem*, 2004, **5**, 1196–1203.
- 46 C. J. Balibar, A. R. Howard-Jones and C. T. Walsh, *Nat. Chem. Biol.*, 2007, **3**, 584–592.
- 47 Hsiao-Ching lin, Wei Xu, Yi Tang, *J. Am. Chem. Soc.*, 2016, **138**, 4002–4005.
- 48 M. Sato, J. E. Dander, C. Sato, Y. S. Hung, S. S. Gao, M. C. Tang, L. Hang, J. M. Winter, N. K. Garg, K. Watanabe and Y. Tang, *J. Am. Chem. Soc.*, 2017, **139**, 5317–5320.
- 49 K. L. Eley, L. M. Halo, Z. Song, H. Powles, R. J. Cox, A. M. Bailey, C. M. Lazarus and T. J. Simpson, *ChemBioChem*, 2007, **8**, 289–297.
- 50 L. M. Halo, J. W. Marshall, A. A. Yakasai, Z. Song, C. P. Butts, M. P. Crump, M. Heneghan, A. M. Bailey, T. J. Simpson, C. M. Lazarus and R. J. Cox, *ChemBioChem*, 2008, **9**, 585–594.
- 51 L. M. Halo, M. N. Heneghan, A. A. Yakasai, Z. Song, K. Williams, A. M. Bailey, R. J. Cox, C. M. Lazarus and T. J. Simpson, *J. Am. Chem. Soc.*, 2008, **130**, 17988–17996.
- 52 K. M. Fisch, *RSC Adv.*, 2013, **3**, 18228.
- 53 W. C. A. Gelderblom, P. G. Thiel and K. J. van der Merwe, *Mutat. Res. - Fundam. Mol. Mech. Mutagen.*, 1988, **199**, 207–214.
- 54 D. W. Brown, R. A. E. Butchko, M. Busman and R. H. Proctor, *Fungal Genet. Biol.*, 2012, **49**, 521–532.
- 55 S. N. Chulze, M. L. Ramirez, A. Torres and J. F. Leslie, *Appl. Environ. Microbiol.*, 2000, **66**, 5312–5315.
- 56 G. Wei, D. Tan, C. Chen, Q. Tong, X. N. Li, J. Huang, J. Liu, Y. Xue, J. Wang, Z. Luo, H. Zhu and Y. Zhang, *Sci. Rep.*, 2017, **7**, 1–12.
- 57 J. P. Côté, S. French, S. S. Gehrke, C. R. MacNair, C. S. Mangat, A. Bharat and E. D. Brown, *MBio*, 2016, **6**, e01714-16.
- 58 C. L. M. Gilchrist, H. Li and Y. H. Chooi, *Org. Biomol. Chem.*, 2018, **16**, 1620–1626.
- 59 A. Doltra, T. Dietrich, C. Schneeweis, S. Kelle, A. Doltra, P. Stawowy and E. Fleck, *Biomed Res. Int.*, **2013**, 676489–676499.
- 60 Y. jie Yang, Y. Wang, *Microb. Cell. Fact.*, 2017, **16**, 142.
- 61 A. A. Wylie, J. Schoepfer, W. Jahnke, S. W. Cowan-Jacob, A. Loo, P. Furet, A. L. Marzinzik, X. Pelle, J. Donovan, W. Zhu, S. Buonamici, A. Q. Hassan, F. Lombardo, V. Iyer, M. Palmer, G. Berellini, S. Dodd, S. Thohan, H. Bitter, S. Branford, D. M. Ross, T. P. Hughes, L. Petruzzelli, K. G. Vanasse, M. Warmuth, F. Hofmann, N. J. Keen and W. R. Sellers, *Nature*, 2017, **543**, 733–737.
- 62 P. Sarkari, H. Marx, M. L. Blumhoff, D. Mattanovich, M. Sauer and M. G. Steiger, *Bioresour.*

- Technol.*, 2017, **245**, 1327–1333.
- 63 S. Zlitni, L. F. Ferruccio and E. D. Brown, *Nat. Chem. Biol.*, 2013, **9**, 796–804.
- 64 T. Katayama, Y. Tanaka, T. Okabe, H. Nakamura, W. Fujii, K. Kitamoto, *Biotechnol. Lett.*, 2016, **38**, 637–642.
- 65 D. Sharma, A. Pramanik and P. K. Agrawal, *3 Biotech*, 2016, **6**, 210–224.
- 66 A. Ear, S. Amand, F. Blanchard, A. Blond, L. Dubost, D. Buisson and B. Nay, *Org. Biomol. Chem.*, 2015, **13**, 3662–3666.
- 67 T. Jiang, M. Wang, L. Li, J. Si, B. Song, C. Zhou, M. Yu, X. Wang, Y. Zhang, G. Ding and Z. Zou, *J. Nat. Prod.*, 2016, **79**, 2487–2494.
- 68 X. Liu and C. T. Walsh, *Biochemistry*, 2009, **48**, 11032–11044.
- 69 Y. Hu, D. Dietrich, W. Xu, A. Patel, J. A. J. Thuss, J. Wang, W. B. Yin, K. Qiao, K. N. Houk, J. C. Vederas and Y. Tang, *Nat. Chem. Biol.*, 2014, **10**, 552–554.
- 70 K. Qiao, Y. H. Chooi and Y. Tang, *Metab. Eng.*, 2011, **13**, 723–732.
- 71 J. W. Sims and E. W. Schmidt, *J. Am. Chem. Soc.*, 2008, **130**, 11149–11155.
- 72 J. Diakur, T. T. Nakashima and J. C. Vederas, *Can. J. Chem.*, 1980, **58**, 1311–1315.
- 73 H. Oikawa, Y. Murakami, *J. Am. Chem. Soc.*, 1994, **116**, 3605–3606.
- 74 L. Hang, N. Liu and Y. Tang, *ACS Catal.*, 2016, **6**, 5935–5945.
- 75 X. Zhang and S. Li, *Nat. Prod. Rep.*, 2017, **34**, 1061–1089.
- 76 K. Ishiuchi, T. Nakazawa, F. Yagishita, T. Mino, H. Noguchi, K. Hotta and K. Watanabe, *J. Am. Chem. Soc.*, 2013, **135**, 7371–7377.
- 77 J. Schumann and C. Hertweck, *J. Am. Chem. Soc.*, 2007, **129**, 9564–9565.
- 78 K. Ishiuchi, T. Nakazawa, F. Yagishita, T. Mino, H. Noguchi, K. Hotta and K. Watanabe, *J. Am. Chem. Soc.*, 2013, **135**, 7371–7377.
- 79 J. A. Hangasky, C. Y. Taabazuing, M. A. Valliere and M. J. Knapp, *Metallomics*, 2013, **5**, 287–301.
- 80 J. E. Baldwin, R. M. Adlington, N. P. Crouch, I. A. C. Pereira, R. T. Aplin and C. Robinson, *J. Chem. Soc. Chem. Commun.*, 1993, 105–108.
- 81 B. Lindblad, G. Lindstedt and S. Lindstedt, *J. Am. Chem. Soc.*, 1970, **92**, 7446–7449.
- 82 S. Wei, V. Episkopou, R. Piantedosi, M. E. Gottesman, E. J. Robertson and W. S. Blaner, *J. Bio. Chem.*, 1994, **270**, 866–870.
- 83 M. J. Ryle, A. Liu, R. B. Muthukumar, R. Y. N. Ho, K. D. Koehntop, J. McCracken, L. Que,

- and R. P. Hausinger, *Biochemistry*, 2003, **42**, 1854–1862.
- 84 W. Min, T. P. Begley, J. Myllyharju and K. I. Kivirikko, *Bioorg. Chem.*, 2000, **28**, 261–265.
- 85 J. Zhou, W. L. Kelly, B. O. Bachmann, M. Gunsior, C. A. Townsend and E. I. Solomon, *J. Am. Chem. Soc.*, 2001, **123**, 7388–7398.
- 86 S. P. Salowe, E. N. Marsh and C. A. Townsend, *Biochemistry*, 1990, **29**, 6499–6508.
- 87 M. D. Lloyd, K. D. Merritt, V. Lee, T. J. Sewell, B. Wha-Son, J. E. Baldwin, C. J. Schofield, S. W. Elson, K. H. Baggaley and N. H. Nicholson, *Tetrahedron*, 1999, **55**, 10201–10220.
- 88 J. E. Baldwin, *J. Chem. Soc. Chem. Commun.*, 1976, 734–736.
- 89 J. E. Baldwin, R. M. Adlington, J. S. Bryans, M. D. Lloyd, T. J. Sewell, C. J. Schofield, K. H. Baggaley and R. Cassels, *Tetrahedron*, 1997, **53**, 7011–7020.
- 90 E. Neil Marsh, M. D. T. Chang and C. A. Townsend, *Biochemistry*, 1992, **31**, 12648–12657.
- 91 T. Bureau, K. C. Lam, R. K. Ibrahim, B. Behdad and S. Dayanandan, *Genome*, 2007, **50**, 1001–1013.
- 92 M. J. Bonifácio, M. A. Vieira-Coelho, N. Borges and P. Soares-da-Silva, *Arch. Biochem. Biophys.*, 2000, **384**, 361–367.
- 93 M. Motomura, N. Chihaya, T. Shinozawa, T. Hamasaki and K. Yabe, *Appl. Environ. Microbiol.*, 1999, **65**, 4987–94.
- 94 Y. Youngdae, Y. Park, Y. S. Yi, Y. Lee, G. Jo, J. C. Park, J. H. Ahn and Y. Lim, *J. Microbiol. Biotechnol.*, 2010, **20**, 1359–1366.
- 95 Y. Zhang, M. Z. Han, S. L. Zhu, M. Li, X. Dong, X. C. Luo, Z. Kong, Y. X. Lu, S. Y. Wang and W. Y. Tong, *Enzyme Microb. Technol.*, 2015, **73–74**, 72–79.
- 96 F. S. Chu, *Mutat. Res. Toxicol.*, 1991, **259**, 291–306.
- 97 D. Bhatnagar, T. E. Cleveland and D. G. I. Kingston, *Biochemistry*, 1991, **30**, 4343–4350.
- 98 T. E. Cleveland and D. Bhatnagar, *Can. J. Microbiol.*, 1987, **33**, 1108–1112.
- 99 J. Yu, J. W. Cary, D. Bhatnagar, T. E. Cleveland, N. P. Keller and F. S. Chu, *Appl. Environ. Microbiol.*, 1993, **59**, 3564–3571.
- 100 D. Sychantha, A. S. Brott, C. S. Jones and A. J. Clarke, *Front. Microbiol.*, 2018, **9**, 1–17.
- 101 U. Oppermann, C. Filling, M. Hult, N. Shafqat, X. Wu, M. Lindh, J. Shafqat, E. Nordling, Y. Kallberg, B. Persson and H. Jörnvall, *Chem. Biol. Interact.*, 2003, **143–144**, 247–253.
- 102 Y. He and R. J. Cox, *Chem. Sci.*, 2016, **7**, 2119–2127.
- 103 M. Nukina, *Agric. Biol. Chem.*, 1987, **51**, 2625–2628.

- 104 M. Nukina and H. C. Found, 2000, **51**, 2625–2628.
- 105 T. Tsurushima, L. D. Don, K. Kawashima, J. Murakami, H. Nakayashiki, Y. Tosa and S. Mayama, *Mol. Plant Pathol.*, 2005, **6**, 605–613.
- 106 M. Binder and C. Tamm, *Angew. Chemie Int. Ed.*, 1973, **12**, 370–380.
- 107 M. Suzuki, T. Sugiyama, M. Watanabe, T. Murayama and K. Yamashita, 1987, **51**, 1121–1127.
- 108 K. Blin, S. Shaw, K. Steinke, R. Villebro, N. Ziemert, S. Y. Lee, M. H. Medema and T. Weber, *Nucleic Acids Res.*, 2019, **47**, W81–W87.
- 109 C. Wang, V. Hantke, R. J. Cox and E. Skellam, *Org. Lett.*, 2019, **21**, 4163–4167.
- 110 H. U. Böhnert, I. Fudal, W. Dioh, D. Tharreau, J.-L. Notteghem and M.-H. Lebrun, *Plant Cell*, 2004, **16**, 2499–513.
- 111 S. Rachid, M. Scharfe, H. Blöcker, K. J. Weissman and R. Müller, *Chem. Biol.*, 2009, **16**, 70–81.
- 112 J. Collemare, M. Pianfetti, A. E. Houille, D. Morin, L. Camborde, M. J. Gagey, C. Barbisan, I. Fudal, M. H. Lebrun and H. U. Böhnert, *New Phytol.*, 2008, **179**, 196–208.
- 113 Z. Song, W. Bakeer, J. W. Marshall, A. A. Yakasai, R. M. Khalid, J. Collemare, E. Skellam, D. Tharreau, M.-H. Lebrun, C. M. Lazarus, A. M. Bailey, T. J. Simpson and R. J. Cox, *Chem. Sci.*, 2015, **6**, 4837–4845.
- 114 J. Kennedy, *Nat. Prod. Rep.*, 2008, **25**, 25–34.
- 115 W. T. Shier, K. L. Rinehart and D. Gottlieb, *Proc. Natl. Acad. Sci. U. S. A.*, 1969, **63**, 198–204.
- 116 M. Hamann, *Curr. Pharm. Des.*, 2005, **9**, 879–889.
- 117 J. F. Hu, J. A. Schetz, M. Kelly, J. N. Peng, K. K. H. Ang, H. Flotow, C. Y. Leong, S. B. Ng, A. D. Buss, S. P. Wilkins and M. T. Hamann, *J. Nat. Prod.*, 2002, **65**, 476–480.
- 118 D. Li, Y. Tang, J. Lin and W. Cai, *Microb. Cell Fact.*, 2017, **16**, 1–13.
- 119 J. Davison, A. Al Fahad, M. Cai, Z. Song, S. Y. Yehia, C. M. Lazarus, A. M. Bailey, T. J. Simpson and R. J. Cox, *Proc. Natl. Acad. Sci. U. S. A.*, 2012, **109**, 7642–7647.
- 120 A. M. Bailey, R. J. Cox, K. Harley, C. M. Lazarus, T. J. Simpson and E. Skellam, *Chem. Commun.*, 2007, **39**, 4053–4055.
- 121 A. Al Fahad, A. Abood, T. J. Simpson and R. J. Cox, *Angew. Chemie - Int. Ed.*, 2014, **53**, 7519–7523.
- 122 N. Yokochi, Y. Yoshikane, T. Yagi, M. Yamasaki and B. Mikami, *Acta Crystallogr. Sect. D Biol. Crystallogr.*, 2004, **60**, 2061–2062.

- 123 S. J. Vollmer and C. Yanofsky, *Proc. Natl. Acad. Sci. U. S. A.*, 1986, **83**, 4869–4873.
- 124 V. Meyer, *Biotechnol. Adv.*, 2008, **26**, 177–185.
- 125 M. L. Nielsen, L. Albertsen, G. Lettier, J. B. Nielsen and U. H. Mortensen, *Fungal Genet. Biol.*, 2006, **43**, 54–64.
- 126 I. Weyda, L. Yang, J. Vang, B. K. Ahring, M. Lübeck and P. S. Lübeck, *J. Microbiol. Methods*, 2017, **135**, 26–34.
- 127 J. F. Martin, G. Nicolas and J. R. Villanueva, *Can. J. Microbiol.*, 1973, **19**, 789–796.
- 128 K. T. Yuyama, L. Wendt, F. Surup, R. Kretz, C. Chepkirui, K. Wittstein, C. Boonlarpradab, S. Wongkanoun, J. Luangsa-ard, M. Stadler and W.-R. Abraham, *Biomolecules*, 2018, **8**, 129.
- 129 R. Kretz, L. Wendt, S. Wongkanoun, J. Luangsa-ard, F. Surup, S. Helaly, S. Noumeur, M. Stadler and T. Stradal, *Biomolecules*, 2019, **9**, 73.
- 130 Kuspa A, Kaiser D, *J. Bacteriol*, 1989, **171**, 2762–2772.
- 131 V. Hantke, E. J. Skellam and R. J. Cox, *Chem. Comm*, 2020, **56**, 2925-2928..
- 132 K. E. Lebe and R. J. Cox, *Chem. Sci.*, 2019, **10**, 1227–1231.
- 133 K. A. K. Pahirulzaman, K. Williams and C. M. Lazarus, *Methods Enzymol*, 2012, **517**, 242-257.
- 134 Larissa M. Podust, *Nat. Prod. Rep.*, 2012, **29**, 1251-1266.
- 135 M. Winn, J. K. Fyans, Y. Zhuo and J. Micklefield, *Nat. Prod. Rep.*, 2016, **33**, 317–347.
- 136 W. Xu, X. Cai, M. E. Jung and Y. Tang, *J. Am. Chem. Soc.*, 2010, **132**, 13604–13607.
- 137 K. Ishiuchi, T. Nakazawa, F. Yagishita, T. Mino, H. Noguchi, K. Hotta and K. Watanabe, *J. Am. Chem. Soc.*, 2013, **135**, 7371–7377.
- 138 K. Qiao, Y. H. Chooi and Y. Tang, *Metab. Eng.*, 2011, **13**, 723–732.
- 139 C. Wang, K. Becker, S. Pfütze, E. Kuhnert, M. Stadler, R. J. Cox and E. Skellam, *Org. Lett.*, 2019, **21**, 8756–8760.
- 140 Y. Xu, T. Zhou, S. Zhang, P. Espinosa-Artiles, L. Wang, W. Zhang, M. Lin, I. Molnár, *Proc. Natl. Acad. Sci. U. S. A.*, 2014, **111**, 12354–12359.
- 141 D. J. Mattern, V. Valiante, S. E. Unkles, *Front. Microbiol.*, 2015, **6**, 775.
- 142 L. M. Halo, J. W. Marshall, A. A. Yakasai, Z. Song, C. P. Butts, M. P. Crump, M. Heneghan, A. M. Bailey, T. J. Simpson, C. M. Lazarus and R. J. Cox, *ChemBioChem*, 2008, **9**, 585–594.
- 143 N. J. Alexander, R. H. Proctor and S. P. McCormick, *Toxin Rev.*, 2009, **28**, 198–215.
- 144 X. Wang, C. Wang, L. Duan, L. Zhang, H. Liu, Y. M. Xu, Q. Liu, T. Mao, W. Zhang, M. Chen, M. Lin, A. A. L. Gunatilaka, Y. Xu and I. Molnár, *J. Am. Chem. Soc.*, 2019, **141**, 4355–4364.

- 145 Y. Xu, T. Zhou, P. Espinosa-Artiles, Y. Tang, I. Molnár, *ACS Chem. Biol.*, 2014, **9**, 1119–1127.
- 146 A. Espada, A. Rivera-Sagredo, J. M. De la Fuente, J. A. Hueso-Rodríguez and S. W. Elson, *Tetrahedron*, 1997, **53**, 6485–6492.
- 147 H. Jayasuriya, K. B. Herath, J. G. Ondeyka, J. D. Polishook, G. F. Bills, A. W. Dombrowski, M. S. Springer, S. Siciliano, L. Malkowitz, M. Sanchez, Z. Guan, S. Tiwari, D. W. Stevenson, R. P. Borris and S. B. Singh, *J. Nat. Prod.*, 2004, **67**, 1036–1038.
- 148 M. B. Rubin and S. Inbar, *J. Org. Chem.*, 1988, **53**, 3355–3358.
- 149 X. Hong, J. M. Mejía-Oneto and A. Padwa, *Tetrahedron Lett.*, 2006, **47**, 8387–8390.
- 150 J. Collemare, M. Pianfetti, A.-E. Houille, D. Morin, L. Camborde, M.-J. Gagey, C. Barbisan, I. Fudal, M.-H. Lebrun and H. U. Böhnert, *New Phytol.*, 2008, **179**, 196–208.
- 151 O. Keller, M. Kollmar, M. Stanke and S. Waack, *Bioinformatics*, 2011, **27**, 757–763.
- 152 M. L. Nielsen, T. Isbrandt, L. M. Petersen, U. H. Mortensen, M. R. Andersen, J. B. Hoof and T. O. Larsen, *PLoS One*, 2016, **11**, e0161199.
- 153 A. Kirschning, F. Taft and T. Knobloch, *Org. Biomol. Chem.*, 2007, **5**, 3245–3259.
- 154 C. M. Gober and M. M. Joullé *J. Org. Chem.*, 2016, **81**, 10136–10144.
- 155 G. Ding, Y. C. Song, J. R. Chen, C. Xu, H. M. Ge, X. T. Wang and R. X. Tan, *J. Nat. Prod.*, 2006, **69**, 302–304.
- 156 P. Zorzete, T. A. Reis, J. D. Felício, A. C. Baquião, P. Makimoto and B. Corrêa, *Food Chem.*, 2011, **129**, 957–964.
- 157 Michio Sato, Kenji Watanabe, Yi Tang, *J. Am. Chem. Soc.*, 2017, **139**, 5317–5320.
- 158 J. Schümann and C. Hertweck, *J. Am. Chem. Soc.*, 2007, **129**, 9564–9565.
- 159 S. Sekita, K. Yoshihir and S. Natori, *Chem. Pharm. Bull. (Tokyo)*, 1983, **31**, 490–498.
- 160 H. M. Ge, W. Yan, Z. K. Guo, Q. Luo, R. Feng, L. Y. Zang, Y. Shen, R. H. Jiao, Q. Xu and R. X. Tan, *Chem. Commun.*, 2011, **47**, 2321–2323.
- 161 B. N. Mijts and C. Schmidt-Dannert, *Curr. Opin. Biotechnol.*, 2003, **14**, 597–602.
- 162 C. D. Murphy, B. R. Clark and J. Amadio, *Appl. Microbiol. Biotechnol.*, 2009, **84**, 617–629.
- 163 K. L. Rinehart, *Pure Appl. Chem.*, 1977, **49**, 1361–1384.
- 164 B. Wilkinson, M. A. Gregory, S. J. Moss, I. Carletti, R. M. Sheridan, A. Kaja, M. Ward, C. Olano, C. Mendez, J. A. Salas, P. F. Leadlay, R. vanGinckel and M. Q. Zhang, *Bioorganic Med. Chem. Lett.*, 2006, **16**, 5814–5817.
- 165 J. M. Cassady, K. K. Chan, H. G. Floss and E. Leistner, *Chem. Pharm. Bull.*, 2004, **52**, 1–26.

- 166 D. M. Rothman, M. E. Vazquez, E. M. Vogel and B. Imperiali, *J. Org. Chem.*, 2003, **68**, 6795–6798.
- 167 C. Ferroni, A. Pepe, Y. S. Kim, S. Lee, A. Guerrini, M. D. Parenti, A. Tesei, A. Zamagni, M. Cortesi, N. Zaffaroni, M. De Cesare, G. L. Beretta, J. B. Trepel, S. V. Malhotra and G. Varchi, *J. Med. Chem.*, 2017, **60**, 3082–3093.
- 168 D. J. Newman and G. M. Cragg, *J. Nat. Prod.*, 2007, **70**, 461–477.
- 169 A. L. Demain and R. P. Blander, *Antonie van Leeuwenhoek, Int. J. Gen. Mol. Microbiol.*, 1999, **75**, 5–19.
- 170 A. W. Alberts, *Cardiology*, 1990, **77**, 14–21.
- 171 K. Scherlach, D. Boettger, N. Remme and C. Hertweck, *Nat. Prod. Rep.*, 2010, **27**, 869–886.
- 172 G. Stork and E. Nakamura, *J. Am. Chem. Soc.*, 1983, **105**, 5510–5512.
- 173 B. H. Patwardhan, M. Flashner, C. A. Miller and S. W. Tanenbaum, *J. Med. Chem.*, 1982, **25**, 663–666.
- 174 E. Skellam, *Nat. Prod. Rep.*, 2017, **34**, 1252–1263.
- 175 N. M. Meghani, H. H. Amin and B. J. Lee, *Drug Discov. Today*, 2017, **22**, 1604–1619.
- 176 L. A. Canalle, S. S. Van Berkel, L. T. De Haan and J. C. M. Van Hest, *Adv. Funct. Mater.*, 2009, **19**, 3464–3470.
- 177 Y. Zhang, H. He, C. Gao and J. Wu, *Langmuir*, 2009, **25**, 5814–5824.
- 178 V. O. Rodionov, V. V. Fokin and M. G. Finn, *Angew. Chemie - Int. Ed.*, 2005, **44**, 2210–2215.
- 179 J. E. Hein and V. V. Fokin, *Chem. Soc. Rev.*, 2010, **39**, 1302–1315.
- 180 L. Jin, D. R. Tolentino, M. Melaimi and G. Bertrand, *Sci. Adv.*, 2015, **1**, e1500304.
- 181 A. Testa, S. J. Hughes, X. Lucas, J. E. Wright and A. Ciulli, *ChemRxiv*, 2019, **2**, online version.
- 182 R. P. Wurz, K. Dellamaggiore, H. Dou, N. Javier, M. C. Lo, J. D. McCarter, D. Mohl, C. Sastri, J. R. Lipford and V. J. Cee, *J. Med. Chem.*, 2018, **61**, 453–461.
- 183 C. E. Berndsen and C. Wolberger, *Nat. Struct. Mol. Biol.*, 2014, **21**, 301–307.
- 184 J. Lohbeck and A. K. Miller, *Bioorganic Med. Chem. Lett.*, 2016, **26**, 5260–5262.
- 185 L. G. Rule, *Indian. Med. Forum*, 1972, **23**, 342–344.
- 186 C. Tian, P. Xiu, Y. Meng, W. Zhao, Z. Wang and R. Zhou, *Chem. Eur. J.*, 2012, **18**, 14305–14313.
- 187 X. Ning, S. Lee, Z. Wang, D. Kim, B. Stubblefield, E. Gilbert and N. Murthy, *Nat. Mater.*, 2011, **10**, 602–607.

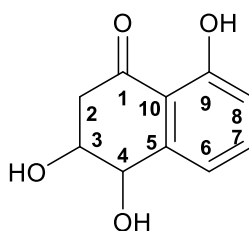
- 188 M. Jezowska, J. Romanowska, B. Bestas, U. Tedebark and M. Honcharenko, *Molecules*, 2012, **17**, 14174–14185.
- 189 T. Honda, T. Janosik, Y. Honda, J. Han, K. T. Liby, C. R. Williams, R. D. Couch, A. C. Anderson, M. B. Sporn and G. W. Gribble, *J. Med. Chem.*, 2004, **47**, 4923–4932.
- 190 B. Hulin, C. L. Lau and E. M. Gibbs, *Bioorganic Med. Chem. Lett.*, 1993, **3**, 703–706.
- 191 C. Ferroni, A. Pepe, Y. S. Kim, S. Lee, A. Guerrini, M. D. Parenti, A. Tesei, A. Zamagni, M. Cortesi, N. Zaffaroni, M. De Cesare, G. L. Beretta, J. B. Trepel, S. V. Malhotra and G. Varchi, *J. Med. Chem.*, 2017, **60**, 3082–3093.
- 192 A. M. Faucher and C. Grand-Maître, *Synth. Commun.*, 2003, **33**, 3503–3511.
- 193 J. Q. Wu and T. D. Pollard, *Science*, 2005, **310**, 310–314.
- 194 T. M. Bunnell, B. J. Burbach, Y. Shimizu and J. M. Ervasti, *Mol. Biol. Cell*, 2011, **22**, 4047–4058.
- 195 R. Grosse and M. K. Vartiainen, *Nat. Rev. Mol. Cell Biol.*, 2013, **14**, 693–697.
- 196 J. E. Estes, L. A. Selden and L. C. Gershman, *Biochemistry*, 1981, **20**, 708–712.
- 197 J. R. Pringle, A. E. M. Adams, D. G. Drubin and B. K. Haarer, *Methods Enzymol.*, 1991, **194**, 565–602.
- 198 R. Joseph, O. P. Srivastava and R. R. Pfister, *Investig. Ophthalmol. Vis. Sci.*, 2012, **53**, 4032–4041.
- 199 T. Jiang, *J. Nat. Prod.*, 2016, **79**, 2487–2494.
- 200 S. Chinthala and S. Raj, *J. Heterocycl. Chem.*, 2018, **55**, 251–257.
- 201 P. P. Mpungose, Z. P. Vundla, G. E. M. Maguire and H. B. Friedrich, *Molecules*, 2018, **23**, 1–24.
- 202 A. V. Martínez, J. I. García and J. A. Mayoral, *Tetrahedron*, 2017, **73**, 5581–5584.
- 203 C. Barnard, *Platin. Met. Rev.*, 2008, **52**, 38–45.
- 204 M. Moreno-Mañas, M. Pérez and R. Pleixats, *J. Org. Chem.*, 1996, **61**, 2346–2351.
- 205 P. B. Dzhevakov, M. A. Topchiy, D. A. Zharkova, O. S. Morozov, A. F. Asachenko and M. S. Nechaev, *Adv. Synth. Catal.*, 2016, **358**, 977–983.
- 206 F. Jiang, A. P. Guo, J. C. Xu, Q. D. You and X. L. Xu, *J. Med. Chem.*, 2018, **61**, 9513–9533.
- 207 R. J. Cox, D. J. Ritson, T. A. Dane, J. Berge, J. P. H. Charmant and A. Kantacha, *Chem. Commun.*, 2005, **1037**, 1037–1039.
- 208 A. P. Xu, H. H. Han, J. Lu, P. P. Yang, Y. J. Gao, H. W. An, D. Zhanng, L. Z. Li, J. P. Zhang, D. Wang, L. Wang and H. Wang, *Dye. Pigment.*, 2016, **125**, 392–398.
- 209 B. K. Hubbard and C. T. Walsh, *Angew. Chemie - Int. Ed.*, 2003, **42**, 730–765.

- 210 P. J. Belshaw and S. L. Schreiber, *J. Am. Chem. Soc.*, 1997, **119**, 1805–1806.
- 211 J. Grunewald and M. A. Marahiel, *Microbiol. Mol. Biol. Rev.*, 2006, **70**, 121–146.
- 212 G. Weber, K. Schörgendorfer, E. Schneider-Scherzer and E. Leitner, *Curr. Genet.*, 1994, **26**, 120–125.
- 213 S. Fadel, Y. Hajbi, M. Khouili, S. Lazar, F. Suzenet and G. Guillaumet, *Beilstein J. Org. Chem.*, 2014, **10**, 282–286.

8. Appendix

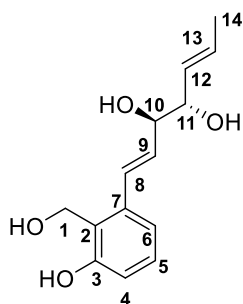
8.1 NMR Data for Chapter 2

Table 8.1 NMR data of compound **157** recorded at 500 MHz in CDCl₃.



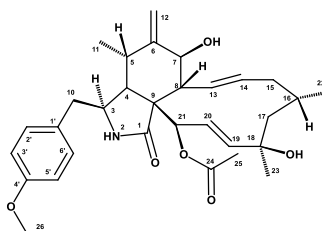
Position	δ_H	M	J_{H-H}/Hz	δ_C	HSQC	HMBC H to C	H-H cosy
1	-	-	-	204.4	-	-	-
2a	2.66	d	8.5	43.6	CH ₂	1,3	3
2b	3.00	d	8.5	-	-	-	-
3	3.99	m	-	70.2	CH	1,5	2,4
4	4.50	d	6.1	71.4	CH	3,8,7,5	2,3
5	-	-	-	145.9	-	-	-
6	6.87	d	6.3	116.4	CH	8,9	7
7	7.56	t	4.2,9.6	137.3	CH	8,5,9	6,8
8	7.07	d	6.8	119.8	CH	1,4,6,9	7
9	-	-	-	161.4	-	-	-
10	-	-	-	115.8	-	-	-

Table 8.2 NMR data of compound **158** recorded at 500 MHz in CDCl₃.



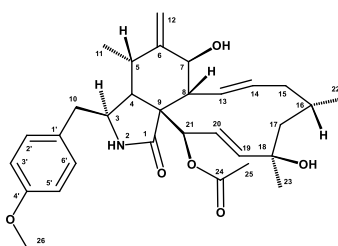
Position	δ_H	M	J_{H-H}/Hz	δ_C	HSQC	HMBC H to C	H-H cosy
1	4.54	Brs	-	54.7	CH ₂	2, 3, 7	-
2	-	-	-	125.23	-	-	-
3	-	-	-	156.12	-	-	-
4	6.71	d	7.8	114.38	CH	3, 5	-
5	7.26	t	3.0, 7.8	128.3	CH	7	-
6	6.88	d	7.8	116.8	CH	5, 7	-
7	-	-	-	138.82	-	-	-
8	6.9	d	7.3	127.9	CH	7	9
9	6.13	dd	7.3, 15.9	133.1	CH	7, 10	8, 10
10	3.97	t	6.4	75.5	CH	9, 11	9, 11
11	3.86	t	6.4	75.4	CH	10, 12	10, 12
12	5.57	m	-	125.6	CH	11	11
13	5.55	m	-	132.8	CH	12	14
14	1.65	d	5.9	18.1	CH ₃	12, 13	13

Table 8.3 NMR data of compound **65a** recorded at 500 MHz in CDCl₃.



Position	δ_H	M	J_{H-H}/Hz	δ_C	HSQC	HMBC H to C	H-H cosy
1	-	-	-	174.4	-	-	-
2	5.58	s	-	-	-	-	-
3	3.23	ddd	4.5, 9.6, 4.6	54.0	CH	1,4,5	4,5,10
4	2.13	dd	4.5, 4.9	50.3	CH	5,6,9,10,21	3,5
5	2.81	m	-	32.9	CH	1',3	3,4,12
6	-	-	-	147.9	-	-	-
7	3.85	dd	10.7, 1.4	69.7	CH	4',5,6,8,11,13	8,12
8	2.94	dd	10.7, 9.8	47.3	CH	1,7,19,21	7,13
9	-	-	-	51.9	-	-	-
10a	2.60	dd	13.6, 9.6	44.7	CH ₂	1',3,4	3,11
10b	2.80	dd	13.6, 4.5	-	-	-	-
11	1.00	d	6.5	14.1	CH ₃	4,5,6	10
12a	5.13	br.s	-	114.1	CH ₂	5,6,7	5,7
12b	5.37	br.s	-	-	-	-	-
13	5.76	ddd	9.6, 15.6, 1.4	127.1	CH	7,9,15,16,20	8,14
14	5.43	ddd	5.2, 15.6, 10.4	138.6	CH	8,16,21	5,13
15a	1.81	m	-	42.8	CH ₂	13,16,19	14,22
15b	2.08	m	-	-	-	-	-
16	1.81	m	-	28.4	CH	15	-
17a	1.58	dd	14.4, 2.9	53.8	CH ₂	18,19,22	-
17b	1.89	m	-	-	-	-	-
18	-	-	-	74.3	-	-	-
19	5.55	dd	17.2, 2.4	138.0	CH	9,20,21,23,24	21
20	5.89	dd	17.2, 2.1	125.8	CH	8,18,19,21	19,21
21	5.57	dd	2.1, 2.3	77.5	CH	19	-
22	1.07	d	6.3	26.4	CH ₃	15,16,17	15
23	1.37	s	-	31.3	CH ₃	17,18,19	-
1'	-	-	-	130.3	-	-	-
2' 6'	7.08	d	8.5	129.9	2×CH	3',4',10	3',5'
3' 5'	6.87	d	8.5	114.2	2×CH	6',4'	2',6'
4'	-	-	-	158.7	-	-	-
24	-	-	-	170.0	-	-	-
25	2.27	s	-	20.9	CH ₃	21,24	21
26	3.81	s	-	55.4	CH ₃	4'	-

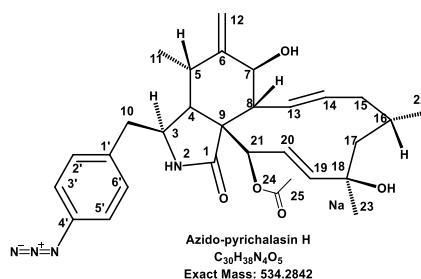
Table 8.4 NMR data of compound **65b** recorded at 500 MHz in CDCl₃.



Position	δ_H	M	J_{H-H}/Hz	δ_C	HSQC	HMBC H to C	H-H cosy
1	-	-	-	174.2	-	-	-
2	5.58	s	-	-	-	-	-
3	3.23	ddd	4.5, 9.6, 4.6	54.2	CH	1,4	4,10
4	2.13	dd	4.5, 4.8	50.3	CH	5,6,10,11	3,5
5	2.81	m	-	32.9	CH	6,11	4,10,11
6	-	-	-	147.9	-	-	-
7	3.84	dd	10.7, 1.4	69.7	CH	5,6,13	8,12
8	2.96	dd	10.7, 9.8	47.3	CH	1,6,7,19,21	7,13
9	-	-	-	51.8	-	-	-
10a	2.61	dd	13.6, 9.6	44.6	CH ₂	1',3,4	3,12
10b	2.80	dd	13.6, 4.5	-	-	-	-
11	1.01	d	6.7	14.4	CH ₃	4,5,6	5
12a	5.13	br.s	-	114.1	CH ₂	5,6,7	7,10
12b	5.37	br.s	-	-	-	-	-
13	5.76	ddd	9.5, 15.6, 1.7	127.1	CH	7,8,15,16	8,14
14	5.42	ddd	5.2, 15.6, 10.4	138.7	CH	8,15,16	13,16
15a	1.82	m	-	42.7	CH ₂	13,14,16,17	22
15b	2.08	m	-	-	-	-	-
16	1.81	m	-	28.4	CH	15	14
17a	1.57	dd	13.4, 2.8	53.7	CH ₂	15,18,19,23	19
17b	1.89	m	-	-	-	-	-
18	-	-	-	74.3	-	-	-
19	5.55	dd	17.3, 2.4	138.0	CH	8,9,20,21,23	17,23
20	5.87	dd	17.3, 2.1	125.9	CH	18,21	21
21	5.57	dd	2.1, 2.4	77.4	CH	8,9,19,20	20
22	1.07	d	6.5	26.5	CH ₃	15,16,17	15
23	1.37	s	-	31.5	CH ₃	16,17,18,19	19
1'	-	-	-	131.5	-	-	-
2' 6'	7.06	d	8.4	129.9	2×CH	3',4',10	3',5'
3' 5'	6.85	d	8.4	114.2	2×CH	6',4'	2',6',26
4'	-	-	-	160.1	-	-	-
24	-	-	-	170.1	-	-	-
25	2.27	s	-	21.1	CH ₃	21,24	-
26	3.81	s	-	55.3	CH ₃	4'	3',5'

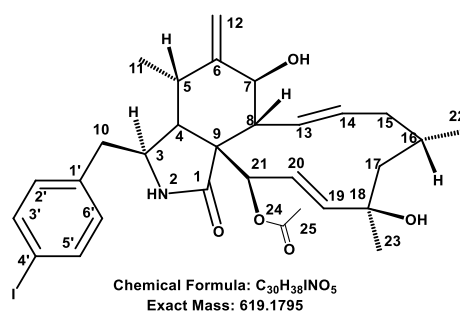
8.2 NMR Data for Chapter 4

Table 8.5 NMR data of compound **258** recorded at 500 MHz in CDCl₃.



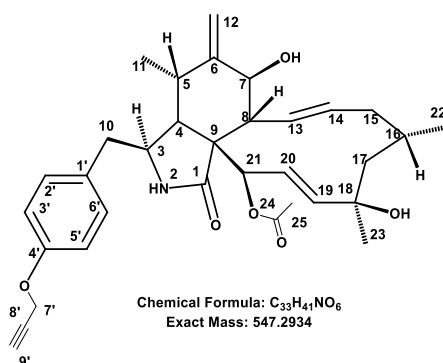
Position	δ_H	M	J_{H-H}/Hz	δ_C	HSQC	HMBC H to C	H-H COSY
1	-	-	-	174.2	-	-	-
2	5.47	brs	-	-	-	-	-
3	3.22	ddd	1.1, 5.0, 9.6	53.7	CH	1', 1, 4, 5	4, 5, 10
4	2.11	dd	3.8, 5.0	50.3	CH	1, 3, 5, 6, 10, 21	3, 5, 10
5	2.77	m	-	32.8	CH	1', 3	4, 11, 12
6	-	-	-	147.7	-	-	-
7	3.84	dd	1.4, 10.2	69.8	CH	5, 6, 8, 12, 13	8, 12
8	2.93	t	10.2	47.3	CH	7, 9, 13, 20, 21	7, 13
9	-	-	-	51.6	-	-	-
10a	2.65	dd	9.3, 13.6	44.9	CH ₂	1', 3	3, 4, 12
10b	2.84	dd	4.9, 13.6	-	-	-	-
11	0.96	d	6.7	14.1	CH ₃	4, 5, 6	5
12a	5.10	brs	-	114.2	CH ₂	5, 6, 7	5, 7, 11
12b	5.35	brs	-	-	-	-	-
13	5.74	ddd	1.4, 9.7, 15.5	127.1	CH	7, 8, 15	8, 14, 15
14	5.42	ddd	4.8, 10.2, 15.5	138.7	CH	9, 15	13, 15
15a	1.82	m	-	42.8	CH ₂	13, 14, 16, 17	13, 14,
15b	2.04	m	-	-	-	-	-
16	1.79	m	-	28.6	CH	13, 14, 17	22
17a	1.58	dd	3.1, 14.3	53.9	CH ₂	18, 19	-
17b	1.87	dd	3.2, 14.3	-	-	-	-
18	-	-	-	74.3	-	-	-
19	5.56	dd	3.8, 15.2	138.1	CH	-	20
20	5.83	m	-	125.8	CH	9, 18, 19	19
21	5.55	brs	-	77.3	CH	19, 20, 24	-
22	1.05	d	6.4	26.6	CH ₃	15, 16, 17	16
23	1.35	s	-	31.3	CH ₃	17, 18, 19	-
1'	-	-	-	133.8	-	-	-
2' 6'	7.14	d	8.4	130.4	2 x CH	3', 4', 5', 10	3', 5'
3' 5'	6.99	d	8.4	119.1	2 x CH	1', 4'	2', 6'
4'	-	-	-	138.9	-	-	-
24	-	-	-	170.2	-	-	-
25	2.25	s	-	21.0	CH ₃	21, 24	-

Table 8.6 NMR data of compound **257** recorded at 500 MHz in CDCl₃.



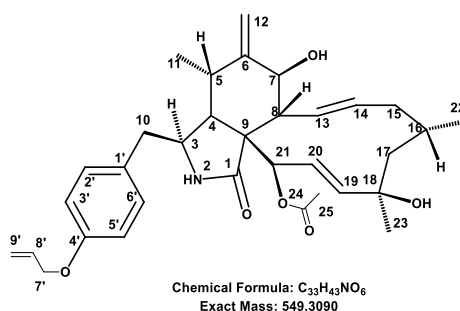
Position	δ_H	M	J_{H-H}/Hz	δ_C	HSQC	HMBC H to C	H-H COSY
1	-	-	-	174.3	-	-	-
2	5.46	brs	-	-	-	-	-
3	3.23	ddd	1.1, 4.8, 9.6	53.5	CH	1', 1, 4, 5	4, 5, 10
4	2.13	dd	3.6, 5.1	50.5	CH	1, 3, 5	3, 5, 10
5	2.80	m	-	32.7	CH	1', 3	4, 11, 12
6	-	-	-	147.9	-	-	-
7	3.84	dd	1.3, 10.8	69.7	CH	5, 6, 8, 12, 13	8, 12
8	2.95	dd	9.8, 10.8	47.2	CH	7, 9, 13, 20, 21	7, 13
9	-	-	-	51.7	-	-	-
10a	2.63	dd	9.5, 13.5	45.2	CH ₂	1', 3	3, 4, 12
10b	2.82	dd	4.8, 13.5	-	-	-	-
11	0.99	d	6.7	14.0	CH ₃	4, 5, 6	5
12a	5.12	brs	-	114.3	CH ₂	5, 6, 7	5, 7, 11
12b	5.37	brs	-	-	-	-	-
13	5.78	ddd	1.4, 9.6, 15.5	127.1	CH	7, 8, 15	8, 14, 15
14	5.43	ddd	4.8, 10.3, 15.5	138.8	CH	9, 15	13, 15
15a	1.82	m	-	42.7	CH ₂	13, 14, 16, 17	13, 14,
15b	2.05	m	-	-	-	-	-
16	1.81	m	-	28.5	CH	13, 14, 17	22
17a	1.60	m	-	53.9	CH ₂	18, 19	-
17b	1.89	m	-	-	-	-	-
18	-	-	-	74.4	-	-	-
19	5.55	brs	-	138.3	CH	-	20
20	5.88	dd	2.9, 16.4	126.0	CH	18, 19	19
21	5.58	brs	-	77.2	CH	8, 9, 19, 20, 23	-
22	1.07	d	6.5	26.4	CH ₃	15, 16, 17	16
23	1.37	s	-	31.1	CH ₃	17, 18, 19	-
1'	-	-	-	131.0	-	-	-
2' 6'	6.93	d	8.2	131.1	2 x CH	3', 4', 5', 10	3', 5'
3' 5'	7.67	d	8.2	138.0	2 x CH	1', 4'	2', 6'
4'	-	-	-	137.3	-	-	-
24	-	-	-	170.2	-	-	-
25	2.27	s	-	20.9	CH ₃	21, 24	-

Table 8.7 NMR data of compound **252** recorded at 500 MHz in CDCl₃.



Position	δ_H	M	J_{H-H}/Hz	δ_C	HSQC	HMBC H to C	H-H COSY
1	-	-	-	174.2	-	-	-
2	5.50	brs	-	-	-	-	-
3	3.24	ddd	1.1, 5.0, 9.6	53.8	CH	1', 1, 4, 5	4, 5, 10
4	2.13	dd	3.8, 5.0	50.5	CH	1, 3, 5, 6, 10, 21	3, 5, 10
5	2.80	m	-	32.9	CH	1', 3	4, 11, 12
6	-	-	-	147.8	-	-	-
7	3.85	dd	1.6, 10.7	69.6	CH	6, 12	8, 12
8	2.96	t	10.7	47.2	CH	7, 9, 13, 20, 21	7, 13
9	-	-	-	51.8	-	-	-
10a	2.61	dd	9.4, 13.6	44.8	CH ₂	1', 3	3, 4, 12
10b	2.82	dd	4.9, 13.6	-	-	-	-
11	1.03	d	6.7	14.1	CH ₃	4, 5, 6	5
12a	5.13	brs	-	114.2	CH ₂	5, 6, 7	5, 7, 11
12b	5.37	brs	-	-	-	-	-
13	5.76	ddd	1.4, 9.7, 15.4	127.1	CH	7, 8, 15	8, 14, 15
14	5.41	ddd	4.8, 10.1, 15.4	138.8	CH	9, 15	13, 15
15a	1.83	m	-	42.8	CH ₂	13, 14, 16, 17	13, 14,
15b	2.05	m	-	-	-	-	-
16	1.81	m	-	28.5	CH	13, 14, 17	22
17a	1.60	dd	3.0, 14.4	53.6	CH ₂	18, 19	-
17b	1.82	dd	3.0, 14.4	-	-	-	-
18	-	-	-	74.4	-	-	-
19	5.54	dd	2.3, 16.2	138.2	CH	-	20
20	5.89	dd	3.0, 16.2	126.0	CH	18, 19	19
21	5.58	dd	2.6, 3.0	77.5	CH	8, 9, 19, 20, 21, 23	-
22	1.07	d	6.3	26.4	CH ₃	15, 16, 17	16
23	1.37	s	-	31.2	CH ₃	17, 18, 19	-
1'	-	-	-	130.4	-	-	-
2' 6'	7.09	d	8.3	130.2	2 x CH	3', 4', 5', 10	3', 5'
3' 5'	6.96	d	8.3	115.4	2 x CH	1', 4'	2', 6'
4'	-	-	-	156.7	-	-	-
24	-	-	-	170.2	-	-	-
25	2.26	s	-	20.9	CH ₃	21, 24	-
7'	4.70	d	2.4	55.9	CH ₂	4', 8', 9'	9'
8'	-	-	-	78.5	-	-	-
9'	2.54	m	-	75.9	CH	7', 8'	7'

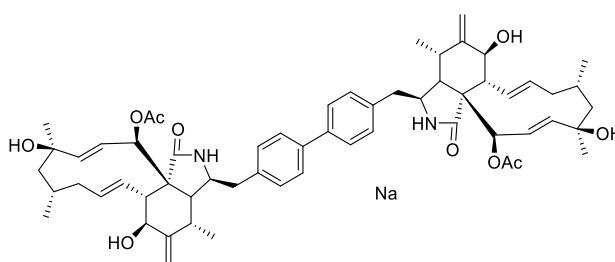
Table 8.8 NMR data of compound **251** recorded at 500 MHz in CDCl₃.



Position	δ_H	M	J_{H-H}/Hz	δ_C	HSQC	HMBC H to C	H-H COSY
1	-	-	-	174.4	-	-	-
2	5.50	brs	-	-	-	-	-
3	3.23	ddd	1.1, 5.0, 9.6	54.0	CH	1', 1, 4, 5	4, 5, 10
4	2.12	dd	3.8, 5.0	50.2	CH	1, 3, 5, 6, 10, 21	3, 5, 10
5	2.79	m	-	33.0	CH	1', 3	4, 11, 12
6	-	-	-	147.9	-	-	-
7	3.87	dd	1.6, 10.7	69.8	CH	6, 12	8, 12
8	2.96	t	10.7	47.3	CH	7, 9, 13, 20, 21	7, 13
9	-	-	-	51.9	-	-	-
10a	2.62	dd	9.4, 13.6	44.8	CH ₂	1', 3	3, 4, 12
10b	2.81	dd	4.9, 13.6	-	-	-	-
11	0.99	d	6.7	14.1	CH ₃	4, 5, 6	5
12a	5.13	brs	-	114.0	CH ₂	5, 6, 7	5, 7, 11
12b	5.37	brs	-	-	-	-	-
13	5.75	ddd	1.4, 9.7, 15.4	127.1	CH	7, 8, 15	8, 14, 15
14	5.42	ddd	4.8, 10.1, 15.4	138.7	CH	9, 15	13, 15
15a	1.84	m	-	42.8	CH ₂	13, 14, 16, 17	13, 14,
15b	2.05	m	-	-	-	-	-
16	1.81	m	-	28.6	CH	13, 14, 17	22
17a	1.60	dd	3.0, 14.4	53.7	CH ₂	18, 19	-
17b	1.89	m	3.0, 14.4	-	-	-	-
18	-	-	-	74.4	-	-	-
19	5.57	dd	2.3, 16.2	138.1	CH	-	20
20	5.89	dd	3.0, 16.2	126.0	CH	18, 19	19
21	5.57	dd	2.6, 3.0	77.4	CH	8, 9, 19, 20, 21 23	-
22	1.07	d	6.3	26.6	CH ₃	15, 16, 17	16
23	1.37	s	-	31.2	CH ₃	17, 18, 19	-
1'	-	-	-	129.5	-	-	-
2' 6'	7.07	d	8.3	130.0	2 x CH	3', 4', 5', 10	3', 5'
3' 5'	6.88	d	8.3	115.1	2 x CH	1', 4'	2', 6'
4'	-	-	-	157.7	-	-	-
24	-	-	-	170.1	-	-	-
25	2.27	s	-	20.9	CH ₃	21, 24	-
7'	4.54	t	1.6	68.8	CH ₂	4', 8', 9'	8', 9'
8'	6.06	dddd	5.3, 10.5, 15.8, 22.6	133.2	CH	7'	7', 9'
9a'	5.30	dd	1.6, 3.2	117.6	CH ₂	7', 8'	7', 8'
9b'	5.41	m	-	-	-	-	-

8.3 NMR Data for Chapter 5

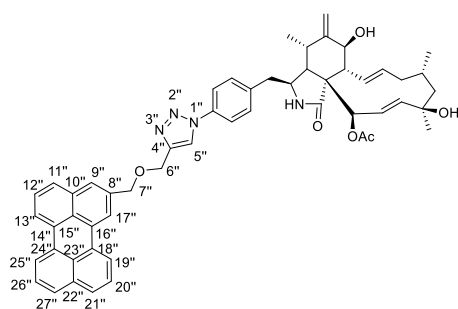
Table 8.9 NMR data of compound **318** recorded at 500 MHz in CDCl₃.



Chemical Formula: C₆₀H₇₆N₂O₁₀
Exact Mass: 984.5500

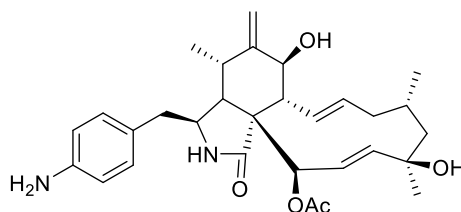
Position	δ_H	M	J_{H-H}/Hz	δ_C	HSQC	HMBC H to C	H-H COSY
1	-	-	-	174.3	-	-	-
2	5.48	brs	-	-	-	-	3
3	3.29	ddd	0.9, 9.6, 4.6	53.4	CH	-	2
4	2.16	dd	4.6, 8.9	50.3	CH	9, 21	5
5	2.81	m	-	32.5	CH	-	4, 11, 12
6	-	-	-	148.1	-	-	-
7	3.83	d	10.8	69.3	CH	6, 12, 13	8, 12
8	2.95	dd	10.2, 10.8	46.9	CH	1, 3, 7, 13, 14	7, 13
9	-	-	-	51.7	-	-	-
10a	2.68	dd	13.5, 9.9	44.9	CH ₂	1', 2', 6', 3	-
10b	2.92	dd	13.5, 4.4	-	-	-	-
11	1.05	d	6.5	13.9	CH ₃	4, 5, 6	5
12a	5.13	brs	-	113.8	CH ₂	5, 6, 7	5, 7
12b	5.37	brs	-	-	-	-	-
13	5.75	ddd	9.7, 15.5, 1.3	126.7	CH	8, 9	8, 14
14	5.41	ddd	15.5, 4.7, 10.0	138.4	CH	-	13, 15
15a	1.80	m	-	42.5	CH ₂	13, 14, 16	14, 17
15b	2.04	m	-	-	-	-	-
16	1.79	m	-	28.2	CH	-	17
17a	1.56	m	-	53.5	CH ₂	18, 19	15, 16
17b	1.88	dd	3.0, 14.4	-	-	-	-
18	-	-	-	74.6	-	-	-
19	5.57	dd	16.6, 2.4	137.8	CH	8, 9, 20	20
20	5.89	dd	16.6, 2.7	125.6	CH	18, 21	21
21	5.58	dd	2.5, 2.7	77.1	CH	19, 20	20
22	1.05	d	6.5	26.2	CH ₃	15, 16, 17	15
23	1.37	s	-	30.8	CH ₃	16, 17, 18, 19	-
1'	-	-	-	129.7	-	-	-
2' 6'	7.22	d	8.1	129.1	2 x CH	3', 4', 5', 10	3', 5'
3' 5'	7.51	d	8.1	127.1	2 x CH	2', 6', 4'	2', 6'
4'	-	-	-	139.6	-	-	-
24	-	-	-	170.3	-	-	-
25	2.26	s	-	20.6	CH ₃	24	-

Table 8.10 NMR data of compound **308** recorded at 500 MHz in CDCl₃.



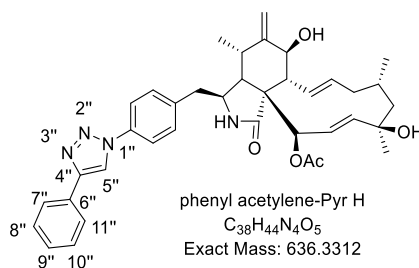
Position	δ_H	M	J_{H-H}/Hz	δ_C	HSQC	HMBC H to C	H-H COSY
1	-	-	-	174.3	-	-	-
3	3.29	m	-	52.9	CH	1', 1, 4, 5	4, 5, 10
4	2.16	dd	3.7, 5.0	49.9	CH	1, 3, 5, 6, 10	3, 5, 10
5	2.81	m	-	32.4	CH	1', 3	4, 11, 12
6	-	-	-	147.7	-	-	-
7	3.88	dd	1.3, 10.8	69.4	CH	6, 12	8, 12
8	2.98	m	-	46.8	CH	7, 9, 13, 20, 21	7, 13
9	-	-	-	51.6	-	-	-
10a	2.74	m	-	44.7	CH ₂	1', 3	3, 4, 12
10b	2.90	m	-	-	-	-	-
11	0.99	d	6.6	13.7	CH ₃	4, 5, 6	5
12a	5.14	brs	-	113.8	CH ₂	5, 6, 7	5, 7, 11
12b	5.39	brs	-	-	-	-	-
13	5.76	ddd	1.4, 9.7, 15.4	126.7	CH	7, 8, 15	8, 14, 15
14	5.42	ddd	4.8, 10.1, 15.4	138.4	CH	9, 15	13, 15
15a	1.83	m	-	42.3	CH ₂	13, 14, 16, 17	13, 14,
15b	2.06	m	-	-	-	-	-
16	1.82	m	-	28.1	CH	13, 14, 17	22
17a	1.61	m	-	53.3	CH ₂	18, 19	-
17b	1.90	m	-	-	-	-	-
18	-	-	-	74.4	-	-	-
19	5.56	brs	-	137.9	CH	-	20
20	5.85	dd	2.2, 17.0	125.4	CH	18, 19	19
21	5.58	brs	-	76.8	CH	8, 9, 19, 20, 23	-
22	1.07	d	6.4	26.1	CH ₃	15, 16, 17	16
23	1.38	s	-	30.8	CH ₃	17, 18, 19	-
1'	-	-	-	138.0	-	-	-
2' 6'	7.27	d	8.5	130.3	2 x CH	3', 4', 5', 10	3', 5'
3' 5'	7.65	d	8.5	120.6	2 x CH	1', 4'	2', 6'
4'	-	-	-	136.0	-	-	-
24	-	-	-	170.2	-	-	-
25	2.28	s	-	20.6	CH ₃	24	-
4''	-	-	-	146.1	-	-	-
5''	7.87	s	-	120.4	CH	4''	-
6''	4.90	s	-	63.4	CH ₂	4'', 5'', 7''	-
7''	5.09	s	-	71.1	CH ₂	6'', 8'', 17''	-
8''	-	-	-	133.0	-	-	-
9''	8.18	s	-	119.2	CH	8'', 10''	-
10''	-	-	-	129.1	-	-	-
11''	8.00	dd	0.9, 8.3	123.2	CH	10'', 13'', 15''	12'', 13''
12''20''26''	7.56	m	-	127.3	3 x CH	13'', 19'', 25'', 16'', 22''	11'', 13''
13''19''25''	8.23	dd	1.0, 7.6	120.0	3 x CH	14'', 15'', 23''	11'', 12''
14''	-	-	-	128.3	-	-	-
15''	-	-	-	132.8	-	-	-
16''	-	-	-	131.1	-	-	-
17''	7.72	d	8.2	127.6	CH	8'', 9'', 16'', 18''	21''
18''	-	-	-	128.5	-	-	-
21''27''	7.52	dd	1.6, 7.8	126.2	2 x CH	19'', 22''	17''
22''	-	-	-	134.7	-	-	-
23''	-	-	-	135.1	-	-	-
24''	-	-	-	132.0	-	-	-

Table 8.11 NMR data of compound **305** recorded at 500 MHz in CDCl₃.



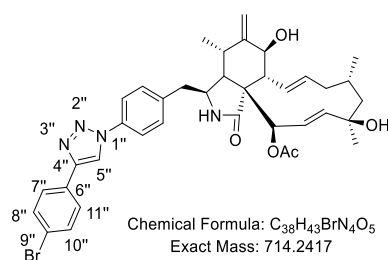
Position	δ_H	M	J_{H-H}/Hz	δ_C	HSQC	HMBC H to C	H-H COSY
1	-	-	-	174.1	-	-	-
2	5.56	brs	-	-	-	-	-
3	3.20	ddd	1.1, 4.7, 9.4	53.9	CH	1', 1, 4, 5	4, 5, 10
4	2.11	dd	4.4, 4.7	50.2	CH	1, 3, 5, 6, 10, 21	3, 5, 10
5	2.80	m	-	32.9	CH	1', 3	4, 11, 12
6	-	-	-	148.1	-	-	-
7	3.86	dd	1.4, 10.8	69.6	CH	6, 12	8, 12
8	2.96	dd	9.8, 10.8	47.2	CH	7, 9, 13, 20, 21	7, 13
9	-	-	-	51.8	-	-	-
10a	2.56	dd	9.8, 13.7	44.8	CH ₂	1', 3	3, 4, 12
10b	2.75	dd	4.6, 13.7	-	-	-	-
11	1.02	d	6.7	14.1	CH ₃	4, 5, 6	5
12a	5.13	brs	-	113.9	CH ₂	5, 6, 7	5, 7, 11
12b	5.37	brs	-	-	-	-	-
13	5.76	ddd	1.3, 9.6, 15.4	127.1	CH	7, 8, 15	8, 14, 15
14	5.40	ddd	4.9, 10.2, 15.4	138.7	CH	9, 15	13, 15
15a	1.82	m	-	42.6	CH ₂	13, 14, 16, 17	13, 14,
15b	2.06	m	-	-	-	-	-
16	1.81	m	-	28.4	CH	13, 14, 17	22
17a	1.58	dd	2.9, 14.3	53.8	CH ₂	18, 19	-
17b	1.89	m	3.1, 14.3	-	-	-	-
18	-	-	-	74.4	-	-	-
19	5.53	dd	2.3, 17.2	138.0	CH	-	20
20	5.89	dd	2.1, 17.2	126.0	CH	18, 19	19
21	5.58	m	-	77.2	CH	8, 9, 19, 20, 21, 23	-
22	1.06	d	6.3	26.5	CH ₃	15, 16, 17	16
23	1.37	s	-	31.2	CH ₃	17, 18, 19	-
1'	-	-	-	130.0	-	-	-
2' 6'	6.95	d	8.3	129.8	2 x CH	3', 4', 5', 10	3', 5'
3' 5'	6.65	d	8.3	115.3	2 x CH	1', 4'	2', 6'
4'	-	-	-	145.3	-	-	-
24	-	-	-	170.1	-	-	-
25	2.25	s	-	20.9	CH ₃	21, 24	-

Table 8.12 NMR data of compound **291** recorded at 500 MHz in CDCl₃.



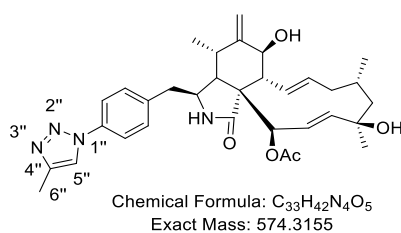
Position	δ_H	M	J_{H-H}/Hz	δ_C	HSQC	HMBC H to C	H-H COSY
1	-	-	-	174.2	-	-	-
2	5.56	brs	-	-	-	-	-
3	3.32	m	-	53.3	CH	1', 1, 4, 5	4, 5, 10
4	2.17	dd	3.8, 5.0	50.2	CH	1, 3, 5, 6, 10	3, 5, 10
5	2.80	m	-	32.7	CH	1', 3	4, 11, 12
6	-	-	-	147.7	-	-	-
7	3.85	dd	1.6, 10.7	69.7	CH	6, 12	8, 12
8	2.95	m	-	47.1	CH	7, 9, 13, 20, 21	7, 13
9	-	-	-	51.6	-	-	-
10a	2.65	m	-	44.9	CH ₂	1', 3	3, 4, 12
10b	2.81	m	-	-	-	-	-
11	0.99	d	6.7	13.9	CH ₃	4, 5, 6	5
12a	5.13	brs	-	114.2	CH ₂	5, 6, 7	5, 7, 11
12b	5.37	brs	-	-	-	-	-
13	5.74	ddd	1.4, 9.7, 15.4	126.9	CH	7, 8, 15	8, 14, 15
14	5.44	ddd	4.8, 10.1, 15.4	138.6	CH	9, 15	13, 15
15a	1.82	m	-	42.8	CH ₂	13, 14, 16, 17	13, 14,
15b	2.05	m	-	-	-	-	-
16	1.79	m	-	28.3	CH	13, 14, 17	22
17a	1.58	dd	2.9, 14.4	53.9	CH ₂	18, 19	-
17b	1.89	m	-	-	-	-	-
18	-	-	-	74.4	-	-	-
19	5.58	brs	2.3, 16.2	138.1	CH	-	20
20	5.87	dd	3.0, 16.2	125.6	CH	18, 19	19
21	5.59	brs	-	77.0	CH	8, 9, 19, 20, 23	-
22	1.06	d	6.5	26.5	CH ₃	15, 16, 17	16
23	1.35	s	-	31.1	CH ₃	17, 18, 19	-
1'	-	-	-	136.3	-	-	-
2' 6'	7.34	d	8.5	130.3	2 x CH	3', 4', 5', 10	3', 5'
3' 5'	7.78	d	8.5	120.8	2 x CH	1', 4'	2', 6'
4'	-	-	-	138.1	-	-	-
24	-	-	-	170.2	-	-	-
25	2.26	s	-	20.9	CH ₃	24	-
4''	-	-	-	148.5	-	-	-
5''	8.18	s	-	117.0	CH	4''	-
6''	-	-	-	129.6	-	-	-
7'' 11''	7.92	dd	1.4, 8.4	125.7	2 x CH	4'', 9''	8'', 10''
9''	7.40	dd	8.4, 18.6	128.5	CH	7'', 11''	8'', 10''
8'' 10''	7.47	dd	7.4, 8.4	128.7	2 x CH	6''	7'', 11''

Table 8.13 NMR data of compound **292** recorded at 500 MHz in CDCl₃.



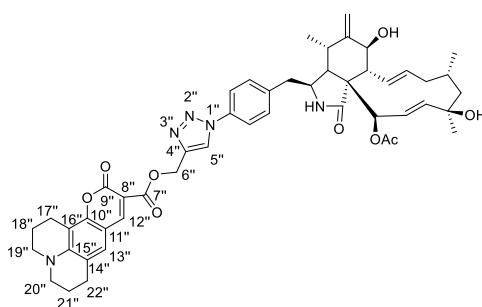
Position	δ_H	M	J_{H-H}/Hz	δ_C	HSQC	HMBC H to C	H-H COSY
1	-	-	-	174.4	-	-	-
2	5.56	brs	-	-	-	-	-
3	3.33	m	-	53.4	CH	1', 1, 4, 5	4, 5, 10
4	2.18	dd	3.8, 5.0	50.3	CH	1, 3, 5, 6, 10	3, 5, 10
5	2.81	m	-	32.7	CH	1', 3	4, 11, 12
6	-	-	-	147.6	-	-	-
7	3.88	dd	1.6, 10.7	69.9	CH	6, 12	8, 12
8	2.95	m	-	47.2	CH	7, 9, 13, 20, 21	7, 13
9	-	-	-	51.7	-	-	-
10a	2.80	m	-	44.9	CH ₂	1', 3	3, 4, 12
10b	2.97	m	-	-	-	-	-
11	1.02	d	6.7	14.1	CH ₃	4, 5, 6	5
12a	5.15	brs	-	114.3	CH ₂	5, 6, 7	5, 7, 11
12b	5.39	brs	-	-	-	-	-
13	5.76	ddd	1.4, 9.7, 15.4	127.0	CH	7, 8, 15	8, 14, 15
14	5.41	ddd	4.8, 10.1, 15.4	138.7	CH	9, 15	13, 15
15a	1.83	m	-	42.7	CH ₂	13, 14, 16, 17	13, 14,
15b	2.06	m	-	-	-	-	-
16	1.81	m	-	28.5	CH	13, 14, 17	22
17a	1.61	dd	2.9, 14.4	53.7	CH ₂	18, 19	-
17b	1.89	dd	3.0, 14.4	-	-	-	-
18	-	-	-	74.4	-	-	-
19	5.58	brs	-	138.3	CH	-	20
20	5.88	dd	3.0, 16.2	125.7	CH	18, 19	19
21	5.58	brs	-	77.1	CH	8, 9, 19, 20, 23	-
22	1.07	d	6.5	26.5	CH ₃	15, 16, 17	16
23	1.35	s	-	31.2	CH ₃	17, 18, 19	-
1'	-	-	-	136.1	-	-	-
2' 6'	7.38	d	8.5	130.5	2 x CH	3', 4', 5', 10	3', 5'
3' 5'	7.78	d	8.5	121.0	2 x CH	1', 4'	2', 6'
4'	-	-	-	120.9	-	-	-
24	-	-	-	170.2	-	-	-
25	2.28	s	-	20.9	CH ₃	24	-
4''	-	-	-	147.5	-	-	-
5''	8.20	s	-	117.4	CH	4''	-
6''	-	-	-	129.1	-	-	-
7'' 11''	7.82	dd	1.4, 8.4	127.4	2 x CH	4'', 9''	8'', 10''
8'' 10''	7.61	dd	7.4, 8.4	132.0	2 x CH	6''	7'', 11''

Table 8.14 NMR data of compound **290** recorded at 500 MHz in CDCl₃.



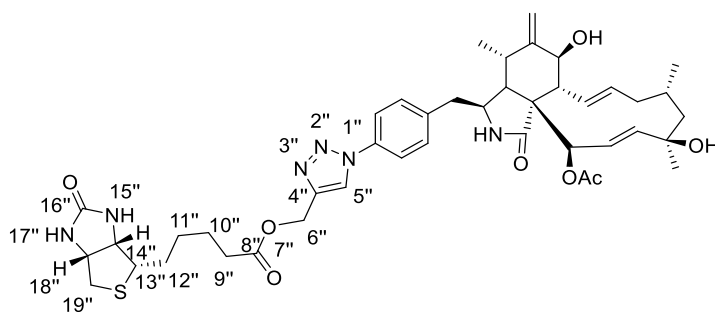
Position	δ_H	M	J_{H-H}/Hz	δ_C	HSQC	HMBC H to C	H-H COSY
1	-	-	-	174.3	-	-	-
2	5.56	brs	-	-	-	-	-
3	3.31	m	-	53.5	CH	1', 1, 4, 5	4, 5, 10
4	2.18	dd	3.8, 5.0	50.2	CH	1, 3, 5, 6, 10	3, 5, 10
5	2.80	m	-	32.7	CH	1', 3	4, 11, 12
6	-	-	-	147.7	-	-	-
7	3.87	dd	1.3, 10.8	70.0	CH	6, 12	8, 12
8	2.96	m	-	47.3	CH	7, 9, 13, 20, 21	7, 13
9	-	-	-	51.7	-	-	-
10a	2.77	m	-	45.1	CH ₂	1', 3	3, 4, 12
10b	2.95	m	-	-	-	-	-
11	1.00	d	6.7	14.1	CH ₃	4, 5, 6	5
12a	5.14	brs	-	114.4	CH ₂	5, 6, 7	5, 7, 11
12b	5.38	brs	-	-	-	-	-
13	5.78	ddd	1.4, 9.7, 15.4	127.0	CH	7, 8, 15	8, 14, 15
14	5.43	ddd	4.8, 10.1, 15.4	138.8	CH	9, 15	13, 15
15a	1.83	m	-	42.7	CH ₂	13, 14, 16, 17	13, 14,
15b	2.06	m	-	-	-	-	-
16	1.81	m	-	28.6	CH	13, 14, 17	22
17a	1.61	m	-	53.8	CH ₂	18, 19	-
17b	1.92	dd	3.0, 14.4	-	-	-	-
18	-	-	-	74.3	-	-	-
19	5.59	brs	-	138.2	CH	-	20
20	5.85	dd	3.0, 16.2	125.9	CH	18, 19	19
21	5.58	brs	-	77.2	CH	8, 9, 19, 20, 23	-
22	1.07	d	6.5	26.6	CH ₃	15, 16, 17	16
23	1.37	s	-	31.2	CH ₃	17, 18, 19	-
1'	-	-	-	137.8	-	-	-
2' 6'	7.33	d	8.5	130.4	2 x CH	3', 4', 5', 10	3', 5'
3' 5'	7.70	d	8.5	120.8	2 x CH	1', 4'	2', 6'
4'	-	-	-	120.9	-	-	-
24	-	-	-	170.2	-	-	-
25	2.28	s	-	21.0	CH ₃	24	-
4''	-	-	-	144.2	-	-	-
5''	7.73	s	-	118.9	CH	4''	-
6''	2.47	s	-	11.0	CH ₃	4'', 5''	-

Table 8.15 NMR data of compound **310** recorded at 500 MHz in CDCl₃.



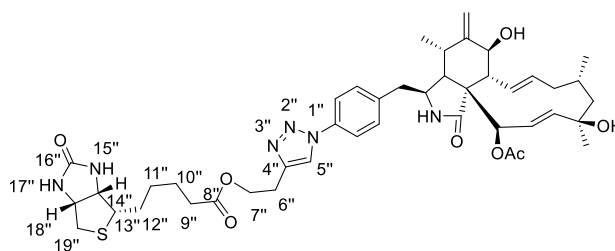
Position	δ_H	M	J_{H-H}/Hz	δ_C	HSQC	HMBC H to C	H-H COSY
1	-	-	-	174.3	-	-	-
3	3.31	m	-	53.3	CH	1', 1, 4, 5	4, 5, 10
4	2.17	dd	3.7, 5.0	50.1	CH	1, 3, 5, 6, 10	3, 5, 10
5	2.79	m	-	32.7	CH	1', 3	4, 11, 12
6	-	-	-	148.9	-	-	-
7	3.86	dd	1.3, 10.8	69.8	CH	6, 12	8, 12
8	2.96	m	-	47.2	CH	7, 9, 13, 20, 21	7, 13
9	-	-	-	51.6	-	-	-
10a	2.77	m	-	45.0	CH ₂	1', 3	3, 4, 12
10b	2.90	m	-	-	-	-	-
11	0.94	d	6.6	14.0	CH ₃	4, 5, 6	5
12a	5.13	brs	-	114.2	CH ₂	5, 6, 7	5, 7, 11
12b	5.37	brs	-	-	-	-	-
13	5.76	ddd	1.4, 9.7, 15.4	127.1	CH	7, 8, 15	8, 14, 15
14	5.41	ddd	4.8, 10.1, 15.4	138.6	CH	9, 15	13, 15
15a	1.82	m	-	42.7	CH ₂	13, 14, 16, 17	13, 14,
15b	2.05	m	-	-	-	-	-
16	1.81	m	-	28.4	CH	13, 14, 17	22
17a	1.58	m	-	53.8	CH ₂	18, 19	-
17b	1.88	m	-	-	-	-	-
18	-	-	-	74.4	-	-	-
19	5.59	brs	-	138.2	CH	-	20
20	5.85	dd	2.2, 17.0	125.8	CH	18, 19	19
21	5.56	brs	-	77.2	CH	8, 9, 19, 20, 23	-
22	1.07	d	6.4	26.5	CH ₃	15, 16, 17	16
23	1.37	s	-	31.2	CH ₃	17, 18, 19	-
1'	-	-	-	138.0	-	-	-
2' 6'	7.33	d	8.5	130.3	2 x CH	3', 4', 5', 10	3', 5'
3' 5'	7.73	d	8.5	121.0	2 x CH	1', 4'	2', 6'
4'	-	-	-	136.0	-	-	-
24	-	-	-	170.2	-	-	-
25	2.27	s	-	20.9	CH ₃	24	-
4''	-	-	-	144.2	-	-	-
5''	8.27	s	-	122.1	CH	4''	-
6''	5.53	s	-	58.0	CH ₂	4'', 5'', 7''	-
7''	-	-	-	164.0	-	-	-
8''	-	-	-	106.1	-	-	-
9''	-	-	-	158.7	-	-	-
10''	-	-	-	153.6	-	-	-
11''	-	-	-	107.3	-	-	-
12''	8.38	m	-	149.6	CH	7'', 8'', 9'', 10'', 13'',	-
13''	6.94	s	-	127.0	CH	10'', 11'', 12'', 22''	-
14''	-	-	-	119.4	-	-	-
15''	-	-	-	149.0	-	-	-
16''	-	-	-	105.8	-	-	-
17''	2.89	d	8.2	20.0	CH ₂	10'', 15'', 16'', 18'', 19''	18''
18''21''	1.98	m	-	20.4	2 x CH ₂	17'', 19'', 16'', 22''	17'', 20'', 22''
19''20''	3.35	m	-	49.8	2 x CH ₂	15'', 18'', 22''	21''
22''	2.77	m	-	27.4	CH ₂	13'', 14'', 15'', 19'', 21'',	21''

Table 8.16 NMR data of compound **298** recorded at 500 MHz in CDCl₃.



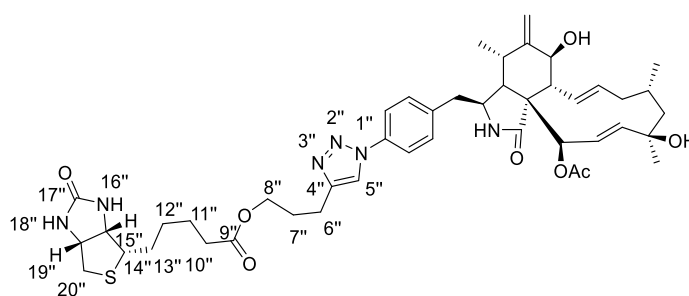
Position	δ_H	M	J_{H-H}/Hz	δ_C	HSQC	HMBC H to C	H-H COSY
1	-	-	-	174.8	-	-	-
3	3.33	m	-	53.7	CH	1', 4, 5	4, 5, 10
4	2.15	t	4.3	50.5	CH	3, 5	3, 5, 10
5	2.82	m	-	32.9	CH	1', 3	4, 11, 12
6	-	-	-	147.9	-	-	-
7	3.86	d	10.8	69.6	CH	5, 6, 8, 12, 13	8, 12
8	2.97	m	-	47.2	CH	1, 7, 9, 13, 21	7, 13
9	-	-	-	51.9	-	-	-
10a	2.74	m	-	45.1	CH ₂	1', 3	3, 4, 12
10b	2.94	dd	4.8, 13.5	-	-	-	-
11	1.07	d	6.7	14.4	CH ₃	4, 5, 6	5
12a	5.15	brs	-	114.2	CH ₂	5, 6, 7	5, 7, 11
12b	5.39	brs	-	-	-	-	-
13	5.74	ddd	1.4, 9.6, 15.5	127.0	CH	7, 8, 15	8, 14, 15
14	5.42	ddd	4.8, 10.3, 15.5	138.8	CH	9, 15	13, 15
15a	1.82	m	-	42.8	CH ₂	13, 14, 16, 17	13, 14,
15b	2.06	m	-	-	-	-	-
16	1.82	m	-	28.5	CH	13, 14, 17	22
17a	1.61	m	-	53.8	CH ₂	18, 19	-
17b	1.91	m	-	-	-	-	-
18	-	-	-	74.3	-	-	-
19	5.58	brs	-	138.2	CH	-	20
20	5.88	dd	2.7, 16.5	125.9	CH	18, 19	19
21	5.52	brs	-	77.4	CH	8, 9, 19, 20, 23	-
22	1.06	d	6.5	26.5	CH ₃	15, 16, 17	16
23	1.35	s	-	31.2	CH ₃	17, 18, 19	-
1'	-	-	-	130.6	-	-	-
2' 6'	7.33	d	8.2	130.6	2 x CH	3', 4', 5', 10	3', 5'
3' 5'	7.75	d	8.2	120.9	2 x CH	1', 4'	2', 6'
4'	-	-	-	138.2	-	-	-
24	-	-	-	170.2	-	-	-
25	2.27	s	-	21.0	CH ₃	21, 24	-
4''	-	-	-	145.1	-	-	-
5''	8.16	s	-	119.6	CH	4''	-
6''	5.34	s	-	25.5	CH ₂	4'', 5'', 7''	7''
8''	-	-	-	173.5	-	-	-
9''	2.43	t	6.9	33.6	CH ₂	8'', 10''	10'', 12''
10''	1.67	m	-	28.3	CH ₂	8'', 9'', 11'', 12'', 13''	9'', 11''
11''	1.48	m	-	28.1	CH ₂	9'', 10'', 12'', 13''	10''
12''	1.73	m	-	24.6	CH ₂	11'', 13'', 14''	9''
13''	3.15	m	-	55.3	CH	11'', 14''	14''
14''	4.25	dd	4.4, 7.8	61.6	CH	16''	13'', 18''
16''	-	-	-	163.3	-	-	-
18''	4.48	m	-	60.1	CH	13'', 16''	14'', 19''
19a''	2.69	m	-	40.6	CH ₂	13'', 18''	18''
19b''	2.94	m	-	-	-	-	-

Table 8.17 NMR data of compound **299** recorded at 500 MHz in CDCl₃.



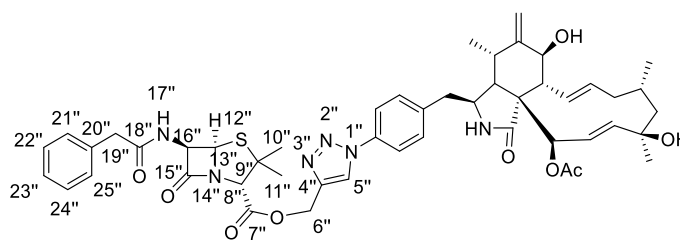
Position	δ_H	M	J_{H-H}/Hz	δ_C	HSQC	HMBC H to C	H-H COSY
1	-	-	-	175.2	-	-	-
3	3.33	m	-	53.9	CH	1', 4, 5	4, 5, 10
4	2.13	m	-	50.4	CH	3, 5	3, 5, 10
5	2.83	m	-	32.9	CH	1', 3	4, 11, 12
6	-	-	-	147.7	-	-	-
7	3.87	dd	1.7, 11.0	69.5	CH	5, 6, 8, 12, 13	8, 12
8	2.97	dd	5.0, 11.0	47.1	CH	1, 7, 9, 13, 21	7, 13
9	-	-	-	52.4	-	-	-
10a	2.73	dd	1.1, 12.9	45.1	CH ₂	1', 3	3, 4, 12
10b	2.93	dd	5.0, 12.9	-	-	-	-
11	1.10	d	6.7	14.3	CH ₃	4, 5, 6	5
12a	5.15	brs	-	114.1	CH ₂	5, 6, 7	5, 7, 11
12b	5.40	brs	-	-	-	-	-
13	5.74	m	-	126.8	CH	7, 8, 15	8, 14, 15
14	5.44	m	-	138.8	CH	9, 15	13, 15
15a	1.80	m	-	42.7	CH ₂	13, 14, 16, 17	13, 14,
15b	2.06	m	-	-	-	-	-
16	1.80	m	-	28.6	CH	13, 14, 17	22
17a	1.61	m	-	53.6	CH ₂	18, 19	-
17b	1.88	m	-	-	-	-	-
18	-	-	-	74.2	-	-	-
19	5.55	brs	-	138.2	CH	-	20
20	5.87	dd	2.9, 16.4	125.7	CH	18, 19	19
21	5.49	brs	-	77.3	CH	8, 9, 19, 20, 23	-
22	1.07	d	6.5	26.5	CH ₃	15, 16, 17	16
23	1.35	s	-	31.2	CH ₃	17, 18, 19	-
1'	-	-	-	130.7	-	-	-
2' 6'	7.34	d	8.2	130.6	2 x CH	3', 4', 5', 10	3', 5'
3' 5'	7.74	d	8.2	120.6	2 x CH	1', 4'	2', 6'
4'	-	-	-	137.9	-	-	-
24	-	-	-	170.1	-	-	-
25	2.26	s	-	20.9	CH ₃	21, 24	-
4''	-	-	-	145.1	-	-	-
5''	7.93	s	-	119.6	CH	4''	-
6''	3.18	m	-	25.6	CH ₂	4'', 5'', 7''	7''
7''	4.21	m	-	61.7	CH ₂	6'', 8''	6''
8''	-	-	-	173.4	-	-	-
9''	2.39	m	-	33.7	CH ₂	8'', 10''	10'', 12''
10''	1.71	m	-	28.2	CH ₂	8'', 9'', 11'', 12'', 13''	9'', 11''
11''	1.46	m	-	28.1	CH ₂	9'', 10'', 12'', 13''	10''
12''	1.69	m	-	24.6	CH ₂	11'', 13'', 14''	9''
13''	3.16	m	-	55.2	CH	11'', 14''	14''
14''	4.34	m	-	61.8	CH	16''	13'', 18''
16''	-	-	-	163.2	-	-	-
18''	4.53	m	-	60.0	CH	13'', 16''	14'', 19''
19a''	2.72	m	-	40.5	CH ₂	13'', 18''	18''
19b''	2.95	m	-	-	-	-	-

Table 8.18 NMR data of compound **300** recorded at 500 MHz in CDCl₃.



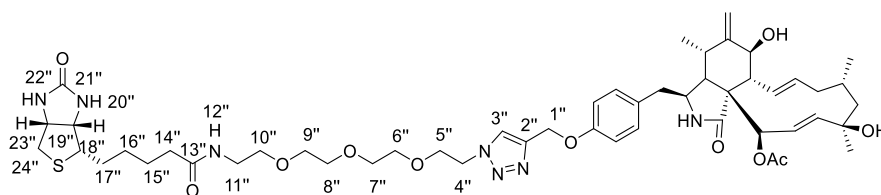
Position	δ_H	M	J_{H-H}/Hz	δ_C	HSQC	HMBC H to C	H-H COSY
1	-	-	-	175.2	-	-	-
3	3.33	ddd	0.9, 4.8, 9.6	53.7	CH	1', 4, 5	4, 5, 10
4	2.15	m	-	50.2	CH	3, 5	3, 5, 10
5	2.81	m	-	32.8	CH	1', 3	4, 11, 12
6	-	-	-	147.7	-	-	-
7	3.88	dd	1.5, 10.8	69.7	CH	5, 6, 8, 12, 13	8, 12
8	2.94	m	-	47.2	CH	1, 7, 9, 13, 21	7, 13
9	-	-	-	52.4	-	-	-
10a	2.75	m	-	45.0	CH ₂	1', 3	3, 4, 12
10b	2.93	m	-	-	-	-	-
11	1.04	d	6.6	14.2	CH ₃	4, 5, 6	5
12a	5.14	brs	-	114.2	CH ₂	5, 6, 7	5, 7, 11
12b	5.39	brs	-	-	-	-	-
13	5.74	ddd	1.4, 9.6, 15.5	127.1	CH	7, 8, 15	8, 14, 15
14	5.45	ddd	4.8, 10.3, 15.5	138.7	CH	9, 15	13, 15
15a	1.82	m	-	42.6	CH ₂	13, 14, 16, 17	13, 14,
15b	2.06	m	-	-	-	-	-
16	1.80	m	-	28.4	CH	13, 14, 17	22
17a	1.61	m	-	53.7	CH ₂	18, 19	-
17b	1.91	m	-	-	-	-	-
18	-	-	-	74.2	-	-	-
19	5.54	brs	-	138.2	CH	-	20
20	5.84	dd	2.7, 16.5	125.8	CH	18, 19	19
21	5.52	brs	-	77.2	CH	8, 9, 19, 20, 23	-
22	1.06	d	6.5	26.2	CH ₃	15, 16, 17	16
23	1.36	s	-	31.3	CH ₃	17, 18, 19	-
1'	-	-	-	130.7	-	-	-
2' 6'	7.33	d	8.2	130.4	2 x CH	3', 4', 5', 10	3', 5'
3' 5'	7.72	d	8.2	120.8	2 x CH	1', 4'	2', 6'
4'	-	-	-	137.9	-	-	-
24	-	-	-	170.1	-	-	-
25	2.27	s	-	21.0	CH ₃	21, 24	-
4''	-	-	-	147.6	-	-	-
5''	7.83	s	-	119.1	CH	4''	-
6''	2.13	m	-	28.1	CH ₂	4'', 5'', 7''	7''
7''	1.89	m	-	27.6	CH ₂	6'', 8''	6''
8''	4.18	m	-	63.1	CH ₂	-	-
9''	-	-	-	173.6	-	-	-
10''	2.37	m	-	33.8	CH ₂	8'', 10''	9'', 11''
11''	1.70	m	-	28.2	CH ₂	8'', 9'', 11'', 12'', 13''	10''
12''	1.48	m	-	28.2	CH ₂	9'', 10'', 12'', 13''	9''
13''	1.69	m	-	24.7	CH	11'', 13'', 14''	14''
14''	3.19	m	-	55.2	CH	11''	13'', 15'', 18''
15''	4.33	m	-	61.7	CH	14'', 17'', 20''	14'', 19''
17''	-	-	-	163.3	-	-	-
19''	4.52	m	-	60.0	CH	13'', 16''	15'', 20''
20a''	2.74	m	-	40.6	CH ₂	13'', 18''	18''
20b''	2.93	m	-	-	-	-	-

Table 8.19 NMR data of compound **304** recorded at 500 MHz in CDCl₃.



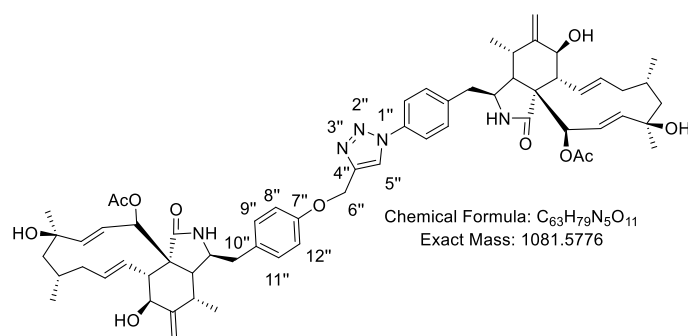
Position	δ_H	M	J_{H-H}/Hz	δ_C	HSQC	HMBC H to C	H-H COSY
1	-	-	-	174.6	-	-	-
3	3.33	m	-	53.2	CH	1', 1, 4, 5	4, 5, 10
4	2.17	m	-	49.9	CH	1, 3, 5, 6, 10	3, 5, 10
5	2.85	m	-	32.6	CH	1', 3	4, 11, 12
6	-	-	-	147.5	-	-	-
7	3.88	d	10.6	69.7	CH	6, 12	8, 12
8	2.96	m	-	47.0	CH	7, 9, 13, 20, 21	7, 13
9	-	-	-	51.9	-	-	-
10a	2.74	m	-	44.7	CH ₂	1', 3	3, 4, 12
10b	2.90	m	-	-	-	-	-
11	0.98	d	6.6	13.8	CH ₃	4, 5, 6	5
12a	5.14	brs	-	114.3	CH ₂	5, 6, 7	5, 7, 11
12b	5.39	brs	-	-	-	-	-
13	5.75	m	-	127.1	CH	7, 8, 15	8, 14, 15
14	5.43	m	-	138.9	CH	9, 15	13, 15
15a	1.82	m	-	42.6	CH ₂	13, 14, 16, 17	13, 14,
15b	2.08	m	-	-	-	-	-
16	1.82	m	-	28.2	CH	13, 14, 17	22
17a	1.61	m	-	53.5	CH ₂	18, 19	-
17b	1.91	m	-	-	-	-	-
18	-	-	-	74.1	-	-	-
19	5.55	brs	-	138.4	CH	-	20
20	5.86	dd	2.6, 16.5	125.8	CH	18, 19	19
21	5.52	brs	-	77.1	CH	8, 9, 19, 20, 23	-
22	1.07	d	6.4	26.3	CH ₃	15, 16, 17	16
23	1.38	s	-	31.4	CH ₃	17, 18, 19	-
1'	-	-	-	129.5	-	-	-
2' 6'	7.34	d	8.5	127.8	2 x CH	3', 4', 5', 10	3', 5'
3' 5'	7.72	d	8.5	121.1	2 x CH	1', 4'	2', 6'
4'	-	-	-	135.7	-	-	-
24	-	-	-	170.2	-	-	-
25	2.26	s	-	21.1	CH ₃	24	-
4''	-	-	-	142.4	-	-	-
5''	8.07	s	-	122.2	CH	4''	-
6''	5.39	s	-	58.1	CH ₂	4'', 5'', 7''	-
7''	-	-	-	173.4	-	-	-
8''	4.42	s	-	70.1	CH	7'', 9'', 10'', 11'', 13'',	-
9''	-	-	-	64.7	-	-	-
10''11''	1.50	s	-	26.9	2 x CH ₃	8'', 9''	-
13''	5.54	d	4.2	67.9	CH	15'', 16''	16''
15''	-	-	-	173.5	-	-	-
16''	5.69	dd	4.2, 9.1	58.5	CH	13'', 15'', 18''	13''
18''	-	-	-	170.3	-	-	-
19''	3.66	s	-	43.4	CH ₂	18'', 20'', 21'', 25''	-
20''	-	-	-	133.8	-	-	-
21''25''	7.30	m	-	129.6	2 x CH	22'' 24''	22'' 24''
22'' 24''	7.39	m	-	129.2	2 x CH	21''25''	21''25''
23''	7.28	m	-	127.6	CH	21'', 22'', 24'', 25''	22'', 24''

Table 8.20 NMR data of compound **302** recorded at 500 MHz in CDCl₃.



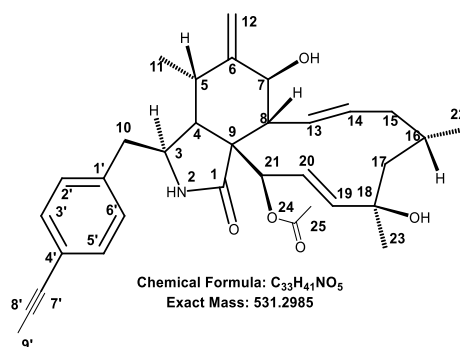
Position	δ_H	M	J_{H-H}/Hz	δ_C	HSQC	HMBC H to C	H-H COSY
1	-	-	-	174.6	-	-	-
3	3.24	m	-	54.0	CH	1', 1, 4, 5	4, 5, 10
4	2.10	m	-	50.2	CH	1, 3, 5, 6, 10	3, 5, 10
5	2.79	m	-	33.0	CH	1', 3	4, 11, 12
6	-	-	-	150.0	-	-	-
7	3.84	dd	1.3, 10.8	69.8	CH	6, 12	8, 12
8	2.96	m	-	47.2	CH	7, 9, 13, 20, 21	7, 13
9	-	-	-	51.9	-	-	-
10a	2.61	m	-	44.5	CH ₂	1', 3	3, 4, 12
10b	2.80	m	-	-	-	-	-
11	1.00	d	6.7	14.3	CH ₃	4, 5, 6	5
12a	5.12	brs	-	114.0	CH ₂	5, 6, 7	5, 7, 11
12b	5.37	brs	-	-	-	-	-
13	5.74	ddd	1.3, 9.7, 15.3	127.2	CH	7, 8, 15	8, 14, 15
14	5.41	ddd	5.1, 10.4, 15.3	138.5	CH	9, 15	13, 15
15a	1.81	m	-	43.0	CH ₂	13, 14, 16, 17	13, 14,
15b	2.07	m	-	-	-	-	-
16	1.82	m	-	28.6	CH	13, 14, 17	22
17a	1.61	m	-	53.9	CH ₂	18, 19	-
17b	1.90	m	-	-	-	-	-
18	-	-	-	74.3	-	-	-
19	5.56	brs	-	138.2	CH	-	20
20	5.88	dd	2.6, 16.6	126.0	CH	18, 19	19
21	5.49	brs	-	77.6	CH	8, 9, 19, 20, 23	-
22	1.06	d	6.4	26.7	CH ₃	15, 16, 17	16
23	1.38	s	-	31.2	CH ₃	17, 18, 19	-
1'	-	-	-	130.1	-	-	-
2' 6'	7.10	d	8.5	130.3	2 x CH	3', 4', 5', 10	3', 5'
3' 5'	6.97	d	8.5	115.2	2 x CH	1', 4'	2', 6'
4'	-	-	-	157.3	-	-	-
24	-	-	-	170.1	-	-	-
25	2.26	s	-	20.9	CH ₃	24	-
1''	5.21	s	-	62.1	-	2'', 3'', 4'	3''
2''	-	-	-	143.9	-	-	-
3''	7.86	s	-	124.0	CH	2''	1'', 4''
4''	4.58	dd	4.5, 5.6	50.3	CH ₂	5''	3'', 5''
5''	3.91	dd	4.5, 5.5	69.4	CH ₂	4'', 6''	4''
6'' 9''	3.58	m	-	70.2	CH ₂	7'', 8''	-
7'' 8''	3.62	m	-	70.4	CH ₂	6'', 9''	-
10''	3.54	m	-	69.9	CH ₂	9'', 11''	11''
11''	3.42	dd	5.3, 10.5	39.2	CH ₂	10'', 13''	10''
12''	6.56	t	5.6	-	-	-	-
13''	-	-	-	173.1	-	-	-
14''	2.19	m	-	35.8	CH ₂	13'', 15'', 16''	15''
15''	1.68	m	-	25.7	CH ₂	13'', 14'', 16''	14'', 16''
16''	1.47	m	-	28.4	CH ₂	14'', 15'', 17'', 18''	15''
17''	1.69	m	-	28.2	CH ₂	18'', 19''	-
18''	3.16	m	-	55.4	CH	17''	-
19''	4.32	m	-	61.8	CH	18'', 21'', 23'', 24''	23''
21''	-	-	-	163.6	-	-	-
22''	-	-	-	-	-	-	-
23''	4.50	m	-	60.1	CH	18'', 19'', 21'', 23''	19'', 24''
24a''	2.74	m	-	40.5	CH ₂	18'', 19''	23''
24b''	2.91	m	-	-	-	-	-

Table 8.21 NMR data of compound **319** recorded at 500 MHz in CDCl₃.



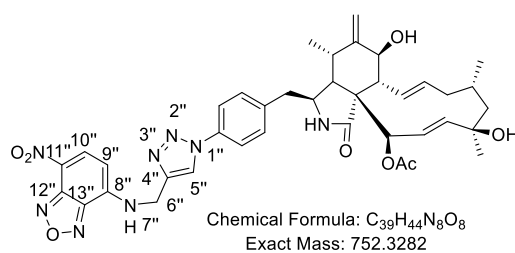
Position	δ_H	M	J_{H-H}/Hz	δ_C	HSQC	HMBC H to C	H-H COSY
1	-	-	-	174.3	-	-	-
3	3.25	m	-	53.8	CH	1', 1, 4, 5	4, 5, 10
4	2.16	dd	3.9, 5.1	50.4	CH	1, 3, 5, 6, 10	3, 5, 10
5	2.80	m	-	32.8	CH	1', 3	4, 11, 12
6	-	-	-	147.9	-	-	-
7	3.86	dd	2.2, 11.8	69.6	CH	6, 12	8, 12
8	2.96	m	-	47.3	CH	7, 9, 13, 20, 21	7, 13
9	-	-	-	51.8	-	-	-
10a	2.79	m	-	44.9	CH ₂	1', 3	3, 4, 12
10b	2.96	m	-	-	-	-	-
11	1.01	d	6.6	14.2	CH ₃	4, 5, 6	5
12a	5.14	brs	-	114.2	CH ₂	5, 6, 7	5, 7, 11
12b	5.38	brs	-	-	-	-	-
13	5.75	m	-	127.9	CH	7, 8, 15	8, 14, 15
14	5.42	m	-	138.8	CH	9, 15	13, 15
15a	1.82	m	-	42.7	CH ₂	13, 14, 16, 17	13, 14,
15b	2.05	m	-	-	-	-	-
16	1.81	m	-	28.6	CH	13, 14, 17	22
17a	1.58	m	-	53.7	CH ₂	18, 19	-
17b	1.91	m	-	-	-	-	-
18	-	-	-	74.7	-	-	-
19	5.56	brs	-	138.2	CH	-	20
20	5.86	m	-	125.8	CH	18, 19	19
21	5.52	brs	-	77.5	CH	8, 9, 19, 20, 23	-
22	1.07	d	6.4	26.5	CH ₃	15, 16, 17	16
23	1.36	s	-	31.3	CH ₃	17, 18, 19	-
1'	-	-	-	138.3	-	-	-
2' 6'	7.34	d	8.5	130.4	2 x CH	3', 4', 5', 10	3', 5'
3' 5'	7.71	d	8.5	121.0	2 x CH	1', 4'	2', 6'
4'	-	-	-	136.0	-	-	-
24	-	-	-	170.2	-	-	-
25	2.26	s	-	21.0	CH ₃	24	-
4''	-	-	-	145.0	-	-	-
5''	8.08	s	-	120.5	CH	4''	-
6''	5.30	s	-	62.0	CH ₂	4'', 5'', 7''	-
7''	-	-	-	157.3	CH ₂	6'', 8'', 17''	-
8'' 12''	7.00	d	8.6	115.2	2 x CH	7'', 9'', 11''	9'', 11''
9'' 11''	7.10	d	8.6	130.2	2 x CH	8'', 10''	8'', 12''
10''	-	-	-	138.3	-	-	-

Table 8.22 NMR data of compound **322** recorded at 500 MHz in CDCl₃.



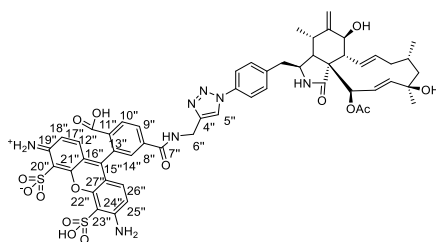
Position	δ_H	M	J_{H-H}/Hz	δ_C	HSQC	HMBC H to C	H-H COSY
1	-	-	-	174.2	-	-	-
3	3.24	ddd	1.1, 4.4, 9.1	53.3	CH	1', 4, 5	4, 5, 10
4	2.13	t	4.4	50.6	CH	3, 5	3, 5, 10
5	2.78	m	-	32.7	CH	1', 3	4, 11, 12
6	-	-	-	147.9	-	-	-
7	3.85	d	10.2	69.6	CH	5, 6, 8, 12, 13	8, 12
8	2.95	t	10.2	47.2	CH	1, 7, 9, 13, 21	7, 13
9	-	-	-	51.7	-	-	-
10a	2.67	dd	9.5, 13.5	45.6	CH ₂	1', 3	3, 4, 12
10b	2.82	dd	4.8, 13.5	-	-	-	-
11	0.98	d	6.7	14.1	CH ₃	4, 5, 6	5
12a	5.12	brs	-	114.2	CH ₂	5, 6, 7	5, 7, 11
12b	5.37	brs	-	-	-	-	-
13	5.76	ddd	1.4, 9.6, 15.5	126.9	CH	7, 8, 15	8, 14, 15
14	5.42	ddd	4.8, 10.3, 15.5	138.4	CH	9, 15	13, 15
15a	1.82	m	-	42.7	CH ₂	13, 14, 16, 17	13, 14,
15b	2.05	m	-	-	-	-	-
16	1.80	m	-	28.7	CH	13, 14, 17	22
17a	1.57	m	-	53.7	CH ₂	18, 19	-
17b	1.91	m	-	-	-	-	-
18	-	-	-	74.4	-	-	-
19	5.54	brs	-	138.0	CH	-	20
20	5.90	dd	2.9, 16.4	126.0	CH	18, 19	19
21	5.60	brs	-	77.5	CH	8, 9, 19, 20, 23	-
22	1.06	d	6.5	26.1	CH ₃	15, 16, 17	16
23	1.37	s	-	31.2	CH ₃	17, 18, 19	-
1'	-	-	-	132.0	-	-	-
2' 6'	7.09	d	8.2	128.8	2 x CH	3', 4', 5', 10	3', 5'
3' 5'	7.36	d	8.2	131.9	2 x CH	1', 4'	2', 6'
4'	-	-	-	122.9	-	-	-
24	-	-	-	170.2	-	-	-
25	2.27	s	-	20.9	CH ₃	21, 24	-
7'	-	-	-	86.2	-	-	-
8'	-	-	-	79.2	-	-	-
9'	2.04	s	-	4.2	CH ₃	3', 4', 5', 7', 8'	-

Table 8.23 NMR data of compound **312** recorded at 500 MHz in CDCl₃.



Position	δ_H	M	J_{H-H}/Hz	δ_C	HSQC	HMBC H to C	H-H COSY
1	-	-	-	174.5	-	-	-
2	5.56	brs	-	-	-	-	-
3	3.35	m	-	53.3	CH	-	4, 5, 10
4	2.17	dd	3.8, 5.0	50.3	CH	1, 3, 5, 6, 10	3, 5, 10
5	2.81	m	-	32.9	CH	1', 3	4, 11, 12
6	-	-	-	147.8	-	-	-
7	3.86	dd	1.6, 10.7	69.7	CH	6, 12	8, 12
8	2.96	m	-	47.3	CH	1, 7, 9, 13, 20, 21	7, 13
9	-	-	-	51.8	-	-	-
10a	2.78	m	-	44.9	CH ₂	1', 3	3, 4, 12
10b	2.98	m	-	-	-	-	-
11	1.03	d	6.7	14.3	CH ₃	4, 5, 6	5
12a	5.14	brs	-	114.3	CH ₂	5, 6, 7	5, 7, 11
12b	5.39	brs	-	-	-	-	-
13	5.74	m	-	126.9	CH	7, 8, 15	8, 14, 15
14	5.43	m	-	138.8	CH	9, 15	13, 15
15a	1.82	m	-	42.8	CH ₂	13, 14, 16, 17	13, 14,
15b	2.06	m	-	-	-	-	-
16	1.81	m	-	28.4	CH	13, 14, 17	22
17a	1.60	m	-	53.9	CH ₂	18, 19	-
17b	1.88	m	-	-	-	-	-
18	-	-	-	74.4	-	-	-
19	5.57	brs	-	138.2	CH	-	20
20	5.85	dd	3.0, 16.2	125.7	CH	18, 19	19
21	5.46	brs	-	77.2	CH	8, 9, 19, 20, 23	-
22	1.07	d	6.5	26.5	CH ₃	15, 16, 17	16
23	1.37	s	-	31.2	CH ₃	17, 18, 19	-
1'	-	-	-	130.7	-	-	-
2' 6'	7.35	d	8.5	130.6	2 x CH	3', 4', 5', 10	3', 5'
3' 5'	7.69	d	8.5	121.2	2 x CH	1', 4'	2', 6'
4'	-	-	-	135.6	-	-	-
24	-	-	-	170.1	-	-	-
25	2.26	s	-	21.0	CH ₃	24	-
4''	-	-	-	144.2	-	-	-
5''	8.04	s	-	119.9	CH	4''	-
6''	4.93	s	-	39.4	CH ₂	-	-
8''	-	-	-	143.1	-	-	-
9''	6.44	d	8.6	99.7	CH	11'', 12''	10''
10''	8.54	d	8.5	135.9	CH	11'', 13''	9''
11''	-	-	-	125.2	-	-	-
12''	-	-	-	144.3	-	-	-
13''	-	-	-	143.4	-	-	-

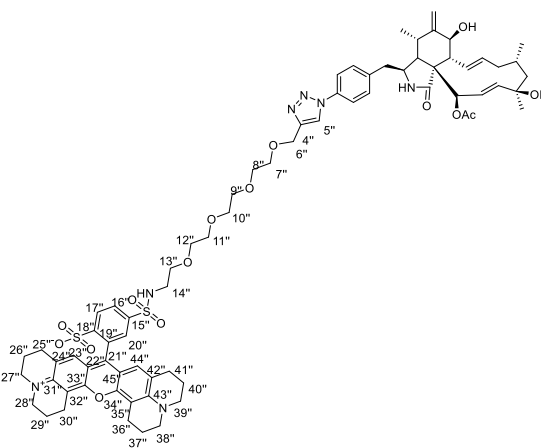
Table 8.24 NMR data of compound **314** recorded at 500 MHz in CDCl₃.



Chemical Formula: C₃₄H₃₈N₇O₁₅S₂
Exact Mass: 1105.3198

Position	δ_H	M	J_{H-H}/Hz	δ_C	HSQC	HMBC H to C	H-H COSY
1	-	-	-	174.6	-	-	-
3	3.15	m	-	53.0	CH	1	10
4	1.97	dd	3.7, 5.0	48.3	CH	3, 5	5
5	2.51	m	-	32.2	CH	1', 3	4
6	-	-	-	146.1	-	-	-
7	3.63	dd	1.3, 10.8	71.0	CH	-	8
8	2.74	m	-	46.6	CH	-	7
9	-	-	-	52.4	-	-	-
10a	2.66	m	-	43.8	CH ₂	1', 3	3
10b	2.85	m	-	-	-	-	-
11	0.48	d	6.6	13.7	CH ₃	4, 5, 6	5
12a	4.84	brs	-	111.8	CH ₂	5, 6, 7	7
12b	5.06	brs	-	-	-	-	-
13	5.54	ddd	1.4, 9.7, 15.4	129.2	CH	7, 8, 15	8
14	5.09	ddd	4.8, 10.1, 15.4	134.9	CH	9, 15	13, 15
15a	1.62	m	-	43.5	CH ₂	114, 16,	13, 14,
15b	1.90	m	-	-	-	-	-
16	1.69	m	-	28.2	CH	13, 14, 17	22
17a	1.39	m	-	54.3	CH ₂	18, 19	-
17b	1.60	m	-	-	-	-	-
18	-	-	-	72.7	-	-	-
19	5.39	brs	-	138.4	CH	-	20
20	5.68	dd	2.2, 17.0	125.8	CH	18, 19	19
21	5.29	brs	-	77.0	CH	19, 20	-
22	0.95	d	6.4	26.7	CH ₃	15, 16, 17	16
23	1.14	s	-	31.4	CH ₃	17, 18, 19	-
1'	-	-	-	138.3	-	-	-
2' 6'	7.35	d	8.5	131.3	2 x CH	3', 4', 5'	3', 5'
3' 5'	7.84	d	8.5	120.0	2 x CH	1', 4'	2', 6'
4'	-	-	-	135.6	-	-	-
24	-	-	-	170.6	-	-	-
25	2.24	s	-	21.1	CH ₃	24	-
4''	-	-	-	146.0	-	-	-
5''	8.65	s	-	121.0	CH	4''	-
6''	4.54	s	-	35.6	CH ₂	4'', 5'', 7''	-
7''	-	-	-	168.7	-	-	-
8''	-	-	-	140.4	-	-	-
9''	8.05	d	7.7	125.3	CH	8''	10''
10''	8.19	d	7.7	129.6	CH	9'', 11'', 12''	9''
11''	-	-	-	130.3	-	-	-
12''	-	-	-	165.5	-	-	-
13''	-	-	-	138.3	-	-	-
14''	7.71	s	-	123.1	CH	12'', 15''	-
15''	-	-	-	129.3	-	-	-
16''	-	-	-	130.0	-	-	-
17''	5.68	dd	8.8, 15.5	138.3	CH	-	-
18''	6.47	d	8.8	114.1	CH	19'', 20''	-
19'', 24''	-	-	-	114.7	2 x CH	-	-
20''	-	-	-	105.2	-	-	-
21''	-	-	-	151.2	-	-	-
22''	-	-	-	149.4	-	-	-
23''	-	-	-	114.6	-	-	-
25''	6.36	d	8.8	129.5	CH	22''	-
26''	5.06	m	-	134.9	2 x CH	-	-
27''	-	-	-	105.5	-	-	-

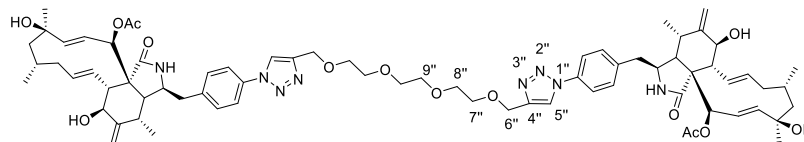
Table 8.25 NMR data of compound **316** recorded at 500 MHz in CDCl₃.



Position	δ_H	M	J_{H-H}/Hz	δ_C	HSQC	HMBC H to C	H-H COSY
1	-	-	-	174.2	-	-	-
3	3.27	m	-	53.6	CH	1', 1, 4, 5	4, 5, 10
4	2.15	dd	3.7, 4.7	50.4	CH	1, 3, 5, 6, 10	3, 5, 10
5	2.80	m	-	32.9	CH	1', 3	4, 11, 12
6	-	-	-	148.0	-	-	-
7	3.85	dd	1.4, 10.8	69.7	CH	6, 12	8, 12
8	2.97	m	-	47.2	CH	7, 9, 13, 20, 21	7, 13
9	-	-	-	51.7	-	-	-
10a	2.77	m	-	45.0	CH ₂	1', 3	3, 4, 12
10b	2.90	m	-	-	-	-	-
11	1.04	d	6.7	14.2	CH ₃	4, 5, 6	5
12a	5.14	brs	-	114.2	CH ₂	5, 6, 7	5, 7, 11
12b	5.38	brs	-	-	-	-	-
13	5.76	ddd	1.4, 9.7, 15.4	127.1	CH	7, 8, 15	8, 14, 15
14	5.45	m	-	138.7	CH	9, 15	13, 15
15a	1.83	m	-	42.7	CH ₂	13, 14, 16, 17	13, 14,
15b	2.05	m	-	-	-	-	-
16	1.81	m	-	28.5	CH	13, 14, 17	22
17a	1.58	m	-	53.8	CH ₂	18, 19	-
17b	1.89	m	-	-	-	-	-
18	-	-	-	74.3	-	-	-
19	5.59	brs	-	138.1	CH	-	20
20	5.91	dd	2.8, 16.5	125.8	CH	18, 19	19
21	5.59	brs	-	77.4	CH	8, 9, 19, 20, 23	-
22	1.08	d	6.5	26.5	CH ₃	15, 16, 17	16
23	1.37	s	-	31.2	CH ₃	17, 18, 19	-
1'	-	-	-	137.7	-	-	-
2' 6'	7.36	d	8.1	128.8	2 x CH	3', 4', 5', 10	3', 5'
3' 5'	7.79	d	8.1	120.8	2 x CH	1', 4'	2', 6'
4'	-	-	-	137.5	-	-	-
24	-	-	-	170.1	-	-	-
25	2.26	s	-	20.9	CH ₃	24	-
4''	-	-	-	145.9	-	-	-
5''	8.36	s	-	121.2	CH	4''	-
6''	4.81	s	-	64.3	CH ₂	4'', 5'', 7''	-
7'', 8'', 9'', 10'', 11'', 12''	3.68	m	-	70.2	6 x CH ₂	7'', 8'', 9'', 10'', 11'', 12''	-
13''	3.79	m	-	69.7	CH ₂	-	14''
14''	3.34	m	-	43.3	CH ₂	-	13''
15''	-	-	-	145.7	-	-	-
16'', 17''	8.01	d	7.9	126.8	2 x CH	18'', 19''	-
18''	-	-	-	127.4	-	-	-
19''	-	-	-	131.5	-	-	-
20''	8.36	s	-	121.2	CH	21'', 22''	-
21''	-	-	-	134.4	-	-	-
22''	-	-	-	126.5	-	-	-
23''	7.27	s	-	127.1	CH	24'', 31''	-
24''	-	-	-	129.1	-	-	-

25", 30"	2.73	m	-	27.4	2 x CH ₂	23", 24"	-
26", 29"	1.28	m	-	29.6	2 x CH ₂	25", 27"	-
27", 28"	3.85	m	-	47.2	2 x CH ₂	26"	-
31"	-	-	-	137.5	-	-	-
32"	-	-	-	73.6	-	-	-
33"	-	-	-	150.0	-	-	-
34"	-	-	-	129.0	-	-	-
35"	-	-	-	151.3	-	-	-
36", 41"	2.66	m	-	27.4	2 x CH ₂	34", 38"	38"
37", 40"	1.97	m	-	20.6	2 x CH ₂	36"	38"
38", 25", 27", 39"	3.47	m	-	50.5	2 x CH ₂	37", 43"	36", 37"
42"	-	-	-	113.7	-	-	-
43"	-	-	-	152.7	-	-	-
44"	6.83	s	-	128.1	CH	41", 42", 43", 45"	-
45"	-	-	-	104.6	-	-	-

Table 8.26 NMR data of compound **321** recorded at 500 MHz in CDCl₃.



Chemical Formula: C₇₂H₉₄N₈O₁₄
Exact Mass: 1294.6889

Position	δ_H	M	J_{H-H}/Hz	δ_C	HSQC	HMBC H to C	H-H COSY
1	-	-	-	174.3	-	-	-
3	3.33	m	-	53.5	CH	1', 1, 4, 5	4, 5, 10
4	2.16	dd	3.8, 5.1	50.3	CH	1, 3, 5, 6, 10	3, 5, 10
5	2.81	m	-	32.8	CH	1', 3	4, 11, 12
6	-	-	-	147.9	-	-	-
7	3.88	dd	1.3, 10.8	69.9	CH	6, 12	8, 12
8	2.96	m	-	47.3	CH	7, 9, 13, 20, 21	7, 13
9	-	-	-	51.8	-	-	-
10a	2.76	m	-	45.1	CH ₂	1', 3	3, 4, 12
10b	2.93	m	-	-	-	-	-
11	1.02	d	6.7	14.2	CH ₃	4, 5, 6	5
12a	5.14	brs	-	114.2	CH ₂	5, 6, 7	5, 7, 11
12b	5.39	brs	-	-	-	-	-
13	5.75	ddd	1.4, 9.7, 15.4	126.9	CH	7, 8, 15	8, 14, 15
14	5.42	ddd	4.8, 10.1, 15.4	138.8	CH	9, 15	13, 15
15a	1.82	m	-	42.7	CH ₂	13, 14, 16, 17	13, 14,
15b	2.06	m	-	-	-	-	-
16	1.81	m	-	28.6	CH	13, 14, 17	22
17a	1.60	m	-	53.6	CH ₂	18, 19	-
17b	1.88	m	-	-	-	-	-
18	-	-	-	74.7	-	-	-
19	5.56	brs	-	138.2	CH	-	20
20	5.88	dd	2.2, 17.0	125.7	CH	18, 19	19
21	5.55	brs	-	77.3	CH	8, 9, 19, 20, 23	-
22	1.07	d	6.3	26.5	CH ₃	15, 16, 17	16
23	1.36	s	-	31.3	CH ₃	17, 18, 19	-
1'	-	-	-	138.3	-	-	-
2' 6'	7.31	d	8.5	130.4	2 x CH	3', 4', 5', 10	3', 5'
3' 5'	7.68	d	8.5	120.8	2 x CH	1', 4'	2', 6'
4'	-	-	-	136.0	-	-	-
24	-	-	-	170.2	-	-	-
25	2.27	s	-	21.0	CH ₃	24	-
4''	-	-	-	145.0	-	-	-
5''	8.04	s	-	120.4	CH	4''	-
6''	4.77	s	-	64.7	CH ₂	4'', 5'', 7''	-
7''	3.76	m	-	69.9	CH ₂	6'', 8'', 17''	-
8'' 9''	3.70	m	-	70.6	CH ₂	8'', 9''	-

Curriculum Vitae

Chongqing Wang was born in 08.10.1987, Anhui, China.

Oct 2016 – Mar 2020	PhD student, Organic Chemistry , Gottfried Wilhelm Leibniz Universität Hannover, Germany
Sep 2012 – Jun 2015	Master, Medicinal Chemistry , Secondary Military Medical University, Shanghai, China
Sep 2007 – Jun 2011	Bachelor, Pharmaceutical Engineering , Wannan Medical College, Anhui, China

List of Publications

1. **Chongqing Wang**, Verena Hantke, Russell J. Cox, Elizabeth Skellam, “Targeted Gene Inactivation Expose Silent Cytochalasins in *Magnaporthe grisea* NI980.” *Org. Lett.*, 2019, 21, 4163-4167.
2. **Chongqing Wang**, Marc Stadler, Russell J. Cox, Elizabeth Skellam, “Investigating the Function of Cryptic Cytochalasin Cytochrome P450 Monooxygenases Using Combinatorial Biosynthesis.” *Org. Lett.*, 2019, 21, 8756-8760.
3. Junhang Jiang[†], **Chongqing Wang**[†], Canhui Zheng, “1-Phenyl-dihydrobenzoinidazoles as novel colchicine site inhibitors: Structural basis and antitumor efficacy” *European Journal of Medicinal Chemistry*, 2019, 177, 448-456. (†: Equal contribution).
4. **Chongqing Wang**, Chen X, Jiang JH, Tang H, Zhu KK, Zhou YJ, Zheng CH, Zhu J, “Acidic rearrangement of benzyl group in flavone benzyl ethers and its regioselectivity.” *Chinese Chemical Letters (IF = 4.6)*, 2015, 26, 793-796.
5. Jiang JH[†], **Chongqing Wang**[†], Wang J, Tian W, Yang C, Song YL, Hu Y, Zhu J, Zhou YJ, “Synthesis and biological evaluation of 5,6,7-trimethoxy-1-benzylidene-3,4-dihydro-naphthalen-2-one as tubulin-polymerization inhibitors.” *Chinese Chemical Letters (IF = 4.6)*, 2015, 26, 607-609. (†: Equal contribution).
6. Verena Hantke, **Chongqing Wang**, Elizabeth J Skellam and Russell J Cox, “Function of Pathway Specific Regulators in the ACE1 and Pyrichalasin H Biosynthetic Gene Cluster.” *RSC Advances*, 2019, 9, 35797-35802.
7. Jiang JH, Canhui Zheng, **Chongqing Wang**, Jiang HL, Zhu J, Luo C, Zhou YJ, “Quantum Chemistry Calculation-Aided Structural Optimization of Combretastatin A-4 like Tubulin Polymerization Inhibitors: Improved Stability and Biological Activity.” *Journal of Medicinal Chemistry*, 2015, 58, 2538-2546.